UNIVERSITA' DEGLI STUDI DI PADOVA

FACOLTÀ DI MEDICINA E CHIRURGIA

Istituto di Anatomia Patologica

SCUOLA DI DOTTORATO DI RICERCA IN SCIENZE MEDICHE, CLINICHE E SPERIMENTALI

INDIRIZZO SCIENZE CARDIOVASCOLARI

XX CICLO

TESI DI DOTTORATO

Genetic analysis in a large cohort of unrelated consecutive patients with Arrhythmogenic Right Ventricular Cardiomyopathy/Dysplasia

Coordinatore : Ch.mo Prof. Gaetano Thiene
Istituto di Anatomia Patologica

Supervisore : **Dr.ssa Alessandra Rampazzo**
Dipartimento di Biologia

Dottorando : Dr.ssa Alessandra Lorenzon

31 gennaio 2008

INDEX

ABSTRACT

Introduction — Arrhythmogenic right ventricular cardiomyopathy/dysplasia (ARVC/D) is an inherited heart muscle disorder that primarily affects the right ventricular myocardium early in the course of disease with later-onset left ventricular involvement. Clinically, it is characterized by ventricular arrhythmias of right ventricular origin, as noted by ventricular tachycardia with a left bundle branch block morphology, commonly associated with syncope or sudden cardiac death in particular in teenagers and in young adults. To date, mutations in 7 genes, including 5 encoding desmosomal proteins, Junctional plakoglobin (JUP), Desmoplakin (DSP), Plakophilin-2 (PKP2), Desmoglein-2 (DSG2) and Desmocollin-2 (DSC2), have been identified in ARVC/D patients.

The study of genetically engineered mice models of ARVC/D, generated through transgenesis and gene targeting, recapitulates the pathogenic characteristics of the disease.

Methods — The study involved a cohort of 110 unrelated consecutive index cases and their available family members. Clinical diagnosis of ARVC/D was based on major and minor criteria established by an international Task Force.

Mutation screening in four desmosomal protein genes (PKP2, DSP, DSG2 and DSC2) was performed by denaturing high-performance liquid chromatography (DHPLC) and direct sequencing in ARVC/D index cases. Desmin (DES) and plakophilin-4 (PKP4) candidate genes were screened in 80 ARVC/D index cases, by DHPLC and direct sequencing as well.

In order to generate a knock−in mouse carrying a targeted mutation in DSG2, the mouse *dsg2* gene was isolated from the λ FIX II 129/SVJ library. A 7041bp genomic fragment was subcloned in the targeting vector, and three nucleotide mutations (G105R, N271S, and K299E) were introduced in mouse *dsg2* exons 4, 7, and 8 by site-directed mutagenesis. Neomycin resistance cassette (Neo) and Thymidine kinase cassette (TK) were cloned in the targeting vector, thus allowing positive-negative selection of the recombination events.

Results — Analysis of coding sequences of PKP2, DSP, DSG2 and DSC2 genes was performed on genomic DNA of 110 ARVC/D index cases. One PKP2 mutation was detected in 16 probands (14.6%), one DSP mutation in 11 (10.0%), one DSG2 mutation in 8 (7.3%), and one DSC2 mutation in 3 subjects (2.7%). Compound or double heterozygosity was identified in 14 probands (12.7%). Available family members of 19 index cases were screened for the detected mutations and clinical investigation showed that clinical expression of ARVC/D mutations is heterogeneous even among relatives, ranging from a complete lack of symptoms and/or clinical manifestations to severe disease phenotype.

According with the hypothesis that ARVC/D is due to desmosomal defects, DES and PKP4 genes were screened in 80 ARVC/D probands. Two variations (K241E and c.736-11A>G) were detected in DES gene in two subjects. Three PKP4 variations (c.245+101A>G, A479A, and P797P) were detected in three subjects. None of the nucleotide changes was found in 300 control subjects from the same population.

To establish a cause and effect relationship between DSG2 mutations and ARVC/D, a knock-in mouse model will be generated. A *dsg2* genomic fragment was cloned in the targeting vector that will be used; by site-directed mutagenesis three *dsg2* pathogenic mutations (G105R, N271S, and K299E) were introduced; also Neo and TK cassettes were cloned. After linearization, the vector will be transfected into the murine embryonic stem cells.

Discussion – ARVC/D is a recognized cause of sudden cardiac death, which may be prevented by timely detection and intervention. Since mutations causing ARVC/D have been identified so far in genes encoding desmosomal proteins, this cardiomyopathy might be considered as "a disease of the desmosome". Mutation screening of the four desmosomal genes PKP2, DSP, DSG2 and DSC2 in 110 ARVC/D unrelated individuals allowed successful genotyping of 52 (47.3%). Emerging data suggest that an important minority of ARVC/D patients are compound heterozygous or double heterozygous (12.7%). Clinical comparison of patients carrying single and multiple mutations showed no significant differences in terms of electrocardiographic and structural abnormalities, major events and disease expression. The only significant difference was that patients carrying DSG2 mutations were found older at diagnosis and at the time of major arrhythmic symptoms than DSP and PKP2 carriers. On the ground of these data, it is impossible to clinically differentiate different forms of ARVC/D due to mutations in different genes.

Since no causing mutations have been identified in more than 50% of patients, additional components of the desmosome-intermediate filament complex and associated proteins were considered the primary candidates disease-genes. The coding regions of DES and PKP4 genes were screened in 80 ARVC/D index cases. Most of the detected nucleotide changes were intronic and synonymous variations that do not change the sequence of the gene product, but might affect splicing (by activating a cryptic splice site). On the basis of present data, it is not possible to exclude the involvement of these genes in the pathogenesis of ARVC/D; thus, mutation screening in ARVC/D genes on DNA of probands should be planned only on the basis of relative prevalence of mutations in different genes.

The identification of the primary genetic causes of ARVC/D has opened the possibility to generate animal models where the events underlying the pathophysiology of this disease can be studied in detail. Gene transfer technology allows the creation of specific mutant genotypes in animals thereby increasing their chance of resembling human diseases at the genetic and phenotypic levels.

The generated targeting vectors will be transfected into the murine embryonic stem cells to create a DSG2 knock−in mouse model. In perspective, such models should prove useful for investigating cellular mechanisms involved in the molecular pathogenesis of ARVC/D and for assessing the effects of selected pharmacological treatments.

SUMMARY IN ITALIAN

Introduzione ─ La cardiomiopatia aritmogena del ventricolo destro (ARVC), nota anche come displasia aritmogena del ventricolo destro (ARVD), è una malattia ereditaria del muscolo cardiaco caratterizzata da alterazioni strutturali e funzionali che tipicamente coinvolgono il ventricolo destro. La disomogeneità del tessuto cardiaco altera la conduzione dell'impulso elettrico e si originano aritmie che occasionalmente portano a fibrillazione ventricolare e morte improvvisa, soprattutto nei giovani.

Attualmente 7 geni sono coinvolti nella determinazione genetica della malattia, 5 dei quali codificano proteine dei desmosomi: Placoglobina (JUP), Desmoplachina (DSP), Placofilina-2 (PKP2), Desmogleina-2 (DSG2) e Desmocollina-2 (DSC2).

Topi geneticamente modificati, creati mediante transgenesi o *gene targeting strategy*, rappresentano un buon modello per studiare i meccanismi patogenetici dell'ARVC/D.

Metodi ─ Lo studio ha coinvolto 110 casi indice, non imparentati tra loro, diagnosticati affetti da ARVC/D in base ai criteri diagnostici della Task Force. Lo *screening* per la ricerca di mutazioni è stato condotto nei casi indice in 4 geni che codificano proteine desmosomali (PKP2, DSP, DSG2 e DSC2) mediante DHPLC (denaturing high-performance liquid chromatography) e sequenziamento diretto. L'analisi genetica è stata successivamente estesa ai familiari disponibili.

I geni candidati DES e PKP4 (codificanti, rispettivamente, desmina e placofilina-4) sono stati analizzati per la ricerca di mutazioni in 80 dei 110 casi indice affetti da ARVC/D, mediante DHPLC e sequenziamento diretto.

Allo scopo di generare un topo knock−in per il gene DSG2, la sequenza genomica del gene *dsg2* murino è stata isolata da una libreria genomica di topo (λ FIX II 129/SVJ *library*). Un frammento di 7041 paia di basi (comprendente gli esoni da 4 a 8) è stato subclonato in un *targeting vector* e, mediante mutagenesi sito specifica, tre mutazioni puntiformi (G105R, N271S, and K299E) sono state introdotte negli esoni 4, 7, and 8. Le cassette Neo (per la resistenza alla neomicina) e TK (codificante la timidina chinasi) sono state clonate nello stesso vettore in modo da permettere la doppia selezione positiva-negativa delle cellule embrionali ricombinanti.

Risultati ─ L'analisi delle sequenze codificanti dei geni PKP2, DSP, DSG2 and DSC2 nei 110 casi indice ha permesso di identificare mutazioni nel 47.3% dei casi. In particolare, 16 soggetti (14.6%) sono risultati portatori di una singola mutazione nel gene PKP2, 11 (10.0%) nel gene DSP, 8 (7.3%) nel gene DSG2 e 3 (2.7%) nel gene DSC2; 14 pazienti (12.7%) sono risultati portatori di più di una mutazione.

E' stato possibile estendere l'analisi molecolare ai familiari di 19 casi indice ed individuare nella famiglia coloro che, avendo ereditato la mutazione, sono verosimilmente a rischio di ammalarsi. L'indagine clinica dei soggetti portatori di mutazione ha confermato la penetranza incompleta della patologia, che risulta manifestarsi con una ampia variabilità fenotipica.

In accordo con l'ipotesi che l'ARVC/D sia una malattia dovuta ad alterazioni delle giunzioni desmosomali, i geni DES e PKP4 sono stati analizzati per la ricerca di mutazioni in 80 casi

indice affetti da ARVC/D. Sono state identificate due variazioni (K241E e c.736-11A>G) nel gene DES e tre (c.245+101A>G, A479A, e P797P) nel gene PKP4. Nessuna delle 5 variazioni nucleotidiche è stata riscontrata in 300 soggetti sani di controllo.

Al fine di realizzare topi knock-in per il gene DSG2 quali modello animale dell'ARVC/D un frammento di 7041 paia di basi del gene *dsg2* murino è stato clonato in un vettore plasmidico e mediante mutagenesi sito-specifica sono state create nei costrutti tre mutazioni puntiformi che riproducono quelle identificate nel gene DSG2 in probandi ARVC/D. Nei vettori sono state successivamente introdotte le sequenze necessarie Neo e TK. I costrutti saranno opportunamente linearizzati e transfettati in cellule embrionali murine.

Discussione – Cinque dei geni ARVC/D finora noti codificano per componenti desmosomali, mentre uno è in grado di modularne l'espressione (TGFβ3); l'ARVC/D può essere quindi considerata "una malattia dei desmosomi".

Lo screening per la ricerca di mutazioni dei geni desmosomali PKP2, DSP, DSG2 e DSC2 in 110 casi indice diagnosticati affetti da ARVC/D ha permesso di identificare mutazioni in 52 di essi (47.3%). In una percentuale importante di essi (12.7%) sono state individuate più mutazioni. Dal confronto clinico tra portatori di mutazioni singole nei diversi geni e portatori di mutazioni multiple non sono emerse differenze significative; solo l'età alla diagnosi e alla manifestazione di sintomi aritmici è risultata più elevata nei portatori di mutazioni nel gene DSG2, se confrontati con portatori di mutazioni nei geni PKP2 e DSP. Sulla base di questi dati, non è perciò possibile associare manifestazioni fenotipiche diverse a mutazioni in geni distinti; lo screening per la ricerca di mutazioni deve quindi interessare tutti i geni più frequentemente implicati nella patologia.

Poiché mutazioni causative non sono state identificate in più del 50% dei casi, altri geni devono essere coinvolti nell'ARVC/D. I geni DES e PKP4, altamente espressi in cardiomiociti e i cui prodotti proteici sono associati al complesso desmosoma-filamento intermedio, sono stati considerati dei buoni geni candidati e sono stati analizzati in 80 casi indice. Le 5 variazioni nucleotidiche identificate (4 delle quali non causano cambiamento aminoacidico, ma potrebbero determinare uno splicing alterato, attivando siti criptici di splicing) non permettono di escludere completamente il coinvolgimento dei due geni nella determinazione dell'ARVC/D.

L'individuazione delle cause genetiche dell' ARVC/D ha offerto la possibilità di generare animali modello che permettano di indagare in dettaglio i meccanismi patofisiologici della malattia. I costrutti generati, una volta transfettati in cellule embrionali staminali murine, permetteranno di ottenere topi Knock-in per il gene DSG2 che consentiranno di indagare sui meccanismi patogenetici dell'ARVC/D e di sperimentare nuovi approcci diagnostici e terapeutici.

1. INTRODUCTION

Arrhythmogenic right ventricular cardiomyopathy/dysplasia (ARVC/D) is a genetically determined heart muscle disease associated with arrhythmia, heart failure, and sudden death (Nava et al., 2000). Autosomal dominant inheritance with incomplete penetrance is characteristic (Nava et al., 1988), although autosomal recessive variants are also recognized (McKoy et al., 2000). The main pathologic feature of the disease is loss of myocardium in the right ventricle, with fatty or fibro-fatty replacement (Thiene et al., 1988). Patients may present with symptoms such as palpitation, dizzy spells and syncope. Sudden cardiac death is often the first manifestation, mainly in young people engaged in physical exercise (Thiene et al., 1988; Fontaine et al., 1988; Furlanello et al., 1998; Corrado et al., 1990; Tabib et al., 1999).

1.1. Epidemiology

The prevalence of approximately 1 in 5,000 people has been estimated (Norman et al., 1999). The exact prevalence of ARVC/D, however, is unknown and could be higher than the estimated because of the existence of many non-diagnosed or misdiagnosed cases.

In the Veneto Region, Italy, the prevalence of the disease has been estimated to vary from 1:2,000 to 1:5,000 (Nava et al., 1989).

1.2. Historical notes

The first description of the disease can be traced to the book *De Motu Cordis et Aneurismatibus*, published in 1736 by Giovanni Maria Lancisi. In the 5th chapter of the book, paragraph 47, Lancisi reported a family with disease recurrence in four generations. Signs and symptoms were palpitations, heart failure, dilatation and aneurysms of the right ventricle, and sudden death, all features consistent with the current diagnostic criteria of the disease (Lancisi, 1736).

It was in 1961 that Professor Dalla Volta, University of Padua, reported cases with "auricularization of the right ventricular pressure" with an amazing fibrofatty, nonischemic pathology of the right ventricle (Dalla Volta et al., 1961). One the those patients survived until 1995, and underwent transplantation due to end-stage cardiac failure: the heart specimen showed severe right ventricular enlargement with a nearly normal left ventricle.

In 1982, Marcus and colleagues reported the first clinical series in 24 adults, first emphasizing the origin of arrhythmias from the RV and the histopathological substrate consisting of fibro-fatty replacement of the RV free wall, accounting for epsilon wave and ventricular arrhythmias of RV origin with left bundle branch block (LBBB) morphology (Marcus et al., 1982).

Same years later, two studies by the Padua research group (Nava A. et al., 1987; Thiene et al., 1988) completely changed the focus on the disease. In the first paper Nava and colleagues demonstrated that the disorder showed polymorphous clinical features and that it could run in

families as a genetic trait. In the family under study there were persons showing massive or minor forms of the disease. There were different types of arrhythmias in affected subjects and most family members appeared asymptomatic. Thiene and colleagues observed an impressive series of sudden deaths in the young (≤35 years), with pathology consisting of ARVC/D, mostly occurring during effort, and all characterized by inverted T-waves in the right precordial leads at electrocardiogram (ECG) and apparently benign ventricular arrhythmias of LBBB morphology (Thiene et al., 1988). They accounted for 20% of all sudden deaths. For the first time it was acknowledged that ARVC/D is another important cause of sudden death in the young (Maron, 1988). Death often occurred during effort; in autopsies of deceased patients areas of fibrolipomatosis in the right ventricle alternating with areas of myocytolysis and healthy myocardium were observed. Consequently, Thiene and colleagues, hypothesized that this disease affected primarily the myocardium with progressive atrophy, unrelated to developmental defects (Thiene et al., 1988).

In the last 20 years, it was possible to report the pathology (Basso et al., 1996), to put forward clinical diagnostic criteria (McKenna et al., 1994) , to find therapeutic measures (Wichter et al., 1992) and, finally, to discover the genetic background (Rampazzo and Danieli, 2007).

1.3. Clinical presentation

Four clinicopathologic phases have been described in natural history of arrhythmogenic right ventricular cardiomyopathy based on the long-term follow-up of clinical data (Thiene et al., 1990).

Subclinical phase with concealed structural abnormalities. This phase is characterised by subtle right ventricular structural changes with or without ventricular arrhythmias during which sudden death may occasionally be the first manifestation of the disease, mostly in young people during competitive sports or intense physical exercise (Thiene et al., 1988).

Overt arrhythmic phase. This phase shows symptomatic right ventricular arrhythmias possibly leading to sudden cardiac arrest associated with overt right ventricular functional and structural abnormalities (Corrado et al., 1990).

Global right ventricular dysfunctional phase. This phase results from the progression and extension of muscle disease with relatively preserved left ventricular function (Corrado et al., 1998).

Final phase. The final stage of bi-ventricular pump failure is caused by pronounced left ventricular involvement. At this stage, ARVC/D mimics biventricular dilated cardiomyopathy of other causes, leading to congestive heart failure and related complications. These data and those produced by other authors confirm that the disease is progressive (Blomstrom-Lundqvist et al., 1987). Progression could occur at any stage of the life but it is more evident in the teenage (Daliento et al., 1995).

Arrhythmogenic right ventricular cardiomyopathy/dysplasia (ARVC/D) was classified as a “cardiomyopathy of unknown origin mainly involving the myocardium at the right ventricle”

(Marcus et al., 1995; Basso et al., 1996). Knowledge on the clinical spectrum of the disease was enhanced by more careful evaluation of the structure and size of the right ventricle, investigated by echocardiography (Foale et al., 1986; Scognamiglio et al., 1989), angiography (Daliento et al., 1990), nuclear magnetic resonance (Casolo et al., 1987) or radionuclide imaging (Manyari et al., 1986), by better definition of diagnostic criteria (McKenna et al., 1994) and by systematic investigation on of family members of affected patients (Nava et al., 1988; Buja et al., 1989; Nava et al., 1990).

In the classical form, in about 80% of cases the disease is manifested in teenagers or in young adults (Marcus et al., 1982; Marcus et al., 1995; Fontaine et al., 1988), but it can be discovered at any age and in both sexes. Clinical presentation is characterized by palpitations, presyncope or syncope in subjects generally considered normal on physical examination. Weakness and dizzy spells are sometimes referred. A 12-leads electrocardiogram during the episodes or a 24-h Holter monitoring demonstrates that symptoms are mainly related to sustained, monomorphic ventricular tachycardia (SVT) with left bundle branch block configuration of QRS complex and superior, intermediate or inferior frontal plane axis.

The main features of the electrocardiogram at rest are as follow: negative T waves on precordial leads V1-V5, incomplete right bundle branch block or prolongation of QRS duration greater than 110 ms on V1-V2, distinct waves of small amplitude after the end of QRS complex, suggesting delayed activation of some portion of right ventricular wall (“epsilon wave”).

In about 24% of cases, palpitations are not exclusively associated with ventricular arrhythmias but with atrial extrasystoles, atrial flutter or fibrillation. This can be explained either by a primary involvement of atrial myocardium, replaced by fibro-fatty infiltration or by atrial dilatation and secondary to hemodynamic impairment of the right ventricle (Fontaine et al., 1988). Some interesting cases complain of chest pain associated with transient alterations of repolarization, such as ST segment elevation or negative T wave on inferior or precordial leads; in some instances, increased CK activity, mimicking angina and ischemia may be observed. For the pathogenetic mechanism of these cases, recurrent episodes of myocarditis of unknown etiology leading to localized areas of necrosis followed by replacement with adipose and fibrous tissue are postulated.

First description of ARVC/D included cases with exclusive or prevalent involvement of the right ventricle. Following the observation of several cases with long-term follow-up, however, it became evident that even left ventricle could be affected by the degenerative process (Marcus et al., 1982; Basso et al., 1996; Pinamonti et al., 1992). In these cases, clinical presentation is again characterized by occurrence of ventricular arrhythmias; the echoangiographic study shows right and left ventricular dysfunction. Recently, ARVC/D phenotypes with early and prominent left-sided involvement was reported (Norman et al., 2005).

It is now recognised that ARVC/D is a cause of sudden unexpected death, particularly in the young; this dramatic event may occur as first presenting symptom of the disease (Marcus et al., 1995; Basso et al., 1996).

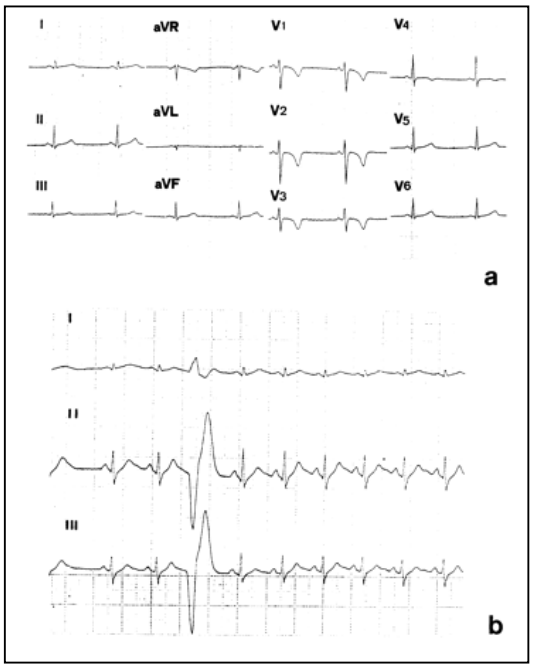

Figure 1.1. An asymptomatic 17-year-old boy died suddenly during a soccer game. Retrospectively, the only signs of the disease were **(a)** basal ECG showing T-wave inversion in right precordial leads up to V4 and **(b)** isolated premature ventricular beat of left bundle-branch block morphology during step test (from Basso et al., 1996).

Morphologic changes accounting for global and/or regional dysfunction are detectable by non-invasive techniques as echocardiography, angiography, radionuclide scintigraphy, or cardiac magnetic resonance imaging (MRI).

Echocardiography represents the first-line imaging approach for evaluating patients with suspected ARVC/D or for screening of family members. Echocardiography also allows serial examinations aimed to assess the disease onset and progression during the follow-up. RV angiography is usually reported as the gold standard for the diagnosis of ARVC/D. Angiographic evidence of akinetic/diskinetic bulgings localized in infundibular, apical and subtricuspid region has a high diagnostic specificity (> 90%) (Daliento et al., 1990). Radionuclide angiography is also an accurate non-invasive imaging technique for detection of global RV dysfunction and regional wall motion abnormalities. Its diagnostic concordance with RV angiography is nearly 90% (Le Guludec et al., 1995).

New tools for improving diagnostic accuracy have been introduced in recent years. Among non-invasive investigations, MRI is an attractive imaging tool has the ability to characterize tissue by distinguishing fat from muscle. However, recent studies have shown a high degree of interobserved variability in assessing fatty deposition, which may be observed even in normal hearts (Tandri et al., 2005). Cine-MRI may be of value in estimating RV volume and wall motion abnormalities with akinesia, dyskinesia and aneurysms. Among invasive procedures, three dimensional electroanatomic mapping shows low-voltage areas which correspond to fibro-fatty myocardial replacement (Corrado et al., 2005). It is able to differentiate ARVC/D from inflammatory cardiomyopathy mimicking ARVC/D, which shows a preserved electrogram voltage and has a better arrhythmic outcome.

1.4. Diagnostic criteria

In the years, many cases of ARVC/D were reported and a heterogeneous pattern of disease expression emerged.

In many individuals the clinical findings were very subtle, and they appeared to be affected by a variant of the same condition. In some of those identified at postmortem, clinical findings antemortem had perhaps not been recognized or interpreted appropriately, and opportunities to institute potentially life-saving measures were missed. Other milder phenotypes were emerging, with patients initially diagnosed as having idiopathic ventricular arrhythmia with “normal hearts”, with subsequent detailed echo or angiographic studies showing evidence of regional or segmental right and/or left ventricular structural or dynamic abnormalities (Nava et al., 1992).

As a result of these difficulties in clinically diagnosing ARVC/D, a Task Force of experienced clinicians in the field of cardiomyopathy was convened under the auspices of the European Society of Cardiology (Working Group on Myocardialand Pericardial Diseases) and the International Society and Federation of Cardiology (Scientific Council). The remit of this Task Force was to agree criteria (concerning structural, histological, electrocardiographical and genetic aspects) on clinical evaluation that would delineate the spectrum of disease that justifiably can be called right ventricular dysplasia in clinical practice (McKenna et al., 1994).

The Task Force looked at clinical criteria in six different groupings. Diagnostic criteria were assigned major or minor status according to their specificity for the condition. A diagnosis of ARVC/D was to be considered fulfilled by the presence of different groups of two major criteria, one major and two minor criteria, or four minor criteria (Table 1.1).

The full complement of cardiac investigation may be unremarkable in the concealed phase of arrhythmogenic right ventricular cardiomyopathy. Pivotal to this concept are reports of patient initially diagnosed with idiopathic right ventricular outflow tract tachycardia on the basis of normal ECG and imaging; arrhythmogenic right ventricular cardiomyopathy was later confirmed after the development of typical clinical features (Kuhn et al., 2000), or post-mortem examination. Arrhythmic events may therefore precede the development of other clinical findings in early arrhythmogenic right ventricular cardiomyopathy. The importance of continued follow-up for patients with presumed idiopathic right ventricular outflow tract tachycardia is also underlined.

Table 1.1. Task Force criteria for diagnosis of ARVC/D (adapted from McKenna et al., 1994).

	Major	Minor
I. Global and/or regional dysfunction and structural alterations*	Severe dilatation and reduction of right ventricular ejection fraction with no (or only mild) left ventricular involvement	Mild global right ventricular dilatation and/or ejection fraction reduction with normal left ventricle
	Localized right ventricular aneurysms (akinetic or dyskinetic areas with diastolic bulgings)	Mild segmental dilatation of the right ventricle
	Severe segmental dilatation of the right ventricle	Regional right ventricular hypokinesia
II. Tissue characteristics of wall	Fibro-fatty replacement of myocardium on endomyocardial biopsy	
III. Repolarization abnormalities		Inverted T-waves in right precordial leads (V2 and V3) in people >12 years, in absence of right bundle branch block
IV. Depolarization / conduction abnormalities	Epsilon waves or localized prolongation (>110ms) of the QRS complex in right precordial leads (V1-V3)	Late potentials (signal-averaged electrocardiography)
V. Arrhythmias	Arrhythmias listed below plus T wave abnormalities - see III Repolarization abnormalities	Sustained or non-sustained ventricular tachycardia wiyh left bundle branch block morphology (documented on electrocardiography, Holter or exercise testing)
		Frequent ventricular extrasystoles (>1000/24 hours, Holter)
VI. Family history	Familial disease confirmed at necropsy or surgery	Family history of premature sudden death (<35 years) due to suspected ARVC/D

* Morphological changes in I as detected by echocardiography, angiography, cardiac magnetic resonance imaging or radionuclide scintigraphy

Even before the publication of the Task Force criteria, study of relatives of probands diagnosed with ARVC/D identified features of disease which were not as marked as in the proband, suggesting considerable heterogeneity of disease expression, even within relatives carrying the same gene mutation. There was evidence supporting both incomplete and age-related penetrance (Nava et al., 1988). The identification of specific gene mutations responsible for ARVC/D has provided evidence of gene carriers with some features of ARVC/D which are insufficient to fulfil the Task Force criteria.

Hamid and colleagues evaluated family members of ARVC/D probands to determine if reliance on Task Force criteria to diagnose ARVC/D would result in significant underreporting in the setting of family screening (Hamid et al., 2002).

The authors therefore propose a modification of the Task Force criteria, which could be used as a diagnostic tool, but only in first degree relatives of a patient with confirmed ARVC/D (Table 1.2). The presence of any one of right precordial T-wave inversion, late potentials on signal-averaged electrocardiogram, ventricular tachycardia with left bundle branch block morphology,

or minor functional or morphological changes of the right ventricle on imaging should be considered diagnostic for familial ARVC/D.

Table 1.2. Proposed modification of Task Force criteria for diagnosis of familial ARVC/D (adapted from Hamid et al., 2002).

Proven ARVC/D in a first-degree relative plus one of the following	
I. Electrocardiogram: T-wave inversion in the right precordial leads (V2 and V3)	**II.** Signal averaged electrocardiogram: Demonstration of late potentials
III. Arrhythmias: Ventricular tachycardia with left bundle branch block morphology (documented on electrocardiogram , Holter monitoring or during exercise testing) >200 ventricular extrasystoles over 24 hours (Holter monitor)	**VI.** Structural or functional abnormality of the right ventricle: Mild global right ventricle dilatation of the right ventricle and/or reduction in ejection fraction with normal left ventricle Mild segmental dilatation of the right ventricle Regional right ventricle hypokinesia

1.5. Pathology

The striking feature of the disease is a diffuse or segmental transmural loss of the myocardium in the right ventricular free wall and its replacement by fatty or fibro-fatty tissue (Figure 1.2), usually in the setting of a normal left ventricle (Thiene et al., 1988). Myocardial atrophy accounts for a parchment-like, translucent look of the wall, even though the distance between the epicardium and the endocardium may be preservert (Figure 1.2).

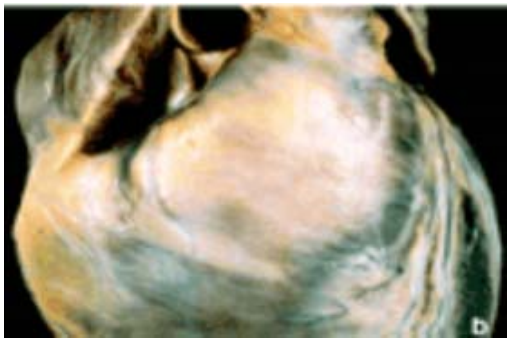

Figure 1.2. A 26-years-old male cyclist died suddenly at rest. Gross view of the heart specimen showing a yellow, dilated pulmonary infundibulum (from Basso et al., 1996).

Histological examination of affected myocardial tissue shows sparse myocytes interspersed among adipocytes and fibrous tissue. The process begins at the epicardium and gradually extends through the myocardium towards the subendocardium. The anterior right ventricular outflow tract (RVOT), the apex, and the inferoposterior wall are most frequently affected (Angelini et al., 1993).

However, there are peculiar alterations of the right ventricle that should draw the attention of the pathologist. Firstly at external examination, the right side of the heart appears yellowish or whitish, compared with the brownish left side, as to indicate a different tissue composition of the underlying myocardium. The suspicion may be easily confirmed by cutting the free wall along the inflow-outflow tracts, which appears fatty, and by checking the wall transparency with a light source (Figure 1.3).

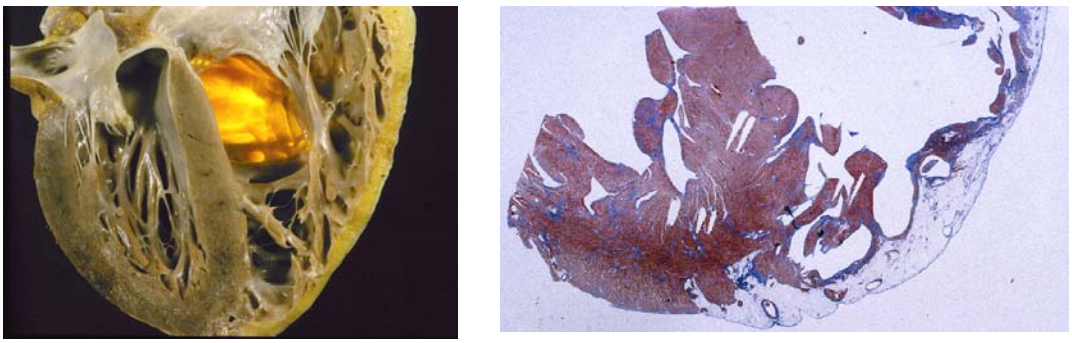

Figure 1.3. Typical case of ARVC/D in a 25-years old man who died suddenly at rest. **(Left)** Four chamber cut of the heart specimen seen from behind: noticeable isolated fatty replacement of the right ventricular free wall and translucent infundibulum. **(Right)** Macrohistological slide confirming that the dystrophic phenomenon is confined to the right ventricular free wall and spares the left ventricle and the ventricular septum. (From Nava, Rossi, Thiene. Arrhythmogenic right ventricular cardiomyopathy/dysplsia).

Other deformities of the right ventricular surface are even more remarkable. Aneurysms of the right ventricular free wall are a feature which actually seems to be pathognomonic of ARVC/D. They may appear as a true external bulging or as an “ex vacuo” hollow, the latter being explained by the empty cavity in the specimen (Figure 1.4).

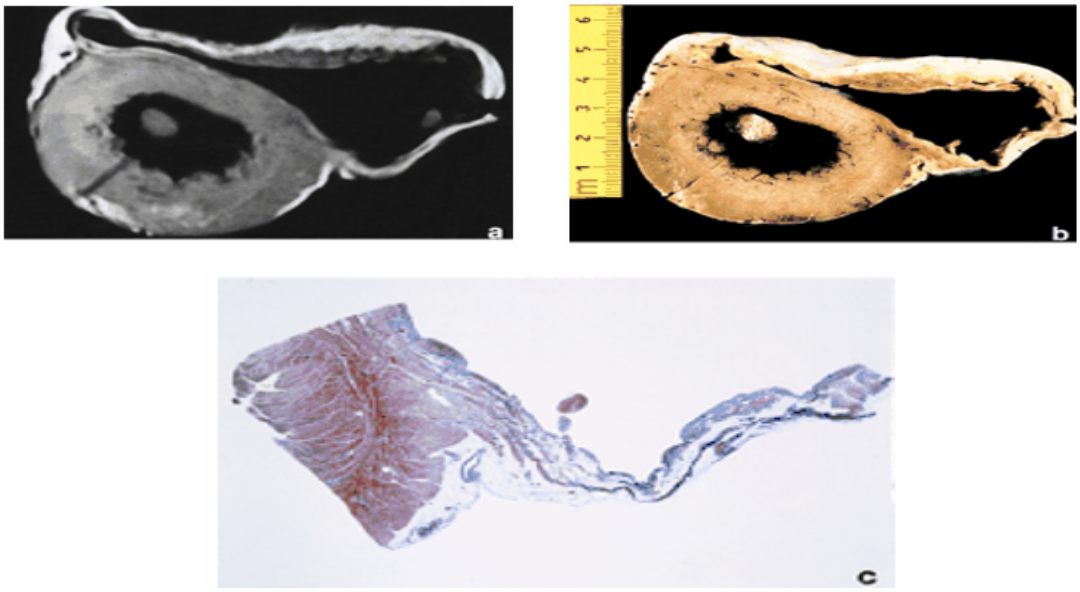

Figure 1.4. ARVC/D with aneurysms of the right ventricle in a 17-years-old boy who died suddenly during a soccer game. **(A)** In vitro MNR cross-sectional view showing a uniformly whitish right ventricular free wall with anterior and inferior aneurysms; note a spotty involvement of the posterolateral wall of the left ventricle. **(B)** Corresponding cross section of the heart specimen with infundibular and inferior subtricuspidal aneurysms. **(C)** Panoramic histological view of the inferior aneurysm showing wall thinning with fibro-fatty replacement (Azan stain). (from Basso et al., 1996).

Thus, a through gross examination of the heart can address immediately the diagnosis: whitish or yellowish appearance of the right ventricular surface, pericardial thickening, lipomatous and translucent appearance of the cut surface of the wall, presence of aneurysms.
In the most severe, long-standing forms endocardial thickening is a usual finding, particularly coincidental with ventricular aneurysms. Residual myocardium is visible only in the trabeculae, which show a thickened endocardium.

1.6. Pathologic substrates

Histologically, two distinct patterns, namely fatty and fibro-fatty, exist.
The *"fatty pattern"* consists of a mostly transmural fatty infiltration of the right ventricle free wall, mainly localized in the anterior wall and infundibulum, in the setting of a wave-front extension from the epicardium to the endocardium. The residual myocytes appear scattered within the fatty tissue. This pattern is regularly associated with a normal or even thickened wall, without scarring or aneurysms (Thiene et al., 1997) (Figure 1.5).
The *"fibro-fatty pattern"* shows a high incidence of right ventricular aneurysms and focal myocarditis, which consists of patchy inflammatory infiltrates of lymphocytes associated with myocardial necrosis (Thiene et al., 1991; Basso et al., 1996). Involved of the left ventricle and ventricular septum, when present, is exclusive to the fibro-fatty variety (Thiene et al., 1997) (Figure 1.5).

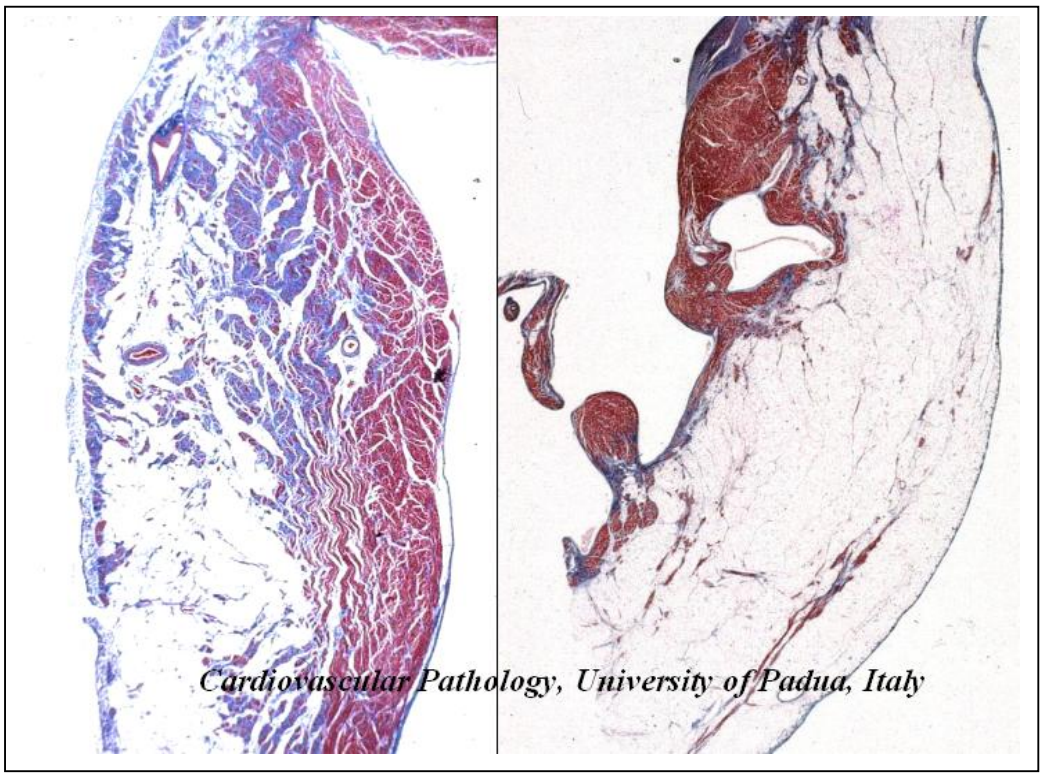

Figure 1.5. (Left) Fibro-fatty pattern of arrhythmogenic right ventricular cardiomyopathy: macrohistologic slide of the free wall of the left ventricle with a large spot of fibro-fatty replacement. **(Right)** Fatty pattern of arrhythmogenic right ventricular cardiomyopathy: macrohistologic slide of the free wall of the left ventricle only with fatty replacement (Tricromica Azan Mallory) (from Basso, Nava, Thiene. Cardiomiopatia aritmogena).

The fibro-fatty replacement of the myocardium interferes with intraventricular conduction of the electric impulse accounting for delay (late potentials, epsilon wave, parietal right bundle branch block) and onset of re-entrant phenomena which are the mechanism of ventricular arrhythmias. Fatty infiltration of the RV has not to be considered "*per se*" a sufficient morphologic hallmark of ARVC/D. A certain amount of intramyocardial fat is present in the RV antero-lateral and apical region even in the normal heart and increases with age and body size. Moreover, ARVC/D should be kept distinct from adipositas cordis. Presence of replacement-type fibrosis and myocyte degenerative changes are essential to provide a clear-cut diagnosis, besides remarkable fat replacement (Basso and Thiene, 2005; Thiene et al., 2007)

1.7. Role of apoptosis

Descriptive studies suggest loss of myocardium and replacement by adipose and fibrous tissue in ARVC/D results from excessive and inappropriate apoptosis of cardiac myocytes. Four groups of investigators have independently observed apoptosis in myocardial sample from patients with arrhythmogenic right ventricular cardiomyopathy (Mallat et al., 1996; Valente et al., 1996; Nishikawa et al., 1999; Nagata et al., 2000). As postnatal involution of the right ventricle results from physiological remodelling, most probably mediated by apoptosis (James et al., 1994), abnormal bouts of recurring or continued apoptosis could lead to progressive myocardial disapparence followed by fibro-fatty replacement in ARVC/D.

In particular, to test the hypothesis of apoptosis in the setting of progressive myocardial loss Valente and colleagues studied by transmission electron microscope (TEM) and TUNEL methods right ventricular endomyocardial biopsies from twenty ARVC/D patients, and calculated the apoptotic index as percentage of positive nuclei in the section stained by TUNEL. Presence of apoptotic myocytes was found in several cases (35%). Apoptosis appeared to be significantly related to clinical history duration and presence of acute symptoms and signs, in particular angina, elevated ESR or CPK titers as well as ST segment elevation on basal 12-lead ECG (Valente et al., 1996).

The evidence of apoptosis as a mechanism of myocyte death opens new avenues not only to get insights into the pathogenesis of ARVC/D, but also to develop new diagnostic and therapeutic strategies. Agents which induce apoptosis are used in tumour theraphy; apoptosis inhibitors should be searched for and investigated to stop or slow down myocyte loss in ARVC/D, and to prevent the electrical instability of the ventricle leading to ominous arrhythmias.

1.8. Possible causative or contributing role of viruses

The presence of myocardial inflammation in more than two-thirds of cases has suggested that some pathologic features of ARVC/D may be considered a sequela of infective myocarditis (Calabrese et al., 2006). Thus, fibro-fatty infiltration may , in part, be viewed as a healing phenomenon in the setting of chronic myocarditis. Enterovirus was first investigated on the

basis of an experimental model in which a mice infected with Coxsackievirus B3 developed selective right ventricular myocardial cell death, acute mononuclear cell infiltration and right ventricular aneurysm formation (Matsumori and Kawai, 1980).

Many DNA and RNA viruses, following infection, can cause genetic alteration in somatic genes; thus, viral infections could play a primary contributing role in the acquired forms of ARVC/D affecting the desmosome primarily by direct disruption. Whereas “pure” genetic forms may be uncommon, a genome-environment interaction could commonly influences virus uptake, migration, and antiviral immunity. In others words, genetic defects of different type could be responsible for increase individual viral susceptibility (Calabrese et al., 2007).

Several researchers have evaluated ARVC/D patients for the presence of enteroviral genome in the myocardium and controversial results have been reported, possibly reflecting different patient selection (Grumbach et al., 1998; Heim et al., 1997; Kearney et al., 1995; Calabrese et al., 2000). Chimenti and colleagues studied thirty patients who were diagnosed with ARVC/D on the basis of having either two major criteria or one major plus at least two minor criteria (McKenna et al., 1994). At histology ARVC/D was confirmed in nine patients, whereas the remaining met the Dallas criteria for myocarditis. The molecular investigation detected viral genome in four patients with myocarditis and in none with ARVC/D (Chimenti et al.,2004).

In Italy, recent experience using molecular viral screening confirmed the presence of different viral genome in seven (19%) of 36 cases with clinical and histological evidence of ARVC/D (Calabrese et al., 2007).

1.9. Treatment

The treatment of patients with ARVC/D encompasses a broad spectrum of the disease, ranging from latent asymptomatic forms to the survivors of repeated cardiac arrest (Marcus et al., 1995). Failure in the management of any of these situations could lead to sudden cardiac death. This event is particularly catastrophic since most of patients affected by ARVC/D are young and have an otherwise almost completely normal heart (Thiene et al., 1988). Therefore they may enjoy a long life expectancy provided that they arrhythmias are controlled.

The treatment of patients with ARVC/D is mostly based on the prevention of sudden cardiac death which results from cardiac arrhythmias.

Patients in whom a diagnosis of arrhythmogenic right ventricular cardiomyopathy is confirmed or strongly suspected are discourage from participating in competitive sports and endurance training. Extreme physical exertion is best avoided in daily activities, as is excessive ingestion of stimulants such as pseudoephedrine.

Evidence for the efficacy of antiarrhythmic agents in ARVC/D is largely anecdotal (Marcus et al., 1989; Wichter et al., 1992). The primary indication for drug treatment is to alleviate symptoms such as recurrent palpitation due to frequent ventricular extrasystoles. The associations of arrhythmic events with strenuous activity, together with the observation that ventricular tachycardia in ARVC/D is often preceded by an increased heart rate (Leclercq et al., 1996),

suggest that sympathetic stimulation may be a precipitant. First-line use β-adrenergic receptor antagonists, when there are no contraindications, is reasonable. Amiodarone is recommended as add-on therapy if β-blockers alone prove ineffective in suppressing ventricular arrhythmia.
ARVC/D patients with good left ventricular ejection fraction are candidates for treatment with automatic implantable cardioverter-defibrillator (AICD) since they generally have a long life expectancy provided that their arrhythmia is correctly controlled. The AICD should achieve the goal of preventing arrhythmic death in the severe forms of the disease (Tavernier et al., 2001).
In current practice, it is first-line therapy for cardiac arrest survivors, and is also offered to patients with arrhythmic syncope, left ventricular involvement , or ventricular tachycardia that is resistant to drug treatment (Tavernier et al., 2001).

1.10. Molecular genetics

Familial occurrence of ARVC/D is rather common, up to 50% of cases (Hamid et al., 2002), and is generally transmitted as an autosomal dominant trait, with some examples of autosomal recessive inheritance.

Since identification of the first ARVC/D locus in 1994 (Rampazzo et al., 1994), 12 loci have been detected, but only seven disease genes have been identified (Table 1.3).

Table 1.3. Known ARVC/D loci and disease-genes identified so far.

Locus	Inh. pattern	Chromosome	Gene	Function	Mutations identified so far	References
ARVD1	AD	14q24.3	TGFb3	cytokine stimulating fibrosis and modulating cell adhesion	Regulatory mutations in 5' and 3' UTRs	Rampazzo et al., 1994 Beffagna et al., 2005
ARVD2	AD	1q42-q43	RYR2	Calcium homeostasis	Missense mutations	Rampazzo et al., 1995 Tiso et al., 2001
ARVD3	AD	14q12-q22	unknown	-	-	Severini et al., 1996
ARVD4	AD	2q32.1-q32.2	unknown	-	-	Rampazzo et al., 1997
ARVD5	AD	3p23	unknown	-	-	Ahmad et al., 1998
ARVD6	AD	10p12-p14	unknown	-	-	Li et al., 2000
ARVD7	AD	10q22.3	unknown	-	-	Melberg et al., 1999
ARVD8	AD	6p24	DSP	Cell-cell adhesion	Missense, nonsense and splice site mutations	Rampazzo et al., 2002
ARVD9	AD	12p11.2	PKP2	Cell-cell adhesion	Missense, nonsense, insertion/deletion and splice site mutations	Gerull et al., 2004
	AR	12p11.2	PKP2	Cell-cell adhesion	Silent mutation affecting splicing	Awad et al., 2006
ARVD10	AD	18q12.1	DSG2	Cell-cell adhesion	Missense, nonsense, insertion/deletion and splice site mutations	Pilichou et al., 2006
ARVD11	AD	18q12.1	DSC2	Cell-cell adhesion	Missense, insertion/ deletion and splice site mutations	Syrris et al., 2006
ARVD12	AD	17q21	JUP	Cell-cell adhesion	Insertion mutation	Asimaki et al., 2007
Naxos disease	AR	17q21	JUP	Cell-cell adhesion	Deletion mutation	McKoy et al., 2000

1.10.1. ARVC/D dominant forms

DESMOPLAKIN

The first disease gene linked to autosomal dominant ARVC/D showing typical right ventricular phenotype was Desmoplakin (DSP) (Rampazzo et al., 2002). In 2002, genome scan in a family with ARVC/D indicated a linkage with a region of chromosome 6 short arm including DSP gene. DNA sequencing of all DSP exons in the affected persons of this family revealed a missense mutation in exon 7 (C1176G; AGC>AGG). The involved amino acid (Ser299Arg) is at the centre of a coiled, charged region, separating the two short helices of DSP sub-domain Z. The amino acid substitution suppresses a putative phosphorylation site which, on the other hand, is fully conserved in related proteins belonging to the same family. This mutation is thought to disrupt a protein kinase C (PKC) phosphorylation site which is involved in plakoglobin binding and in clustering of desmosomal cadherin-plakoglobin complexes.

Desmoplakin, together with plakoglobin, anchors to desmosomal cadherins, forming an ordered array of non-transmembrane proteins, which bind to keratin intermediate filaments (IF) (Leung et al., 2002). The primary structure of desmoplakin contains three functional domains: the N-terminal, which binds to the desmosome via connection with plakoglobin and plakophilin; the rod segment, which is predicted to form a dimeric coil; and the C-terminal domain, which bind IF's (Choi et al., 2002). Alternative splicing of the protein produces two isoforms, desmoplakin I and desmoplakin II. The cDNAs encoding these two highly related proteins differ in a 1.8 Kbase sequence that is missing in DSPII, most likely due to differential splicing of a longer transcript (Virata et al., 1992).

Mutations in desmoplakin have been reported for various disorders of skin and heart, which are striate palmoplantar keratoderma II (Armstrong et al., 1999), dilated cardiomyopathy with woolly hair and keratoderma (Norgett et al., 2000), skin fragility–woolly hair syndrome (Whittock et al., 2002).

Desmoplakin mutations were identified in four out of 25 (16%) Italian ARVC index patients studied, later confirmed in a larger series from the same population (Pilichou et al., 2006); Yang and colleagues identified desmoplakin mutations in four out of 66 (6%) ARVC/D patients from the north American ARVC/D registry (Yang et al., 2006). Detected mutations include missense, nonsense and splice-site mutations.

PLACOPHILIN-2

In 2004, Gerull and colleagues selected Plakophilin2 (PKP2) as candidate gene because a homozygous deletion caused a lethal cardiac defect in mice (Grossman et al., 2004). PKP2 gene encodes Plakophilin-2, an essential protein of the cardiac desmosome. By sequencing all 14 exons of the PKP2 gene, including flanking intronic splice sequences, the authors identified 25 different heterozygous mutations (12 insertion-deletion, 6 nonsense, 4 missense and 3 splice site mutations) in 32 out of 120 unrelated ARVC/D probands (Gerull et al., 2004). Plakophilin-2 is an armadillo-related protein, located in the outer dense plaque of desmosomes. It links

desmosomal cadherins to desmoplakin and the intermediate filament system. Plakophilins are also present in the nucleus, where they may play a role in transcriptional regulation (Mertens et al, 2001). Gerull et al. speculated that lack of plakophilin-2 or incorporation of mutant plakophilin-2 in the cardiac desmosomes might impair cell-cell contacts and, as a consequence, might disrupt association between adjacent cardiomyocytes.

The frequency of PKP2 mutations among ARVC/D cases ranged from 11% to 43% in different studies (Syrris et al., 2006; Van Tintelen et al., 2006; Dalal et al., 2006); these differences might be attributed to origin of cases or simply to selection bias.

DESMOGLEIN-2

Recently, by candidate gene approach, 50 Italian ARVC/D index cases were investigated for mutations in DSG2 gene. Desmoglein2 is a cadherins family member and isoforms 2 is the only one expressed in cardiac myocytes. Nine heterozygous mutations were detected in 8 out of 50 (12%) unrelated individuals with ARVC/D. Among these, 5 were missense mutations, 2 were insertion-deletions, 1 was a nonsense and 1 was a splice site mutation; one patient had two different DSG2 mutations (compound heterozygote). Endomyocardial biopsy, obtained from 5 patients, showed extensive loss of myocytes with fibro-fatty tissue replacement. In 3 patients, electron microscopy showed intercalated disc paleness, decreased desmosome number, and intercellular gap widening (Pilichou et al., 2006). Mutations in DSG2 gene were also detected in an independent study (Awad et al., 2006). It is interesting to note that, in this study, there was one patient with compound-heterozygous mutations in DSG2.

DESMOCOLLIN-2

DSC2 is the desmosomal protein most recently causally related to ARVC/D. DSC2, like DSG2, is a major constituent of desmosomal cadherins, and was therefore considered an important candidate gene. Syrris and colleagues found mutations in four out of 77 (5%) desmoplakin/JUP/ PKP2/DSG2-negative ARVC/D patients, with incomplete penetrance in the families studied (Syrris et al., 2006). Simultaneously, Heuser and colleagues identified a splice-site mutation in one out of 88 PKP2/DSG2-negative patients (Heuser et al., 2006). Two DSC2 heterozygous mutations were also identified in two Italian probands and in four family members; these N-terminal amino acid changes affected the normal localisation of DSC2, that was predominantly localised in the cell cytoplasm (Beffagna et al., 2007).

PLAKOGLOBIN

Asimaki and colleagues described a dominant mutation in the JUP gene, encoding plakoglobin, in a German family with arrhythmogenic right ventricular cardiomyopathy. The mutation was predicted to result in the insertion of an extra serine residue after Ser39 in the N-terminus of the protein. There was no dermatological manifestation such those seen in Naxos disease, a recessive disorder also due to recessive mutation in JUP gene. Analysis of a biopsy sample of the right ventricle from the proband showed markedly decreased localization of plakoglobin,

desmoplakin, and connexin-43 at intercalated discs in cardiac myocytes. Taken together with other observations it was concluded that the insertion mutation affected the structure and distribution of mechanical and electrical cell junctions (Asimaki et al, 2007).

TRANSFORMING GROWTH FACTOR-β3

In two families with ARVC/D the exonic sequences of 6 candidate genes (included in the critical region of 14q23-q24 and expressed in the heart) were screened to identify gene involved in ARVD1. Five of them (POMT2, KIAA0759, KIAA1036, C14orf4 and TAIL1) were unsuccessfully screened for pathogenic ARVC/D mutations (Rampazzo et al, 2003; Rossi et al, 2004). Transforming growth factor-β3 (TGFβ3) appeared to be a good candidate, since it encodes a cytokine stimulating fibrosis and modulating cell adhesion. After previous analyses failed to detect any mutation in the coding region of this gene, mutation screening was extended to the promoter and untranslated regions (UTRs). A nucleotide substitution (c.-36G>A) in 5'UTR of TGF β3 gene was detected in all affected subjects belonging to a large ARVD1 family. After the investigation was extended to 30 unrelated ARVC/D index patients, an additional mutation (c.1723C>T) was identified in the 3'UTR of one proband. In vitro expression assays of constructs containing the mutations showed that mutated UTRs were twofold more active than wild-type (Beffagna et al., 2005).

TGFβ3 is a member of the transforming growth factor superfamily, which includes a diverse range of proteins regulating many different physiological processes. TGFβ1, -β2, and -β3 are the prototype of the TGFβ superfamily. They inhibit proliferation in most types of cells and induces apoptosis of epithelial cells. Conversely, they stimulate mesenchymal cells to proliferate and produce extracellular matrix and they induce a fibrotic response in various tissues *in vivo*.

Finding TGFβ3 mutations associated with ARVC/D is very interesting, since it is well established that TGFβs stimulate mesenchymal cells to proliferate and to produce extracellular matrix components. Since mutations in UTRs of TGFβ3 gene, detected in ARVC/D, showed enhanced gene expression *in vitro*, it is likely that they could promote myocardial fibrosis *in vivo*. Myocardial fibrosis may disrupt electrical and mechanical behavior of myocardium and extracellular matrix abnormalities may predispose to re-entrant ventricular arrhythmias. In agreement with this hypothesis, endomyocardial biopsy in the two probands in which TGFβ3 UTR mutations were detected showed extensive replacement-type fibrosis. Moreover, it has been shown that TGFβs modulate expression of genes encoding desmosomal proteins in different cell types. cDNA microarray analysis, performed on RNA from cardiac fibroblasts incubated in the presence or in the absence of exogenous TGFβs, revealed increased expression of different genes, including plakoglobin (Kapoun et al., 2004). Yoshida and colleagues reported that TGFβ1 exposure of cultured airway epithelial cells increases the content of desmoplakins I and II. This suggests that regulation of cell-cell junctional complexes may be an important effect of TGFβs (Yoshida et al, 1992). Therefore, overexpression of TGFβ3, caused by UTRs mutations, might affect cell-to-cell junction stability, thus leading to

disease expression similar to that observed in ARVC/D due to mutations of genes encoding desmosomal proteins.

CARDIAC RYANODINE RECEPTOR-2

The first identified ARVC/D gene in a dominant form was RYR2, the cardiac ryanodine receptor, involved in ARVD2 (Tiso et al., 2001). The distinctive feature of this form is the presence of polymorphic, effort-induced arrhythmias (Figure 1.6). RYR2 is one of the largest human genes (105 exons), enconding a 565Kda protein located in the membrane of smooth sarcoplasmic reticulum. The homo-tetrameric structure known as cardiac ryanodine receptor plays a pivotal role in intracellular calcium homeostasis and excitation-contraction coupling in cardiomyocytes (Stokes and Wagenknecht, 2000; Missiaen et al., 2000). All RYR2 mutations detected in ARVD2 patients were missense resulting in substitutions involving amino acids highly conserved through evolution in critical domains of the protein (Tiso et al., 2001; Bagattin et al., 2004).

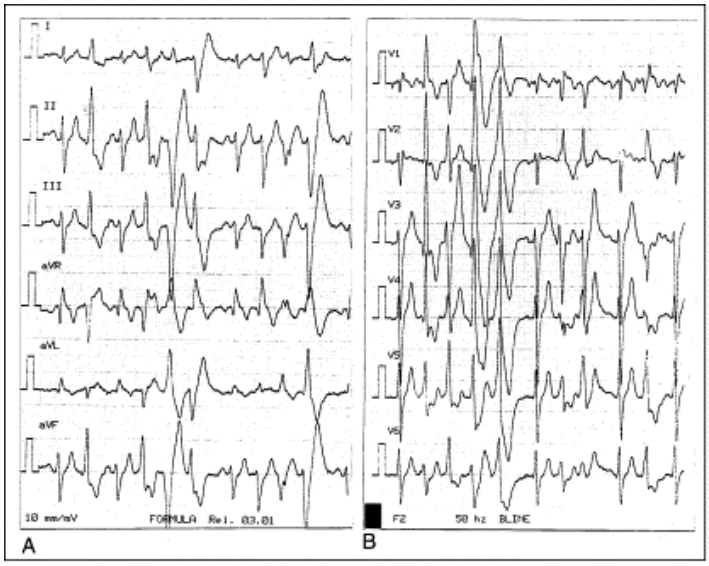

Figure 1.6. (A) Standard and augmented limb leads. **(B)** Precordial leads. Electrocardiogram during and exercise stress test of a 15-year-old patient. Polymorphic tachycardia appeared at 150 W (from Bauce et al., 2000).

Mutations in the human RYR2 gene have also been associated with catecholaminergic polymorphic ventricular tachycardia (CPVT; OMIM 604772) (Priori et al., 2001, 2002) and familial polymorphic ventricular tachycardia (FPVT; OMIM 604772) (Laitinen et al., 2001, 2003). Putative pathogenic mutations in RYR2 have been reported in 20 out 240 patients with a diagnosis of long-QT syndrome (Kopplin et al., 2004).

All RYR2 mutations described to date cluster in three specific domains: the N-terminal amino-acid residues 176-433, the centrally located residues 2246-2504, and the C-terminal residues 3778-4959. Detection of RYR2 mutations in both ARVD2 and CPVT patients raises the question

of the possible existence of a single genetic defect different phenotypes of which might be simply due to variable expression and incomplete penetrance. Both ARVD2- and CPVT-RyR2 missense mutations would alter the ability of the calcium channel to remain closed. Intense adrenergic stimulation due to emotional or physical stress can lead to calcium overload, thus triggering severe arrhythmias. The functional role of mutations R176Q, L433P, N2386I and T2504M, previously detected in ARVD2 patients (Tiso et al., 2001) was recently investigated (Thomas et al., 2004). RyR2 mutants N2386I and R176Q/T2504M exhibited enhanced sensitivity to caffeine activation and increased Ca^{2+} release, in agreement with the current hypothesis that defective RyR2 cause Ca^{2+} leak. In contrast, RyR2 L433P mutation showed reduced response to caffeine activation. This mutation might be interpreted as a "loss-of-function". Therefore, RyR2 mutations might be either "gain-of-function" or "loss-of-function", thus suggesting heterogeneity in functional consequences of RyR2 mutations. Even with this additional information, the question of whether ARVD2 and CPVT are different diseases due to different mutations of the RYR2 gene still remains unsettled.

1.10.2. ARVC/D recessive forms

PLACOGLOBIN

To date, one plakoglobin mutation has been implicated in Naxos disease, a syndrome characterised by arrhythmogenic right ventricular cardiomyophaty associated with palmoplantar keratoderma and peculiar woolly hair. It was identified by Protonotarios and colleagues amongst families originating from the Hellenic Naxos island (Protonotarios et al., 1986). This followed his observation of an association between recurrent ventricular tachycardia and/or sudden death and palmoplantar keratoderma. The syndrome was called Naxos syndrome, because of the concentration of cases in the Naxos island (Protonotarios et al., 1986).

All patients had diffuse, not transgressing, palmoplantar keratoderma and tight woolly hair unlike other family members. The pattern of disease stereotyped in all cases. At birth woolly hair was present. At that time or shortly after, palmar erythema occurred, and when the infants started to use their hands keratoderma developed. Later, when they started to ambulated, plantar erythema occurred which was followed by keratoderma, producing the typical pattern.

The cardiac abnormality presented later. All patients presented electrocardiographic and/or echocardiographic abnormalities fulfilling the criteria of ARVC/D (McKenna et al., 1994).

Cardiac biopsies revealed fibro-fatty replacement of right ventricular myocardium. The right ventricle showed extensive myocardial loss with fibro-fatty replacement at subepicardial and mediomural layers (Figure 1.7).

A 2-basepair deletion mutation in JUP gene (2157delTG) was identified in 13 Greek families end one Turkish family with Naxos disease. Twenty-nine clinically unaffected family members were heterozygous for the mutation. This deletion causes a frame shift and premature

termination of translation resulting in a truncated protein at the C-terminal domain (McKoy et al., 2000).

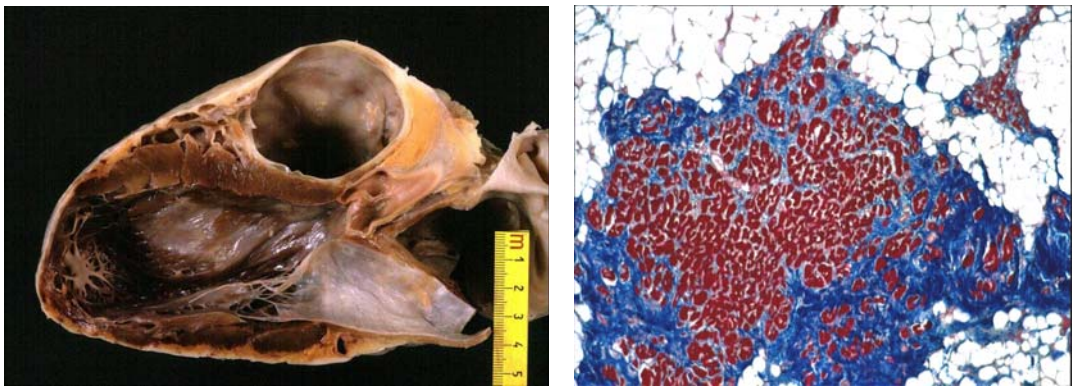

Figure 1.7. (Left) Autopsy finding from a Naxos' patient who died suddenly. **(Right)** High magnification hystologic picture of the right ventricle free wall. Note the remarkable myocardial atrophy with fatty replacement and interstitial fibrosis (gently provided by Prof. Thiene and Prof. Basso).

DESMOPLAKIN

The first autosomal recessive mutation in desmoplakin to be reported comprised a homozygous mutation, 7901delG, detected in three Equadorian families. The frameshift mutation occurs close to the 3' end of the gene and leads to a truncated desmoplakin protein with part of the C domain of the tail region missing, and disrupts desmoplakin–intermediate filament interaction (Norgett et al., 2000). It results in a clinical syndrome of dilated cardiomyopathy, woolly hair and keratoderma. Affected family members with this condition, known as Carvajal syndrome (OMIM 605676), suffer with heart failure in their teens (Carvajal-Huerta, 1998).

A further homozygous missense mutation, G2375A, in desmoplakin gene was identified in one Arab family (Alcalai et al., 2003). The substitution in C-terminal of protein has been found to underlie a case of acral skin blistering, woolly hair and cardiomyopathy.

Finally, a nonsense mutation in desmoplakin (C3799T) in association with a polymorphism in plakoglobin (T2089A) was found to cause a severe form of cardiocutaneous syndrome in Turkish family. This mutation lead to loss of most of the desmoplakin isoforms 1, particularly affecting the C-terminal area.

All identified desmoplakin mutations that cause recessive cardiac phenotype affect the protein domain at the inner dense plaque of desmosomes and result in skin and hair phenotype similar to that of plakoglobin mutation.

PLAKOPHILIN-2

The first case of recessive ARVC/D caused by mutation in PKP2 gene was recently reported. Candidate gene analysis in DNA of a proband with typical form of ARVC/D identified a homozygous mutation predicted to be translationally silent (G828G). Analysis of the proband's mRNA showed that this mutation causes predominantly cryptic splicing, with a 7bp deletion in

exon 12, and the ensuing frame shift disrupts the last portion of plakophilin-2 molecule. Heterozygous family members produce approximately 60% of properly spliced PKP2 and do not have manifestation of the disease (Awad et al., 2006).

1.11. Desmosomal abnormalities and pathophysiological mechanisms

Since mutations causing ARVC/D have been identified so far in more genes encoding desmosomal proteins, this cardiomyopathy might be considered as "a disease of the desmosome".

Desmosomes provide mechanical attachment between cells by anchoring desmin intermediate filaments. In addition, they protect the other junctions (gap junctions and adherens junctions) from mechanical stress and are involved in structural organization of the intercalated disc (Kaplan et al., 2004). Notably, desmosomes are also believed to play a role in cell–cell signaling themselves (Ko et al., 2001). Desmosomes are found in tissues that experience mechanical stress; epidermis and myocardium in particular. Mutant desmosomes are probably able to maintain tissue integrity unless subjected to excessive mechanical stress. In this respect, the thinnest portions of the right ventricle, i.e. the right ventricular outflow tract, inflow tract and the apex (the 'triangle of dysplasia') are the most vulnerable.

Desmosomes are multiprotein structures in the cell membrane and consist of three protein families: transmembraneous proteins (cadherins): desmogleins (DSG) and desmocollins (DSC); linker-(armadillorepeat) proteins: plakoglobin and plakophilin; and plakins: desmoplakin (DSP) and plectin (Figure 1.8). Within desmosomes, cadherins interact with armadillo proteins, which for their part are connected to plakins. The latter anchor desmosomes to intermediate filaments, mainly desmin, thereby forming a threedimensional scaffolding that provides tissues with mechanical strength (Garrod et al., 2002; Green and Simpson, 2007). Although desmosomal proteins are widely expressed, mutations in specific components lead to myocardial dysfunction only, because some are specifically expressed in myocardial tissue. Some desmosomal proteins (e.g. desmoplakin and plakoglobin) also participate in desmosomes of other tissues. This is exemplified by the fact that mutations in these components, in addition to cardiomyopathy, lead to skin and hair abnormalities.

Mutations in genes encoding components of this complex might lead to:

- haploinsufficiency and thus insufficient incorporation of the protein;
- the absence of essential protein–protein interactions;
- the incorrect incorporation of mutant proteins in the desmosome (it will result in disturbed formation or reduced numbers of functional desmosomes).

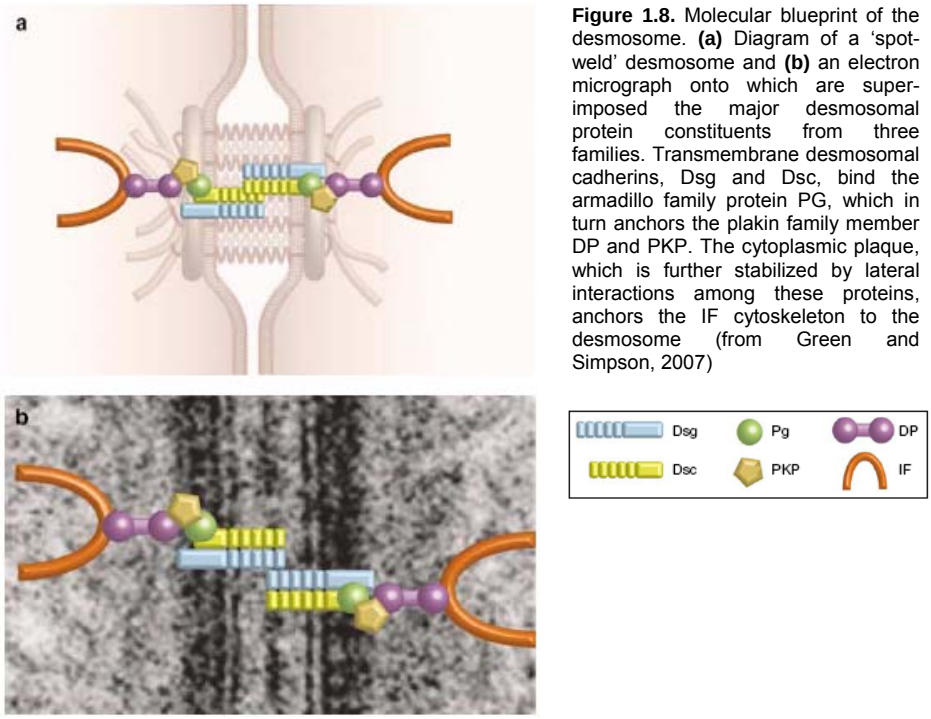

Figure 1.8. Molecular blueprint of the desmosome. **(a)** Diagram of a 'spot-weld' desmosome and **(b)** an electron micrograph onto which are super-imposed the major desmosomal protein constituents from three families. Transmembrane desmosomal cadherins, Dsg and Dsc, bind the armadillo family protein PG, which in turn anchors the plakin family member DP and PKP. The cytoplasmic plaque, which is further stabilized by lateral interactions among these proteins, anchors the IF cytoskeleton to the desmosome (from Green and Simpson, 2007)

This was exemplified by studies of Basso and colleagues, which showed decreased desmosome numbers, and increased desmosome lengths in myocardial tissue of mutation carriers (Basso et al., 2006) (Figure 1.9).

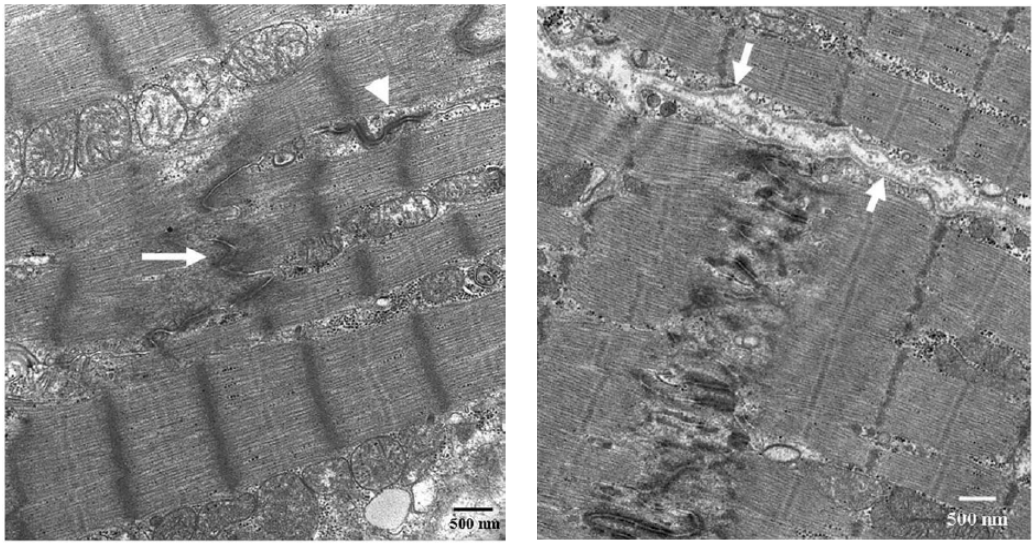

Figure 1.9. Panoramic view of cardiac myocyte intercalated discs. **(Left)** ARVC/D patient with desmoplakin gene splice site mutation. Note the abnormal position of long desmosomess (arrowhead) and the widened gap of fascia aherens (arrow). **(Right)** Control case. Regular membrane (arrows) and intercalated disc between adjacent myocytes. Original magnification: x15 000 (from Basso et al., 2006)

Mechanical stress might induce the disruption of these desmosomal structures, resulting in reduced mechanical contacts and the detachment of cardiomyocyte cells. Desmosome impairment is believed to predispose to tissue damage under conditions of mechanical stress, leading to the disruption and subsequent degeneration of cardiomyocytes and their replacement by (fibro)-fatty tissue (Kostetskii et al., 2005).

Moreover, the destabilization of cell adhesion complexes may perturb the kinetics of gap junction turnover, resulting in heterogeneous conduction, a potential contributor to arrhythmogenesis in ARVC/D (Kaplan et al., 2004; Kostetskii et al., 2005).

It has recently been discovered that desmosomes or desmosome components participate in intercellular signalling networks via the Wnt/β-catenin pathway (Getsios et al., 2004). Wnt signaling is involved in a variety of developmental processes, including cell proliferation and differentiation, and the development of tissues and organs. Several studies have implicated that desmosome dysfunction results in the delocalization and nuclear translocation of plakoglobin. As a result, competition between plakoglobin and β-catenin will lead to the inhibition of Wnt/b-catenin signaling, resulting in a shift from a myocyte fate towards an adipocyte fate of cells (Garcia-Gras et al., 2006).

In conclusion, together, these processes will lead to cardiomyocyte death, (fibro)-fatty replacement, slow conduction, and thus facilitates re-entrant ventricular arrhythmias.

1.12. Animal models

In recent years, animal models have been used to recapitulate human disease, including Cardiomyopathies (Dalloz et al., 2001). In some cases, transgenic animals have been developed while other models have been knock-out, knock-in, or over-expression models. Based on the finding of the desirable pathology, mechanism studies have been pursued. It is based on these models that the current data on mechanisms of disease rely. To date, animal models for RyR2, PKP2, JUP and DSP have been reported.

RYR2 MUTANT MURINE MODELS

Using homologous recombination in embryonic stem cells, a point mutation in exon 8 of the RyR2 gene, R176Q, was engineered in C57Black/6 (C57BL/6) mice using a knock-in strategy (Kannankeril et al, 2006). This mutation, which was previously shown to cosegregate with ARVC/D in humans, leading to the effort-induced polymorphic VT and mild ARVC/D histologically characteristic of the ARVC2 form of disease, demonstrated germline transmission in these mice and once grown were studied clinically and by use of pathologic analysis. Histologic analysis of hearts from mutant ($RyR2^{R176Q/+}$) and wild-type (WT) mice revealed no evidence of structural abnormalities or fibrofatty infiltration. This model was inconclusive regarding the phenotype but appeared more consistent with a CPVT phenotype than that of a classic form of ARVC/D.

PLAKOPHILIN-2 MUTANT MURINE MODELS

A null mutation of the plakophilin-2 (PKP2) gene was created by homologous recombination in embryonic stem cells whereby an early stop of PKP2 translation after exon 1 (43 amino acids) was engineered (Grossmann et al., 2004). Generation of homozygous mutants led to no live offspring, consistent with embryonic lethality. At E11.5, the number of viable embryos declined significantly. In addition, reduced trabeculations within the ventricles and atrial wall thinning was observed. Confocal microscopy demonstrated lack of the normal co-localization of desmoplakin to the junctions and intercalated disks, instead being dispersed over the cytoplasm, mostly distant from the intercalated disks. In addition electron microscopy confirmed abnormalities of cytoskeletal organization. In the latter case, intermediate filament arrays appearing as extensive swirls of disordered filaments around dense desmoplakin aggregates were seen. Hence, these findings were consistent with the concept that abnormalities of PKP2 lead to cardiac abnormalities with an unusual form of cardiomyopathy due to desmosomal destabilization. These findings are supportive of the human mutations in PKP2 that are believed to cause ARVC/D.

JUNCTIONAL PLAKOGLOBIN MUTANT MURINE MODELS

Using homologous recombination in which mutation in the junction between exons 3 and 4 of the plakoglobin gene was engineered in embryonic stem cells and injected into C57Black/6 (C57BL/6) mice, generated null JUP mice (Ruiz et al., 2006). Homozygous mutants ($JUP^{-/-}$) were found to be embryonic lethal between days 12-16 of embryogenesis (E12-E16) while heterozygous mutants ($JUP^{+/-}$) and WT animals were born with normal development.

Evaluation of homozygous embryos between days E10-E16 of gestation demonstrated reduced ventricular contraction in E11.5 embryos, consistent with systolic dysfunction; immunofluorescence microscopy showed the homozygous mutant animals lack desmosomes, which are replaced by extended adherens junctions that contain desmosomal proteins such as desmoplakin, but have impaired architectural stability and function. Interestingly, the skin of these animals was unaffected.

DESMOPLAKIN MUTANT MURINE MODELS

Using the Cre-LoxP system (Agah et al., 1997) a cardiac-restricted exon 2 deletion in DSP was created in mice (Garcia-Gras et al., 2006). Homozygous ($DP^{-/-}$) mutant mice had a high rate of embryonic lethality, consistent with data previously reported in germline DSP-null mice (Gallicano et al., 1998, 2001). These homozygous mutant mouse embryos exhibited growth arrest at embryonic stage E10-E12. Histopathologic evaluation revealed poorly formed hearts with no chamber specification and unorganized cardiac myocytes. Furthermore, an excess number of cells resembling adipocytes, dispersed between myocytes and localized to adjacent areas, were also detected. In comparison, cardiac phenotype was normal in $DP^{+/+}$ and $DP^{+/-}$ embryos, with and without transgene. $DP^{+/-}$ mice were born with normal development, but had age-dependent penetrance of heart involvement. Gross pathologic analysis of both $DP^{+/-}$ and

$DP^{-/-}$ animals demonstrated grossly enlarged cardiac chambers and increased heart weight. The gross anatomic findings were further supported by echocardiographic measurements which revealed thin ventricular walls, increased LV end-diastolic and end-systolic dimensions, and depressed systolic function with reduced ejection fraction. Histologic examination revealed poorly organized myocytes with large areas of patchy fibrosis; in the $DP^{-/-}$ animals, fibrosis was seen in up to 30-40% of the myocardium.

In addition to these pathologic abnormalities, the authors showed that JUP, a member of the armadillo repeat protein family that plays a role in regulation of gene expression, interacts and competes with β-catenin, the effector of the canonical Wnt signalling (Klymkowsky et al., 1999) having a negative effect on this pathway. They were able to show that plakoglobin was translocated to the nucleus in cardiac-restricted DP-deficient mice and that expression levels of gene targets of the canonical Wnt/β-catenin pathway were reduced.

Another animal model of mutant desmoplakin was recently described (Yang et al., 2006). This model, a transgenic mouse with cardiac-restricted overexpression of a C-terminal DSP mutant (R2834H), demonstrated histological evidence of increased cardiomyocyte apoptosis, cardiac fibrosis and lipid accumulation. Echocardiography and cardiac magnetic resonance imaging revealed ventricular enlargement and cardiac dysfunction of both ventricles, which was confirmed on necropsy. The mutant mice also displayed interruption of the DSP-desmin interaction at intercalated disks and marked ultrastructural abnormalities of the intercalated disks. The intercalated disks were irregularly shaped with markedly widened gaps between adjacent anchoring sarcomeres, affecting both the adherens junctions and desmosomes.

This animal models support the notion that ARVC/D is a disease of the desmosome (Vatta et al., 2007). Future animal models will continue to focus on desmosomal and other adherens junction proteins and other genes responsible for this disorder is likely to be identified. The next series of important steps in better understanding this paradigm disorder include defining the mechanisms responsible for the fatty infiltrative process, the mechanisms responsible for the disruption of the junctions and intercalated disks, and the mechanisms responsible for the development of arrhythmia (Nerbonne, 2004; MacRae et al., 2006).

2. AIM OF THE STUDY

Arrhythmogenic right ventricular cardiomyopathy is a clinically and genetically heterogeneous disease, inherited as autosomal trait; it significantly increases the risk of sudden death, in particular in teenagers and in young adults. Sudden death may occur as first presenting symptom of the disease; therefore, early diagnosis and/or early detection of susceptible genotypes by DNA testing is particularly relevant to prevent juvenile sudden deaths.

Identification of genes involved in this disease is a way to develop novel diagnostic tools for early identification of carriers of pathogenic mutations causing ARVC/D.

The present thesis aims to provide an estimate of relative prevalence of mutations among ARVC/D genes encoding desmosomal proteins (PKP2, DSP, DSG2, and DSC2) in a large cohort of unrelated consecutive index cases and available family members. Clinical correlations in a large series of ARVC/D patients carrying mutations in different ARVC/D genes will be performed, in order to possibly differentiate clinical phenotypes.

Moreover, candidate genes, such as DES and PKP4 will be screened for mutations to investigate their involvement in ARVC/D pathogenesis. Discovering additional disease-genes should enable mutation identification in a growing number of ARVC/D index cases.

The identification of the primary genetic causes of ARVC/D opens the possibility to generate animal models where the events underlying the pathophysiology of this disease can be studied in detail. Gene targeting, has been choice as strategy to generate the first knock−in mouse carrying a targeted mutation in *Dsg2* gene as animal model for ARVC/D.

Understanding the true mechanistic basis of ARVC/D could enable both diagnosis and development of targeted therapies for those patients who have already developed this life−threatening disease.

3. MATERIALS and METHODS

3.1. CLINICAL EVALUATION

One hundred-ten unrelated index cases of Italian descent were clinically evaluated in the University of Padua Medical School – Azienda Ospedaliera. Informed consent was obtained from all individuals. Clinical evaluation consisted of a detailed personal/family history, physical examination, 12-lead ECG, 2-dimensional echocardiogram, signal-averaged ECG (SAECG), and stress test ECG (Nava et al, 2000). Invasive studies including angiography and right ventricular endomyocardial biopsy were performed in selected cases when deemed necessary for the diagnosis. Clinical diagnosis of ARVC/D was made on the basis of the established European Society of Cardiology/International Society and Federation of Cardiology Task Force major and minor criteria (McKenna et al, 1994).

3.1.1. Statistical analysis

All continuous variables were expressed as the mean value ± SD. An unpaired Student t-test was employed for comparison of normally distributed data. A Chi-square test was used to compare non-continuous variables expressed as proportions.

Event-free survival rates were estimated by the Kaplan-Meier method, and comparison were performed using the log-rank test. The p-values are two-sided and considered significant when <0.05. Calculations were performed with SPSS 10 software (SPSS inc, Chicago, Illinois).

3.2. GENETIC STUDY PROTOCOLS

3.2.1. Mutation screening

DNA for genetic analysis was isolated from peripheral blood samples according to the salting-out procedure. PKP2, DSP, DSG2 and DSC2 genes was screened for mutations in all 110 study subjects; DES and PKP4 ARVC/D candidates genes was screened for mutations in 80 subjects. The screening, performed by denaturing high-performance liquid chromatography (DHPLC) and direct sequencing, included all coding sequences and also 50 to 150bp of flanking intronic sequences. Polymerase chain reaction (PCR) primers were designed by PRIMER3 software. Some exons were split into different and overlapping fragments (for amplicons size, primers sequences, amplification and analysis conditions see Appendix, Tables 7.1 to 7.6).

A control group of 200 healthy and unrelated subjects (400 alleles) from the Italian population was used to exclude (through DHPLC analysis, or cleavage by restriction enzymes, or ARMS test) that detected mutations could be common DNA polymorphisms. All the controls were matched to the probands by ancestry.

Mutation screening was performed in all available family members of index cases in which a ARVC/D mutation was detected.

For analysis of the splice site mutations, mRNA was isolated from whole blood of the patient, the corresponding cDNA was obtained from a reverse transcriptase (RT)–PCR reaction with the use of 1μg total RNA. The nested PCR products were size separated by agarose gel electrophoresis, gel isolated, and directly sequenced or subcloned.
All considered cDNA and translation sequences for human ARVC/D genes and human candidate ARVC/D genes are available in NCBI website; the ID numbers are reported below (Table 3.1).

Table 3.1. ID numbers of considered cDNA and translation sequences for human ARVC/D genes and candidate ARVC/D genes.

Human gene	*cDNA sequence ID*	*translation sequence ID*
PKP2	NM_001005242	NP_001005242
DSP	NM_004415	NP_004406
DSG2	BC099657	NP_001934
DSC2	NM_004949	NP_004940
DES	NM_001927	NP_001918
PKP4	NM_003628	NP_003619.2

3.2.2. Salting-out DNA extraction

This is a modification of a salting-out procedure (as described by Miller et al, 1988), evaluated at the Human Genetic Laboratory, University of Padua, Italy. In the following protocol genomic DNA was extracted from peripheral blood leucocytes using 5mL of whole blood obtained from ARVC/D probands and available family members under informed consent.

MATERIALS:

- N-N solution (NaCl 0.9%; Nonidet 0.1%)
- TEN buffer (Tris-HCL 10mM; EDTA 2mM, pH 8.0; NaCl 400mM)
- 20% SDS solution
- Saturated NaCl solution
- Chloroform
- Isopropanol
- 70% ethanol
- TE buffer (10mM Tris-HCl; 1mM EDTA; pH 8.0)
- Vacuette EDTA K3 tube (evacuated blood collection system, Greiner bio-one)
- 15mL tubes
- 50mL tubes
- Sterile Pasteur pipettes
- Centrifuge
- Vortex mixer
- Oven

PROCEDURE:

Collect whole blood in disodium-EDTA containers and store at -20ºC. To facilitate haemolysis of Red Blood Cells it is recommended to store a fresh sample for a few hours in a freezer as freezing destroys red cells.

After thawing, transfer 5mL of whole blood to a sterile conical centrifuge tube (50mL volume) to which 40mL of N-N solution must be added.

Leave the solution for 10 minutes at room temperature with occasional mixing by inversion followed by centrifugation for 30 minutes at 3000xg at 4°C.

After centrifugation discard the supernatant. Wash the pellet another time by adding 30mL of N-N solution, then repeat previous step (it is important to breakdown the pellet and rinse it well in N-N solution in order to clean the white blood cells).

Remove red supernatant by aspiration and add 4mL TEN buffer.

Vortex well to break up pellet, add 300µL of 20% SDS and incubate tubes for 3 hours at 80°C under vigorous mixing.

After the incubation, add 1mL of saturated NaCl solution to the samples.

The tubes are mixed vigorously (on a vortex), then centrifuge the emulsion for 10 minutes at 3000xg at room temperature.

Transfer the upper aqueous phase (containing the DNA) into a clean and sterile conical centrifuge tube (15mL volume), and add an equal volume of chloroform.

Invert and swirl to mix and centrifuge for 10 minutes at 3000xg at room temperature.

Transfer the upper aqueous phase into a clean and sterile conical centrifuge tube (15mL volume), and add an equal volume of isopropanol.

DNA is precipitated by gentle swirling of the tube and is observed visually as a white thread like strand.

Centrifuge for 15 minutes at 4000 rpm at room temperature.

Discard the supernatant and add 1-2mL of 70% ethanol and centrifuge for 10 minutes at 3000xg at room temperature.

After centrifugation discard the supernatant and repeat the previous step.

After discarding the supernatant the pellet is dried, from excess ethanol, by leaving the tubes open and inverted at room temperature for one hour.

Resuspend the DNA pellet in 300-500µL TE buffer.

Check DNA concentration on spectrophotometer and quality on gel.

3.2.3. DNA quantification

Two methods were used to measure the amount of DNA in a preparation. If the amount of nucleic acid is more than 250ng/mL, spectrophotometric measurement of the ultraviolet irradiation absorbed by the bases is simple and accurate. If the amount of nucleic acid is very low or if the sample contains significant quantities of impurities (such as proteins, phenol, or other nucleic acids), the concentration of DNA can be estimated from the intensity of fluorescence emitted by ethidium bromide onto an agarose gel.

a. Spectrophotometric quantification of DNA:

MATERIALS:

- DNA samples
- spectrophotometer cuvette
- Spectrophotometer (GeneQuant pro RNA/DNA Calculator, GE Healthcare)

PROCEDURE:

For quantifying DNA, readings should be taken at wavelengths of 260nm and 280nm.

The reading at 260nm allows calculation of the concentration of nucleic acid in the sample.

1 OD at 260nm for double-stranded DNA = 50ng/μL

1 OD at 260nm for single-stranded DNA = 40ng/μL

The reading at 280nm gives the amount of proteins in the sample.

The ratio OD_{260}/OD_{280} provides an estimate of the purity of the sample. Pure preparations of DNA have ratio values of 1.8 and 2.0. A ratio less than 1.8 indicates that there may be proteins and/or other ultraviolet (UV) absorbers in the sample, in which case it is advisable to re-precipitate the DNA. A ratio higher than 2.0 indicates the samples may be contaminated with chloroform or phenol and should be re-precipitated with ethanol.

10μL of each sample obtained with salting out DNA extraction were diluted in 490μL of water (dilution factor = 50). Whole 500μL were put in spectrophotometer cuvette.

The DNA concentration was calculated as follow:

DNA concentration (ng/μL) = OD_{260} x 50ng/μL x dilution factor / 1000

b. Ethidium Bromide fluorescent quantification of DNA:

The simplest way to check for the presence of DNA fragments is to load a sample (i.e., PCR products) onto an agarose gel which contains ethidium bromide (Sharp et al., 1973). Because the amount of fluorescence is proportional to the total mass of DNA, the quantity of DNA is estimated by comparing the fluorescent yield of the sample with that of a series of appropriate standards. As little as 1-5ng of DNA can be detected by this method.

Using gels of different concentrations it is possible to resolve a wide size range of DNA molecules (i.e., 0.9% w/v agarose gel separates efficient linear DNA molecules of 0.5-7kb, 2.0% w/v agarose gel separates efficient linear DNA molecules of 0.1-2 kb).

MATERIALS:

- DNA samples
- Agarose electrophoresis grade (Invitrogen)
- TAE running buffer (0.04M Tris-acetate; 0.001M EDTA)
- Ethidium bromide solution (10mg/mL, Invitrogen)
- Orange G gel-loading 5X buffer (10mM EDTA; 30% glycerol; 0.25% orange G)

- DNA molecular-weight marker (100bp DNA Ladder, Invitrogen)
- Microwave oven
- Electrophoresis tank and power supply
- UV light transilluminator

PROCEDURE:

Melt the agarose with TAE buffer and heat the mixture to boiling using the microwave oven.

Allow the agarose to cool for 3-5 minutes at room temperature before adding the ethidium bromide solution (1mg/mL concentration, 1µL per 100mL of TAE used).

Pour the agarose solution into the casting tray, add the comb, and leave the gel to cool and solidify.

While the gel is cooling, prepare 3µL of each DNA samples by adding 3µL of orange G gel-loading buffer (tracking dye that increase the density of the sample, so it falls into the well of the gel and provides a visible marker to monitor the loading process).

Transfer the gel completely set in the electrophoresis tank, in the presence of the TAE buffer, and carefully remove the comb.

Carefully pipette each prepared sample into a well in the gel. Load one well with the DNA ladder.

Close the lid of the gel tank and connect the electrical leads so that the DNA will migrate toward the anode. Apply a voltage of 1-5V/cm.

Run the gel until the tracking dye is approximately 3/4 the way across the gel.

Place the gel on the transilluminator, examine the gel by UV light (250-320nm), and photograph the gel.

By comparing product bands with bands from the known molecular-weight markers, any product fragment can be detected and quantified.

3.2.4. DNA amplification by PCR

PCR is designed to permit selective amplification of a specific target DNA sequence(s), lies between two regions of known sequence, within a heterogeneous collection of DNA sequences. Two oligonucleotides are used as primers for a series of synthetic reactions that are catalysed by a DNA polymerase. PCR consists of a series of cycles of three successive reactions:

- *denaturation*, typically set to be at about 93-95°C for human genomic DNA;
- *primer annealing* at temperatures usually from about 50°C to 70°C depending on the melting temperature (T_m) of the expected duplex (the reannealing temperature is typically set to be about 5°C below the calculated melting temperature);
- *DNA synthesis*, typically at about 70-75°C. The DNA polymerase used is heat-stable (it needs to elongate efficiently at 70–75°C and should not be adversely affected by the denaturation steps). In the presence of a suitably heat-stable DNA polymerase and DNA precursors (the four deoxynucleoside triphosphates, dATP, dCTP, dGTP and dTTP), the primers initiate the

synthesis of new DNA strands which are complementary to the individual DNA strands of the target DNA segment.

The orientation of the primers is deliberately chosen so that the direction of new strand synthesis occurring from one primer is towards the other primer binding site. As a result, the newly synthesized strands can in turn serve as templates for new DNA synthesis, causing a *chain reaction* with an exponential increase in product (Figure 3.1).

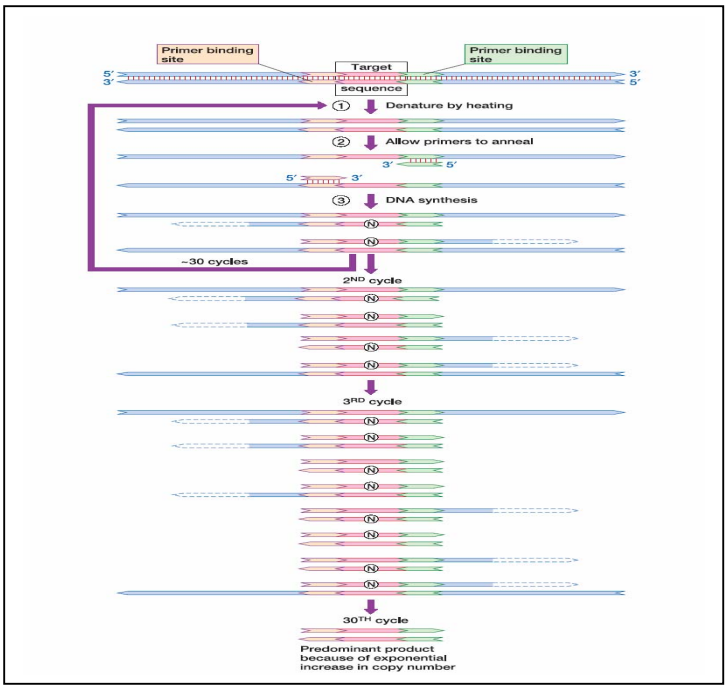

Figure 3.1. Exponential amplification in PCR. PCR is an in vitro method for amplifying DNA sequences using defined oligonucleotide primers. It consists of cycles of denaturation, annealing of primers and then DNA synthesis in which the primers are incorporated into the newly synthesized DNA strands. After 30 cycles or so there is a massive increase (amplification) of this type of product (from Strachan, 2003).

DNA fragments to be analyzed for the presence of mutations are PCR amplicons of ARVC/D genes or candidate ARVC/D genes; nucleotide sequence of these genes is available in NCBI website. Primers flanking the target regions for mutation detection were designed by design software package (http://www.genome.wi.mit.edu/cgi-bin/primer/primer3.cgi).

a. Standard PCR

Each fragment was amplified from patient genomic DNA (for amplicons size, primers sequences and amplification conditions see Appendix, Tables 7.1 to 7.6).

MATERIALS:

- DNA template
- Primers (10pmol/μL, Sigma Genosys or MWG)
- Deoxinucleotide triphosphate (dNTPs 1mM, Invitrogen)
- DNA Taq Gold polymerase (5U/μL, Applied Biosystems)
- 10X PCR Buffer II (Applied Biosystems)
- $MgCl_2$ solution (25mM, Applied Biosystems)

- MilliQ water
- sterile micro centrifuge tubes
- Thermal cycler (MJ Research)

PROCEDURE:

Place approximately 50ng of DNA solution in a sterile micro centrifuge tube.

Carry out the PCR in a 25μL volume containing 400nM of each primer, 100μM deoxinucleotide triphosphate, 1X PCR Buffer II, 1.5mM $MgCl_2$ and 0.8U of DNA Taq polymerase.

After activation of the enzyme (95°C for 12 minutes), repeat cycling conditions (denaturation at 95°C for 30 sec, annealing at the working temperature for 30 sec, extension at 72°C for 45 sec) 35 times in a termal cycler.

The presence of the PCR product can be checked loading the sample onto an agarose gel.

b. GC-RICH PCR

The sequences of primers flanking exon 1 of PKP2 gene were kindly provided by Syrris P. The amplicon nucleotide sequence showed high GC content, thus the amplification was performed by using the GC-RICH PCR System (Roche diagnostic GmbH).

MATERIALS:

- DNA template
- Primers (10pmol/μL, Sigma Genosys or MWG)
- Deoxinucleotide triphosphate (dNTPs 1mM, Invitrogen)
- GC-RICH PCR System (Roche diagnostic GmbH):
  GC-RICH Enzyme (2U/μL)
  GC-RICH 5X Reaction Buffer
  GC-RICH Resolution Solution (5M)
  $MgCl_2$ solution (25mM)
  PCR grade water
- sterile micro centrifuge tubes
- Thermal cycler (MJ Research)

PROCEDURE:

Place approximately 50ng of DNA solution in a sterile micro centrifuge tube.

Store the reagents on ice.

Prepare the “Master Mix 1” mixing 400nM of each primer, 100μM deoxinucleotide triphosphate, 1.5mM $MgCl_2$, 1M Resolution Solution and water to give a final volume of 9μL.

Prepare the “Master Mix 2” mixing 1X Reaction Buffer and 0.5U of GC-RICH Enzyme in a final volume of 2.5μL.

Combine 9μL of “Master Mix 1” and 2.5μL of “Master Mix 2” in the sterile micro centrifuge tube containing the DNA and gently vortex the misture.

Start thermal cycling immediately. After activation of the enzyme (95°C for 3 minutes), repeat cycling conditions (denaturation at 95°C for 30 sec, annealing at 60°C for 30 sec, extension at 72°C for 45 sec) 35 times.
The presence of the PCR product can be checked loading the sample onto an agarose gel.

c. TD-PCR

A frequently encountered problem in PCR amplification of target gene sequence, is the appearance of spurious smaller bands in the product spectrum. This is usually interpreted to be due to mispriming by one or both of the oligonucleotide amplimers internal or external to the target template. A way of increasing the specificity of a PCR reaction is to perform a touch-down (TD) PCR. The thermal cycler is programmed to perform runs in which the annealing temperature is lowered incrementally during the PCR cycling from an initial value above the expected T_m to a value below the T_m. By keeping the stringency of hybridization initially very high, the formation of spurious products is discouraged, allowing the expected sequence to predominate (Don et al., 1991).

d. Allele-specific PCR

Allele-specific PCR, or ARMS (amplification refractory mutation system) method, was performed to permit distinct amplification of alleles that differ at just a single nucleotide, based on the crucial dependence of correct base pairing at the extreme 3' end of bound primers. Primers were designed with their 3' end nucleotides designed to base-pair with the variable nucleotide which distinguishes the two alleles, and with the remaining primer sequence designed to be complementary to the sequence immediately adjacent to the variable nucleotide. Under suitable experimental conditions amplification will not take place where the 3' end nucleotide is not perfectly base-paired thereby distinguishing the two alleles.
ARMS test was used to screen the control population for the presence of two variations in DES gene, in order to exclude that they could be common DNA polymorphisms. Sequence of primers, size of amplicons and amplification annealing temperatures, are reported in Table 3.2.

Table 3.2. Sequence of primers, size of amplicons and amplification annealing temperatures used in ARMS test.

Gene	Nucleotidic variation	Size (bp)	Forward 5'-3'	Reverse 5'-3'	PCR T_{ann} °C
DES	721A>G	463	des-3asoAF aggagatcgcgttccttaaga des-3asoGF aggagatcgcgttccttaagg	des-3asoR gatgagcaagggagcatgaa	65
DES	736-11A>G	261	des-4asoAF gggactgaagcccagtca des-4asoGF gggactgaagcccagtcg	des-4asoR taccacaggcagcacatcc	65

3.2.5. DNA cleavage by restriction enzymes

Restriction enzymes bind specifically to and cleave double-stranded DNA at specific sites within or adjacent to a particular sequence known as the recognition sequence. The vast majority of

type II restriction enzymes recognizes short sequences that display twofold symmetry (palindromes); few enzymes, however, recognize longer sequences or degenerated sequences. Some enzymes cleave both strands exactly, generating DNA fragments that carry blunt ends; others cleave each strand at similar locations on opposite sides, creating DNA fragments that carry protruding single-stranded termini.

Many restriction enzymes have been use for digestions (e.g., in genomic control DNA, to verify SNPs that cause a loss or gain of a restriction site polymorphisms or RSPs, Figure 3.2), linearization of plasmid DNA and molecular cloning.

Each enzyme has specific requirement to achieve optimal activity. Ideal assay conditions favour the most activity and highest fidelity in a particular enzyme's function. Temperature, pH, enzyme cofactor(s), salt composition and ionic strength affect enzyme activity and stability.

Each time, optimal reaction conditions must be assessed. Usually, 1U of enzyme preparation is sufficient to digest 1μg of DNA in one hour. One unit is defined as the amount of enzyme required to completely digest 1μg of lambda DNA in one hour at 37°C in 50μL assay buffer containing Acetylated BSA added to a final concentration of 0.1mg/mL.

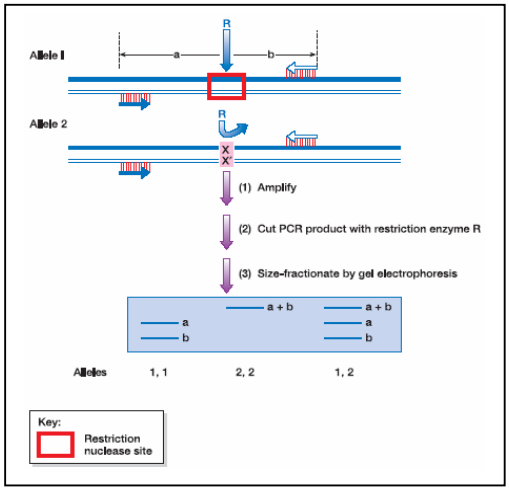

Figure 3.2. Typing of restriction site polymorphisms. Alleles 1 and 2 are distinguished by a polymorphism which alters the nucleotide sequence of a specific restriction site for restriction nuclease (R). Allele 1 possesses the site, but allele 2 has an altered nucleotide(s) X, X' and so lacks it. PCR primers, designed from sequences flanking the restriction site, produce a short fragment. Digestion of the PCR product with enzyme R and size-fractionation can result in simple typing for the two alleles (from Strachan, 2003).

MATERIALS:

- DNA sample
- Restriction enzyme (10 or 12U/μL, Promega or New England BioLabs)
- Appropriate 10X digestion buffer (Promega or New England BioLabs)
- 37-50°C heating block

PROCEDURE:

Place the DNA solution in a sterile micro centrifuge tube and mix with sufficient water to give a final volume of 20-100μL, based upon DNA concentration.

Add the appropriate volume of the 10X digestion buffer.

Add the restriction enzyme (generally 2U of enzyme were used to digest each μg of DNA), and mix by tapping the tube.

Incubate the mixture at the appropriate temperature (37°C or 50°C, specific for each enzyme) for the required period of time (around 1-2 hours).

The DNA digestion can be directly analyzed on an agarose gel.

3.2.6. Mutation screening by DHPLC

Denaturing high performance/pressure liquid chromatography (DHPLC) is a high-capacity technique that exploits the differential melting properties of homoduplex and eteroduplex DNA fragments, in order to detect mutations. It is an ion-pair reversed-phase chromatography. The cartridge contains a nonporous alkylated polystyrene-divinylbenzene separation matrix. DNA sample, injected onto a chromatography column, binds to the column hydrophobic matrix via interactions mediated by triethylammonium acetate (TEAA); acetonytrile disrupts this interaction and causes DNA elution out of the column. Elution of the sample appears as a peak of absorbance at 260nm versus time.

At a non-denaturing temperature, the concentration of acetonytrile required to remove any given fragment depends on the size and sequence. Therefore, any DNA fragment elutes at a characteristic point in a linear gradient of acetonytrile, which corresponds to a characteristic retention time on a plot of absorbance versus time. When the temperature of the column is increased, elution takes place at progressively lower acetonytrile concentrations as the DNA fragment starts to denaturate.

Heteroduplex (mismatched) DNA fragment has different melting characteristics to homoduplex, and under condition of partial denaturation (at high temperatures, opportunely chosen in the range of 50–70°C, depending on the GC-content of the DNA under investigation) have a reduced retention on the chromatographic separation matrix. As a consequence, one or more additional peaks appear in the chromatogram, with different mutations yielding, in most but not all instances, distinctively different peak profiles. Typically, a single peak from a wild type sample changes to multiple peaks from sample which contain sequence variations(Figure 3.3).

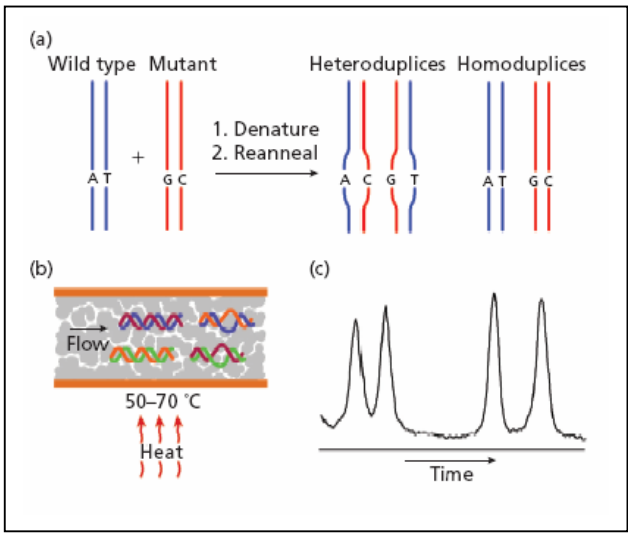

Figure 3.3. Principle of DHPLC. (a) Prior to chromatography, a DNA fragment is amplified by means of PCR from at least two chromosomes. In the presence of a mutation in one of the chromosomes, two original homoduplex and two different heteroduplex species are formed after denaturation. (b) A column temperature typically in the range of 50–70°C is maintained to induce partial denaturation. The thermally less stable heteroduplex denature more extensively and, consequently, are retained shorter on the stationary phase. (c) Example of chromatographic separation of the homoduplex and heteroduplex (adapted from Premstaller and Oefner P, 2000).

Several studies have estimated dHPLC to be a highly sensitive and specific technique. While it is clear that analysis at multiple temperature can increase the detection rate (Jones et al., 1999; Arnold et al., 1999; Ellis et al., 2000; Bagattin et al., 2004), there are still mutations which remain undetected after analysis at all temperatures. The true sensitivity of DHPLC must therefore be under 100%.

a. Sample preparation for dHPLC (quality and quantity)

Samples suitable for mutation detection by dHPLC are PCR products in the range 100-700 base pairs (Xiao and Oefner, 2001). Fragments larger than 700 base pairs can be run but the sensitivity may be reduced. Fragments of less than 100-200 base pairs do not give satisfactory results, as the fragment melt over at a too narrow temperature range. Poor quality PCR products will produce poor quality results. PCR products do not require purification, un-incorporated nucleotides and primers will elute significantly ahead of the sample peak. Primer-dimers, smears and contaminating products of a similar size to the sample could interfere with analysis. These contaminants should be eliminated by optimization of the PCR. The PCR product should be sufficiently concentrated (at least 20ng/μL). Usually 3-10μL (approximately 50-200ng) of sample would be injected onto the column.

b. Identification of mutations

Mutations are only detected in the form of heteroduplex, and are easily formed by heating the sample, in the presence of a wild type DNA spike if necessary, to 95°C for 5 minutes, followed by slow cooling to room temperature.

Heteroduplex have different retention properties on the column to homoduplex. The presence of heteroduplex, and hence of a mutation in the sample, is detected as a change in the number of peaks. Depending on several factors, including, among others, size of the fragments, influence of nearest neighbour on the stability of both matched and mismatched base pairs, and column temperature, either all four species (two homoduplex and two heteroduplex) may be resolved completely or only in part. The wild type peak pattern is changed to a two, three or four peak pattern. Two peak pattern account for the majority of mutations.

In principle, homozygous mutations can be detected on the basis of a shift in retention time of more than 0.1 minutes (Gross et al., 1999). In practice, this is not reliable as the retention time shifts are often within the range of normal variation (Ellis et al., 2000). To detect homozygous mutations, heteroduplex must be generated by mixing equal quantities of mutant and wild type samples.

Sample showing a change in dHPLC pattern is identified as containing potential mutations and re-amplified for direct sequencing.

MATERIALS:

- PCR products
- Thermal cycler (MJ Research)
- Wave DNA Fragment Analysis System 35000HT equipped with DNASep Cartridge (Transgenomic)
- Wave Navigator™ software (Transgenomic)
- Dual buffer system (Transgenomic):
  Buffer A (0.1M TEAA; pH 7.0)
  Buffer B (0.1M TEAA; pH 7.0; 25% ACN)

PROCEDURE:

Amplify DNA fragments from patient genomic DNA and verify quality and quantity on agarose gel using ethidium bromide and UV light.

Denature PCR fragments for 5 minutes at 95°C and then leave to reanneal slowly for 30 minutes at room temperature to promote possible formation of heteroduplex.

Inject each DNA sample onto the chromatography column of the Wave DNA Fragment Analysis System. Eluent conditions are sequence dependent and are predicted by Wave Navigator™ software, which use a modified Fixman-Freire algorithm (Fixman and Freire , 1977). Eluent flow rates for all analyses were 0.9mL/min in the Standard Analysis Mode or 1.5mL/min in the Rapid Analysis Mode.

Mutation detection under partially denaturing conditions is automatically performed at column temperature(s) specific for each fragment (the analyzing temperatures are chosen based on the software predicted temperatures). Whenever fragments showed distinct melting domains, additional analyzing temperatures are performed.

For amplicons size and analysis conditions see Appendix.

Chromatograms are recorded at a wavelength of 260nm. Sample showing a change in DHPLC pattern are identified as containing potential mutations and re-amplified for direct sequencing.

3.2.7. Automated DNA sequencing

PCR products showing aberrant patterns by DHPLC were reamplified and sequenced. Same amplicons were amplified and sequenced directly.

Automated DNA sequencing uses fluorescence labelling: the DNA is labelled by incorporating a specific primer and dNTPs carrying four different fluorophores. The sequencing primer binds specifically to a region 3' of the desired DNA sequence and primes synthesis of a complementary DNA strand in the 5'-3' direction. Four parallel base-specific reactions are automatically carried out, each with all four dNTPs and with one ddNTP. Dideoxy DNA sequencing relies on random incorporation of base-specific chain terminators during in vitro DNA synthesis. During electrophoresis a monitor detects and records the fluorescence signal of the incorporated ddNTPs in order of appearance and the correct sequence data are provided.

MATERIALS:

- PCR products
- Thermal cycler (MJ Research)
- PCR Product Pre-sequencing kit (USB, Amersham Pharmacia Biotech):
  Shrimp Alkaline Phosphatase, SAP (2U/μL)
  Exonuclease I, ExoI (10U/μL)
- Automated ABI Prism 3730XL DNA Sequencer (Applied Biosystems)
- CHROMAS software (release 1.5; Technelysium Pty Ltd)
- DNASTAR Lasergene software

PROCEDURE:

Purify PCR amplicons whit the PCR Product Pre-sequencing kit: the two hydrolytic enzymes used in this kit, SAP and ExoI, effectively remove unincorporated dNTPs and excess primers present in the final PCR product reaction mixture. Add 0.5μL of each enzyme to 5μL of the PCR product mixture, incubate at 37°C for 15 minutes, and then inactivate at 80°C for other 15 minutes. The result is a cleaner PCR product, ready to be sequenced with standard sequencing reagents.

The sequencing reaction needs 3ng of DNA every 100 base pairs of length of the fragment and 10pmol of primer.

DNA sequencing is carried out from the BMR-Genomics (Padua, Italy) through the automated sequencer.

Use the appropriate software to edit, assemble, and translate sequences. Amplicons showing putative mutations were resequenced, with the product of an independent PCR reaction used as template.

3.2.8. RNA isolation

For analysis of splice site mutations, RNA of patients and healthy donors was isolated from lymphocytes using the PAXgene™ Blood RNA Kit (Qiagen). The kit allows the isolation of total RNA from 2.5mL human whole blood collected in the PAXgene Blood RNA tube (Qiagen).

Typical yields of RNA isolated are between 4 to 20μg. However, the yield is highly donor-dependent, and in some cases higher or lower yields may be achieved.

MATERIALS:

- 2.5mL human whole blood
- PAXgene™ Blood RNA tube (Qiagen)
- PAXgene™ Blood RNA Kit (Qiagen):
  Buffer BR1 (Resuspension Buffer)
  Buffer BR2 (Binding Buffer)
  Buffer BR3 (Wash Buffer)

Buffer BR4 (Wash Buffer)
Buffer BR5 (Elution Buffer)
RNase-free water
Proteinase K
PAXgene Blood RNA Spin Columns
2mL Processing tubes
Secondary Hemogard closures
1.5mL Elution tubes

- 100% ethanol
- Centrifuge
- 55-65°C shaker-incubator or heating block
- Vortex mixer
- Microcentrifuge

PROCEDURE:

Before starting the RNA purification procedure, ensure that the tube has been incubated at room temperature (18-22°C) for at least two hours in order to ensure complete cell lysis.

Centrifuge the PAXgene Blood RNA Tube for 10 minutes at 3000-5000xg .

Remove the supernatant by decanting or pipetting.

Add 5mL Rnase-free water to the pellet, and close the tube using a fresh secondary Hemogard closure.

Thoroughly resuspend the pellet by vortexing, and centrifuge for 10 minutes at 3000-5000xg.

Remove and discard the entire supernatant.

Resuspend the pellet in 360µL Buffer BR1 by vortexing; transfer the sample into a 2mL microcentrifuge tube.

Add 300µL Buffer BR2 and 40µL Proteinase K. Mix by vortexing, and incubate for 10 minutes at 55°C using a shaker-incubator (at 1400rpm), or heating block.

Centrifuge for 3 minutes at maximum speed in a microcentrifuge; transfer the supernatant to a fresh 2mL microcentrifuge tube.

Add 350µL 100% ethanol. Mix by vortexing, and centrifuge briefly (1-2 seconds at 1000xg) to remove drops from the inside of the tube lid.

Apply 700µL sample to the PAXgene column sitting in a 2mL processing tube, and centrifuge for 2 minutes at 8000xg. Place the PAXgene column in a new 2mL processing tube, and discard the old processing tube containing flow-through.

Apply the remaining sample to the PAXgene column, and centrifuge for 2 minutes at 8000xg. Place the PAXgene column in a new 2mL processing tube, and discard the old tube.

Add 700µL Buffer BR3 to the PAXgene column, and centrifuge for 2 minutes at 8000xg. Place the PAXgene column in a new 2mL processing tube, and discard the old tube.

Add 500µL Buffer BR4 to the PAXgene column, and centrifuge for 2 minutes at 8000xg. Place the PAXgene spin column in a new 2mL processing tube, and discard the old tube.

Add another 500µL Buffer BR4 to the PAXgene column. Centrifuge for 3 minutes at maximum speed to dry the PAXgene column membrane, and discard the old tube.
To elute the RNA, transfer the PAXgene column to a 1.5mL elution tube, pipet 40µL Buffer BR5 directly on the PAXgene column membrane. Centrifuge for 2 minutes at 8000xg.
Repeat the elution step using another 40µL Buffer BR5.
Incubate the eluate for 5 minutes at 65°C in a heating block.
Following incubation, chill immediately on ice.

3.2.9. Spectrophotometric quantification of RNA

MATERIALS:

- RNA sample
- spectrophotometer cuvette
- Spectrophotometer (GeneQuant pro RNA/DNA Calculator, GE Healthcare)

PROCEDURE:
As for quantifying DNA, readings should be taken at wavelengths of 260nm and 280nm (for the procedure see Spectrophotometric quantification of DNA).
1 OD at 260nm for RNA = 33ng/µL
The RNA concentration was calculated as follow:
RNA concentration (ng/µL) = OD_{260} x 33ng/µL x dilution factor / 1000

3.2.10. RNA DNase treatment

To remove contaminating genomic DNA from RNA preparations, isolated RNA was treated with DNA*free*™ Kit (AMBION, Applied Biosystems), designed to digest trace to moderate amounts of DNA (up to 50µg DNA/mL RNA) from purified RNA to levels below the limit of detection by RT-PCR. DNase and divalent cations are then rapidly and easily removed.

MATERIALS:

- RNA preparation
- DNA*free*™ DNase Treatment and Removal Reagents (AMBION, Applied Biosystems):
  rDNase I (2U/µL)
  10X DNase I Buffer (100mM Tris-HCl, pH 7.5, 25mM $MgCl_2$, 5mM $CaCl_2$)
  DNase Inactivation Reagent
  Nuclease-free Water
- 0.5mL tubes
- 37°C heating block
- Microcentrifuge

PROCEDURE:

Transfer up to 10 μg of RNA preparation in a 0.5mL tube.

Add 5μL 10X DNase I Buffer and 1μL rDNase I to the RNA in a 50μL reaction volume, and mix gently.

Incubate at 37°C for 20–30 min.

Add resuspended DNase Inactivation Reagent (typically 0.1 volume) and mix well.

Incubate 2 minutes at room temperature, mixing occasionally.

Centrifuge at 10000xg for 1.5 minutes and transfer the supernatant containing the RNA into a fresh tube and keep at –20°C.

3.2.11. RT—PCR

Reverse transcription polymerase chain reaction (RT-PCR) is a technique for mRNA detection, quantification and amplification. The RNA strand (isolated from whole blood of patients) is first reverse transcribed into its complementary DNA (cDNA); then the resulting cDNA is amplified with specific primers by using simple or nested PCR.

In order to sequence the aberrant transcript of patient carrying the c.423-1G>A mutation in DSP gene, the following primers were used to amplify the fragment corresponding to exons 3-5 from cDNA (T_{ann} 62°C). Primer forward: 5'ATCAGAGAGATGCGGCAGAT3'; primer reverse: 5'GCTGTTAATGTGCTGCTCCA3'.

In order to investigate the effect of the intronic nucleotide change c.245+101A>G in PKP4 gene, amplification of the fragment corresponding to exons 3-6 was performed from patient cDNA by TD PCR (T_{ann} 75>65°C) using following primers. Primer forward: 5'ACCCGAGAACTGGAAGTGGA3'; primer reverse: 5'TGCTGCTGTCTGTTGTCTGC3'.

MATERIALS:

- Human RNA
- Random Primers (500ng/mL, Promega)
- Deoxinucleotide triphosphate (dNTPs 10mM, Invitrogen)
- ImProm-II 5X Reaction Buffer (Promega)
- $MgCl_2$ Solution (25mM, Promega)
- rRNAsin RNase Inhibitor (40U/μL, Promega)
- ImProm-II Reverse Transcriptase (Promega)
- Nuclease-free water
- Thermal cycler (MJ Research)

PROCEDURE:

Activate 1μg of mRNA from human RNA adding 1μg random primers in a 5μL volume, and incubating 5 minutes at 70°C and 5 minutes at 4°C.

Keep the sample on ice.

Reverse-transcribe the activated RNA in a final volume of 25µL using 10mmol dNTPs, 1X Buffer, 60mmol $MgCl_2$, 40U rRNAsin and 1µL Reverse Transcriptase.

Carry out the reverse-transcription steps (annealing at 25°C for 5 minutes, extension at 42°C for an hour, enzyme inactivation at 70°C for 15 minutes, and the stop of reaction at 4°C for 10 minutes) in a termal cycler.

The generated cDNA is used as a template for PCR (§ 3.2.4) or for nested PCR (1µL cDNA in a reaction volume of 25µL).

Check for the presence of PCR product onto an agarose gel.

3.2.12. Nested PCR

Nested polymerase chain reaction is a modification of PCR intended to increase the specificity of a PCR reaction reducing the contaminations in products due to the amplification of unexpected primer binding sites. The product of an initial amplification reaction is diluted and used as the starting DNA source for a second reaction in which a different set of primers is used, corresponding to sequences located close, but internal, to those used in the first reaction.

The nested PCR was performed from cDNA to investigate the effect of three splice site mutations detected in ARVC/D genes, and two exonic nucleotidic variations detected in PKP4 gene. Sequence of primers used in the first round PCR and in the nested PCR, size of amplicons and amplification annealing temperatures are reported in Table 3.3.

The nested PCR products were size separated by agarose gel electrophoresis, gel isolated, and directly sequenced or cloned into the pCR2.1 plasmid (Invitrogen).

Table 3.3. Nucleotidic variations investigated in four different genes by nested PCR. Sequence of primers used in the first round PCR and in the nested PCR, size of amplicons and amplification annealing temperatures are reported (* = amplification performed by TD PCR).

Gene and Nucleotidic variation	Amplicon	Size (bp)	Forward 5'-3'	Reverse 5'-3'	PCR T_{ann} °C
DSP c.542+5G>A	DSPex1-4	733	GGTAGCGAGCAGCGACCTC	CTCATCCACCCCAAACATTC	60
	DSPnested	267	GACCTGCGCTACGAGGTGA	CTGGGCAAAACACTCATCCA	62
DSG2 c.1881-2A>G	DSG2ex12-15	904	CAGTTTGTGAGTGTCTGCATGG	ACTGGGAAGCTACTGCCAGA	62
	DSG2nested	668	CACAGCATGACTCCTATGTGG	GCGGTCATCTAGCTCTCCTT	60
DSC2 c.631-10C>T	DSC2ex3-9	949	TTGTCCTCGGAGAAGAGAAGTTTT	TGCCATTTTCATTGCCCTTT	62
	DSC2nested	502	TGGGCTCCAATTCCTTGTTC	TCACGCCTGTAGTTGGATGC	65
PKP4 c.1437G>A	PKP4ex7-11	954	GGACCAACCCCTCAATACCA	GGCAGGTATCCCACCAACAT	62
	PKP4nested-a	389	CCAAACCATGGAACTGTGGA	AAGCACAGGTGCTGCAGGTA	68>58*
PKP4 c.2391G>T	PKP4ex11-16	834	GATGCAGAAGTAAGGGAGCTTGTTA	GTTGCGAACATCTAGTGCCATATTC	62
	PKP4nested-b	465	GGAAGAAGCTCGGAAGCAAA	TTCCAGTTGCCAGCAGAGAG	65

3.2.13. Purification of DNA fragments

The Wizard SV Gel and PCR Clean-Up System (Promega) was used to extract and purify DNA fragment (linear DNA and supercoiled plasmid DNA of 100bp to 10kb) from agarose gel, or to purify PCR product directly from a PCR amplification. This system is based on the ability of the

DNA to bind to silica membranes of the minicolumns in the presence of chaotropic salts. After electrophoresis to separate the DNA fragments, the band of interest was excised and dissolved in the presence of guanidine isothiocyanate (Membrane Binding solution). Alternatively, after amplification, an aliquot of PCR reaction was added to the Membrane Binding solution and directly purified. DNA was isolated using micro centrifugation to force the dissolved gel slice or PCR reaction through the membrane while simultaneously binding the DNA on the surface of the silica. After washing the isolated DNA fragment or PCR product, the DNA was eluted in water.

MATERIALS:

- DNA sample
- Agarose gel (only for gel purification)
- TAE running buffer (0.04M Tris-acetate; 0.001M EDTA) (only for gel purification)
- 50-65°C heating block (only for gel purification)
- Microcentrifuge
- Wizard® SV Gel and PCR Clean-Up System (Promega):
  - Membrane Binding Solution
  - Membrane Wash Solution
  - Nuclease-Free Water
  - Wizard® SV Mini columns
  - Collection Tubes (2mL volume)

PROCEDURE:

To purify DNA fragments from agarose gel:

Load and run the gel using established protocol. Visualize the DNA using UV lamp and excise the DNA fragment of interest in a minimal volume of agarose using a clean razor blade. Transfer the gel slice to a micro centrifuge tube and record the weight of the gel slice (the gel slice may be stored at 4°C or –20°C for one week in a tightly closed tube under nuclease-free conditions before purification). Add 10μL Membrane Binding Solution per 10mg of gel slice. Vortex and incubate at 50-65°C until gel slice is completely dissolved (DNA fragments that are larger than 5Kb should be mixed gently to prevent shearing). Proceed to “DNA purification by centrifugation”.

To purify PCR products from a PCR amplification:

Amplify target of choice using standard amplification conditions. Add an equal volume of Membrane Binding Solution to the PCR reaction. Proceed to “DNA purification by centrifugation”.

DNA purification by centrifugation:

Transfer the dissolved gel mixture or prepared PCR product to the SV Mini column placed in a Collection Tube and incubate for 1 minute at room temperature (the maximum binding capacity is approximately 40μg per column).

Centrifuge the SV Mini column assembly in a micro centrifuge at 16000xg for 1 minute. Discard flow through and reinsert Mini column into Collection Tube.

For gel or PCR volumes >700μL, continue to pass the sample through the column until all of the sample has been processed.

Wash the column by adding 700μL of Membrane Wash Solution (previously diluted with 95% ethanol).

Centrifuge at 16000xg for 1 minute. Discard flow through and reinsert Mini column into Collection Tube.

Repeat the wash with 500μL of Membrane Wash Solution and centrifuge at 14000rpm for 1 minute.

Empty the Collection Tube and re-centrifuge the column assembly for 5 minutes to allow evaporation of any residual ethanol.

Carefully transfer Mini column to a clean micro centrifuge tube.

Add 50μL of Nuclease-Free Water to the Mini column. Incubate at room temperature for 1 minute and centrifuge at 16000xg for 1 minute.

Discard Mini column and store the micro centrifuge tube containing the eluted DNA at 4°C or -20°C.

3.2.14. Fragment DNA Cloning

TOPO TA Cloning System (Invitrogen) is a efficient method for cloning PCR products into a plasmid vector (the vector should yield greater than 95% cloning efficiency).

Specific DNA segment isolated by amplification (with 3'A overhangs added by *Taq* DNA polymerase) is ligated into the pCR2.1-TOPO plasmid vector with Topoisomerase I (the vector - size 3890bp - has been engineered to be linearized with 3'T overhangs). The 3'A overhangs of the PCR product complement the 3'T overhangs of the vector and allow for ligation with the Topoisomerase I. The plasmid can then be transformed into competent bacterial cells.

Other useful features of the vector are: its ampicillin and kanamycin resistance that allows for selection of bacterial colonies that take up the vector plasmid during transformation; the lacZ gene in bacteria, that causes colonies to have a blue color, but if PCR DNA is inserted in the vector it will insert in the middle of the lacZ gene causing the colonies to be white and easily selected; the T7 promoter region that allows for *in vitro* RNA transcription/translation by the T7 phage; the EcoR I sites on either side of the insert that enable the insert to be easily removed by EcoR I restriction enzymes; the f1 origin of replication that makes single-strand rescue possible (Figure 3.4).

TOPO TA Cloning System was used to detect different DSC2 transcripts in patient carrying the c.631-10C>T intronic nucleotidic variation. The nested PCR product was size separated by agarose gel electrophoresis, gel isolated, and cloned into the pCR2.1 plasmid.

MATERIALS:

- PCR or nested PCR product
- TOPO TA Cloning Kit (Invitrogen):
  pCR2.1-TOPO plasmid vector (10ng/μL)
  Salt Solution
- 0.5mL sterile microcentrifuge tubes

PROCEDURE:

Produce and gel-purify the PCR product with 3'A overhangs (DSC2ex3-9 fragment of 949bp and DSC2nested fragment of 502bp).

Set up cloning reaction: transfer in a sterile microcentrifuge tube 4μL fresh PCR purified product, 1mL Salt Solution and 1mL pCR2.1-TOPO vector.

Mix reaction gently and incubate for 5 minutes at room temperature (22-23°C).

Place the reaction on ice and proceed to cells transformation.

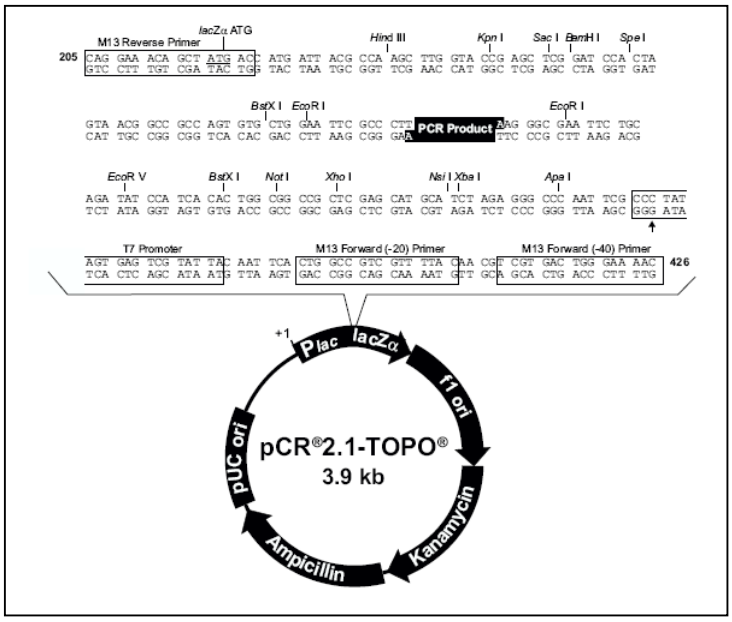

Figure 3.4. The map shows the features of pCR2.1-TOPO plasmid vector and the sequence surrounding the cloning site. Restriction sites are labelled to indicate the actual cleavage site. The arrow indicates the start of transcription for T7 polymerase.

3.2.15. Chemical transformation of competent *E.coli* (TOP10)

The plasma membrane of cells is selectively permeable and does not normally admit large molecules such as long DNA fragments. Cells can be treated so that the permeability properties of the plasma membranes are altered. As a result, a fraction of the cells become competent:

they are capable of taking up foreign DNA from the extra-cellular environment. These cells normally take up only one foreign DNA molecule (which can, however, subsequently replicate many times within a cell).
TOP10 commercial competent *E.coli* cells are available with TOPO TA Cloning Kit (Invitrogen). This strain allows blue/white screening.

MATERIALS:

- Cloning reaction (final volume 6µL)
- TOP10 Competent Cells (Invitrogen)
- SOC medium (Invitrogen)
- 42°C water bath
- 37°C shaking and non-shaking incubator
- LB-Agar plates containing 100µg/mL Ampicillin:
  bacto-tryptone 10g
  bacto-yeast extract 5g
  NaCl 10g
  bacto-agar 10g
  to 1L with deionized H_2O; shake until the solutes have dissolved; adjust the pH to 7.0 with 5N NaOH; sterilize by autoclaving; allow the medium to cool to 50°C before adding 100µg/mL thermolabile ampicillin; pour 25mL of medium per 90mm Petri plate.

PROCEDURE:
Thaw on ice a vial (50µL) of TOP10 Competent Cells.
Add 6µL of cloning reaction to the cells and mix gently.
Incubate tube on ice for 30 minutes.
Heat shock cells for 30 seconds in a 42°C water bath without shaking.
Immediately place the tube on ice for 1-2 minutes.
Add 250µL of room temperature SOC medium and shake the tube horizontally (200 rpm) at 37°C for 1 hour.
Spread up 10µL and about 50µL of transformation on pre-warmed selective plates (plate two different volumes to ensure that at least one plate will have well-spaced colonies).
Incubate plates overnight at 37°C.
The day after, pick 10 white or light blue colonies for analysis (an efficient TOPO Cloning reaction will produce hundreds of colonies).

3.2.16. Extraction and purification of plasmid DNA

Methods to purify plasmid DNA from bacteria involve three steps: growth of the bacterial culture in liquid medium, harvesting and lysis of the bacteria, purification of plasmid DNA.

Small-scale preparations of plasmid DNA

Mini preparations of plasmid DNA was obtained by the alkaline lysis method of the Wizard® Plus SV Minipreps DNA Purification System (Promega). This system can be used to isolated any plasmid from E.coli hosts but works most efficiently when the plasmid is less than 20,000bp in size. It routinely yields 3.5-5μg of plasmid DNA using pGEM Vector and DH5α™ cells in 1.5mL of LB medium.

MATERIALS:

- Colonies on selective agar plates
- 1.5mL microcentrifuge tubes
- Shaking incubator
- Microcentrifuge
- LB medium containing 100μg/mL Ampicillin:
  bacto-tryptone 10g
  bacto-yeast extract 5g
  NaCl 10g
  to 1L with deionized H_2O; shake until the solutes have dissolved; adjust the pH to 7.0 with 5N NaOH; sterilize by autoclaving; allow the medium to cool to 50°C before adding 100μg/mL thermolabile ampicillin.
- Wizard Plus SV Minipreps DNA Purification System (Promega):
  Cell Resuspension Solution
  Cell Lysis Solution
  Alkaline Protease Solution
  Neutralization Solution
  Column Wash Solution
  Wizard SV Mini columns
  Collection Tubes (2mL volume)
  Nuclease-Free Water

PROCEDURE:

Transfer a single, well-isolated colony from selective agar plates into 1.2mL of LB medium containing the appropriate antibiotic (Ampicillin) in a 2mL micro centrifuge tube for a secondary amplification step.

Incubate the culture overnight at 37°C under vigorous shaking.

Use the Wizard Plus SV Minipreps DNA Purification System for isolation of plasmid DNA.

Centrifuge the culture at 12,000xg for 30 seconds at 4°C.

Remove the medium by aspiration and resuspend the cells in 250μL of Cell Resuspension Solution.

Add 250mL of Cell Lysis Solution and mix by inverting the tube 4 times (do not vortex). Incubate for 5 minutes at room temperature.

Add 10μL of Alkaline Protease Solution, mix by inverting the tube 4 times and incubate for 5 minutes at room temperature.
Add 350μL of Neutralization Solution and immediately mix by inverting the tube 4 times.
Centrifuge the bacterial lysate at maximum speed (around 14,000xg) for 10 minutes at room temperature.
Transfer the cleared lysate to the prepared Spin Column by decanting (prepare plasmid DNA purification units by inserting one Spin Column into one 2mL Collection Tube for each sample).
Centrifuge the supernatant at maximum speed for 1 minute at room temperature.
Remove the Spin Column from the tube, discard the flow through from the Collection Tube and reinsert the Spin Column into the Collection Tube.
Add 750μL of Column Wash Solution to the Spin Column.
Centrifuge at maximum speed for 1 minute at room temperature.
Remove the Spin Column from the tube, discard the flow through and reinsert the Spin Column into the Collection Tube.
Repeat the wash procedure using 250μL of Column Wash Solution.
Centrifuge at maximum speed for 2 minutes at room temperature.
Transfer the Spin Column to a new, sterile 1.5ml micro centrifuge tube, being careful not to transfer any of the Column Wash Solution with the Spin Column.
If the Spin Column has Column Wash Solution associated with it, centrifuge again for 1 minute at maximum speed.
Transfer the Spin Column to a new, sterile 1.5mL micro centrifuge tube.
Elute the plasmid DNA by adding 100μL of Nuclease-Free Water to the Spin Column.
Centrifuge at maximum speed for 1 minute at room temperature.
After eluting the DNA, discard the Spin Column and store the purified plasmid DNA at 20°C or below.
Check DNA concentration and quality on agarose gel.

3.2.17. Analysis of positive clones

Plasmid DNA isolated from selected bacterial colonies was analyzed by *Eco*R I digestion and agarose gel electrophoresis to test fragment ligation in the vector. Then M13 Forward and M13 Reverse primers (included in TOPO TA Cloning Kit, Invitrogen) allowed direct sequencing of insert.

3.2.18. Real-time PCR

Quantitative real-time polymerase chain reaction (Real-Time PCR) is a method used to quantify changes in gene expression. It is a form of quantitative PCR using a fluorescence-detecting thermocycler machine to amplify specific nucleic acid sequences and simultaneously measure

their concentrations with excellent sensitivity and precision in every cycle (Gibson et al., 1996; Heid et al., 1996).

Intercalating dye SYBR Green I provides the simplest and most economical format for detecting and quantitating PCR products in real-time reactions. Unbound SYBR Green I emits minimal fluorescence, so the background signal during the first few cycles of PCR is usually very low. When SYBR Green I intercalates double-stranded DNA during the hybridization (annealing) and extension steps of PCR, the fluorescence increases significantly. The fluorescent signal increases proportionally as the amount of amplification product increases (Figure 3.5). Data analysis, including standard curve generation and copy number calculation, is performed automatically.

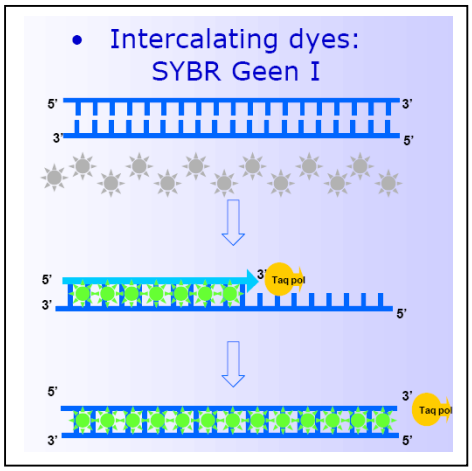

Figure 3.5. Intercalating dye SYBR Green I. Unbound SYBR Green I emits very little fluorescence. Fluorescent signal significantly increases as SYBR Green I intercalates the double-stranded DNA.

Used quantitation approach is the comparative C_T (threshold cycle, the fractional cycle number at which the fluorescence passes the fixed threshold) method. This involves comparing the C_T values of the samples of interest (cDNA from lymphocytes RNA of healthy controls and of patient carrying c.631-10C>T intronic variation in DSC2 gene) with a control or calibrator (cDNA from commercial heart RNA). The C_T values of both the calibrator and the samples of interest are normalized to an appropriate endogenous house keeping gene. β-actin was used as internal control gene.

MATERIALS:

- cDNA from patient and healthy controls RNA
- cDNA from commercially available human total RNA (Clontech)
- Primers (10pmol/μL, Promega)
- 2X SYBR green PCR Master Mix (Applied Biosystems)
- ABI prism 7000 Sequence Detection System (Applied Biosystems)

PROCEDURE:

Utilized β-actin primers (forward: 5'CGAGCGCGGCTACAGCTT3' and reverse: 5'CCTTAATGTCACGCACGATT3') and DSC2 primers (forward: 5'TCCAATTCCTTGTTCGATG CT3' and reverse: 5'TGGGCCGTGTCAGATTGAA3'), were designed through the Primer Express software (Applied Biosystems).

Perform reactions in a final volume of 25μL using, for each sample, three serially diluted cDNA (dilution factor 1:2, 1:4, 1:8) reverse-transcribed from RNA, 1X SYBR green PCR Master Mix, and 300nM of each primer. Amplify all samples in tripled.

Amplification profile consists of an initial denaturation step at 95°C for 10 minutes, followed by 45 cycles of 95°C for 15 seconds and 60°C for 1 minute.

DSC2 expression is determined using a standard curve of serially diluted heart cDNA generated from commercially available total RNA. Quantification of the β-actin house keeping gene is utilized to monitor cDNA input for each sample; β-actin normalized DSC2 expression is reported as a percentage of DSC2 expression in the available heart positive control.

3.2.19. DES and PKP4 genes expression analysis

cDNAs from heart, skin, skeletal muscle, kidney, and liver (MTC Multiple Tissue cDNA Panel I) and cDNA from lymphocytes (from a healthy donor) were available to verify and compare DES and PKP4 genes expression across tissues.

MTC Multiple Tissue cDNA Panel I (Clontech) is a commercial set of first-strand cDNAs (length 0.1-6Kb) from different human tissues, virtually free of genomic DNA. The MTC panel is normalized to several different house-keeping genes to ensure accurate assessment of target mRNA abundance.

Primers used to amplify the fragment corresponding to exons 2-5 of DES gene from cDNAs (T_{ann} 62°C) are as follow: Primer forward: 5'AGAACAATTTGGCTGCCTTC3'; primer reverse: 5'CGTCAATCTCGCAGGTGTAG3'.

Primers used to amplify the fragment corresponding to exons 7-8 of PKP4 gene from cDNAs (T_{ann} 60°C) are as follow: Primer forward: 5'GGACCAACCCCTCAATACCA3'; primer reverse: 5'AGACACGGCAGAACGAAGGT3'.

3.3. SCREENING OF λ-LIBRARY

3.3.1. Mouse 129/Svj genomic library in λ-FIX II vector

The Mouse 129/Svj genomic λ-library (Stratagene) is a commercial collection of λ FIX II vectors containing total mouse 129/SVJ genomic DNA from spleen (partial digests with *Sau*3A I).

The λ FIX II vector is a replacement vector used for cloning large fragments of genomic DNA. The wild-type virus particle (virion) contains a genome of close to 50kb of linear double-

stranded DNA packaged within a protein coat and has evolved a highly efficient mechanism of infecting *E.coli* cells (XL1-Blue MRA (P2) host strain). Only DNA molecules from 37 to 52kb in length can be stably packaged into the λ particle. The central segment of the λ genome contains genes that are required for the lysogenic cycle but are not essential for lytic function. As a result, it can be removed and replaced by a foreign DNA fragment (Figure 3.6). Using this strategy, it is possible to clone foreign DNA up to 23kb in length, and such vectors are normally used for making genomic DNA libraries. The unique arrangement of the polylinker for the λ FIX II vector permits the isolation of the insert.

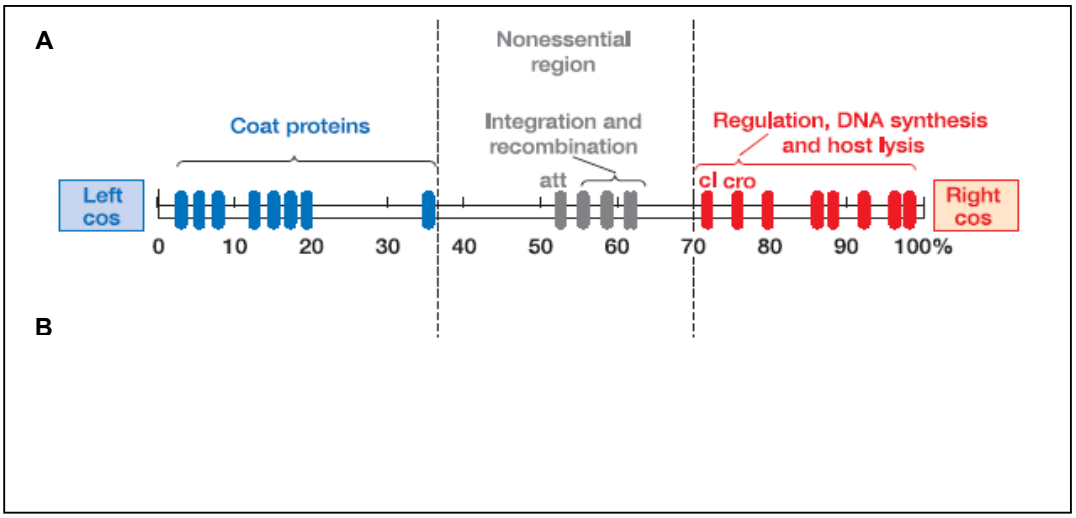

Figure 3.6. (A) Map of the λ genome, showing positions of genes (vertical bars) and cohesive sequence (cos) at the extreme termini. In λ replacement vectors, the nonessential region is removed by restriction endonuclease digestion, leaving a left λ arm and a right λ arm. A foreign DNA fragment is ligated to the two arms in place of the original 'stuffer' fragment, providing maximal insert size of 23kb (from Strachan, 2003). **(B)** Multiple cloning site sequence of the λ FIX II replacement vector.

Aliquots (50μL/aliquot) were removed from λ-library stock solution and stored at -80°C (the titer of libraries stored at -80°C should remain stable for years). A single tube stored at 4°C was used to work (it should be stable for 6 months).

The library was supplied with bacterial host strain for library plating (XL1-Blue MRA (P2) *E.coli* cells). Aliquots (50μL/aliquot) were removed from stock solution and stored at -80°C, host strains in use were stored at -20°C.

To isolate all DSG2 mouse gene genomic sequence, library was screened for three times by hybridization, by using each time mix of two DNA radioactively labeled probes simultaneously.

Normally 15,000 plaques/90mm plate and 45,000/140mm plate were plated and were left to grow until begin to touch. For each screening 10-12 plates (140mm) were plated out: that is from 450,000 to 540,000 pfu.

The plaques which are formed on an agar surface (following lysis of bacterial cells by phage vectors) contain residual phage particles. Plaques which contain recombinant DNA were identified and selected by hybridisation (Figure 3.7).

A nylon membrane was placed on top of the agar plate and when removed from the plate constituted a faithful copy of the phage material in the plaques, a so called *plaque-lift* (two replicate filters of each plate were prepared to confirm detected positive signals by autoradiography).

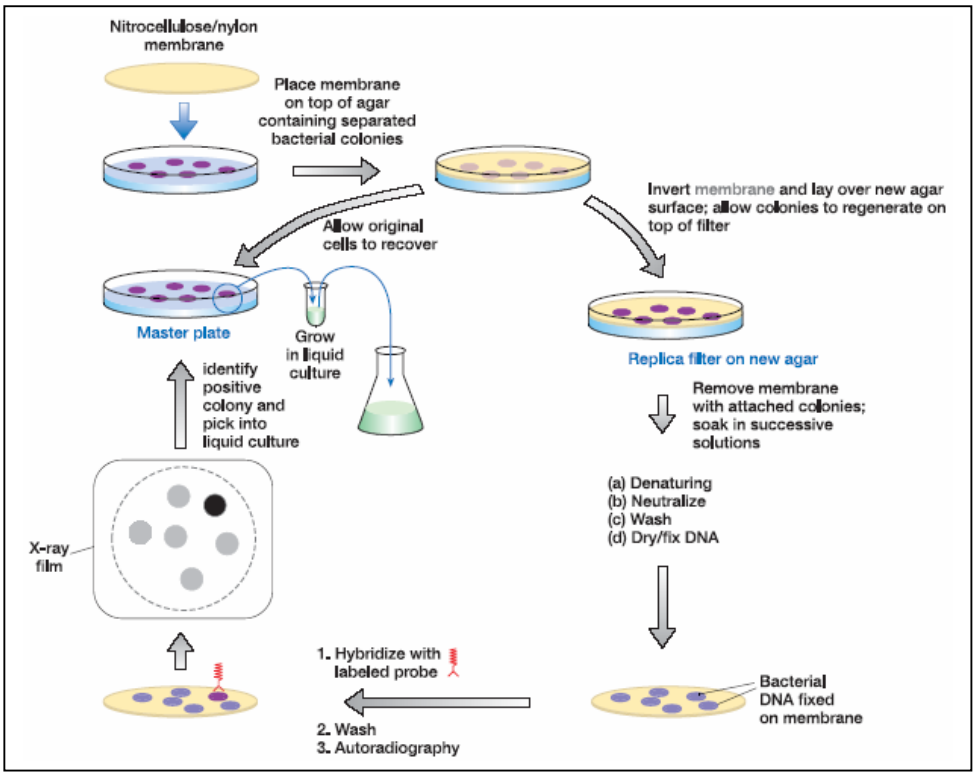

Figure 3.7. Plaques blot hybridization involves replicating colonies on to a durable membrane prior to hybridization with a labelled nucleic acid probe. This method is used to identify plaques containing recombinant DNA, should a suitable labelled probe be available (from Strachan, 2003).

The membrane was then exposed to alkali to denature the DNA prior to hybridizing with a labelled probe. After hybridization, the probe solution was removed, and the filter was washed extensively, dried and submitted to autoradiography using X-ray film. The position of strong radioactive signals was related back to a master plate containing the original pattern of colonies, in order to identify plaques containing DNA related to the probe. These plaques were individually isolated and resuspended in SM solution prior to DNA extraction and purification of the phage DNA.

3.3.2. Growing the bacterial host strain cells

XL1-Blue MRA (P2) *E.coli* cells were used as host strain.

To check the titer of the library or to plate out the library always use fresh bacteria.

MATERIALS:

- XL1-Blue MRA (P2) cells stock solution
- LB-Agarose plates:
  bacto-tryptone 10g
  bacto-yeast extract 5g
  NaCl 10g
  agarose electrophoresis grade 10g
  to 1L with deionized H_2O; shake until the solutes have dissolved; adjust the pH to 7.0 with 5N NaOH; sterilize by autoclaving; pour 25mL of medium per 90mm Petri plate.
- LB-Maltose-$MgSO_4$ medium:
  bacto-tryptone 10g
  bacto-yeast extract 5g
  NaCl 10g
  $MgSO_4$ solution to a final concentration of 10mM
  to 1L with deionized H_2O; shake until the solutes have dissolved; adjust the pH to 7.0 with 5N NaOH; sterilize by autoclaving; allow the medium to cool to room temperature before adding sterile filtered maltose solution to a final concentration of 0.2% (maltose induces higher expression in *E.coli* cells of the lambda receptor).

PROCEDURE:

Streak out bacteria on a primary working LB-Agarose plate and incubate overnight at 37°C.
The day after pick a single colony and transfer to a tube with 20mL LB-Maltose-$MgSO_4$ medium.
Grow overnight at 37°C.
The bacteria can be stored at 4°C.

3.3.3. Checking the titer of library

The lysate titer is the value obtained when the library was constructed. Theoretical noted titer of λ-library was $7.8x10^9$pfu/mL.
It was important to check the most accurate titer of the library before screening.

MATERIALS:

- λ-library stock solution
- Fresh *E.coli* cells in LB-Maltose-$MgSO_4$ solution
- SM buffer:
  NaCl 0.1M
  $MgSO_4 \cdot 7H_2O$ 0.1M
  Tris-HCl 50mM (pH7.5)
  Gelatine 0.01%
  sterilize by autoclaving; store at 4°C.

- Top agarose:
  bacto-tryptone 10g
  bacto-yeast extract 5g
  NaCl 10g
  agarose electrophoresis grade 7g
  to 1L with deionized H_2O; shake until the solutes have dissolved; adjust the pH to 7.0 with 5N NaOH; sterilize by autoclaving; add $MgSO_4$ to a final concentration of 10mM.
- λ–plates:
  bacto-tryptone 10g
  bacto-yeast extract 5g
  NaCl 10g
  agarose electrophoresis grade 16g
  to 1L with deionized H_2O; shake until the solutes have dissolved; adjust the pH to 7.0 with 5N NaOH; sterilize by autoclaving; add $MgSO_4$ to a final concentration of 10mM; pour 25mL of medium per 90mm Petri plate.
- Microcentrifuge tubes
- 15mL tubes
- 37°C oven
- 50°C water bath
- Microwave oven

PROCEDURE:

Make a dilution series of the library: take out 10μL of the library stock solution and transfer to 990μL SM solution, this will be the ($7.8x10^7$pfu/mL) "10^8" stock solution. Make a 1/100 dilution of the 10^8 stock, (10^6 mix), a 1/100 dilution of the 10^6 mix (10^4 mix), a 1/100 dilution of the 10^4 mix (10^2 mix), and a 1/10 dilution of the 10^2 mix (10^1 mix).

Transfer bacterial cells to 3 eppendorf tubes, 100μL in each. Add 2μL of the 10^6 mix, 2μL of the 10^4 mix, 2μL of the 10^2 mix, and 2μL of the 10^1 mix.

Incubate 15-20 minutes at 37°C to let the phage particles adhere to the *E.coli* cells.

Melt the top agarose in microwave oven, transfer 3mL to 15mL tubes and keep in a water bath at 50°C.

Transfer various diluitions of phages/cells mixtures to the 3mL λ-top agarose (in 15mL tubes). Invert the tube a couple of times and pour the top agar on a pre-warmed λ-plate.

Wait until the λ-top agarose has solidified and incubate the plates at 37°C until plaques appear (10-12 hours).

Count the plaques to determine titer of the library as follow:

Titer (pfu/mL) = (pfu counted / pfu theoretical) x theoretical titer (pfu/mL)

3.3.4. Plating out the library for screening

Plate out 10 plates (140mm), 450,000 pfu.

MATERIALS:

- λ-library stock solution
- Fresh *E.coli* cells in LB-Maltose-$MgSO_4$ solution
- Top agarose (§ 3.3.3)
- 10 λ-plates, 140mm (§ 3.3.3)
- 15mL tubes
- 37°C oven
- Microwave oven

PROCEDURE:

Take out 600μL of fresh *E.coli* cells (grown in LB-Maltose-$MgSO_4$ solution), and transfer to 15mL tube. Prepare 10 tubes.

Add to each tube 45,000 pfu from library (dilution based on the titer obtained) and incubate 30 minutes at 37°C.

Transfer 8mL top agarose (melted in microwave oven and kept in a water bath at 50°C) to each 15mL tube. Invert the tube a couple of times and pour the top agar on a pre-warmed λ-plate (it is important that plates are "dried out" a bit before to use them; pouring the top agarose onto a "wet" newly made plate can give problems with filter lifts later).

Plate out all the phage (10 tubes).

Let the top agarose solidify and incubate the plates at 37°C until plaques appear (10-12 hours).

When the λ–top agarose library plates are ready store them at 4°C overnight.

3.3.5. Taking lifts of the plates (transferring the λ-phage to nylon membranes)

MATERIALS:

- λ–top agarose library plates
- Hybond-NX nylon membranes/filters, 132mm (Amersham Biosciences)
- Denaturation solution (NaCl 1.5M, NaOH 0.5M)
- Neutralization solution (NaCl1.5M, Tris-Cl pH8.0 0.5M)
- 20X SSC solution (NaCl 3M, Na citrate•$2H_2O$ 0.3 M)
- 3MM filter paper
- Needle
- Flat forceps
- UV light transilluminator

PROCEDURE:

Label (number) the filters.

Place a filter on top of the top agarose for about 2 minutes.

Then using a needle mark the filter with needle assymmetrical holes (holes are necessary later to align the filters and exposed films). Mark the needle holes at the back side of the plate with a marker (this makes it easier to align the exposed films against the plates).

Using flat forceps, gently lift the filter off the plate, making sure the top agarose stays on the plate.

Place the duplicate filter on the top agarose for 4 minutes and marked similarly as the first filter.

The lambda phage is now transferred to the filters.

Soak the filter in alkaline denaturation solution for 2 minutes.

Soak the filter in neutralization solution for 5 minutes.

Wash the filter 2X SSC solution for 30 seconds.

Lay on 3MM filter paper to dry.

UV fixate the filter for 2-5 minutes (crosslinking procedure).

The filters are ready for use. They should be stored in a dry place at room temperature.

Keep the λ–top agarose library plates good wrapped at 4°C to avoid that they dry out.

3.3.6. Probe labelling

a. Probe synthesis

DNA fragments to be utilized as probes in library screening were amplified from 129/SVJ mouse genomic DNA. cDNA and translation sequences of mouse *dsg2* gene is available in NCBI website (NM_007883 and NP_031909, respectively). Primers were designed by software package (http://www.genome.wi.mit.edu/cgi-bin/primer/primer3.cgi). Sequence of primers, size of amplicons, and amplification annealing temperatures are reported in Table 3.4.

Table 3.4. Probes utilized in library screening. Sequence of primers, size of amplicons and amplification annealing temperatures are reported.

Probe	Size (bp)	Forward 5'-3'	Reverse 5'-3'	PCR T_{ann} °C
Probe 1	691	GTCCCGCAGAGTCAGAGAAG	GATGATGGTGGCTTCGATTT	60
Probe 4-5	864	ACCTGCCTCCTGTCCATACC	AAAGAGCCTGGAGTAATGGGTTT	60
Probe 9	636	CATCACTGTCAAGGTCAAGAACG	TCTGCCCCACTTTTCTATTTTCA	60
Probe 11	711	TACGGAGTGTCTGTGAGGATGAA	TTGGATTGTGAGACCATGAATTG	60
Probe 12	720	ACAGCCACCCATTTTCATCC	TGACGGGCTAGAGGTCCATT	60
Probe 15	806	TCCAGGCAGAGTCAGAAGGT	CCATCCCCCAATAATCACAG	60

For each probe, PCR was carried out in 6 vials, each in a final volume of 25μL (§ 3.2.4). After activation of the enzyme (DNA Taq Gold polymerase, Applied Biosystems; activation at 95°C for

12 minutes), cycling conditions (denaturation at 95°C for 30 sec, annealing at the working temperature for 30 sec, extension at 72°C for 1 minute) were repeated 35 times.
Six PCR products were mixed, loaded and run onto an agarose gel using established protocol.
After gel purification (§ 3.2.13), probe concentration was checked on gel electrophoresis and probes stored at -20°C.
All probes were radioactively labelled.
Probe1 and Probe15 were used simultaneously in the first library screening; Probe4-5 and Probe12 were mixed for the second screening; to complete *dsg2* mouse gene sequence isolation, Probe9 and Probe11 were designed and used in the third library screening.

b. Random primer DNA labelling

Random sequence hexanucleotides are used to prime DNA synthesis on denatured template DNA at numerous sites along its length (Feinberg and Vogelstein B, 1983). The primer-template complex is a substrate for the 'Klenow' fragment of DNA polymerase1. By substituting a radiolabelled nucleotide for a non-radioactive equivalent in the reaction mixture newly synthesized DNA is made radioactive (Figure 3.8). The absence of the 5'-3' exonuclease activity associated with DNA polymerase1 ensures that labelled nucleotides incorporated by the polymerase are not subsequently removed as monophosphates. Radioactive labelled fragments can then be used as sensitive hybridization probes for a wide range of filter based applications.

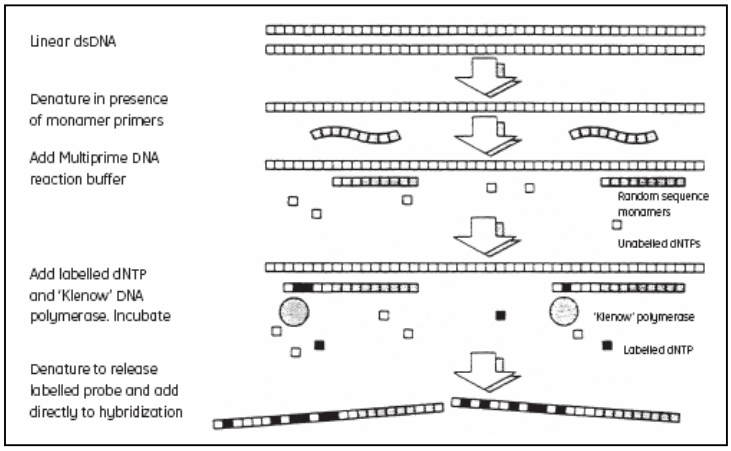

Figure 3.8. Preparation of labelled probes using random hexanucleotides primers.

Then, removal of unincorporated labelled nucleotides is desirable to reduce background produced by the probe during hybridization (it is considered important particularly if the radioactive probe has to be used several days later or the incorporation is less than 50%). Columns containing Sephadex (ProbeQuant G-50 Micro Columns, GE Healthcare) are designed for the quantitative removal of unincorporated nucleotides from a DNA labelling reaction by the process of gel filtration: molecules smaller than 1 x 10^3Da (or 20bp) are retained in the matrix whereas larger molecules are eluted. Percent label incorporation may be

calculated by a radiation detector. The interaction of the radiation with the detector element causes an electronic pulse: this is recorded and displayed as a radioactive "counts" per unit time (for example, counts per minute, cpm).

MATERIALS:

- DNA probe
- Megaprime DNA Labelling System (Amersham Biosciences):
  Random nonamer primers
  Labelling Buffer (dATP, dGTP, dTTP in Tris-HCl; pH 7.5; 2-mercaptoethanol; $MgCl_2$)
  DNA polymerase1, Klenow fragment 1U/µL
- α [^{32}P] dCTP 10µCurie/µL (GE Healthcare)
- Boiling water bath
- ProbeQuant G-50 Micro Columns (GE Healthcare)
- 1.5mL microcentrifuge tubes
- Microcentrifuge
- Scintillation vials
- Scintillant
- Scintillation counter

PROCEDURE:

Place 25ng of DNA template into a micro centrifuge tube.

Add 5µL of primers and the appropriate volume of water to give a total volume of 50µL in the final Megaprime reaction.

Denature by heating to 100°C for 5 minutes in a boiling water bath and chill on ice for 5 minutes.

Add 10µL of labelling buffer, 5µL of radio-labelled dCTP, and 2µL of enzyme.

Mix gently by pipetting and incubate at 37°C for 10 minutes.

Stop the reaction by the addition of 5µL of 0.2M EDTA.

Purify probes to remove unincorporated labelled nucleotides by ProbeQuant G-50 Micro Columns:

Resuspend the resin in the column by vortexing.

Loosen the cap one-quarter turn, snap off the bottom closure, place the column in the supplied collection tube for support, and pre-spin the column for 1 minute at 735xg.

Place the column in a new 1.5mL micro centrifuge tube and slowly apply 50µL of the labelled sample to the top-centre of the resin.

Spin the column at 735xg for 2 minutes. The purified sample is collected in the bottom of the 1.5mL tube. This is the ‘COLUMN’ sample.

Determine the percent incorporation of the radiolabel:

For each sample to be assayed, mix 2µL of the ‘COLUMN’ sample with 598µL of water buffer in a micro centrifuge tube.

Prepare an identical dilution using the 2µL sample reserved prior to column purification (this sample represents the 'TOTAL' cpm added to the labelling reaction).
Add 2µL aliquots of the diluted 'COLUMN' and 'TOTAL' samples directly to scintillation vials containing 10mL scintillant, capped and inverted to mix.
Count the samples using an appropriate ^{32}P counting program.
Percent label incorporation may be calculated using the formula:

% label incorporation = cpm for 'COLUMN' sample / cpm for 'TOTAL' sample x 100

Percent incorporation values obtained using this system vary from 50-75%.
Determination of cpm/µL of purified labelled probe is obtained dividing cpm for 'COLUMN' sample by two.
To determine the total cpm incorporated into the purified sample, multiply cpm/µL by the volume of the sample recovered from the column, and by the dilution factor (300).
The specific activity of the probe should be more than $8x10^8$cpm/µg, and the final concentration $1–2x10^6$cpm/mL of hybridization solution.
Denature the labelled DNA to be used in a hybridization by heating to 100°C for 5 minutes, then chill on ice.

3.3.7. Filter hybridization

a. Pre-hybridization

MATERIALS:

- 10 filters and 10 duplicate filters (carrying fixed phage DNA)
- Rapid-Hyb Buffer (Amersham Biosciences)
- Appropriate containers
- 65°C oven with shaker

PROCEDURE:
Place filters on an empty appropriate container and cover with 50mL of Rapid-Hyb Buffer.
Place duplicate filters on an other appropriate container and cover similarly as first filters.
Incubate at 65°C in a oven with shaker for 2-3 hours.

b. Hybridization

MATERIALS:

- 2 radioactively labelled probes
- Containers with pre-hybridized filters (filters and duplicates filters)
- Rapid-Hyb Buffer (Amersham Biosciences)
- 65°C oven with shaker

PROCEDURE:

Boil a labelled probe by heating to 100°C for 5 minutes.

Chill it quickly on ice and then dilute it into 5mL of pre-warmed Rapid-Hyb Buffer.

Mix gently and add 2.5mL of probe/Rapid-Hyb Buffer solution to each container.

Repeat previous steps for the second labelled probe.

Filters are now hybridized with two probes simultaneously.

For high stringency screening incubate at 65°C with shaker for 5 hours.

c. Washing

The filters were washed in SSC/SDS solutions after the hybridization. The washing solutions and temperatures depend on probe and stringency conditions.

MATERIALS:

- Hybridized filters (filters and duplicate filters)
- Low stringency solution (2X SSC, 0.1% SDS)
- Medium stringency solution (1X SSC, 0.1% SDS)
- 50mL centrifuge tubes
- 3MM paper
- 65°C oven with shaker
- Geiger counter

PROCEDURE:

Pour out the hybridization solution into a 50mL centrifuge tube if it has to be reused (probes can be reused within a couple of weeks, and must be boiled 5 minutes and chilled on ice before reuse).

Add a generous amount (100-200 mL) of wash solution.

Wash the filters with low stringency solution at room temperature for 5 minutes.

Discard the wash solution and repeat the washing 2-3 times.

Wash the filters with medium stringency solution for 30 minutes at 65°C with shaker.

Discard the wash solution and repeat the previous washing.

Dab the filters on 3MM paper to get rid of excess liquid.

Check the activity of the filters with a geiger counter: at this point the geiger counter should not (or just barely) detect counts on the filters (that is unless you have 10-100 of positive clones per filter). Too high activity normally means that the background signal is high.

Store the filters overnight at room temperature.

3.3.8. Autoradiography

MATERIALS:

- 3MM paper
- Kodak XAR5 films
- Autoradiography cassette
- Phosphorescent markers (Stratagene)
- Kodak GBX 5X Develop solution
- Kodak GBX 5X Fixer solution

PROCEDURE:

Put the filters with Kodak films between 3MM paper in a autoradiography cassette, applying some phosphorescent markers.

Proceed with autoradiography using an intensifying screen to enhance the signal, and take an exposure at -80°C for 1-3 days.

Develop the films: place them in 1x Develop solution at room temperature for 5 minutes; transfer in H_2O for 1-2 minutes, and then place them in 1x Fixer solution for 5 minutes.

Wash well the films with H_2O and let dry at room temperature.

3.3.9. Identification of positive plaques and rescreening

PROCEDURE:

After developing, align film with filters and corresponding duplicate filters to locate positive plaques.

In cases where a single, isolated positive plaque cannot be picked, remove an agar plug containing several plaques into 400μL of sterile SM dilution buffer.

Let the plug elute at 4°C overnight.

Add a drop of chloroform and incubate at 25°C for 1 hour with shaking.

Spin in a microcentrifuge at 8,000xg for 2 minutes to remove debris.

Titer the supernatant (§ 3.3.3).

Replate supernatant to obtain 200–1,000 plaques on a 140mm plate.

Rescreen these plaques (secondary screening and eventually tertiary screening; steps are similar to the ones described above).

Pick a single, well-isolated plaque for the plate stock. The plate stock is then used for further analysis.

3.3.10. Phage stock preparation

MATERIALS:

- λ-plate stock
- SM buffer (§ 3.3.3)
- Chloroform
- Microcentrifuge tubes
- 50mL tubes
- Microcentrifuge
- Centrifuge
- Shaking incubator
- Vortex mixer

PROCEDURE:

Transfer an agar plug containing a single, well-isolated plaque to a microcentrifuge tube containing 1mL of sterile SM buffer.

Let the plug elute at 4°C overnight.

Add some drop of chloroform and incubate at 25°C for 1 hour with shaking.

Spin in a microcentrifuge at 8,000xg for 2 minutes to remove debris.

Titer the supernatant (§ 3.3.3).

Plate about 60,000 lytic phage per 140mm plate (§ 3.3.4) and incubate at 37°C overnight.

The day after, add 12mL of SM dilution buffer to the plate, and incubate at 4°C for 24 hours with gently constant shaking.

Pour the liquid (containing phage lysate) from the plate into a sterile 50mL tube.

Add 2mL of chloroform to the phage lysate, and vortex for 2 minutes.

Centrifuge at 7,000xg for 10 minutes.

Collect the supernatant and store at 4°C (this is a high-titer stock: titer should be approximately 10^{10} pfu/mL).

3.3.11. Lysate processing and λ-DNA extraction

MATERIALS:

- High-titer phage lisate stock
- Chloroform
- RNase A (10mg/mL, Sigma Genosys)
- Proteinase K (20mg/mL, Boehringer Mannheim GmbH)
- 10% SDS
- Phenol-chloroform (Invitrogen)
- Isopropanol

- 3M NaOAc
- Isopropanol
- 70% ethanol
- sterile H_2O
- 15mL tube
- microcentrifuge tube
- Centrifuge
- Microcentrifuge
- Oven

PROCEDURE:

Transfer 1-3mL of phage lisate into a 15mL tube and add an equal volume of chloroform.

Vortex and centrifuge at 10,000xg for 2 minutes.

Transfer the supernatant in a new 15mL tube, add an equal volume of chloroform, vortex and repeat the centrifugation.

To the supernatant, add RNasi A to 10µg/mL, and incubate at 37°C for 30 minutes.

Add proteinase K to 50 µg/mL and 10% SDS to 0.5% final concentration.

Mix gently, incubate at 56°C for 1 hour, and then let chill at room temperature.

Add an equal volume of phenol-chloroform, and mix by gentle inversion.

Centrifuge at 10,000xg for 2 minutes.

Transfer the supernatant in a new 15mL tube, add an equal volume of phenol-chloroform, mix by gentle inversion, and repeat the centrifugation.

To the supernatant, add an equal volume of chloroform (only to remove any residual phenol), mix by gentle inversion, and centrifuge at 10,000xg for 2 minutes.

Collect the supernatant.

Add 1/10 volume of 3M NaOAc and 1 volume of isopropanol for DNA precipitation.

Mix by gentle inversion and incubate at room temperature for 10 minutes.

Centrifuge the DNA at 10,000xg for 5 minutes.

Discard the supernatant and wash twice the pellet with 500µL 70% ethanol.

Centrifuge the DNA at 10,000xg for 2 minutes and pour off the supernatant.

Let the pellet dry until the edges of the pellet begin to turn clear.

Allow the pellet to resuspend in 100-300µL of sterile H_2O at 4°C overnight.

Transfer the purified λ-DNA in a microcentrifuge tube and store at -20°C.

The DNA should be analyzed by restriction enzyme digestion and run on an agarose gel.

3.4. TARGETING VECTOR GENERATION FOR DEVELOPMENT OF A DSG2 KNOCK-IN MOUSE MODEL

In order to generate a knock−in mouse carrying a targeted mutation in DSG2 gene, three targeting vector were created from murine *dsg2* genomic clones identified from the λ FIX II 129/SVJ library. Sequencing reactions and restriction analysis were used to characterize λ–inserts and subclone a 7041bp fragment (709bp upstream exon 4 to 2249bp downstream exon 8) in *Sac*I site of the pBS-plyA vector. Three missense mutations (detected in DSG2 gene of ARVC/D patients) (Table 3.5) were introduced in mouse *dsg2* exons by site-directed mutagenesis, in order to generate three different targeting vectors. A neomycin resistance cassette (Neo, kindly provided by Prof. Bonaldo P., University of Padua) was cloned into *Bln*I site of *dsg2* intron 8 sequence and a herpes simplex virus thymidine kinase gene cassette (TK, kindly provided by Prof. Bonaldo P., University of Padua) was cloned in *Xho*I – *Sal*I sites of each targeting vector. Two cassettes will allow positive-negative selection of the recombination events.

Table 3.5. Pathogenic mutations detected in DSG2 gene of ARVC/D patients (cDNA and translation sequences BC099657 and NP_001934, respectively), and corresponding mouse mutations introduced in *dsg2* gene (cDNA and translation sequences NM_007883 and NP_031909, respectively) by site-directed mutagenesis.

exon	DSG2 Human mutation		*dsg2* Mouse mutation	
	Nucleotide change	Amino acid change	Nucleotide change	Amino acid change
4	c.298G>C	G100R	c.313G>C	G105R
7	c.797A>G	N266S	c.812A>G	N271S
8	c.880A>G	K294E	c.895A>G	K299E

3.4.1. pBluescript II KS (+) plasmid vector

Map of pBluescript II KS (+) plasmid vector (GenBank/EMBL accession number X52327), is presented below.

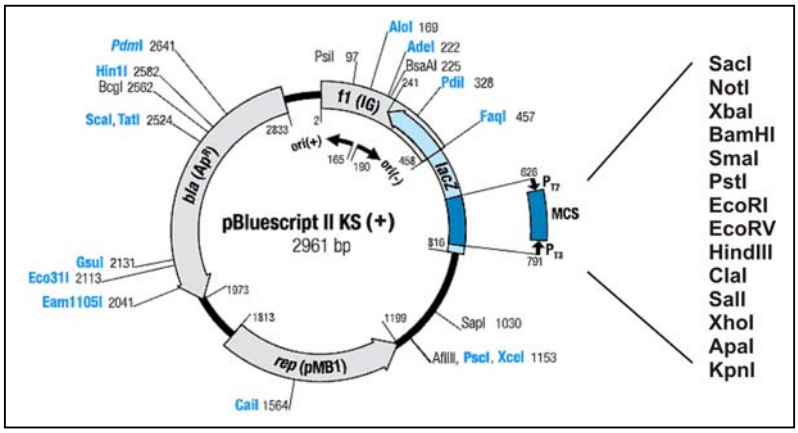

Figure 3.9. The map shows enzymes that cut pBluescript II KS (+) DNA once (enzymes produced by Fermentas are shown in blue). The coordinates refer to the position of first nucleotide in each recognition sequence. The exact position of genetic elements is shown on the map (termination codons included) (http://www.fermentas.com/techinfo/nucleicacids/mappbluescriptiiskks.htm).

The pBluescript II KS vector is 2961bp long. KS represents the orientation of the MCS (multiple cloning site or polylinker) in which *lacZ* transcription proceeds from KpnI to SacI (l*acZ is* gene encoding the N-terminal fragment of beta-galactosidase). (+) symbol indicates the orientation of the cloned phage f1 intergenic (IG) region carrying the sequences required in *cis* for initiation and termination of phage f1 DNA synthesis and for packaging of DNA into bacteriophage particles.

pBluescript II phagemids contain: f1 (IG), the intergenic region of phage f1; *rep* (pMB1), the pMB1 replicon responsible for the replication of phagemid (DNA replication initiates at position 1213 +/- 1 and proceeds in the direction indicated); *bla* (ApR) gene, coding for beta-lactamase that confers resistance to ampicillin; *lacZ,* 5'-terminal part of *lacZ* gene encoding the N-terminal fragment of beta-galactosidase (this fragment allows blue/white screening of recombinant phagemids). Other codons in the same reading frame come from f1 DNA.

MCS was modified to obtain a plasmid named pBS-plyA (Figure 3.10).

3.4.2. DNA cleavage by restriction enzymes

Many restriction enzymes have been used for digestions, linearization of plasmid DNA and molecular cloning (§ 3.2.5).

3.4.3. Dephosphorylation of Plasmid DNA

To prevent the re-circularization and religation of linearized cloning vector DNA during ligation and to enhance the introduction of DNA fragments into the cloning vector, a dephosphorylation of 5' termini can be performed. A phosphatase catalyzes the removal of 5' phosphate groups from linearized cloning vector DNA. It is effective on 3' overhangs, 5' overhangs and blunt ends. The re-circularization can happen only with insertion of phosphorylated DNA fragments.

MATERIALS:

- linearized DNA plasmid
- Thermosensitive Alkaline Phosphatase TSAP (1U/μL, Promega)
- MULTI-CORE™ 10X Buffer (Promega)
- 37-74°C heating block

PROCEDURE:

Digest the plasmid with the desired enzyme (§ 3.2.5).

When the digestion has been completed, heat-inactivate the restriction enzyme according to the directions provided with the restriction enzyme. If the restriction enzyme cannot be heat-inactivated, purify the digested DNA using the Wizard® SV Gel and PCR Clean-Up System (§ 3.2.13).

Add 10X buffer to a final concentration of 1X before to add 1µl of TSAP for reactions containing up to 1µg of digested DNA.

Incubate the reaction at 37°C for 15 minutes. This is a sufficient amount of time to dephosphorylate all vector DNA overhang types (3', 5' or blunt).

Inactivate irreversibly TSAP by incubating at 74°C for 15 minutes. Therefore, a DNA clean up step is not required before proceeding to a ligation reaction.

3.4.4. DNA ligation

Several strategies are available to ligate fragments of foreign DNA to plasmid vectors. The choice among them depends on the nature of the termini of the foreign DNA fragment and of plasmid vector (Table 3.6).

Ligation is accomplished using the enzyme DNA ligase (usually from the bacteriophage T4). It requires ATP and magnesium ions to catalyze the reaction of a 3'-hydroxyl group and a 5'-phosphate group on double-stranded DNA to form a phosphodiester bond. The DNA ends can be cohesive ends, such as those formed between molecules that have been digested with the same restriction endonuclease, or they can be blunt ends. Ligation between cohesive-ended molecules is much more efficient than ligation between blunt-ended molecules. Because of this, when ligating blunt-ended molecules, the DNA and ligase concentrations must be higher than when ligating cohesive-ended molecules.

During the ligation reaction, the foreign DNA and the plasmid have the capacity to circularize and to form tandem oligomers. It is therefore necessary to carefully adjust the concentrations of the two types of DNA to optimize the number of "correct" ligation products. Recircularization of plasmid DNA is minimized by removing the 5'-phosphates from both termini of the linear DNA with phosphatase (§ 3.4.3).

Table 3.6. Ligation of fragments of foreign DNA to plasmid vectors (from Maniatis, 1989).

Termini carried by foreign DNA fragment	Requirements for cloning	Comments
Blunt-ended	High concentrations of DNAs and ligase	Background of non-recombinant clones can be high; restriction sites at junctions between plasmid and foreign DNAs may be eliminated; recombinant plasmids may carry tandem copies of foreign DNA.
Different protruding termini	For maximum efficiency requires purification of plasmid vector after digestion with two restriction enzymes	Restriction sites at junctions between plasmid and foreign DNAs are usually conserved; background of non-recombinant clones is low; foreign DNA is inserted in only one orientation within recombinant plasmid.
Identical protruding termini	Phosphatase treatment of linear plasmid DNA	Restriction sites at junctions between plasmid and foreign DNAs are usually conserved; foreign DNA can be inserted in either orientation; recombinant plasmids may carry tandem copies of foreign DNA.

MATERIALS:

- foreign DNA fragment
- linearized plasmid DNA
- dephosphorylated (linearized) plasmid DNA
- T4 DNA Ligase (400 Cohesive End U/mL, New England Biolabs)
- 10X T4 DNA Ligase Buffer (New England Biolabs)

PROCEDURE:

Set up three different test ligations to assess whether dephosphorylation has been successful: ligation A (dephosphorylated plasmid DNA), ligation B (dephosphorylated plasmid DNA plus foreign DNA fragment carrying compatible phosphorylated termini), ligation C (linearized plasmid DNAthat has not been treated with phosphatase). Generally Insert:Vector molar ratio 3:1 is optimal for single insertions. Use 0.1-1µM total DNA.

ng DNA fragment = [50ng DNA vector x size (bp) DNA fragment / size (bp) DNA vector] x 3

To each test ligation, add appropriate volume of the 10x buffer and 1µL of T4 DNA Ligase (one Cohesive End Unit is defined as the amount of enzyme required to give 50% ligation of *Hind*III fragments of λ DNA, 5' DNA termini concentration of 0.12µM, 300µg/mL, in a total reaction volume of 20µL in 30 minutes at 16°C in 1X T4 DNA Ligase Reaction Buffer).
Mix and incubate the reactions at 16°C for 4 hours to overnight (alternatively T4 DNA Ligase can also be used at room temperature for one hour).
Purify the ligation (§ 3.2.13).
Dry the purified ligation solutions to 5µL and freeze at –20°C for the transformation.

3.4.5. pBS-plyA plasmid vector

pBS-plyA plasmid vector was obtained by restriction of pBluescript II KS (+) plasmid with *Kpn*I and *Sac*I enzymes and ligation of a new polylinker. Polylinker oligonucleotides (forward: 5'agcggccgcctcgagtgtcgacaagcttactagtgagctcgcatgcgcggccgcaagct3' and reverse: 5'tgcggccgcgcatgcgagctcactagtaagcttgtcgacactcgaggcggccgctgtac3') were designed to insert a new multiple cloning site (Figure 3.10).

MATERIALS:

- Polylinker oligonucleotides (150pmol/µL, Sigma Genosys)
- T4 Polynucleotide Kinase (10U/µL, Promega)
- Kinase 10X Reaction Buffer (Promega)
- Deoxiadenosine triphosphate (dATP 100pM, Invitrogen)
- pBluescript II KS (+) plasmid
- *Kpn*I and *Sac*I enzymes (10U/µL, Promega)

- 10X Digestion Buffer J (Promega)
- MilliQ water
- microcentrifuge tubes
- 37°-80°C heating block

PROCEDURE:

Place 10μL of two oligonucleotides in a sterile microcentrifuge tube.

Incubate at 80°C for 5 minutes; then let chill to 37°C allowing polylinker annealing.

Carry out polylinker DNA phosphorylation in a 20μL final volume containing 2μL polylinker DNA (about 6μg), 15pM dATP, 1X Kinase Buffer, and 15U of T4 Kinase (T4 Kinase catalyzes the transfer of the γ-phosphate from dATP to the 5'-terminus of polylinker).

Incubate at 37°C for one hour; store for ligation reaction.

Digest 6μg pBluescript II KS (+) plasmid with *Kpn*I and *Sac*I enzymes simultaneously in a volume of 50μL containing 1X Buffer J and 50U of each enzyme.

Incubate at 37°C for 2 hours.

Check digestion on an agarose gel; purify the digested plasmid using the Wizard SV Gel and PCR Clean-Up System (§ 3.2.13); dephosphorilate the digested plasmid (§ 3.4.3)and store for ligation reaction.

Set up ligation reaction using Polylinker:Vector molar ratio 10:1, optimal for single insertions.

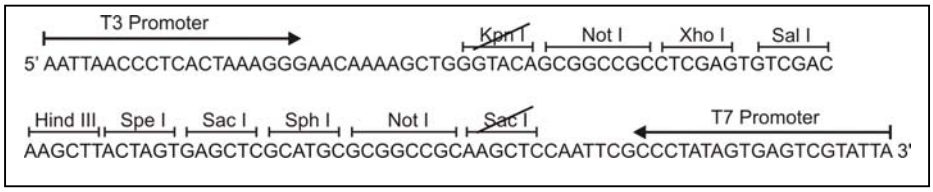

Figure 3.10. Multiple cloning site (polylinker) sequence inserted in pBS-plyA plasmid vector.

3.4.6. Site-specific mutagenesis PCR

Site-directed mutagenesis by PCR was used to introduce base substitutions in exons 4, 7 and 8 of mouse *dsg2* gene.

The mutagenesis results in an amplified product with a specific pre-determined mutation located in a central segment (Figure 3.11). Two PCR reactions (A and B) are envisaged as amplifying overlapping segments of DNA containing an introduced mutation (by deliberate base mismatching using mutant primers: 1M reverse and 2M forward). Then the two products are combined, denatured and allowed to reanneal, the DNA polymerase can extend the 3' end of heteroduplexes with recessed 3' ends. Thereafter, a full-length product with the introduced

mutation in a central segment can be amplified by using the outer primers (1forward and 2reverse) only.

Mismatched primers mutagenesis were designed to be complementary to the target site, exception made for a specific position, in which the nucleotide variation was introduced; the outer primers were designed to include restriction sites useful to allow wild-type fragments substitution with mutated fragments in targeting vector (Table 3.7).

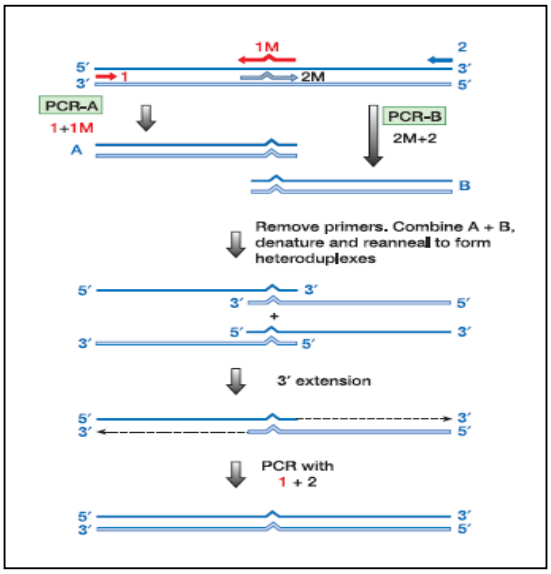

Figure 3.11. Site-specific mutagenesis. Two mutagenic reactions (A and B) are designed in which the two separate PCR products have partially overlapping sequences containing the mutation. The denatured products are combined to generate a larger product with the mutation in a more central location (1, primer forward 1F; 1M, mutant primer reverse 1MR; 2M, mutant primer forward 2MF; 2, primer reverse 2R). (from Strachan, 2003).

MATERIALS:

- Template DNA
- Primers (10pmol/μL, Sigma Genosys)
- Deoxinucleotide triphosphate (dNTPs 10mM, Invitrogen)
- Phusion High-Fidelity DNA Polymerase (2U/μL, Finnzymes)
- 5X Phusion HF Buffer (Finnzymes)
- MilliQ water
- microcentrifuge tube
- Thermal cycler (MJ Research)

PROCEDURE:

Amplifying overlapping segments (PCRs A and B):

Place approximately 1ng of DNA template (7041bp *dsg2* fragment cloned into pBS-plyA plasmid) in a sterile microcentrifuge tube.

Carry out PCRs in quadruple in a 50μL volume containing 250nM of each primer, 250μM deoxinucleotide triphosphate, 1X HF Buffer, and 1U of Phusion HF DNA Polymerase.

After activation of the enzyme (98°C for 30 sec), repeat cycling conditions (denaturation at 98°C for 8 sec, annealing at the working temperature for 20 sec, extension at 72°C for 15 sec) 30 times in a termal cycler.

For each PCR, mix four volumes, load and run onto an agarose gel, and gel purify the band using the Wizard SV Gel and PCR Clean-Up System (§ 3.2.13).

Check PCR concentration on gel electrophoresis.

Combining PCRs A and B to generate final product:

Place 2ng of PCR A and PCR B in a sterile microcentrifuge tube.

Carry out the first step in 6 vials in a 45μL volume adding 250μM deoxinucleotide triphosphate, 1X HF Buffer, and 1U of Phusion HF DNA Polymerase.

Activate the enzyme at 98°C for 3 minutes, and repeat cycling conditions (denaturation at 98°C for 8 sec, annealing at the working temperature for 20 sec, extension at 72°C for 20 sec) 10 times in a termal cycler, allowing products combination, denaturation and extension.

Add 500nM of each outer primer and proceed with second step repeating cycling conditions (denaturation at 98°C for 8 sec, annealing at the working temperature for 20 sec, extension at 72°C for 20 sec) 25 times, to allow amplification of full-length product.

Mix six PCR volumes, load and run onto an agarose gel.

Purify the band from gel using the Wizard SV Gel and PCR Clean-Up System (§ 3.2.13) and check the final product concentration on gel electrophoresis.

Digest the fragment with the desired enzyme (on the basis of the restriction sites included in the outer primers sequence) and clone in targeting vector, substituting the wild-type fragment.

Table 3.7. Sequence of primers, size of amplicons and amplification annealing temperatures used to generate *dsg2* mutations by site-specific mutagenesis PCR.

dsg2 mutation (exon)	PCR	Size (bp)	Forward 5'-3'	Reverse 5'-3'	PCR T_{ann} °C
G105R (ex4)	A	818	1F: acaagcttactagtgagctctccactagcac	1MR: aagacgaatatgcGgaaaggcggttctg	65
	B	504	2MF: cagaaccgcctttcCgcatattcgtctt	2R: agtgcctgtaactagtttcaggggatccg	65
	Final	1294	1F: acaagcttactagtgagctctccactagcac	2R: agtgcctgtaactagtttcaggggatccg	65
N271S (ex7)	A	407	1F: ctttgtttgaagaattcatctcctaagac	1MR:caggtatattgtcaCtgacatccaatat	65
	B	444	2MF: atattggatgtcaGtgacaatatacctg	2R: agcaatgctggtaccaactgatgtc	65
	Final	823	1F: ctttgtttgaagaattcatctcctaagac	2R: agcaatgctggtaccaactgatgtc	62
K299E (ex8)	A	580	1F: ctttgtttgaagaattcatctcctaagac	1MR: gcatcggtcacttCgatccgcatg	65
	B	267	2MF: catgcggatcGaagtgaccgatgc	2R: agcaatgctggtaccaactgatgtc	65
	Final	823	1F: ctttgtttgaagaattcatctcctaagac	2R: agcaatgctggtaccaactgatgtc	62

Base mismatching is reported in capital letter in mutant primers (2MF and 2MR). Outer primers (1F and 2R) for G105R mutation include *Spe*I restriction sites (5'actagt3'). Outers primers for N271S and K299E mutations were the same: 1F carries *EcoR*I restriction site (5'gaattc3') and 2R carries *Kpn*I restriction site (5'ggtacc3').

3.4.7. Chemical transformation of competent *E.coli* (DH5α)

DH5α commercial competent cells transformation efficiency should be greater than $1x10^6$ transformants/μg of cyclized DNA.

Because circular DNA (even nicked circular DNA) transforms much more efficiently than linear DNA, most of the cell transformants will contain cyclized products rather than linear recombinant DNA concatemers and, if an effort has been made to suppress vector cyclization (e.g. by dephosphorylation), most of the transformants will contain recombinant DNA.

MATERIALS:

- DH5α™ Competent Cells (Invitrogen)
- 5μL (1-10ng) of purified ligation solution
- 1.5mL microcentrifuge tubes
- Water bath
- LB medium:
  bacto-tryptone 10g
  bacto-yeast extract 5g
  NaCl 10g
  to 1L with deionized H_2O; shake until the solutes have dissolved; adjust the pH to 7.0 with 5N NaOH; sterilize by autoclaving.
- LB-Agar plates containing 100μg/mL Ampicillin:
  bacto-tryptone 10g
  bacto-yeast extract 5g
  NaCl 10g
  bacto-agar 10g
  to 1L with deionized H_2O; shake until the solutes have dissolved; adjust the pH to 7.0 with 5N NaOH; sterilize by autoclaving; allow the medium to cool to 50°C before adding 100μg/mL thermolabile ampicillin; pour 25mL of medium per 90mm Petri plate.
- 37°C oven.

PROCEDURE:

Thaw on ice one tube of DH5α Competent Cells. Place 1.5mL micro centrifuge tubes on wet ice.

Aliquot 50μL of cells for each transformation into a 1.5mL micro centrifuge tube.

Add 5μL of purified ligation solution (see § X) to the cells and mix gently.

Incubate tubes on ice for 30 minutes.

Heat shock cells for 1 minute in a 42°C water bath without shaking.

Place tubes on ice for 1-2 minutes.

Add 1mL of pre-warmed LB medium to each tube and incubate at 37°C for 1 hour with shaking at 2250rpm.

Centrifuge the cells for some seconds at 8000 rpm and resuspend the pellet in 200μL of LB medium.

Spread up to 200μL of transformation on pre-warmed selective plates.

Incubate plates overnight at 37°C.

The day after, count the number of colonies on each plate. Dephosphorylation should reduce the transformation efficiency of linear plasmid DNA by a factor of at least 50 (ligation A versus ligation C). Ligation of foreign DNA (ligation B) to dephosphorylated linear plasmid DNA should increase the transformation frequency by a factor of at least 5 (ligation B versus ligation C).

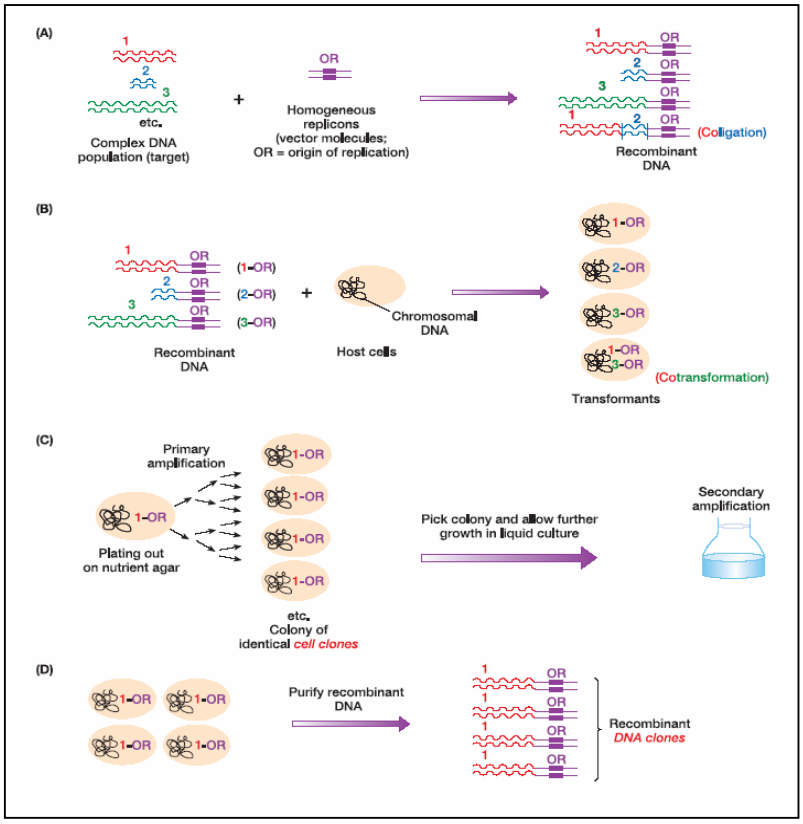

Figure 3.12: Essential steps of cell-based DNA cloning. (A) Formation of recombinant DNA. Note that, in addition to simple vector–target ligation products, co-ligation events may occur whereby two unrelated target DNA sequences may be ligated in a single product (e.g. sequences 1 plus 2 in the bottom example). OR, origin of replication. (B) Transformation. Cells normally take up only one foreign DNA molecule. Note that occasionally, however, co-transformation events are observed. (C) Amplification to produce numerous cell clones. After plating out the transformed cells, individual clone colonies can be separated on a dish and then individually picked into a secondary amplification step to ensure clone homogeneity. (D) Isolation of recombinant DNA clones(from Strachan, 2003).

3.4.8. Extraction and purification of plasmid DNA

a. Small-scale preparations of plasmid DNA

Mini preparations of plasmid DNA from DH5α colonies was obtained by the alkaline lysis method of the Wizard Plus SV Minipreps DNA Purification System (Promega) (§ 3.2.16).

b. Large-scale preparations of plasmid DNA

Midi preparations of plasmid DNA was obtained by Pure Yield Plasmid Midiprep System (Promega). This system is designed to purify (by a combination of centrifugation and vacuum) 100-200μg of plasmid from a large volume (50-250mL) overnight culture of bacteria.

MATERIALS:

- DH5α bacterial cell culture
- Vacuum manifold
- PureYield Plasmid Midiprep System (Promega):
  Cell Resuspension Solution (CRA)
  Cell Lysis Solution (CLA)
  Neutralization Solution (NSB)
  Endotoxin Removal Wash
  Column Wash Solution
  PureYield Clearing Columns
  PureYield Binding Columns
  Nuclease-Free Water
- 1.5mL tubes
- Centrifuge
- 50mL centrifuge tubes
- 37°C oven

PROCEDURE:

Grow 150mL of transformed bacterial cell culture overnight at 37°C.

Pellet the cells using centrifugation at 5000×g for 10 minutes and discard supernatant.

Use the PureYield Plasmid Midiprep System for isolation of plasmid DNA.

Resuspend the cell pellets in 4mL of Cell Resuspension Solution.

Add 4mL of Cell Lysis Solution, mix by gently inverting the tube 3-5 times and incubate for 3 minutes at room temperature.

Add 6.6mL of Neutralization Solution to the lysed cells and mix by gently inverting the tube 5-10 times.

Centrifuge the lysate at 15000×*g* for 15 minutes. This centrifugation will pellet the bulk of the cellular debris. Remaining debris is removed using the Clearing Columns.

Assemble a column stack by nesting a Clearing Column into the top of a Binding Column. Place the assembled column stack onto the vacuum manifold.

Decant the cleared lysate into the Clearing Column and apply vacuum. Continue the vacuum until all the liquid has passed through both columns: the DNA will bind to the binding membrane in the Binding Column.

Slowly release the vacuum and remove the Clearing Column.

Add 5mL of Endotoxin Removal Wash to the Binding Column, and allow the vacuum to pull the solution through the column.

Add 20mL of Column Wash Solution to the Column, and allow the vacuum to draw the solution through.

Dry the membrane by applying a vacuum for 30 seconds to 1 minute to remove ethanol excess.

Remove the Binding Column from the vacuum manifold and place the column into a new 50mL conical centrifuge tube.
To elute the DNA, add 600µL of Nuclease-Free Water to the DNA binding membrane in the Binding Column.
Centrifuge the Binding Column at 2,000×*g* for 5 minutes.
Collect the filtrate from the 50mL tube and transfer to a 1.5mL tube.
Check DNA concentration on spectrophotometer and quality on gel.
Store the midi-prep DNA at -20°C.

3.4.9. Analysis of positive clones

Plasmid DNA isolated from selected bacterial colonies was analyzed by enzyme digestion and agarose gel electrophoresis to test fragment ligation in the vector. Then T7 and T3 primers flanking pBS-plyA polylinker allowed direct sequencing of insert.

3.4.10. Glycerol stock solution

Every construct in *E.coli* strains was stored and maintained as a glycerol stock at -80°C in medium containing 30% glycerol.

MATERIALS:

- *E.coli* colonies on LB-Agar plates containing 100µg/mL Ampicillin
- LB medium, 100µg/mL Ampicillin (see§X)
- Sterile glycerol 100%
- 2mL screw-cap vials
- 37°C oven

PROCEDURE:
Pick a single colony of the clone off of a plate and grow overnight at 37°C in the appropriate selectable liquid medium (LB-Ampicillin).
The day after, add 1mL *E.coli* liquid colture and 0.5mL sterile glycerol to a sterile 2mL screw-cap vial.
Vortex the vial vigorously to ensure even mixing of the bacterial culture and the glycerol.
Freeze the glycerol stock at -80°C.

3.5. BIOINFORMATIC TOOLS

BCM SERCH LAUNCHER (Baylor College of Medicine Search Launcher)
(http://searchlauncher.bmc.tmc.edu)
Integrated set of Web pages that organize molecular biology-related search and analysis services available by function by providing a single point of entry for related searches. Launch pages provide access to nucleic acid sequence searches, protein sequence searches, multiple and pair-wise sequence alignments, gene feature searches, protein secondary structure prediction, and miscellaneous sequence utilities. The BCM Search Launcher also provides a mechanism to extend the utility of other services by adding supplementary hypertext links to results returned by remote servers.

BLAST (Basic Local Alignment Search Tool)
(http://www.ncbi.nlm.nih.gov/BLAST)
Program provided by NCBI for comparing nucleotide or protein sequences to library or database of sequences and calculates the statistical significance of matches. BLAST can be used to infer functional and evolutionary relationships between sequences as well as help identify members of gene families.

CLUSTAL W
(http://www2.ebi.ac.uk/clustalw/)
General purpose multiple sequence alignment program (provided by European Bioinformatics Institute) for DNA or proteins. It produces biologically meaningful multiple sequence alignments of divergent sequences. It calculates the best match for the selected sequences, and lines them up so that the identities, similarities and differences can be seen.

dbSNP (Single Nucleotide Polymorphism Database)
(http://www.ncbi.nlm.nih.gov/projects/SNP)
One of the most important data sources for the geneticist involved in disease mapping. The dbSNP is a division of GenBank. The NCBI astablished the dbSNP in september 1998 as a central repository for both SNPs and short INDEL polymorphisms. In December 2007 dbSNP contain more than 7.0 millions SNPs from 16 organisms. These SNPs collapse into a non-redundant set of these RefSNPs do not currently map to the draft human genome. These quantities of SNPs give a high level of coverage across the genome.

Ensembl
(http://www.ensembl.org)
Joint project between EMBL - European Bioinformatics Institute (EBI) and the Wellcome Trust Sanger Institute (WTSI). The Ensembl database, launched in 1999, was the first to provide a window to the draft genome, curating the results of a series of computational analyses. Until January 2002 Ensembl used the UCSC draft sequence assemblies as its starting point but it is

now based upon NCBI assemblies. The Ensembl analysis consist of a ruled-based system designed to mimic decision made by a human annotator. The idea is to identify "confirmed" genes that are computationally predicted and also supported by a significant BLAST match to one or more expressed sequence or proteins. The total set of Ensambl genes should therefore be a much more accurate reflection of reality than *ab initio* prediction alone but it is clear that many novel genes are missed. Many other genomic features have been included in Ensembl: different repeat classes, cytological bands, CpG island prediction, tRNA gene prediction, expressed sequence cluster from the UniGene database, SNPs from the dbSNPs database, disease gene found in the draft genome from the OMIM database, and regions of homology to mouse draft genomic sequences.

Entrez

(http://www.ncbi.nlm.nih.gov/entrez)

Integrated, text-based search and retrieval system used at NCBI for the major databases, including PubMed, Nucleotide and Protein Sequences, Protein Structures, Complete Genomes, Taxonomy, and others. The current version is listed as a build number on the genome view page and includes an accompanying set of statistics and released notes.

GDB (Genome Database)

(http://www.gdb.org)

Established ahead of most other genetics databases in 1990 as a central repository for mapping information from the human genome project, throughout the early 1990s GDB was the dominant genome database and served as the primary repository for genetic map-related information.

Today GDB is still one of the most comprehensive sources for some forms of genetic data, including tandem repeat polymorphisms, it also contains an electric range of information on fragile sites, deletions, disease genes and mutations, collected by a mixture of curation and direct submission. GDB development is ongoing and the historical focus of the database on genetic maps is broadening to a more integrated view of the genome ultimately down to the sequence level.

GenBank

(http://www.ncbi.nlm.nih.gov/Genbank)

Sequence database produced at NCBI annotating collection of all publicly available nucleotide sequences and their protein translations from more than 100,000 distinct organisms. GenBank continues to grow at an exponential rate, doubling every 10 months. Release 155, produced in August 2006, contained over 65 billion nucleotide bases in more than 61 million sequences.

GeneCards

(http://www.genecards.org)

Database of human genes, their products and their involvement in diseases. It offers concise information about the functions of all human genes that have an approved symbol, as well as selected others. The information presented in GenCards has been automatically extracted from various resources. GeneCards is particulary useful for people who wish to find information about genes of interest in the context of functional genomics and proteomics. This resource also features a new type of navigation support system that guides its users to the information. Important parts of this guidance system are the spell corrector, and the automatically generated tips for query reformulation.

NCBI (National Center for Biotechnology Information)

(http://www.ncbi.nlm.gov)

Established in 1988 as a division of the National Library of Medicine (NLM) at the National Institutes of Health (NIH), NCBI represent a national resource for molecular biology information; it creates public databases, conducts research in computational biology, develops software tools for analyzing genome data, and disseminates biomedical information - all for the better understanding of molecular processes affecting human health and disease.

NEB CUTTER V2.0

(http://tools.neb.com/NEBcutter2/index.php)

On-line DNA sequence tool (from New England BioLabs) to find large, non-overlapping, open reading frames and sites for all restriction enzymes.

OMIM (Online Mendelian Inheritance in Man)

(http://www.ncbi.nlm.nih.gov/OMIM)

On-line catalogue of human genes and their associated mutations, based on the long running catalogue Mendelian Inheritance in Man (MIM) stated in 1967 by Victor McKusick at Johns Hopkins. OMIM is an excellent resource for providing a brief background biology on genes and diseases, it includes information on the most common and clinically significant mutations and polymorphisms in genes. As the name suggest, this focuses on mendelian monogenic disorders, although it also offers some coverage of complex disease. As a manually curated digest of the literature extracted from the full text of publications it can contain more information than PubMed. Although this has the disadvantage that not all entries are fully comprehensive or current, the database usually captures the most salient information and is therefore a good place to start. In addition OMIM is fully integrated with the NCBI database family. This facilitates rapid and direct linking between disease, gene sequence and chromosomal locus.

Primer3

(http://frodo.wi.mit.edu/primer3/)

Program developed and supported from WI/MIT, used for building PCR primers. Some of the most important issues in primer picking can be addressed only before using Primer3. These are sequence quality and avoiding repetitive elements. Sequence quality can be controlled by manual trace viewing and quality clipping or automatic quality clipping programs. Low-quality bases should be changed or can be made part of Excluded Regions. The beginning of a sequencing read is often problematic because of primer peaks, and the end of the read often contains many low-quality or even meaningless called bases. Therefore when picking primers from single-pass sequence it is often best to use the Included Region parameter to ensure that Primer3 chooses primers in the high quality region of the read.

TrEMBL

(http://www.ebi.ac.uk/trembl/index.html)

Protein sequence database of nucleotide translated sequences. UniProt/TrEMBL is a computer-annotated protein sequence database complementing the UniProt/Swiss-Prot Protein Knowledgebase. UniProt/TrEMBL contains the translations of all coding sequences (CDS) present in the EMBL/GenBank/DDBJ Nucleotide Sequence Databases and also protein sequences extracted from the literature or submitted to UniProt/Swiss-Prot. The database is enriched with automated classification and annotation.

UCSC Human Genome Browser

(http://genome.ucsc.edu)

Browser (HGB) that bears many similarities to Ensembl: it too provides annotation of the NCBI assemblies and it displays a similar array of features, including confirmed genes fron Ensembl. An useful feature of HGB is the detailed description of the genomic sequence assemblies. Graphical representation of the fragments making up a region of draft genome can be displayed, showing the relative size and overlaps of each fragment and also whether any gaps between fragment are bridged by mRNAs or paired BAC end sequences. This means that one can get an idea of the likely degree of misassembly in a draft region. There is an increasing amount of data becoming available from large-scale gene expression studies.

UniProt-SwissProt

(http://www.ebi.ac.uk/swissprot/)

Annotated protein sequence database established in 1986 maintained collaboratively by the Swiss Institute for Bioinformatis (SIB) and the European Bioinformatics Institute (EBI). It provides a high level of annotation, a minimal level of redundancy and high level of integration with other databases. UniProt, a "one-stop shop" that allows easy access to all publicly available information of protein sequence annotation.

WI/MIT (Whitehead Institute for Biomedical Research / MIT Center for Genome Research) (http://frodo.wi.mit.edu)

Web site from Whitehead Institute for Biomedical Research sharing a teaching affiliation with Massachusetts Institute of Technology. They run pioneering programs in cancer research, immunology, developmental biology, stem cell research, regenerative medicine, genetics and genomics programs with a record of success

4. RESULTS

4.1. MUTATION SCREENING IN KNOW ARVC/D GENES

The study population consisted of 110 index cases (75 males and 35 females; all Italian, exception made for the German patient #105). All of them satisfied task force diagnostic criteria. For about 50% of them, family history reported the occurrence of additional cases of ARVC/D.
Main clinical characteristics of the study population are summarized in Table 4.1.
Mutation screening of coding regions of such genes was performed by denaturing high-performance liquid chromatography (DHPLC) and direct sequencing. Temperatures for DHPLC analyses were predicted using the NAVIGATOR™ software (Trangenomic). Samples showing a change in DHPLC elution pattern were directly sequenced. Some exons were analyzed only by direct sequencing, because of the presence of GC-rich segments or repeats.
A control group of 200 healthy and unrelated subjects (400 alleles) from the Italian population was used to exclude (by DHPLC analysis or cleavage with restriction enzymes) that detected mutations could be common DNA polymorphisms. DNA variations detected in more than 1% of healthy controls chromosomes were considered as polymorphisms.

Table 4.1. Main clinical features in ARVC/D study population (110 subjects).

	n	%
Male	75	68
Mean age (years)	42±16	
Mean age at presentation (years)	33±14	
Family history of ARVC/D	51	46
Non sustained VT	49	45
Sustained VT/VF	37	34
Biventricular involvement	31	28
RV dilatation	91	83
Pathological ECG	78	71
Localized QRS prolongation in V1–V3	38	35
Complete RBBB	14	13
TWI V1-V2±V3	24	22
TWI extending beyond V3	27	25
TWI lateral leads only	7	6
Presence of late potentials	76	69
Presence of epsilon wave	11	10
ICD implantation	14	13
RVEDV (mL/m^2)	89±29	
RVEDA (cm^2)	24±5	
RVEF (%)	53±10	

VT, ventricular tachycardia; VF, ventricular fibrillation; RV, right ventricular; RBBB, right bundle-branch block; TWI: T-wave inversion, ICD, implantable cardioverter defibrillator; RVEDV, right ventricular end-diastolic volume; RVEDA, right ventricular end-diastolic area; RVEF, right ventricular ejection fraction.

4.1.1. Mutations in PKP2 gene

All 110 ARVC index cases were investigated for mutations in 14 exons of PKP2 gene. Sixteen heterozygous mutations (eight novel: E58D, Q62DfsX22, N76S, K112N, S209R, Q211X, I778T, and T816RfsX9) were identified in twenty-two of them (Table 4.2).

PKP2 cDNA and translation sequences were compared to reference sequences NM_001005242 and NP_001005242, respectively.

Table 4.2. Variations detected in PKP2 gene.

Mutation	Amino Acid Change	Type of mutation	Exon	Position (protein domain)	# Index case	Reference
145_148delCAGA	T50SfsX60	deletion, frameshift	1	N-terminal	16,34,57,62, 80	Gerull et al., 2004 Syrris et al., 2006 Dalal et al., 2006
174G>T	E58D	missense	1	N-terminal	36	novel
184C>A	Q62K	missense	1	N-terminal	40	Van Tintelen et al., 2006 (unclassified variant) Lahtinen et al., 2007
184_185delCA	Q62DfsX22	deletion, frameshift	1	N-terminal	89	novel
227A>G	N76S	missense	2	N-terminal	24	novel
336G>T	K112N	missense	2	N-terminal	107	novel
397C>T	Q133X	nonsense	3	N-terminal	61	Van Tintelen et al., 2006
419C>T	S140F	missense	3	N-terminal	106	Gerull et al., 2004 Syrris et al., 2006 Dalal et al., 2006
627C>G	S209R	missense	3	N-terminal	18	novel
631C>T	Q211X	nonsense	3	N-terminal	39	novel
1642delG	G548VfsX14	deletion, frameshift	7	A-4	50,96	Gerull et al., 2004 Dalal et al., 2006
1759G>A	V587I	missense	8	A-4	54	Basso et al., 2006
2010delC	K672RfsX11	deletion, frameshift	10	A-5	2,6,81	Dalal et al., 2006 Basso et al., 2006
2119C>T	Q707X	nonsense	10	A-5	40	Basso et al., 2006
2333T>C	I778T	missense	12	A-7	39	novel
2447_2448delCC	T816RfsX9	deletion, frameshift	12	A-8	3,18,73	novel
Polymorphism	**Amino Acid Change**	**Type of variation**	**Exon**	**Position (protein domain)**	**# Index case**	**Reference**
76G>A	D26N	missense	1	N-terminal	110	Van Tintelen et al., 2006 (unclassified variant)
209G>T	S70I	missense	1	N-terminal	49	novel
2431C>A	R811S	missense	12	A-8	93	novel

Among the 16 mutations identified, 5 were deletions, 3 nonsense (resulting in a premature termination codon), and 8 missense mutations. Six missense mutations were not detected in control population and resulted to affect conserved residues in functional domains of plakophilin-2; on the contrary, the novel E58D variation and the previously described Q62K variant (Van Tintelen et al., 2006; Lahtinen et al., 2007) affect a residue highly variable among species in the N-terminal not conserved domain of plakophilin; E58D was found in control population at a frequency of 0.7%, Q62K was detected in nether of 200 healthy controls.

Four mutations were identified in more than one index case. The previously described deletion c.145_148delCAGA was detected in five patients; this mutation causes a frame shift that leads to a premature termination codon (T50SfsX60) within the N-terminal domain of plakophilin-2. The known single base pair deletions c.1642delG and c.2010delC, detected in two and three patients respectively, are located in the conserved Arm repeat domains and result in frame shifts and premature termination of translation several amino acid residues downstream (G548VfsX14, K672RfsX11). In particular, mutation c.2010delC causes deletion of one among four consecutive cytosines (c.2010-2013); since it is impossible to establish which of them is involved in the deletion, we decided to consider the first cytosine as the deleted one. Thus, it is impossible to exclude that the previously reported 2011delC (Dalal et al., 2006) corresponds to the same deletion; in any case, the resulted truncated protein should be the same. A novel deletion in exon 12 (2447_2448delCC) was detected in three patients: it causes the addition of eight amino acid residues before a premature stop codon is introduced (T816RfsX9); the predicted truncated plakophilin-2 molecule lacks the last Arm domain.

Three index patients carried two PKP2 variants. Subject #18 was heterozygote for a missense mutation in exon 3 (S209R) and for the novel two base pairs deletion in exon 12 resulting in predicted truncated protein (T816RfsX9). Subject #39 carried a nonsense mutation (Q211X) causing premature termination of translation within the exon 3, and a missense mutation (I778T) in exon 12. In subject #40 Q62K missense variant was identified exon 1 and Q707X stop mutation in exon 10. The molecular analysis of available parents demonstrated that such mutations are carried in *trans*.

Relative position of mutations detected by the study is reported in Figure 4.1.

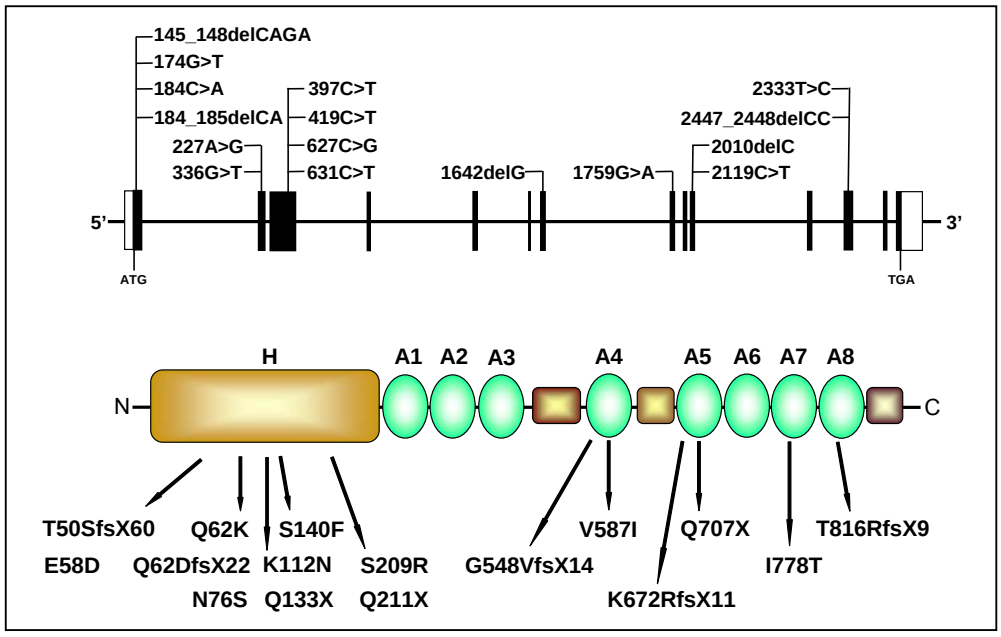

Figure 4.1. (Top) Schematic organization of the human PKP2 gene (exons are represented by vertical black boxes, and introns are represented by horizontal lines). **(Bottom)** The encoded protein PKP2, includes a head domain (H) followed by 8 Arm domains (A1-A8). Position of the 16 PKP2 mutations detected by the study is indicated.

In the course of the screening, some intronic and exonic single nucleotide polymorphisms (SNPs) were detected. Novel SNPs (not reported in dbSNP) are indicated in Table 4.2. The amino acid change D26N, described by Van Tintelen (Van Tintelen et al., 2006) as an "unclassified variant", since it involves a residue not conserved among different species, was detected in healthy controls with a frequency of 2.4% and therefore considered a polymorphism. Two novel PKP2 exonic single nucleotide polymorphisms were identified. They involve amino acids conserved among species causing missense changes S70I and R811S; both variations were found in control population with a frequency of 2.4%.

4.1.2. Mutations in DSP gene

Mutations screening for coding regions (exons 1 to 24) of DSP gene was performed in all 110 index cases. Eighteen heterozygous variants (ten novel: Q273X, N375I, N458Y, E1068VfsX18, R1113X, D1258E, M1601I, L1654P, S2108X and R2541K) were identified in eighteen index patients (Table 4.3).

DSP cDNA and translation sequences were compared to reference sequences NM_004415 and NP_004406, respectively.

Table 4.3. Variations detected in DSP gene.

Mutation	Amino Acid Change	Type of mutation	Exon	Position (protein domain)	# Index case	Reference
88 G>A	V30M	missense	1	N-terminal	8,29,83	Yang et al., 2006
273+5G>A	-	splice site	intr 2	N-terminal	23	Basso et al., 2006
423-1G>A	-	splice site	intr 3	N-terminal	46	Bauce et al., 2005
817 C>T	Q273X	nonsense	7	N-terminal	105	novel
897C>G	S299R	missense	7	N-terminal	44	Rampazzo et al., 2002
1124A>T	N375I	missense	9	N-terminal	97	novel
1372A>T	N458Y	missense	11	N-terminal	71	novel
1408A>G	K470E	missense	11	N-terminal	38	Basso et al., 2006
1696G>A	A566T	missense	13	N-terminal	38	Basso et al., 2006
3203_3204delAG	E1068VfsX18	deletion, frameshift	23	Rod domain	88	novel
3337C>T	R1113X	nonsense	23	Rod domain	5	novel
3764G>A	R1255K	missense	23	Rod domain	39	Bauce et al., 2005
3774C>A	D1258E	missense	23	Rod domain	103	novel
4803G>A	M1601I	missense	23	Rod domain	45	novel
4961T>C	L1654P	missense	23	Rod domain	40	novel
5324G>T	R1775I	missense	23	Rod domain	92	Bauce et al., 2005
6323C>G	S2108X	nonsense	24	C-terminal	102	novel
7622G>A	R2541K	missense	24	C-terminal	83	novel

Polymorphism	Amino Acid Change	Type of variation	Exon	Position (protein domain)	# Index case	Reference
273+10C>T	-	intronic	intr 2	-	21,47	novel
777+84C>T	-	intronic	intr 6	-	108	novel
1141-146C>T	-	intronic	intr 9	-	4	novel
1574+14G>T	-	intronic	intr12	-	37	novel
3963G>A	Q1321Q	synonymous	23	Rod domain	28,98	novel
4773G>A	R1591R	synonymous	23	Rod domain	62,64	novel

Twelve were missense mutations, two were splice mutations, three were nonsense mutations, and one was a single base pair deletion.

Neither of missense variants was detected among 400 healthy control chromosomes; all (exception made for V30M and R2541K) involved residues conserved among species.

In one patient (#38), two different desmoplakin missense mutations (K470E and A566T) were detected (Basso et al., 2006).

One mutation (V30M) occurred in three unrelated patients: two of them recruited as isolated cases, the other one belonged to a family showing additional ARVC/D cases. This latter patient (#83) was found to carry V30M and R2541K mutations with *in trans*. Both Val30 and Arg2541 residues are not highly conserved among species (Figure 4.2). The V30M mutation occurs in the head region of desmoplakin, involved in binding to the linker proteins (JUP and PKPs) of desmosomes. Recent studies *in vitro* demonstrated that this missense mutation affect the normal localization of DSP, probably causing loss of binding to JUP as shown by protein–protein interaction analysis; in addition, overexpression of the N-terminal mutant in embryonic mouse hearts can induce embryonic lethality (Yang et al., 2006).

On the contrary, pathogenic effect of R2541K variation (involving C-terminal domain) cannot be established until functional assays will be performed also for such variation.

Homo_sapiens	ESGPDLRYEVTSGG-----	DAIDKGLVDRKFFDQYRSG	NP_004406
Pan_troglodytes	----------\----------	DAIDKGLVDRKFFDQYRSG	XM_001165463
Mus_musculus	ESGPDLRYEMTSGG-----	DAIDKGLVDRKFFDQYRSG	XM_001481272
Rattus_norvegicus	ESGPDLRYEMTYSG-GGGG	DAIDKGLVDRKFFDQYRSG	XM_001058477
Bos_taurus	ESGPDLRYEMTCGGVGGGG	DTIDKGLIDRKFFEQYRSG	XM_876261
Gallus_gallus	DSGTDLRYEMSSHVVGGGG	DAIDKGLVEKKFFDQYRSG	XM_001231410
Danio_rerio	----------\----------	ESLQRGIINKQTLEKYRAG	XM_677652

Figure 4.2. ClustalW alignment of two not highly conserved regions of desmoplakin protein among species. Organism names and GenBank accession numbers are reported on sides. V30 and R2541 (that change in M and K, respectively, in index patient #83) are reported on a pink background. Not conserved residues are reported in blu.

Mutation c.273+5G>A (Basso et al., 2006) alters the donor splicing site of intron 2. After reverse transcription of lymphocytes RNA from patient #23, DSP cDNA corresponding to exons 1-3 was nested-PCR amplified and direct sequenced. Analysis failed to detect aberrant transcripts and showed only the wild-type allele, suggesting that the aberrant transcripts would be degraded, most likely through nonsense-mediated mRNA decay.

Mutation c.423-1G>A (Bauce et al., 2005) alters the acceptor splicing site of intron 3. Sequencing of the DSP transcript obtained from lymphocytes RNA of the probands #46 showed the skipping of exon 4 (Figure 4.3). This aberrant spliced mRNA contains a premature stop codon and should code for a truncated protein of 200 amino acids in length.

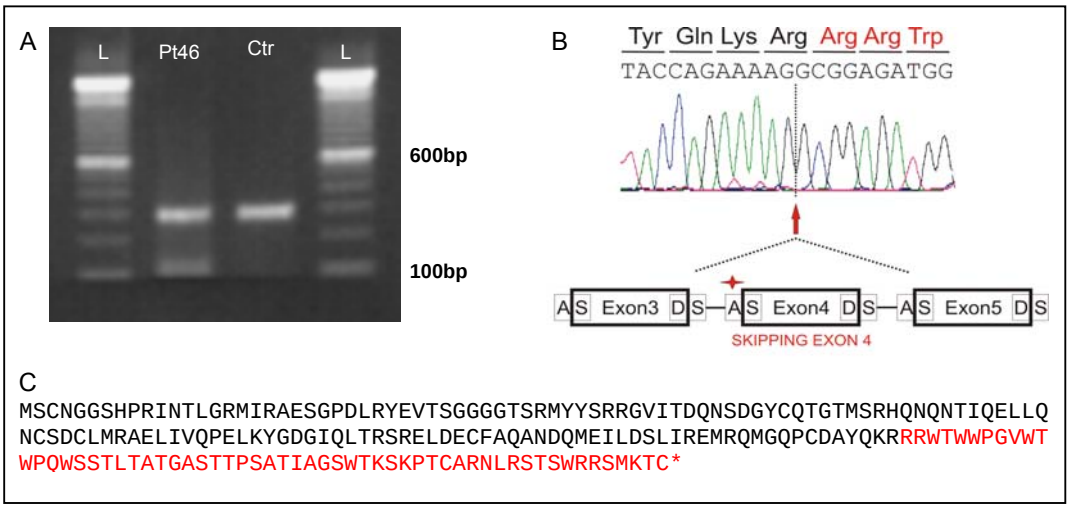

Figure 4.3. (A) RT-PCR analysis confirming the splice mutation c.421-1G>A. Index patient #46 (Pt46) shows mRNA wild-type of 288bp in length (same the healthy control cDNA, Ctr) and an aberrant spliced mRNA of 113bp in length resulting from the skipping of exon 4 (L=ladder 100pb). **(B)** Sequence electropherogram and schematic representation of altered splicing and skipping of exon 4 (AS=acceptor splice site; DS=donor splice site; asterisk=splice mutation c.421-1G>A). **(C)** Sequence of predicted protein containing only 200 amino acids for presence of a premature stop codon (*). The change introduced by the mutation is shown in red.

Relative position of DSP mutations detected by the study is reported in Figure 4.4.

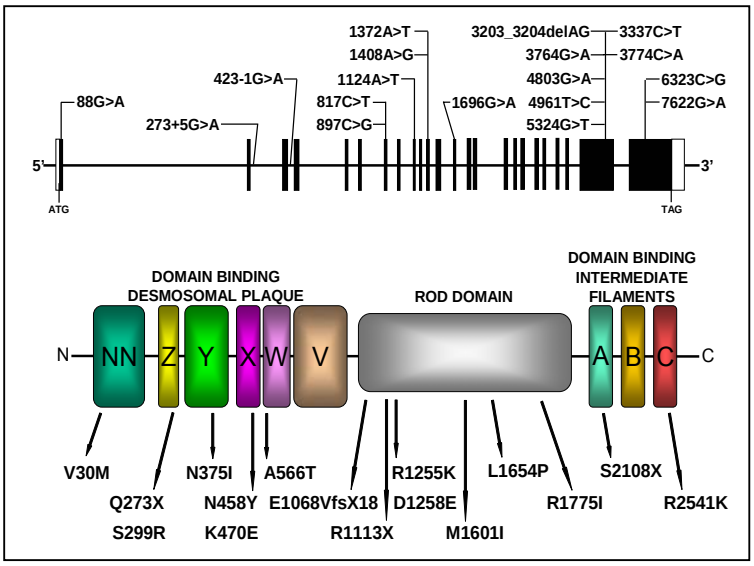

Figure 4.4. (Top) Schematic organization of the human DSP gene (24 exons are represented by vertical black boxes, and introns are represented by horizontal lines). **(Bottom)** The DSP protein contains several subdomains. A series of α-helical bundles, designated NN, Z, Y, X, W and V of the N-terminus protein are adjacent to the plasma membrane and interacts with armadillo proteins (including plakoglobin and plakophilins-2 and 4), as well as the cadherins desmocollin-2 and desmoglein-2. Flanking the central Rod Domain are the C-terminal A, B and C subdomains, that interact with desmin intermediate filament. Position of the 18 DSP detected mutations is indicated.

Four intronic and two exonic novel polymorphisms (SNPs) were detected in DSP sequence. Only SNPs not reported in dbSNP were indicated in Table 4.3.

4.1.3. Mutations in DSG2 gene

The coding regions of DSG2 gene (exons 1 to 15) was screened for mutations in all 110 study subjects. Seventeen DSG2 mutations have been identified in seventeen index cases (Table 4.4): one previously described (Syrris et al., 2007), nine recently published (Pilichou et al., 2006), and seven novel (R146H, E230G, D297G, G638R, L831F, P925S, and G997VfsX19). DSG2 cDNA and translation sequences were compared to reference sequences BC099657 and NP_001934, respectively.

Table 4.4. Variations detected in DSG2 gene.

Mutation	Amino Acid Change	Type of mutation	Exon	Position (protein domain)	# Index case	Reference
260A>G	Y87C	missense	4	EC1	7	Pilichou et al., 2006
298G>C	G100R	missense	4	EC1	33	Pilichou et al., 2006
437G>A	R146H	missense	5	EC1	18	novel
689A>G	E230G	missense	6	EC2	92	novel
797A>G	N266S	missense	7	EC2	10	Pilichou et al., 2006
880A>G	K294E	missense	8	EC3	85	Pilichou et al., 2006
890A>G	D297G	missense	8	EC3	92	novel
991G>A	E331K	missense	8	EC3	42	Pilichou et al., 2006
1174G>A	V392I	missense	9	EC4	62	Syrris et al., 2007
1254_1257insATGA	E418EfsX1	insertion, frameshift	9	EC4	87	Pilichou et al., 2006
1672C>T	Q558X	nonsense	12	EA	100	Pilichou et al., 2006
1881-2A>G	-	splice site	intr12	EA	42	Pilichou et al., 2006
1912G>A	G638R	missense	13	IA	34,97	novel
2036delG	G678AfsX2	deletion, frameshift	14	IA	91	Pilichou et al., 2006
2491C>T	L831F	missense	15	ICS	12,14,17	novel
2773C>T	P925S	missense	15	RUD	88	novel
2983delG	G997VfsX19	deletion, frameshift	15	RUD	87	novel

Polymorphism	Amino Acid Change	Type of variation	Exon	Position (protein domain)	# Index case	Reference
2137G>A	E713K	missense	14	IA	several	Basso et al., 2006

Among the 17 DSG2 mutations, 11 were missense, 3 insertion-deletions, 1 a nonsense, and 1 a splice site mutation. None of the detected nucleotide changes was found in the control group of 200 healthy and unrelated subjects.

Only one missense mutation (L831F) occurred in a residue not conserved in all considered species (Figure 4.5). It was detected in three index cases.

```
Homo_sapiens      DRFLDDLGLKFKTLAEV  NM_001943
Mus_musculus      DLFLDDLGLKFKTLAEV  NM_007883
Pan_troglodytes   DRFLDDLGLKFKTLAEV  XP_512079
Canis_familiaris  DGFLDDLGFKFRTLAEI  XP_547622
Macaca_mulatta    DRFLDDLGLKFKTLAEV  XM_001098597
Gallus_gallus     DHFLDDLGDKFKTLAEI  XP_426083
```

Figure 4.5. ClustalW alignment of a conserved region of desmoglein-2 protein among species, in which the L831 residue is reported on a yellow background. Organism names and GenBank accession numbers are reported on sides. Not conserved residues are reported in blu.

One mutation (G638R), located in the highly conserved transmembrane domain, occurred in two unrelated patients.

Three index patients resulted to carry two different DSG2 mutations. Molecular analysis of available family members demonstrated that such mutations are carried in *trans*.

Subject #42 carried a missense mutation in exon 8 (E331K) and a splice mutation (c.1881-2A>G) that affects the acceptor splice site of intron 12. Analysis of the aberrant DSG2 transcript was performed by nested-PCR from lymphocytes RNA of the proband. Amplification products were size separated by agarose gel electrophoresis, gel isolated, and directly sequenced; they showed that this mutation activates an alternative cryptic splice site in exon 13, located 38bp downstream from the authentic 3' splice acceptor site (Figure 4.6). This aberrant spliced mRNA contains a 38bp deletion and should code for a truncated protein of 646 amino acids in length, missing the cytoplasmic domain.

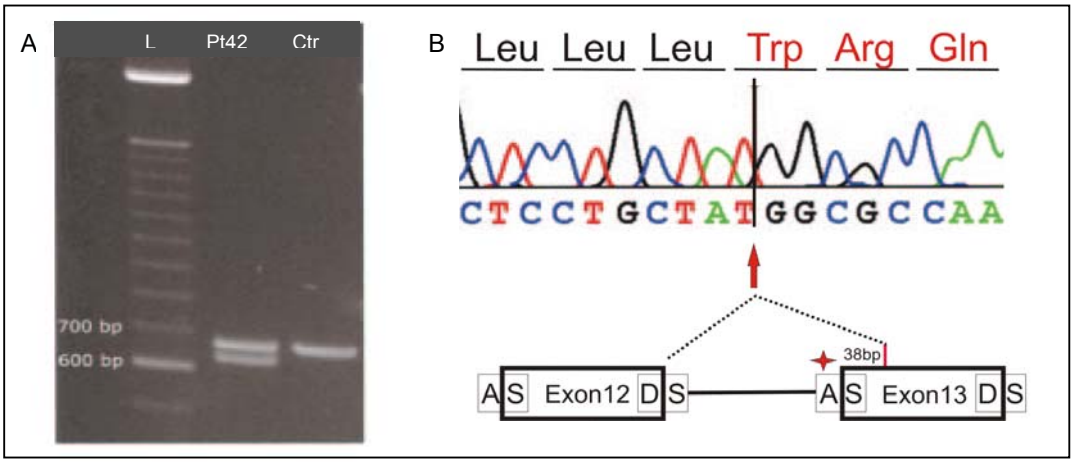

Figure 4.6. (A) Gel electrophoresis showing normal (668bp in length) and mutant (630bp) RT-PCR fragments caused by the DSG2 splice-site mutation (1881-2A>G). Index patient #42 (Pt42)shows both the wild-type and the aberrant spliced fragment (L=ladder 100pb; Ctr=Healthy Control cDNA). **(B)** Sequence electropherogram of the aberrant fragment and schematic representation of mutation (asterisk) that affects the acceptor splice site (AS) of intron 12 and activates an alternative cryptic splice site in exon 13 (DS=donor splice site). Predicted protein containing only 646 amino acids for presence of a premature stop codon. The change introduced by the mutation is shown in red.

The subject #87 was heterozygote for two DSG2 mutations: a four base pair insertion in exon 9 (c.1254_1257insATGA) that causing addition of an amino acid residue before a premature stop signal is introduced (E418EfsX1), and a single base pair deletions in exon 15 (c.2983delG) resulting in frameshifts and premature termination of translation several amino acid residues downstream (G997VfsX19). The predicted truncated DSG2 molecules would lack transmembrane and cytoplasmic components, and portion of cytoplasmic domain, respectively.

Two novel missense mutations were detected in subject #92. Both E230G and D297G occurred in residues highly conserved in different species and located in the extracellular cadherin (EC) domains. Cadherin domains are important for homophilic intercellular associations and form Ca^{2+}-dependent rodlike structures. All the inherent amino acid changes may destabilize the rod structure and influence the homophilic binding.

Relative position of DSG2 mutations detected by the study is reported in Figure 4.7.

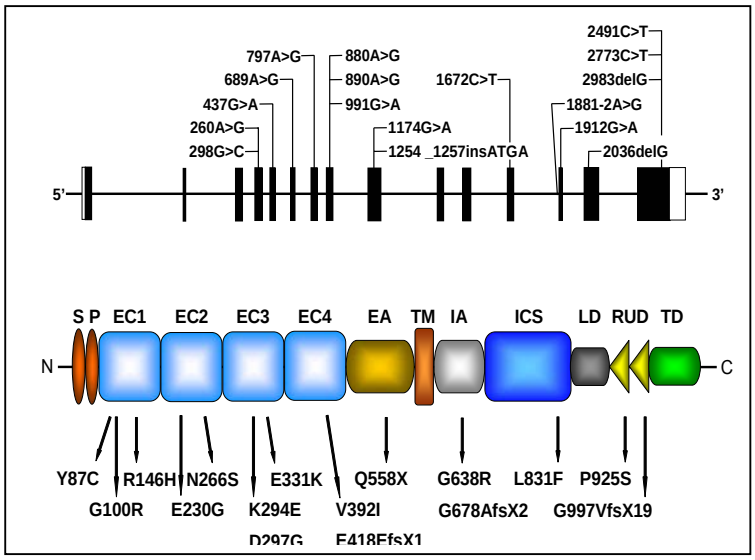

Figure 4.7. (Top) Schematic organization of the human DSG2 gene (15 exons are represented by vertical black boxes, and introns are represented by horizontal lines). **(Bottom)** The encoded DSG2 protein comprises a signal (S) domain and a preprotein (P) domain (both S and P domains lack in the functional protein) followed by 5 extracellular domains (EC1, EC2, EC3, EC4, and EA), a transmembrane domain (TM), an intracellular anchor domain (IA), an intracellular cadherin-typical segment domain (ICS), a linker domain (LD), a repeat unit domain (RUD) and a terminal domain (TD) . Position of the 17 detected mutations is indicated.

A polymorphism (E713K) was detected in exon 14 of DSG2 gene in several ARVC/D index cases. Although E713 was a residue conserved among species, the same amino acidic change was found in control population with an allelic frequency of 5%.

4.1.4. Mutations in DSC2 gene

Exon-by-exon analysis of coding sequences of DSC2 gene was performed on genomic DNA of all 110 ARVC index cases. Four mutations (one novel: c.631-10C>T) were identified in 5 of them (Table 4.5).

DSC2 cDNA and translation sequences were compared to reference sequences NM_004949 and NP_004940, respectively.

Table 4.5. Variations detected in DSC2 gene.

Mutation	Amino Acid Change	Type of mutation	Exon	Position (protein domain)	# Index case	Reference
304G> A	E102K	missense	3	P	78	Beffagna et al., 2007
631-10C>T	-	splice site	intr 5	-	60	novel
1034C>T	I345T	missense	10	EC2	55	Beffagna et al., 2007
2687_2688insGA	E896EfsX4	insertion, frameshift	16	ICS	7,36,97	Syrris et al., 2006
Polymorphism	**Amino Acid Change**	**Type of variation**	**Exon**	**Position (protein domain)**	**# Index case**	**Reference**
351A>G	T117T	synonymous	3	P	89	novel
2393G>A	R798Q	missense	15	IA	several	novel

Two heterozygous point substitutions c.304G>A and c.1034T>C were detected in two patients (Beffagna et al., 2007). None of the detected nucleotide changes was found in the control group of 200 healthy and unrelated subjects from Italian population. Mutations were confirmed by restriction digest. Two variations result in predicted E102K and I345T amino acid substitutions, respectively. The mutated amino acids shows completely different physico-chemical properties when compared to the wild type. Mutation E102K replaced a negatively-charged residue in the propeptide domain by a positively-charged one, whereas mutation I345T replaced a non polar hydrophobic amino acid by a polar hydrophilic amino acid in the second extracellular cadherin (EC2) domain.

The insertion c.2687_2688insGA, previously described as a recurrent mutation (Syrris et al., 2006), was detected in three patients. This mutation (E896EfsX4) would affect the intracellular cadherin-typical segment (ICS) domain of desmocollin-2a isoform by altering 4 amino acidic residues before a termination codon is prematurely introduced. If compared with the wild type, only the last 5 amino acids, which are not conserved among mammals (Figure 4.8), were altered in the mutated protein, three have changed and the last two were lost. By DHPLC analysis of control subjects DNA, the frequency of such variant resulted to be 2%. However, since most of frameshift mutations leads to functional effects, it has been provisionally reported as a mutation.

Homo_sapiens	QEEDGLEFLDNLEPKFRTLAEACMKR	AAH63291.1
Macaca_mulatta	QEEDGLEFLDNLEPKFRTLAEACMKR	XP_001102096.1
Pan_troglodytes	QEEDGLEFLDNLEPKFKTLAEACMKR	XP_512077.2
Bos_taurus	QEEDGLEFLDHLGPKFRTLAETCMKR	XP_615164.2
Mus_musculus	QEEDGLEFLDHLEPKFRTLAEVCAKR	AAH57867.1
Rattus_norvegicus	QEEDGLEFLDHLEPKFRTLAEVCAKR	NP_001028860.1
Canis familiaris	QEEDGLEFLDHLEPKFRTLAEACIKR	CAA05309.1

Figure 4.8. ClustalW alignment of the last portion of intracellular cadherin-typical segment (ICS) domain of desmocollin-2a isoform among species. Five amino acids (involved by mutation E896EfsX4) show relative variance. Organism names and GenBank accession numbers are reported on sides.

An intronic nucleotidic variation (c.631-10C>T) was found in subject #60. Because of its close proximity to the wild-type AG splice-site, mutation c.631-10C>T could alter the acceptor splice site of exon 6. DSC2 cDNA corresponding to exons 4 to 7 was nested-PCR amplified from lymphocytes RNA of the patient. Amplification products were size separated by agarose gel electrophoresis, gel isolated, and cloned into the pCR2.1 plasmid (using the TOPO-TA cloning kit). Plasmid DNA from 54 different clones was purified and sequenced with M13 forward and reverse primers. The analysis failed to detect aberrant transcripts and showed only the wild-type allele, thus suggesting that the aberrant transcripts would be degraded, most likely through nonsense mediated mRNA decay. To assess this hypothesis, real-time quantitative RT-PCR analysis was performed on total RNA obtained from peripheral blood of the patient #60 and of six healthy donors. Figure 4.9 shows that DSC2 expression in the healthy donors resulted highly variable. Therefore, it will be necessary to increase the number of healthy controls, in order to evaluate the range of normal DSC2 expression.

Actually, the pathogeneity cannot be established with certainty and the possibility of being a rare polymorphism cannot be excluded.

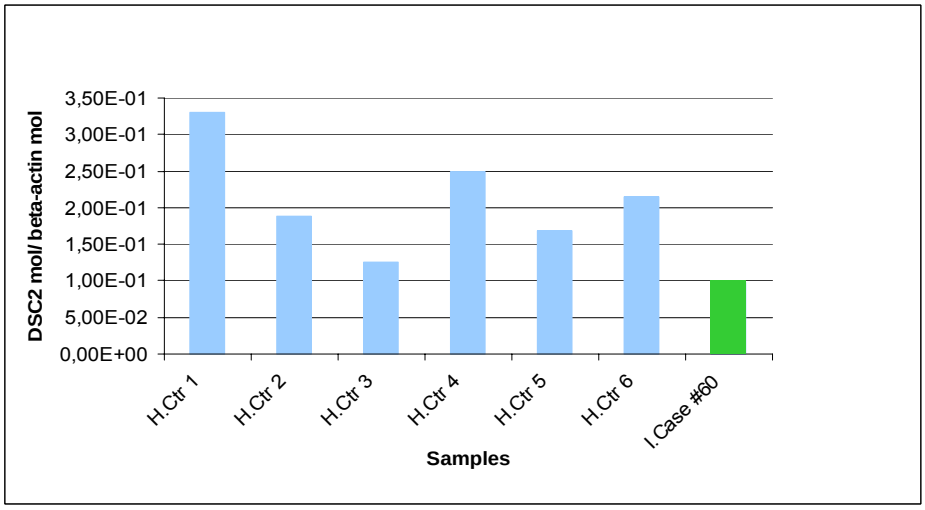

Figure 4.9. RT-PCR analysis of DSC2 expression in six healthy donors (H.Ctr1 to 6) and in the Index Case #60 (I.Case #60). DSC2 expression results highly variable.

Relative position of DSC2 mutations detected by the study is reported in Figure 4.10.

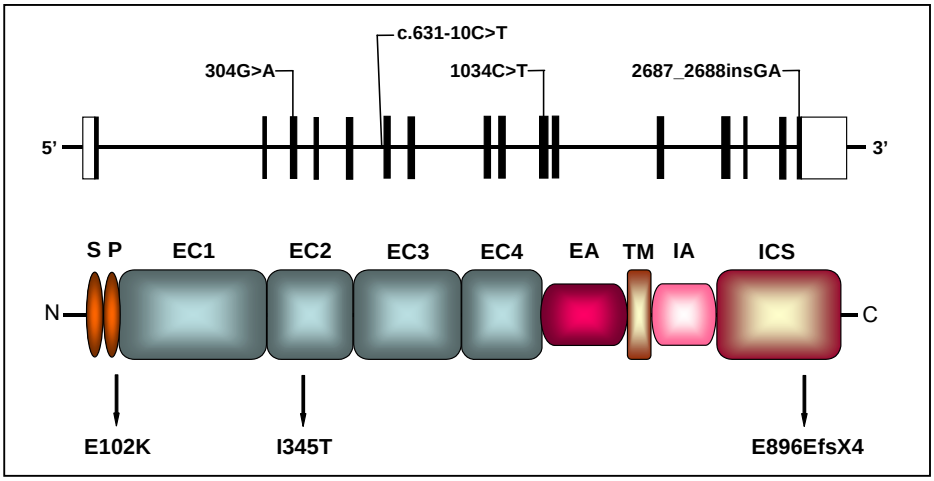

Figure 4.10. (Top) Schematic organization of the human DSC2 gene (16 exons are represented by vertical black boxes, and introns are represented by horizontal lines). **(Bottom)** The encoded DSC2 protein comprises a signal (S) domain and a preprotein (P) domain (both S and P domains lack in the functional protein), followed by 5 extracellular domains (EC1, EC2, EC3, EC4, and EA), a transmembrane domain (TM), an intracellular anchor domain (IA),and an intracellular cadherin-typical segment domain (ICS). Position of the 4 detected mutations is indicated.

Two novel DSC2 exonic single nucleotide polymorphisms were identified. c.351A>G was a synonymous variation involving T117 detected in patient #89 and found in control population with a frequency of 1.6%. c.2393G>A involves a amino acid conserved among species causing the missense change R798Q in IA domain; it was detected in several index cases and in control subjects showing a frequency of 3.5%.

4.1.5. Mutations in the study population

Mutation screening of four desmosomal ARVC/D genes (PKP2, DSP, DSG2, and DSC2) in 110 ARVC/D index cases enabled to estimate the proportion of mutations in different disease genes. Data are reported in Table 4.6.

Table 4.6. Mutations detected in 110 ARVC/D index cases.

# Index case	PKP2 gene mutations	DSP gene mutations	DSG2 gene mutations	DSC2 gene mutations	Variation detected
2	K672RfsX11	-	-	-	1
3	T816RfsX9	-	-	-	1
5	-	R1113X	-	-	1
6	K672RfsX11	-	-	-	1
7	-	-	Y87C	E896EfsX4	2
8	-	V30M	-	-	1
10	-	-	N266S	-	1
12	-	-	L831F	-	1
14	-	-	L831F	-	1
16	T50SfsX60	-	-	-	1
17	-	-	L831F	-	1
18	T816RfsX9; S209R	-	R146H	-	3
23	-	c.273+5G>A	-	-	1
24	N76S	-	-	-	1
29	-	V30M	-	-	1
33	-	-	G100R	-	1
34	T50SfsX60	-	G638R	-	2
36	E58D	-	-	E896EfsX4	2
38	-	K470E; A566T	-	-	2
39	Q211X; I778T	R1255K	-	-	3
40	Q62K; Q707X	L1654P	-	-	3
42	-	-	E331K; c.1881-2A>G	-	2
44	-	S299R	-	-	1
45	-	M1601I	-	-	1
46	-	c.423-1G>A	-	-	1
50	G548VfsX14	-	-	-	1
54	V587I	-	-	-	1
55	-	-	-	I345T	1
57	T50SfsX60	-	-	-	1
60	-	-	-	c.631-10C>T	1
61	Q133X	-	-	-	1
62	T50SfsX60	-	V392I	-	2
71	-	N458Y	-	-	1
73	T816RfsX9	-	-	-	1
78	-	-	-	E102K	1
80	T50SfsX60	-	-	-	1
81	K672RfsX11	-	-	-	1
83	-	V30M; R2541K	-	-	2
85	-	-	K294E	-	1
87	-	-	E418EfsX1; G997VfsX19	-	2
88	-	E1068VfsX18	P925S	-	2
89	Q62DfsX22	-	-	-	1
91	-	-	G678AfsX2	-	1
92	-	R1775I	E230G; D297G	-	3
96	G548VfsX14	-	-	-	1
97	-	N375I	G638R	E896EfsX4	3
100	-	-	Q558X	-	1
102	-	S2108X	-	-	1
103	-	D1258E	-	-	1
105	-	Q273X	-	-	1
106	S140F	-	-	-	1
107	K112N	-	-	-	1
Total	25 (16 different)	20 (18 different)	20 (17 different)	6 (4 different)	71 (55 different)

Nucleotide polymorphisms (for which no functional effect is suspected) were not included.

Mutations were detected in the screened genes in 52 out 110 ARVC/D index cases (47.3%): 16 subjects (14.6%) resulted to carry one plakophilin-2 mutation, 11 (10.0%) one desmoplakin mutation, 8 (7.3%) a single desmoglein-2 mutation, and 3 (2.7%) one desmocollin-2 mutation; in 14 index patients (12.7%), multiple mutations were detected.

A total of seventy-one mutations (55 different mutations, including 28 novel ones) were identified. 25 of them (35.2%) occurred in PKP2 gene, 20 (28.2%) in DSP gene, 20 (28.2%) in DSG2 gene, and 6 (8.4%) in DSC2 gene. Therefore, genes most frequently involved in ARVC/D among index patients of this series were PKP2, DSP and DSG2.

Among the 55 different mutations, 34 (62%) altered single amino acids (missense mutations), 10 (18%) were insertions or deletions causing a frame shift, 7 (13%) coded for premature stop codons (nonsense mutations), and 4 (7%) were putative splice donor or acceptor site mutations located in the introns (Table 4.7).

Table 4.7. Type and number of different mutations detected in desmosomal ARVC/D genes (PKP2, DSP, DSG2 and DSC2) in 110 ARVC/D index cases.

Type of mutation	PKP2 gene mutations	DSP gene mutations	DSG2 gene mutations	DSC2 gene mutations	Total
Missense	8	12	12	2	34
Frame shift	5	1	3	1	10
Nonsense	3	3	1	-	7
Splice site	-	2	1	1	4
Total	16	18	17	4	55

The clinical features of genotyped ARVC/D index cases are summarised in below.

Table 4.8. Clinical characteristics of ARVC/D index cases with PKP2, DSP, DSG2 and DSC2 mutations.

# Index case	Mutations	Sex	Family history (Major)	Family history (minor)	Age (yrs)	Age at diagnosis (yrs)	Non sustained VT	Sustained VT / VF	Major events	Age at major event (yrs)	ICD	Biventricular involvement	ECG abnormalities	Late potentials	2D-echo RV Abnormalities	2D-echo LV Abnormalities
2	PKP2	M	-	+	41	32	-	-	+	42	+	-	+	+	+	+
3	PKP2	M	-	+	65	58	-	-	-	65	-	+	+	+	+	-
5	DSP	F	+	-	42	35	-	-	-	42	-	+	+	+	-	-
6	PKP2	M	-	-	33	28	-	+	+	33	-	+	+	+	+	-
7	MULTIPLE	M	-	-	52	45	+	-	-	52	-	-	+	-	-	-
8	DSP	M	-	+	22	16	+	-	-	22	-	-	+	+	+	+
10	DSG2	F	-	+	63	50	-	+	+	55	+	+	+	+	+	-
12	DSG2	F	-	+	66	60	+	-	+	60	-	-	-	+	+	-
14	DSG2	M	-	-	66	64	-	+	+	66	-	-	+	-	+	-

16	PKP2	M	-	+	50	48	+	-	-	50	-	-	+	-	+	-
17	DSG2	M	-	-	26	21	+	-	-	26	-	-	+	-	+	-
18	MULTIPLE	M	-	-	51	39	-	+	+	39	+	+	+	+	+	+
23	DSP	M	-	-	47	32	-	+	+	45	-	-	+	+	+	+
24	PKP2	M	-	-	31	17	+	-	-	31	-	-	-	+	+	+
29	DSP	M	-	-	64	38	-	+	+	64	-	+	+	-	+	-
33	DSG2	M	-	-	55	42	-	+	+	55	-	+	+	+	-	-
34	MULTIPLE	M	-	-	53	50	-	+	+	50	-	-	+	+	+	-
36	MULTIPLE	F	-	+	63	60	+	-	-	63	-	-	+	+	+	-
38	MULTIPLE	M	-	+	35	16	-	+	+	16	+	+	+	+	+	+
39	MULTIPLE	M	-	-	43	40	-	+	+	40	-	-	+	-	+	-
40	MULTIPLE	F	-	+	44	30	+	-	+	44	+	+	+	+	+	-
42	MULTIPLE	F	-	+	65	63	-	+	+	63	-	-	+	+	+	-
44	DSP	M	-	+	38	18	-	+	+	18	-	+	+	+	+	+
45	DSP	M	-	+	40	39	-	-	-	40	-	-	-	+	+	-
46	DSP	M	-	-	33	27	-	+	+	28	-	+	+	+	+	+
50	PKP2	M	-	+	74	60	-	-	+	74	-	-	+	+	+	-
54	PKP2	M	-	-	49	37	+	-	-	49	-	+	+	-	+	+
55	DSC2	M	-	-	55	50	-	+	+	50	+	+	+	+	+	-
57	PKP2	M	-	+	59	35	-	+	+	35	-	-	+	+	+	-
60	DSC2	M	-	-	39	25	+	-	-	39	-	-	+	+	+	-
61	PKP2	M	-	-	32	19	+	-	-	32	-	-	+	+	+	+
62	MULTIPLE	M	+	-	49	34	+	-	-	49	-	-	-	+	+	-
71	DSP	M	-	+	27	15	+	-	-	27	-	-	+	+	+	-
73	PKP2	M	-	-	36	25	-	+	+	25	+	-	+	+	-	-
78	DSC2	M	-	+	28	19	+	-	-	28	-	-	-	+	+	-
80	PKP2	F	-	-	49	37	-	+	+	37	-	-	+	+	+	-
81	PKP2	F	-	+	23	16	-	+	+	23	+	-	+	+	+	-
83	MULTIPLE	F	-	+	47	38	-	+	+	47	-	+	+	+	+	-
85	DSG2	F	-	+	70	38	+	-	-	70	-	+	+	+	+	-
87	MULTIPLE	M	-	-	22	14	+	-	-	22	-	+	+	+	+	-
88	MULTIPLE	M	-	+	29	22	-	+	+	29	-	-	+	+	+	-
89	PKP2	F	-	+	57	40	+	-	-	57	-	-	+	-	-	-
91	DSG2	M	-	-	37	32	+	-	-	37	-	+	+	+	+	-
92	MULTIPLE	F	-	+	46	38	-	+	+	46	+	-	+	+	+	-
96	PKP2	M	-	-	36	18	-	+	+	18	-	-	+	+	+	-
97	MULTIPLE	F	-	-	49	38	-	+	+	38	-	-	-	+	+	-
100	DSG2	M	-	+	19	11	+	-	-	19	-	-	+	+	+	-
102	DSP	M	-	-	34	26	-	+	+	26	+	+	+	+	+	-
103	DSP	M	-	+	23	15	+	-	-	23	-	-	-	+	+	-
105	DSP	F	-	+	67	40	+	-	+	65	-	+	+	+	+	-
106	PKP2	F	-	-	63	42	-	+	+	63	-	-	+	-	+	-
107	PKP2	M	-	-	21	19	-	+	+	19	-	-	+	+	+	-

Major events: sustained VT, ventricular fibrillation, heart failure, death, unexplained syncope.

4.1.6. Mutations in familial forms of ARVC/D

Family members of 19 ARVC/D index cases were available for clinical and genetic testing. They were clinically investigated at the Department of Clinical and Experimental Medicine of the University of Padua, by Prof. Nava and colleagues.

Clinical findings of subjects carrying mutation are reported in Table 4.9. Clinical screening revealed an interfamilial variability as far as degree of disease extent and electrical instability. Among gene carriers younger than 10 yrs, none was found to be affected.

Table 4.9. Clinical characteristics of family members carrying mutations in PKP2, DSP, DSG2 and DSC2 genes.

# Family	# Family subject	Mutations	Sex	Family history (Major)	Family history (minor)	Age (yrs)	Age at diagnosis (yrs)	Non sustained VT	Sustained VT / VF	Major events	Age at major event (yrs)	ICD	Biventricular involvement	ECG abnormalities	Late potentials	2D-echo RV Abnormalities	2D-echo LV Abnormalities
23	III,1	DSP	F	-	+	20	18	-	-	-	-	-	-	-	-	+	-
38	III,4	MULTIPLE	M	-	+	62	50	+	-	-	-	-	-	-	+	+	-
40	I,1	MULTIPLE	M	+	-	80	70	+	-	-	-	-	-	+	+	+	-
40	I,2	PKP2	F	+	-	83	71	+	-	-	-	-	-	-	-	np	np
40	II,7	MULTIPLE	M	+	-	50	40	-	+	+	42	+	+	+	+	+	+
40	III,1	DSP	M	+	-	35	26	+	-	-	-	-	-	-	-	-	+
40	III,3	PKP2	M	+	-	30	12	-	-	-	-	-	-	+	-	-	-
42	II,2	MULTIPLE	F	-	-	64	62	+	-	-	-	-	-	+	np	+	-
45	II,3	DSP	M	-	-	52	43	-	+	-	-	-	-	+	-	-	-
45	II,5	DSP	F	-	-	57	47	+	-	-	-	-	-	+	+	+	-
45	III,2	DSP	M	-	-	18	18	-	+	-	-	-	-	-	-	-	-
45	III,3	DSP	M	-	-	25	16	+	-	-	-	-	-	+	+	+	-
46	II,2	DSP	M	+	-	66	40	-	-	+	40	-	-	+	+	-	+
62	II,3	DSG2	M	+	-	82	65	+	-	-	-	-	-	+	-	-	-
62	III,1	DSG2	M	+	-	80	68	+	-	-	-	-	-	+	-	-	-
62	III,9	DSG2	F	+	-	55	20	-	-	-	-	-	-	-	+	+	-
71	II,2	DSP	F	-	+	59	59	+	-	-	-	-	-	-	-	-	-
71	II,4	DSP	M	-	+	60	60	+	-	-	-	-	-	-	-	-	-
78	II,1	DSC2	M	-	+	26	24	-	-	-	-	-	-	-	-	+	-
78	II,3	DSC2	M	-	+	26	25	-	-	-	-	-	-	-	-	+	-
83	II,7	DSP	F	+	-	56	56	+	-	-	-	-	-	+	+	+	-
83	III,1	DSP	M	+	-	14	14	+	-	-	-	-	-	-	-	-	-
83	III,3	DSG2	F	+	-	23	18	-	-	-	-	-	-	-	-	+	-
83	III,4	DSG2	M	+	-	21	15	+	-	-	-	-	-	+	+	+	-
83	III,8	DSP	M	+	-	24	24	+	-	-	-	-	-	-	-	+	-
85	III,4	DSG2	F	-	+	36	18	-	+	+	18	-	-	+	+	+	+
85	III,5	DSG2	M	-	+	35	35	+	-	-	-	-	-	-	-	+	-
88	I,2	DSP	F	-	+	63	60	+	-	-	-	-	-	+	-	-	-
88	II,2	MULTIPLE	F	-	+	20	14	+	-	-	-	-	-	+	+	+	-
97	II,7	MULTIPLE	M	-	+	50	42	-	-	-	-	-	-	-	-	-	+
100	I,1	DSG2	M	-	+	48	48	+	-	-	-	-	-	-	-	+	-
105	II,4	DSP	F	-	+	60	48	+	-	-	-	-	-	+	-	-	-
105	II,6	DSP	M	-	+	60	34	-	+	+	34	+	+	+	+	+	+
105	II,8	DSP	F	-	+	55	48	-	-	-	-	-	-	-	-	+	-
105	III,1	DSP	M	-	+	43	24	+	-	+	35	-	-	+	+	+	-

Major events: sustained VT, ventricular fibrillation, heart failure, death, unexplained syncope.

a. Families with a single mutation

Family #5

Patient #5 (III,7 of Family #5, Figure 4.12) was a female aged 42 years with a classic form of ARVC/D; she showed a family history for premature sudden death.

DHPLC analysis of fragment 23b of DSP gene showed an abnormal elution profile (Figure 4.11). By direct sequencing the c.3337C>T transition in exon 23 was identified (Figure 4.11). This nucleotide change causes the introduction of a termination codon in position 1113 (R1113X), within the rod domain (from 1056 to 1909 amino acids) of desmoplakin protein. The predicted truncated molecules lack most central rod domain forming desmoplakin dimeric coiled coil, and completely lack C-terminal domain interacting with desmin intermediate filaments.

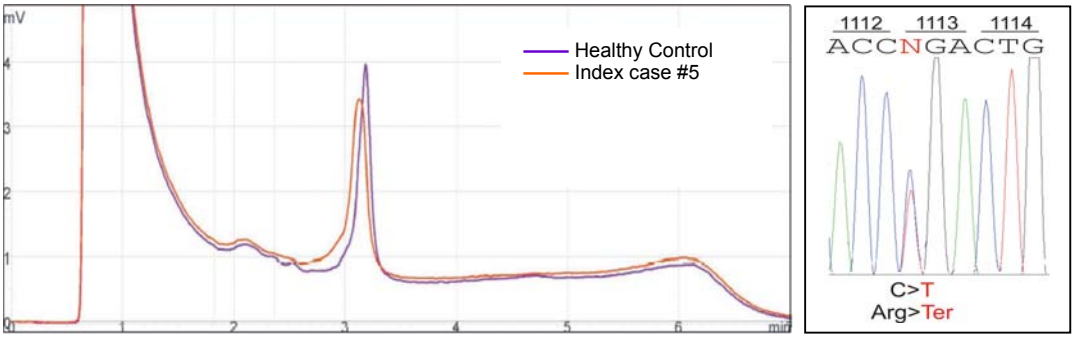

Figure 4.11. (Left) DHPLC elution profiles of PCR DSP fragment 23b in the Healthy Control and in Index case #5 at analysis temperature of 58.0°C. **(Right)** DNA sequencing of PCR DSP 23b fragment revealing c.3337C>T transition (R1113X).

The genetic study was extended to available family members. Only three subjects (IV,2; IV,3; IV,4), aged 9 to 18 years, and actually clinically unaffected, resulted to carry the DSP mutation. Tissue was not available for genetic analysis in any of the suddenly deceased individuals (II,3; II,4).

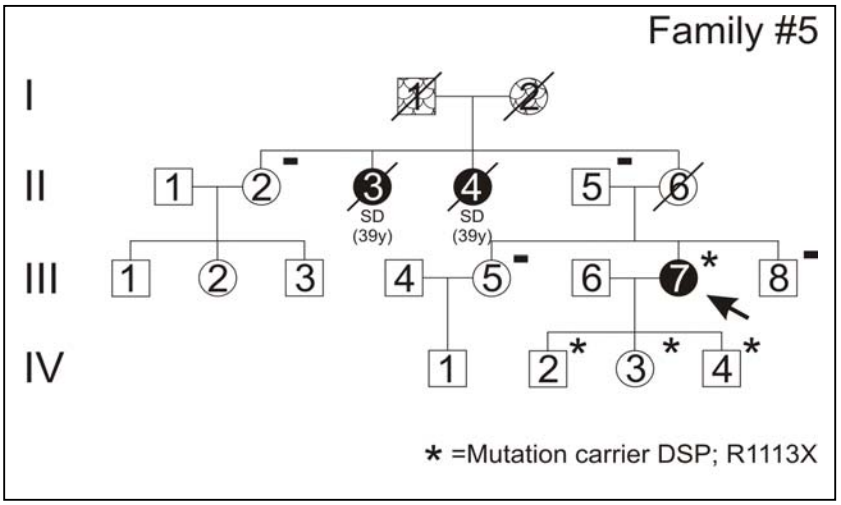

Figure 4.12. Pedigree of Family #5. Index patient #5 is indicated by arrow. Black, white, and shaded symbols represent clinically affected individuals, unaffected individuals, and individuals of unknown disease status, respectively. Presence (symbol) or absence (-) of the genes mutations is indicated. SD=sudden death.

Family #23

Patient #23 (II,1 in Family #23, Figure 4.14) is a male with a typical form of ARVC/D. By means of DHPLC analysis of DSP exon 2, an abnormal elution profile was identified, and by sequencing of this amplicon a nucleotide change was identified in the donor splice site of exon 2 of DSP gene (c.273+5G>A) (Figure 4.13). This variation was not detected in the SNP database and was never observed in 300 control subjects screened by DHPLC analysis (the number of healthy control individuals was increased because this is a change occurring in a non-coding region).

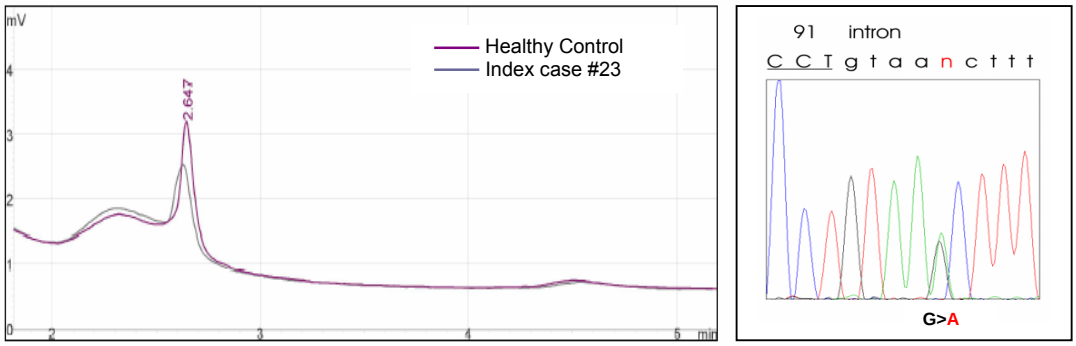

Figure 4.13. (Left) DHPLC elution profiles of PCR DSP fragment 2 in the Healthy Control and in Index case #23 at analysis temperature of 60.5°C. **(Right)** DNA sequencing of PCR DSP 2 fragment revealing c.273+5G>A transition.

The c.273+5G>A change occurred in one of the conserved sequence important for splicing. The patient cDNA analysis failed to detect aberrant transcripts and showed only the wild-type allele, thus suggesting that the aberrant transcripts would be degraded, most likely through nonsense mediated mRNA decay (Maquat et al., 2004).

The genetic study was extended to available family members. The two young healthy daughters of the index case resulted to carry the detected mutation; only one (III,1) showed minor signs of the disease.

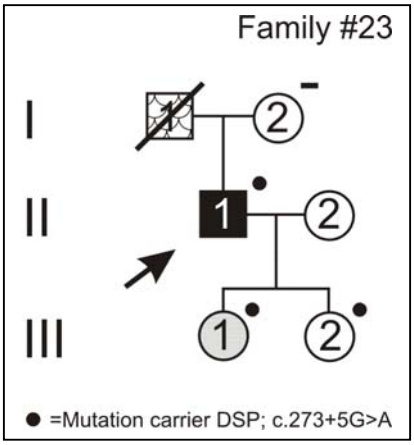

Figure 4.14. Pedigree of Family #23. Index patient #23 is indicated by arrow. Black, white, and grey symbols represent clinically affected, unaffected, and showing minor signs of the disease individuals, respectively; shaded square, individual of unknown disease status; the line through symbol, deceased individual. Presence (symbol) or absence (-) of the DSP mutation is indicated.

Family #45

Patient #45 (II,1 of Family #45, Figure 4.16) is a male aged 40 years with a classic form of ARVC/D; he showed family history of the disease.

DHPLC analysis of fragment 23f of DSP gene showed an abnormal elution profile (Figure 4.15). The identified c.4803G>A transition in exon 23 (Figure 4.15) resulted in the substitution of a methionine with a isoleucine (M1601I) in the rod domain of desmoplakin protein predicted to form the dimeric coil. Both Methionine and isoleucine are hydrophobic amino acids, nevertheless this change occurred in a residue conserved among species; it was not detected in 400 control chromosomes screened by restriction digest with NlaIII enzyme (New England Biolabs), and it co-segregate with the disease in the family.

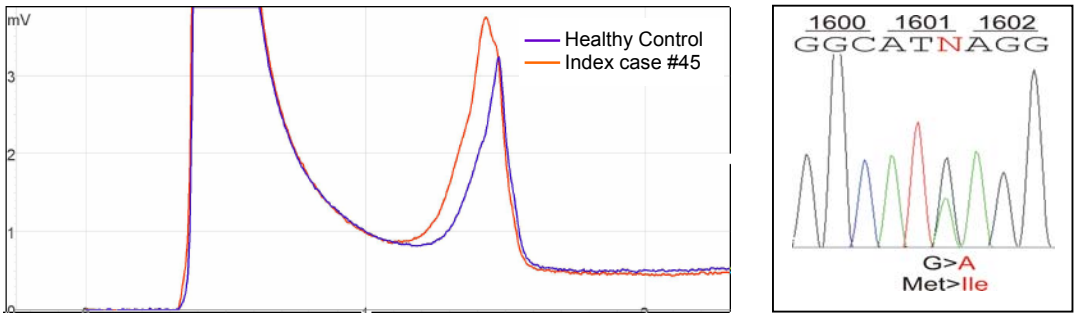

Figure 4.15. (Left) DHPLC elution profiles of PCR DSP fragment 23f in the Healthy Control and in Index case #45 at analysis temperature of 61.6°C. **(Right)** DNA sequencing of PCR DSP 23f fragment revealing c.4803G>A transition (M1601I).

The heterozygous M1601I mutation was detected in 5 individuals: the proband (II,1) and two family members (II,5 and III,3) fulfilled clinical diagnostic criteria, two subjects (II,3 and III,2) did not fulfil diagnostic criteria but raised a suspicion of incomplete disease expression.

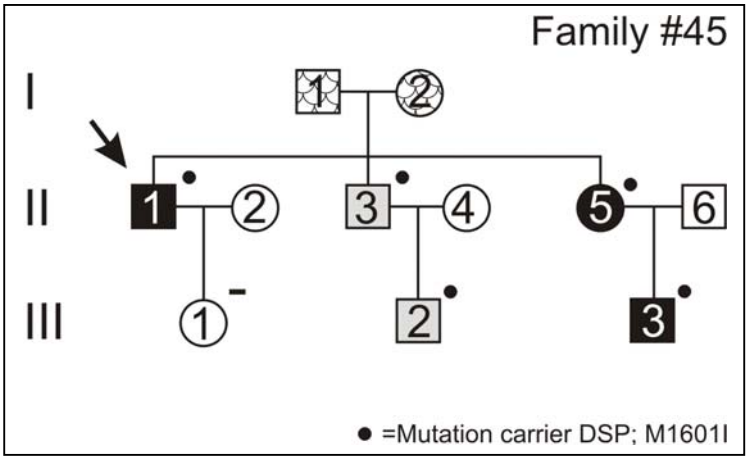

Figure 4.16. Pedigree of Family #45. Index patient #45 is indicated by arrow. Black, white, and grey symbols represent clinically affected, unaffected, and showing minor signs of the disease individuals, respectively; shaded symbols, individuals of unknown disease status. Presence (symbol) or absence (-) of the DSP mutation is indicated.

Family #46

Patient #46 (III,1 of Family #46, Figure 4.18) is a young man affected with a severe form of arrhythmogenic right ventricular cardiomyopathy. He died suddenly at age of 33 years in the course of the follow-up.

By means of DHPLC analysis of DSP exon 4, an abnormal chromatogram showing two peaks was identified (Figure 4.17). By direct sequencing of this amplicon, a novel nucleotide change in the acceptor splice site of exon 4 of DSP gene (c.423-1G>A) was identified (Figure 4.17). This variation was not detected in the SNP database and was never observed in 600 control chromosomes screened by DHPLC analysis.

The alteration c.423-1G>A was confirmed to be a mutation, as the RT-PCR resulted in an alternatively spliced product. In fact, c.423-1G>A alter the acceptor splicing site of intron 3, which could result in the skipping of exon 4 (Fig.23). This aberrant spliced mRNA should contain a premature stop codon and it should code for a truncated protein of 200 amino acid in length.

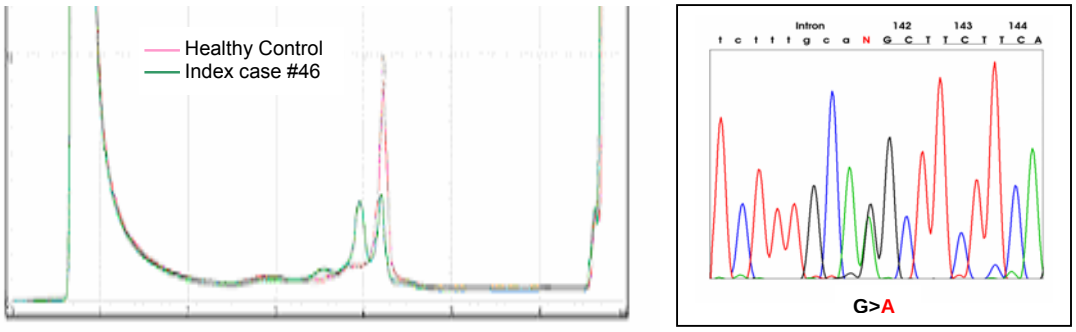

Figure 4.17. (Left) DHPLC elution profiles of PCR DSP fragment 4 in the Healthy Control and in Index case #46 at analysis temperature of 58.6°C. **(Right)** DNA sequencing of PCR DSP fragment 4 revealing c.423-1G>A splice site mutation.

The genetic study was extended to additional family members. The proband's father (II,2) was clinically affected with ARVC/D, whereas a young subject (III,2) resulted asymptomatic.

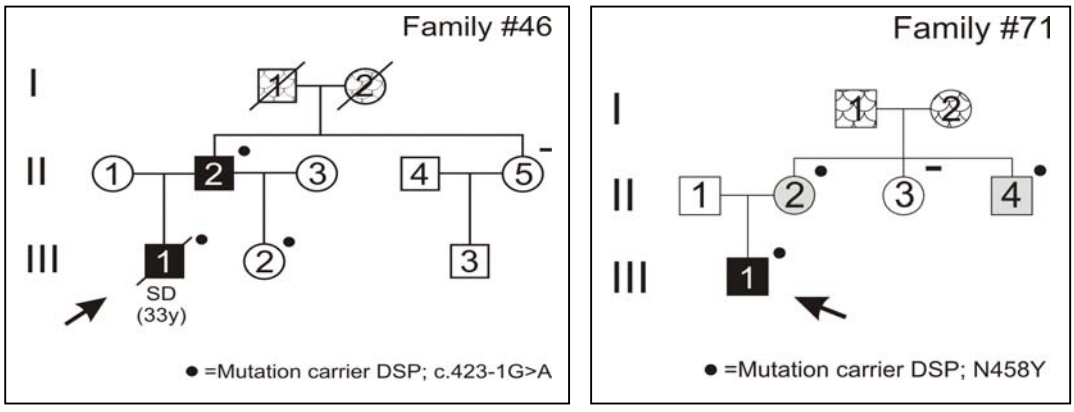

Figure 4.18. (Left) Pedigree of Family #46. **(Right)** Pedigree of Family #71. Index patients are indicated by arrow. Black, white, and grey symbols represent clinically affected, unaffected, and showing minor signs of the disease individuals, respectively; shaded symbols, individuals of unknown disease status. The line through symbols represents deceased individuals. SD=sudden death. Presence (symbol) or absence (-) of the gene mutation is indicated.

Family #71

Patient #71 (III,1 of Family #71, Figure 4.18) is a young male with a classic form of ARVC/D.
By DHPLC analysis, abnormal elution profile for DSP exons 11 was identified, and sequencing of the amplicon showed a novel heterozygous nucleotide change, c.1372A>T (N458Y) (Figure C), not detected in Italian control population. It involved a asparagine conserved residue among species, substituted by a tyrosine, an amino acid having an aromatic ring that may destabilize the N-terminus of DSP molecules.

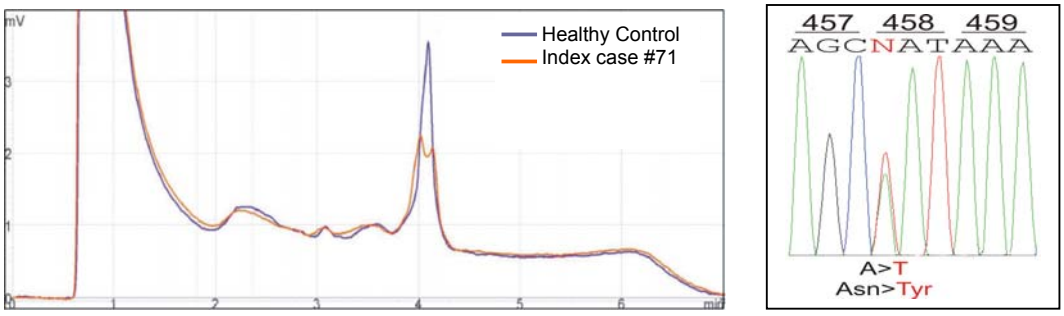

Figure 4.19. (Left) DHPLC elution profiles of PCR DSP fragment 11 in the Healthy Control and in Index case #71 at analysis temperature of 56.4°C. **(Right)** DNA sequencing of PCR DSP fragment 11 revealing c.1372A>T (N458Y) mutation.

In Family #71, the missense mutation was detected in two additional individuals (II,2 and II,4). They did not fulfilled diagnostic criteria but raised a suspicion of incomplete disease expression.

Family #78

The patient #78 (II,2 of Family #78, Figure 4.22) was examined at the age of 19 years due to premature ventricular beats with left bundle branch block morphology. The ECG showed the presence of incomplete right bundle branch block, whereas late potentials were present at 40-80 filter setting. Two-D echocardiogram demonstrated a dilated right ventricle with kinetic abnormalities and decreased ejection fraction. The left ventricle was dilated as well.
Variation c.304G>A, resulting in predicted E102K amino acid substitution, was detected by DHPLC analysis followed by sequencing of DSC2 exon 3 (Figure 4.20).

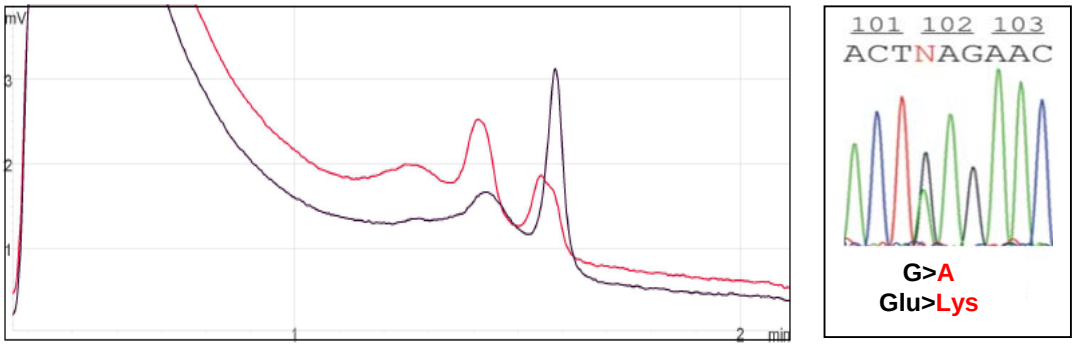

Figure 4.20. (Left) DHPLC elution profiles of PCR DSC2 fragment 3 in the Healthy Control and in Index case #7 at analysis temperature of 54.8°C. **(Right)** DNA sequencing of PCR DSC2 fragment 3 revealing c.304G>A (E102K) mutation.

Mutation E102K occurred in a residue conserved among species in the propeptide domain, although in mouse and rat desmocollin-2 protein E102 is replaced by aspartic acid (Figure 4.21). However, these two amino acids show very similar physico-chemical properties; on the contrary, the detected substitution replaced a negatively-charged residue by a positively-charged one. The detected nucleotide change was not found in a control group of 250 healthy and unrelated subjects (500 control chromosomes) from Italian population.

Homo_sapiens	SFTILLSNTENQEKKKIFV	AAH63291.1
Canis_familiaris	SFSILLSNTENQEEKKILV	XP_001102096.1
Bos_taurus	SFTILLSNTETQEEKEILV	XP_512077.2
Macaca_mulatta	SFTILLSNTENQEKKKIFV	XP_615164.2
Pan_troglodytes	SFTILLSNTENQEKKKIFV	AAH57867.1
Mus_musculus	SFTIWLFSTDSQEKREISV	NP_001028860.1
Rattus_norvegicus	SFTIWLFNTDSQEERELSV	CAA05309.1

Figure 4.21. Evolutionary conservation of the DSC2 missense mutation E102K among 7 species. The mutated amino acid is coloured, and not conserved residues are reported in blu.

DSC2 missense mutation was detected in three patient's relatives: one (I,1) resulted asymptomatic, and two (II,1 and II,3) not fulfilled the current diagnostic criteria for ARVC/D.

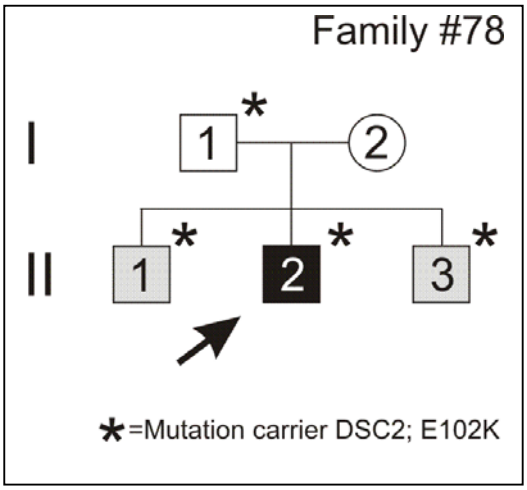

Figure 4.22. Pedigree of Family #48. Index patient is indicated by arrow. Black, white, and grey symbols represent clinically affected, unaffected, and not fulfilling the current diagnostic criteria for ARVC/D individuals, respectively. Presence (symbol) of the DSC2 mutation is indicated.

Family #85

Patient #85 (II,4 of Family #85, Figure 4.23), a female aged 70, was diagnosed at age of 38 years with a classic form of ARVC/D.

Direct sequencing of DSG2 fragment 7-8 showed the c.880A>G transition in exon 8 resulting in the substitution of a lysine with a glutamic acid (K294E) in a residue conserved among species, in the extracellular cadherin domains. Cadherin domains are important for homophilic intercellular associations and the amino acid change may destabilize the rod structure and influence the homophilic binding.

In Family #85, the missense mutation was detected in 3 individuals, two clinically affected with ARVC/D: the proband and her daughter (III,4). The proband's son (III,5) manifested ventricular arrhythmias and shoved 2D-Echo abnormalities, but he doesn't fulfil ARVC/D diagnostic criteria. None of the family members without DSG2 mutation presented symptoms or signs of the disease.

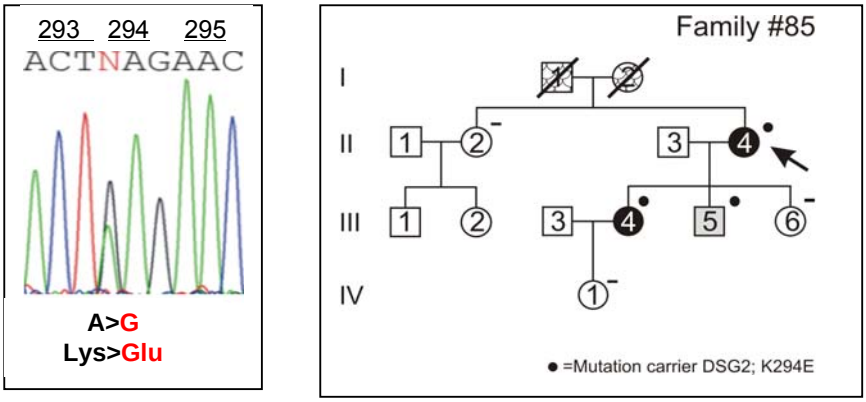

Figure 4.23. (Left) DNA sequencing of DSG2 exon 8 revealing c.880A>G (K294E) mutation in index patient #85. **(Right)** Pedigree of Family #85 (index patient is indicated by arrow). Black, white, and grey symbols represent clinically affected, unaffected, and showing minor signs of the disease individuals, respectively; shaded symbols, individuals of unknown disease status. The line through symbol represents deceased individuals. Presence (symbol) or absence (-) of the

Family #100

Patient #100 (II,1 of Family #100, Figure 4.24) was a young male diagnosed with a classic form of ARVC/D at age of 11 years.

Mutation c.1672C>T was identified by direct sequencing of DSG2 exon 12 (Figure 4.24). Nucleotide change generates a termination codon (Q558X), leading to DSG2 molecules lacking transmembrane and cytoplasmic domains.

The genetic study was extended to available first-order relatives. Proband's father and sister carried DSG2 stop mutation; only the father showed minor 2D-Echo abnormalities.

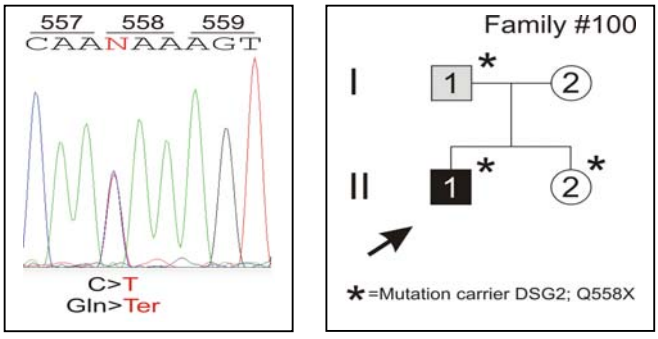

Figure 4.24. (Left) DNA sequencing of DSG2 exon 12 revealing c.1672C>T (Q558X) mutation. **(Right)** Pedigree of Family #100 (index patient is indicated by arrow). Black, white, and grey symbols represent clinically affected, unaffected, and showing minor signs of the disease individuals, respectively. Presence (symbol) of the DSG2 mutation is indicated.

b. Families carrying multiple mutations

Family #18

Patient #18 (III,1 in Family #18, Figure 4.26) was a men aged 51 diagnosed with a severe form of ARVC/D.

Direct sequencing of exons 3 and 12 of PKP2 gene showed two nucleotide changes (Figure 4.25). The transversion c.627C>G led to the replacement of a polar serine in position 209 by a positive-charged arginine in the N-terminal portion of plakophilin-2 (S209R). This change was not found in 400 alleles from the control population. A deletion of two nucleotides (2447_2448delCC) was detected exon 12: it causes the addition of eight amino acid residues before a premature stop signal is introduced (T816RfsX9); the predicted truncated plakophilin-2 molecule lacks portion of Arm domain 8.

By direct sequencing of DSG2 exon 5 an additional mutation was detected in the patient DNA (Figure 4.25). The transition c.437G>A resulted in a missense mutation R146H in the extracellular domain (EC1) of desmoglein-2. In this position an arginine, conserved among different species, was substituted by an histidine, an hydrophilic amino acid, having an aromatic ring. In this protein region, all the inherent amino acid changes may destabilize the rod structure and influence the homophilic intercellular associations.

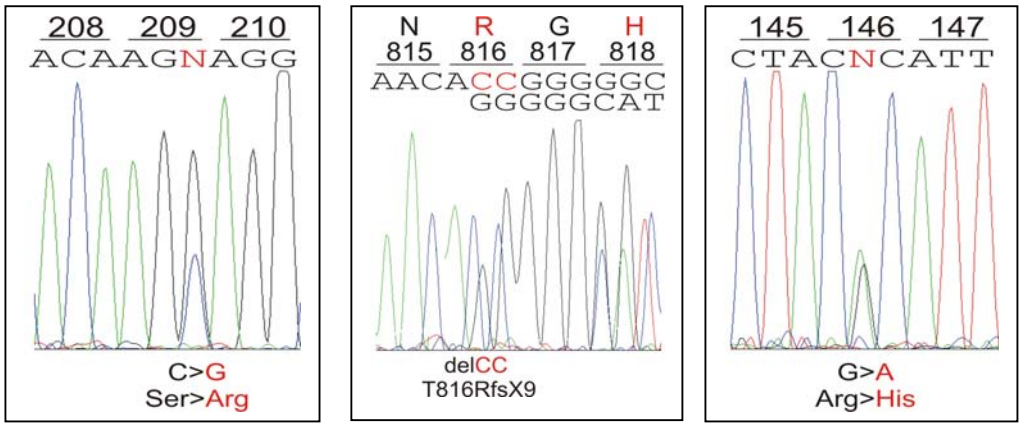

Figure 4.25. (Left) DNA sequencing of PKP2 exon 3 revealing c.627C>G (S209R) mutation. **(Center)** DNA sequencing of PKP2 exon 12 showing c.2447_2448delCC (T816RfsX9) mutation. **(Right)** DNA sequencing of DSG2 exon 5 revealing c.437G>A (R146H) mutation.

Three family members were available for genetic testing. The PKP2 T816RfsX9 was inherited from the mother (II,2). Since father's DNA was not available for clinical investigation, it was not possible to establish if two missense variations PKP2 S209R and DSG2 R146H have been inherited from the father or have to be considered de novo mutations.

Two relatives who carried PKP2 mutation were fully symptomatic.

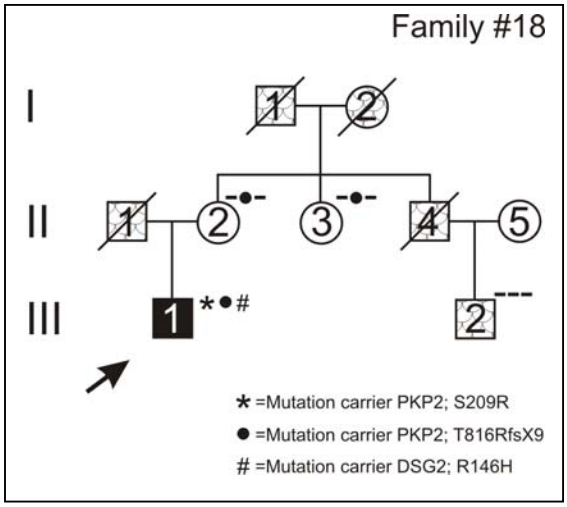

Figure 4.26. Pedigree of Family #18. Index patient #18 is indicated by arrow. Black and white symbols represent clinically affected and unaffected individuals, respectively; shaded symbols, individual of unknown disease status. The line through symbols represents deceased individuals. Presence (symbol) or absence (-) of the three mutations is indicated.

Family #38

Patient #38 (IV,1 of Family #38, Figure 4.28) was a male aged 55, diagnosed with a severe form of ARVC/D who received an implantable cardioverter defibrillator.

By DHPLC analysis, abnormal elution profiles for DSP exons 11 and 13 were identified. Sequencing analysis of the two amplicons showed two novel heterozygous nucleotide changes: c.1408A>G in exon 11 and c.1696G>A in exon 13 that led to causes K470E and A566T amino acidic substitutions, respectively (Figure 4.27). These mutations were not identified in the SNP database and were not observed in 200 control chromosomes screened by DHPLC analysis.

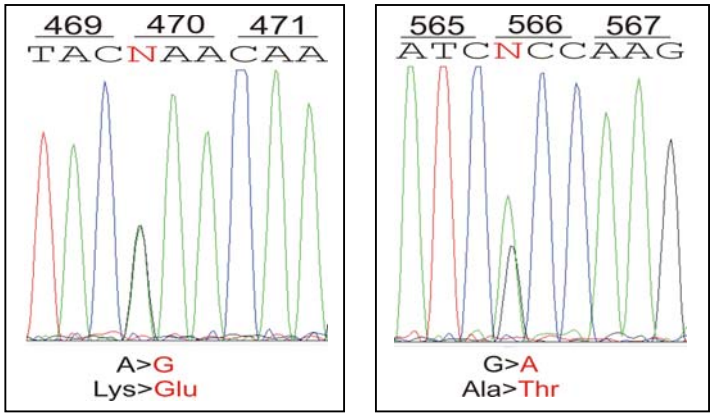

Figure 4.27. Sequencing analysis confirms the presence of heterozygous A>G transition (c.1408A>G, K470E) in DSP exon 11 (on the left) and of heterozygous G>A transition (c.1696G>A, A566T) in DSP exon 13 (on the right), in patient #38, in with the heteroduplex peaks were detected by DHPLC analysis.

Both K470E and A566T mutations are located in the N-terminal domain of desmoplakin, which is predicted to bind the desmosomal plaque. They occurred in residues conserved among

species. The first detected substitution replaced a positively-charged residue by negatively-charged a one; the second amino acid change introduce a new –OH group in position 566.

The genetic study was extended to the other members of the family. It demonstrated that the proband inherited mutations from the mother (III,2), suddenly death at 40 years. A maternal cousin (III,4) carried the two mutations, thus suggesting that such mutations are carried in *cis* orientation; he showed minor signs of the disease.

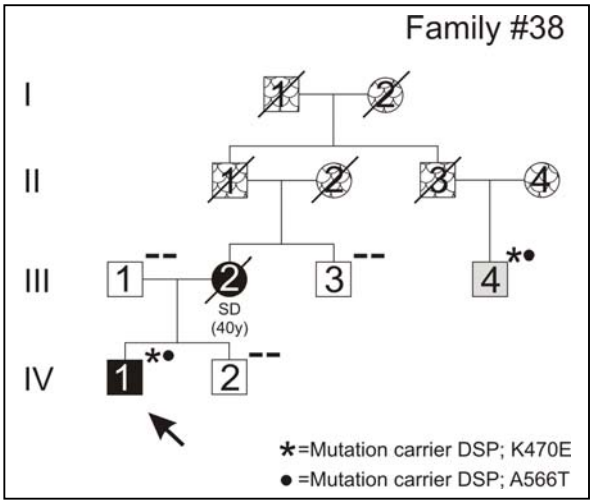

Figure 4.28. Pedigree of Family #38. Index patient is indicated by arrow. Filled square or circles represent affected patients; open square or circles, unaffected individuals; the line through symbol represent deceased individuals. Black, white, and grey symbols represent clinically affected, unaffected, and showing minor signs of the disease individuals, respectively; shaded symbols, individuals of unknown disease status. The line through symbols represents deceased individuals. SD=sudden death. Presence (symbol) or absence (-) of the two DSP mutations is indicated.

Family #39

Patient #39 (II,1 in Family #39, Figure 4.30) was a male with a severe form of ARVC/D who received an implantable cardioverter defibrillator.

He resulted to carry three heterozygous mutations. By DHPLC analysis followed by direct sequencing of DSP amplicon 23c, and by direct sequencing of PKP2 exons 3 and 12, the presence of three nucleotide changes was demonstrated (Figure 4.29).

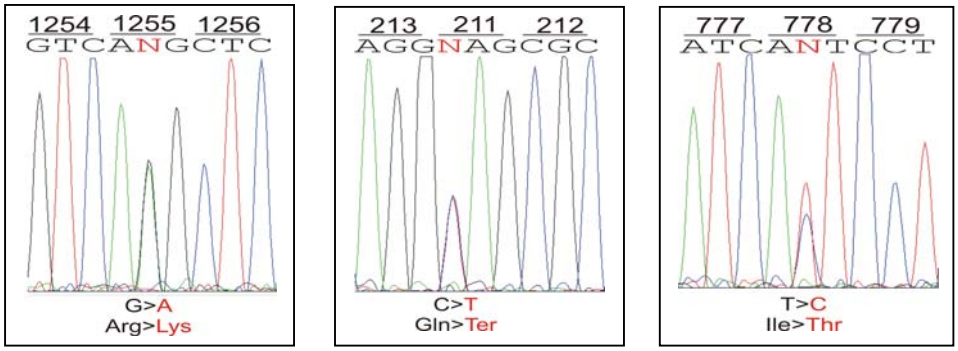

Figure 4.29. Sequencing analysis shows the presence of heterozygous G>A transition (c.3764G>A, R1255K) in DSP exon 23 (on the left), of heterozygous C>T transition (c.631C>T, Q211X) in PKP2 exon 3 (on the center), and of heterozygous T>C transition (c.2333T>C, I778T) in PKP2 exon 12 (on the right) in patient #39.

The first nucleotide change c.3764G>A, detected in DSP exon 23, leads to causes an R1255K substitution. This variation was not identified in the SNP database and was never observed in 200 control chromosomes screened by DHPLC analysis. It is located in the rod domain of desmoplakin (from 1056 to 1909 amino acid), which is predicted to form the dimeric coil. Both arginine and lysine are hydrophilic amino acids, nevertheless arginine could establish higher number of hydrogen bonds than lysine.

The second nucleotide change c.631C>T, detected in PKP2 exon 3, causes a nonsense mutation (Q211X) that insert the premature termination codon within the N-terminal domain of plakophilin-2.

The third nucleotide change c.2333T>C, detected in PKP2 exon 12, results in the change I778T disrupting a highly conserved residue in functional Arm-7 domain of plakophilin-2. In fact, a hydrophobic isoleucine residue is substituted by an ambivalent threonine.

The genetic study was extended to available relatives.

The *trans* orientation of two PKP2 nucleotidic mutations was demonstrated. Proband (II,1) resulted to inherit DSP missense mutation and PKP2 stop mutation from his mother (I,2), and the missense PKP2 mutation from the father (I,1). In all proband's sons at least one mutation was detected. A proband's cousin (II,4) died suddenly at the age 30, but no autoptic data were available.

In the family, all clinically investigated mutation carriers, excluding the proband, were fully asymptomatic.

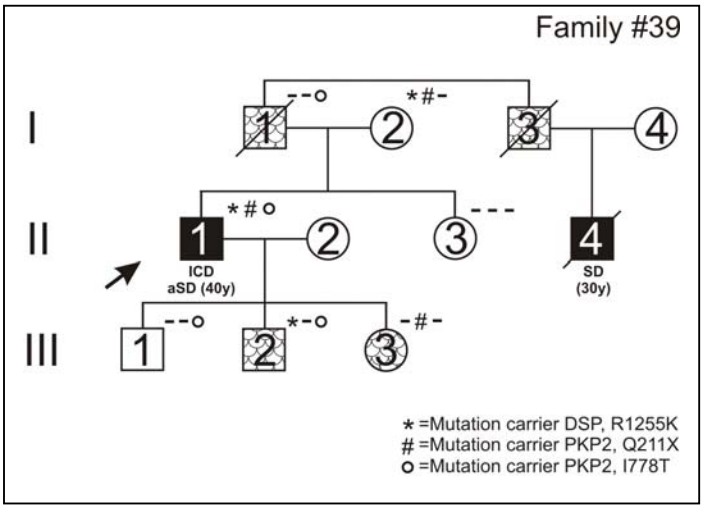

Figure 4.30. Pedigree of Family #39, index patient is indicated by arrow. Filled square or circles represent affected patients; open square or circles, unaffected individuals; shaded symbols, individuals of unknown disease status. the line through symbol represent deceased individuals. The line through symbols represents deceased individuals. ICD= implantable cardioverter defibrillator; aSD=aborted sudden death; SD=sudden death. Presence (symbol) or absence (-) of all three mutations is indicated.

Family #40

Patient #40 (III,9 in Family #40, Figure 4.32) was a female aged 44 years with a severe form of ARVC/D; she showed family history for juvenile sudden death.

Mutation detection analysis of the DSP gene showed a mutation (c.4961T>C) in exon 23 leading to a replacement of a leucine by proline (L1654P) (Figure 4.31). The novel nucleotide change was absent in 400 unrelated normal chromosomes and involved a residue highly

conserved in different species. Leucine residue in position 1654 is placed in the “core” of the alpha-helical coiled-coil rod-domain of desmoplakin. Leucine is a hydrophobic amino acid found as a structural element on the interior of proteins (alpha-helix or beta-sheet). Proline does not fit into the regular part of either helix or sheet structures because it does not have a backbone-NH available to take part in an hydrogen-binding. Thus, this mutation possibly destroy the alpha-helix.

However, analysis of all the family members showed that one clinically affected subject didn’t carried this mutation.

The DHPLC screening of PKP2 gene followed by sequencing of the abnormal profiles allowed to identify a missense mutation in exon 1 (c.184C>A, Q62K) and a nonsense mutation in exon 10 (c.2119C>T, Q707X) (Figure 4.31). None of the detected nucleotide changes was found in 400 control chromosomes. The missense variation Q62K has been previously reported as “unclassified variant” (Van Tintelen et al., 2006), because it is not located in highly conserved amino acid, but it was absent in 300 control alleles.

Analysis of all the available family members showed that the proband inherited the DSP L1654P mutation and PKP2 Q62K from the father (II,1) and the Q707X mutation from the mother (II,2).

Eight subjects resulted to carry the DSP L1654P mutation, five subjects carried the PKP2 Q62K variant, whereas nine carried the PKP2 Q707X mutation. Seven subjects resulted to be heterozygous for two mutations.

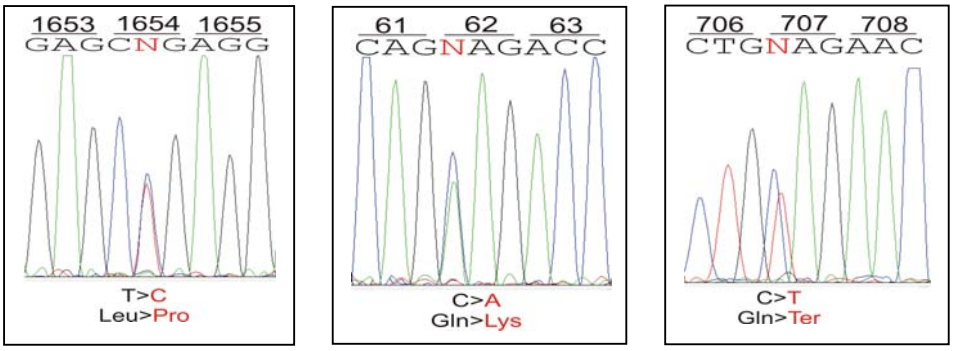

Figure 4.31. Sequencing analysis shows the presence of heterozygous T>C transition (c.4961T>C, L1654P) in DSP exon 23 (on the left), of heterozygous C>A transversion (c.184C>A, Q62K) in PKP2 exon 1 (on the center), and of heterozygous C>T transition (c.2119C>T, Q707X) in PKP2 exon 10 (on the right) in patient #40.

Two subjects (III,3 and III,4) died suddenly at the age 22 and 24 during emotion and effort respectively. No clinical or autoptic data were available.

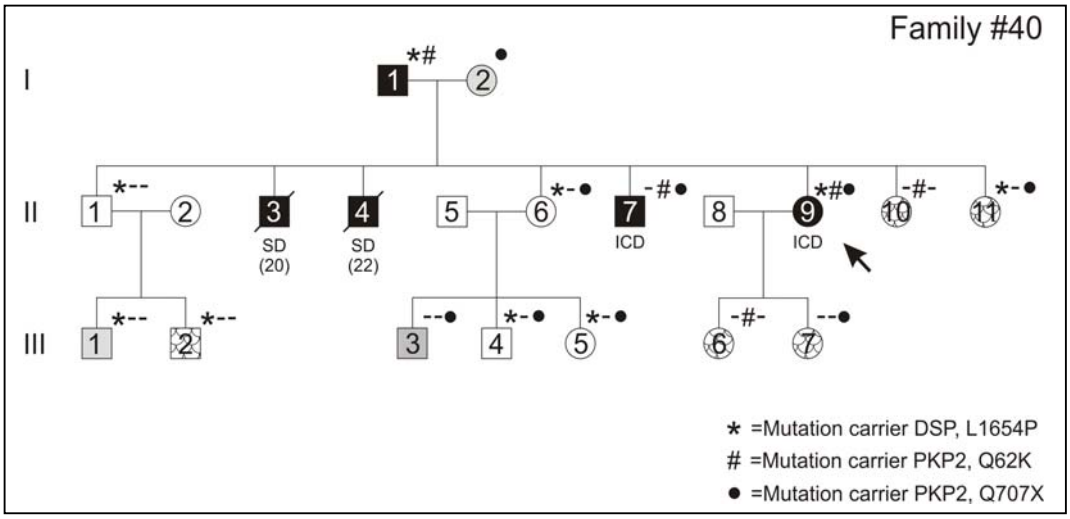

Figure 4.32. Pedigree of Family #40, index patient is indicated by arrow. Black, white, and grey symbols represent clinically affected, unaffected, and showing minor signs of the disease individuals, respectively; shaded symbols, individuals of unknown disease status. The line through symbol, deceased individuals. ICD= implantable cardioverter defibrillator; SD=sudden death. Presence (symbol) or absence (-) of all three mutations is indicated.

Family #42

Patient #42 (II,4 in Family #42, Figure 4.34) was a female aged 62 years diagnosed with a severe form of ARVC/D.

The DHPLC analysis and the direct sequencing for mutation screening in DSG2 gene revealed the presence of two heterozygous nucleotide changes: a missense mutation c.991G>A in exon 8 (E331K), and a splice mutation (c.1881-2A>G) that affects the acceptor splice site of intron 12 (Figure 4.33).

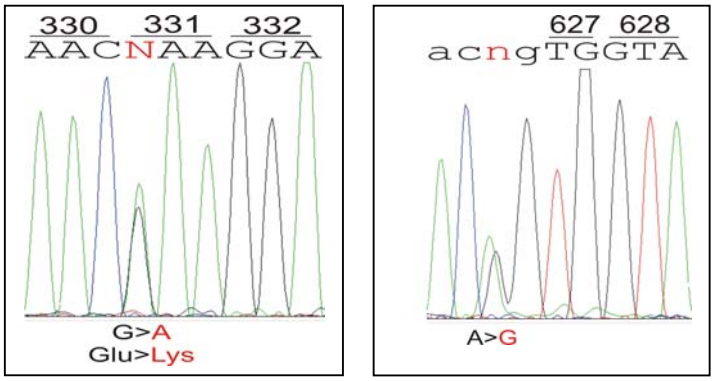

Figure 4.33. Sequencing analysis shows the presence of heterozygous G>A transition (c.991G>A, E331K) in DSG2 exon 8 (on the left) and of heterozygous A>G transition (c.1881-2A>G) in DSG2 acceptor splice site of intron 12 (on the right), in patient #42.

The amino acid change E331K involved a residue highly conserved among species, sited in extracellular cadherin (EC3) domain important for homophilic intercellular associations and

forming Ca^{2+}-dependent rodlike structures. This substitution lead to a negatively-charged glutamic acid change with a positively-charged lysine in EC3 domain.

Analysis of the aberrant DSG2 transcript showed that c.1881-2A>G mutation activates an alternative cryptic splice site in exon 13, located 38bp downstream from the authentic 3' splice acceptor site. This aberrant spliced mRNA contains a 38bp deletion and should code for a truncated plakophilin-2 protein of 646 amino acids in length, missing the cytoplasmic domain.

Family members were available for molecular analysis, but few of them were available for clinical investigation.

The *trans* orientation of two mutation was demonstrated. Subjects carrying both mutations (the proband II,4 and her sister II,2) were affected with a severe form of ARVC/D, whereas investigated single mutation carriers (I,2 and III,7) were fully negative.

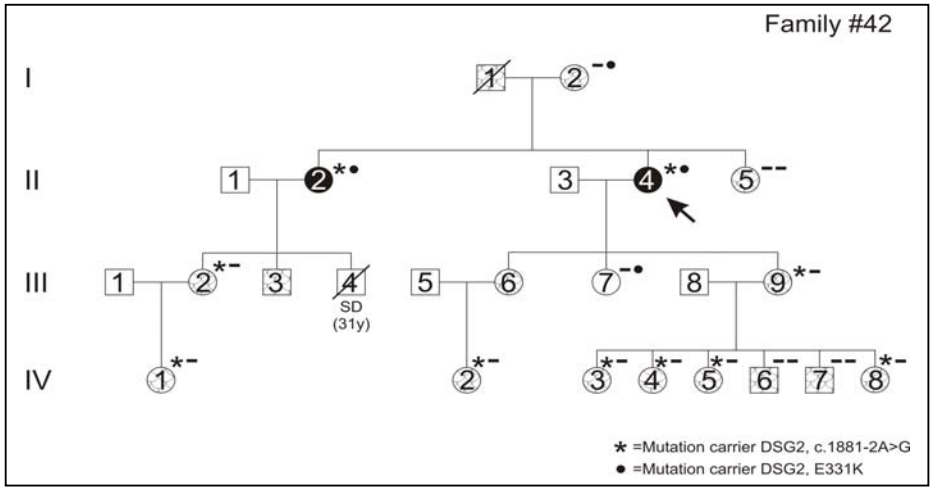

Figure 4.34. Pedigree of ARVC/D index patient #42 (indicated by arrow). Black, white, and shaded symbols represent clinically affected individuals, unaffected individuals, and individuals of unknown disease status, respectively. The line through symbol, deceased individuals. SD=sudden death. Presence (symbol) or absence (-) of the DSG2 mutations is indicated.

Family #62

Patient #62 (III,10 in Family #62, Figure 4.36) was a men aged 49, diagnosed with a severe form of ARVC/D at 34 years. He showed family history for juvenile sudden death.

Mutation detection analysis of desmosomal encoding genes involved in ARVC/D showed the transition c.1174G>A in DSG2 exon 9, leading to a replacement of a valine by isoleucine (V392I) (Figure 4.35). DHPLC analysis of 400 unrelated normal chromosomes failed to detect the abnormal profile corresponding to the mutation. In addition, this amino acid is highly conserved in different species. This mutation has been previously reported (Syrris et al., 2006).

Moreover, sequencing of PKP2 exon 1 allowed to identify a 4bp deletion, c.145_148delCAGA, leading to a frame shift and premature termination of the protein (T50SfsX60) (Figure 4.35). This mutation has been previously reported by different groups (Gerull et al., 2004; Syrris et al., 2006; Dalal et al., 2006; Van Tintelen et al., 2006), named S50fsX110 or T50fsX60.

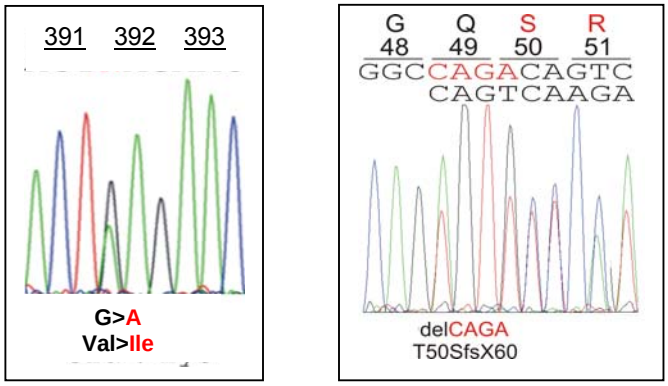

Figure 4.35. Sequencing analysis showing the presence of heterozygous G>A transition (c.1174G>A, V392I) in DSG2 exon 9 (on the left) and of heterozygous 4-bp deletion (c.145_148delCAGA, T50SfsX60) in DSG2 exon1 (on the right), in patient #62.

Segregation analysis in family members assigned the DSG2 V392I mutation to the paternal side and the PKP2 T50SfsX60 mutation to the maternal one.

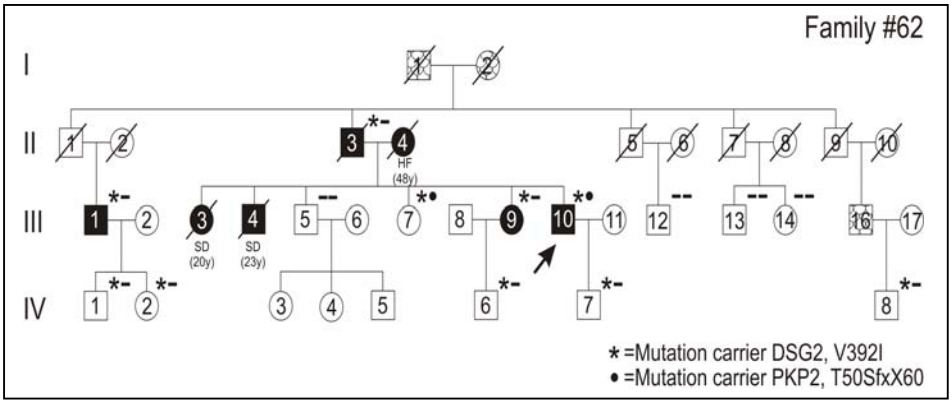

Figure 4.36. Pedigree of ARVC/D index patient #62 (indicated by arrow). Black, white, and shaded symbols represent clinically affected individuals, unaffected individuals, and individuals of unknown disease status, respectively. The line through symbol, deceased individuals. SD=sudden death; HF=heart failure. Presence (symbol) or absence (-) of the two mutations is indicated.

Two subjects resulted to carry the PKP2 mutation (III,7 and III,10), whereas ten subjects carried the DSG2 mutation (II,3; III,1; III,7; III,9; III,10; IV,1; IV,2; IV,6; IV,7 and IV,8). The index case (III,10) and his sister (III,7) resulted to be heterozygous for the two mutations.

Family #83

Patient #83 (II,5 in Family #83, Figure 4.38) was the proband of a family with recurrence of ARVC/D and high occurrence of sudden death.

The proband resulted to carry the two nucleotide substitutions c.88G>A and c.7622G>A in DSP exon 1 and exon 24, respectively (Figure 4.37). None of the nucleotide changes were detected in 200 control subjects from the Italian population.

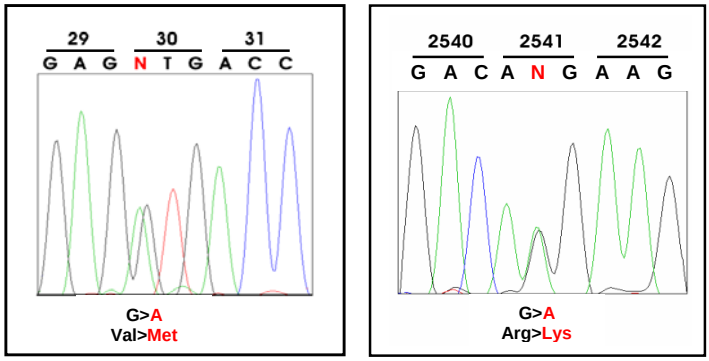

Figure 4.37. Sequencing analysis showing the presence of heterozygous G>A transition (c.88G>A, V30M) (on the left) and of heterozygous G>A transition (c.7622G>A, R2541K) (on the right), in DSP exon 1 and exon 24, respectively.

Substitution c.88G>A, leading to a replacement of a valine by methionine (V30M), has been previously demonstrated to be pathogenic (Yang et al., 2006). The methionine at position 30 has not been well conserved during the evolution of vertebrate desmoplakins. Strict conservation is seen, however, in the immediately upstream positions (residues 1-29).

Variation c.7622G>A leads to substitution R2541K occurring in a residue placed in a region of link between plakin repeat domains of the desmoplakin C-terminal, not well conserved among species. Although arginine 2541 changes with a lysine in *Gallus gallus* and in *Danio rerio* and both residues are hydrophilic amino acids, nevertheless arginine could make a major number of hydrogen bonds than lysine, and, consequently, the plakin repeat domains could be destabilized by this change.

Analysis of all the available family members showed that the proband inherited the V30M mutation from the mother (I,3) and the R2541K variant from the paternal side.

Subject II,4 was affected by a severe form of ARVC/D and died suddenly at the age of 43 after two years of follow-up. Autopsy confirmed the clinical diagnosis of ARVC/D. Subject I,5 was affected by a biventricular form of ARVC/D and died due to refractory heart failure at the age of 64 yrs. Among the living relatives, two fulfilled the diagnostic criteria (II,7 and III,4), and three had only minor clinical sign, whereas five mutation carriers did not show any cardiac abnormalities.

Mutation V30M was found in five additional subjects and the variation R2541K in seven. In this family, each of the two distinct mutations was responsible for the ARVC phenotype.

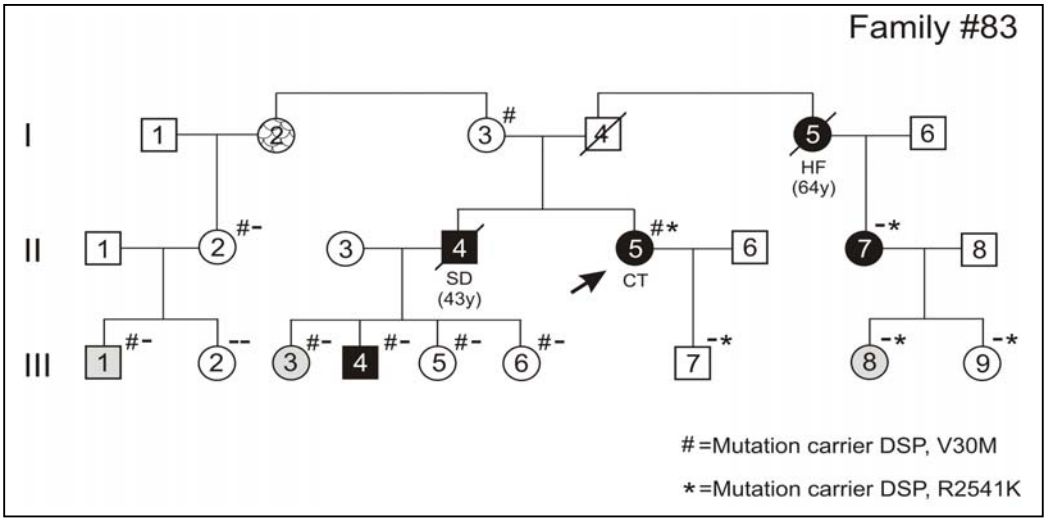

Figure 4.38. Pedigree of ARVC/D index patient #83 (indicated by arrow). Black, white, and grey symbols represent clinically affected, unaffected, and individuals showing minor signs of the disease, respectively; shaded symbols, individuals of unknown disease status. The line through symbol, deceased individuals. SD=sudden death; HF=heart failure; CT= cardiac transplantation. Presence (symbol) or absence (-) of the two mutations is indicated.

Family #87

Patient #87 (III,2 in Family #87, Figure 4.40) was a young male asymptomatic, clinically examined because of ECG abnormalities detected at pre-participation screening for sport activity at age of 14 years.

By DHPLC analysis of coding regions of DSG2 gene, abnormal chromatograms for amplicons of exons 9 and 15 were detected. To confirm the presence of heterozygous nucleotide changes, two amplicons were sequenced (Figure 4.39). A 4bp insertion was identified in exon 9 (1254_1257insATGA) causing the addition of an amino acid residue before a premature stop signal is introduced (E418EfsX1). A single bp deletions (c.2983delG) was identified in exon 15 resulting in frameshifts and premature termination of translation several amino acid residues downstream (G997VfsX19). Both mutations led to predicted truncated DSG2 molecules lacking transmembrane and cytoplasmic components, and portion of cytoplasmic domain, respectively.

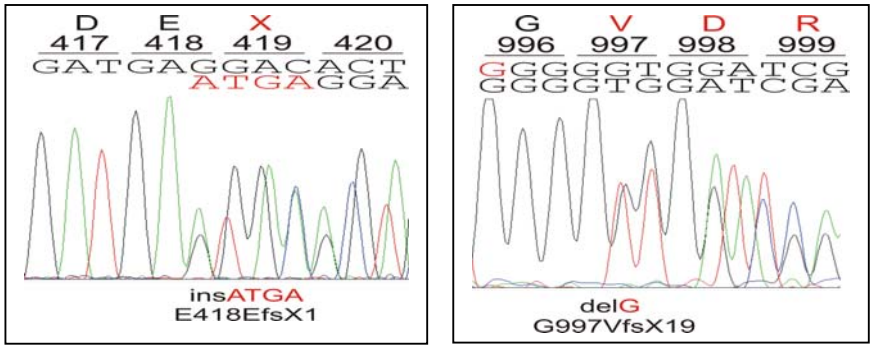

Figure 4.39. Sequencing analysis showing the presence of heterozygous 4-bp insertion (1254_1257insATGA, E418EfsX1) in DSG2 exon 9 (on the left) and of heterozygous single bp deletions (c.2983delG, G997VfsX19) in DSG2 exon 15 (on the right), in patient #87.

Patient #87 resulted compound heterozygous for the two mutations.

The genetic study was extended to additional members of the family. The *trans* orientation of two mutation was demonstrated: E418EfsX1 mutation was detected in proband's father (II,1), G997VfsX19 mutation in maternal side (I,1 and II,2). None of single mutation carriers presented symptoms or signs of the disease.

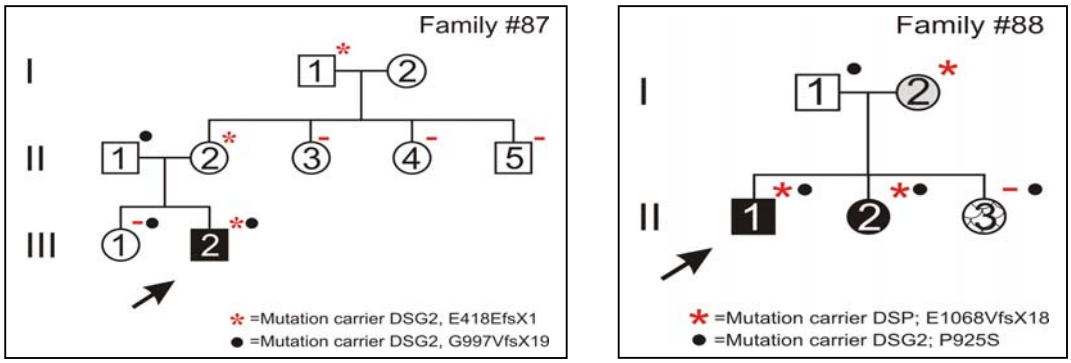

Figure 4.40. (Left) Pedigree of Family #87. **(Right)** Pedigree of Family #88. Index patients are indicated by arrow. Black, white, and grey symbols represent clinically affected, unaffected, and showing minor signs of the disease individuals, respectively; shaded symbols, individuals of unknown disease status. Presence (symbol) or absence (-) of the genes mutations is indicated.

Family #88

Patient #88 (II,1 in Family #88, Figure 4.40) was a men of 29 years affected with a severe form of ARVC/D.

By genetic screening he was identified as a double heterozygote, with a mutation (c.3203_3204delAG, E1068VfsX18) in exon 23 of DSP gene and a mutation (c.2773C>T, P925S) in exon 15 of DSG2 gene (Figure 4.41). Two mutations were detected by DHPLC analysis followed by sequencing of samples showing a change in DHPLC pattern. DSP mutation caused a frameshift that led to a premature termination codon within the rod domain of desmoplakin. DSG2 missense mutation, not found in 200 healthy controls, involved a residue highly conserved among species, sited in cytoplasmic domain of desmoglein-2; moreover, P925 is substituted with a serine showing very different physico-chemical properties.

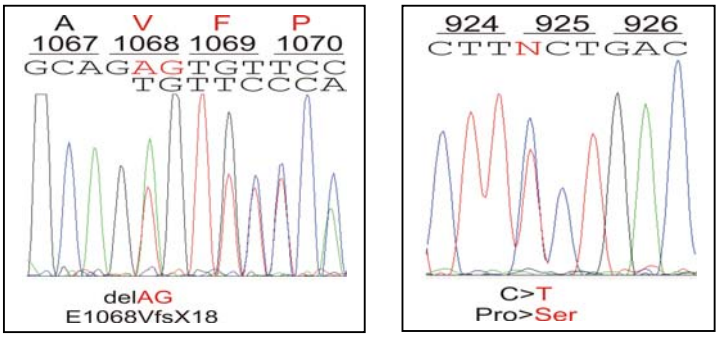

Figure 4.41. Sequencing analysis showing the presence of heterozygous 2bp deletions (c.3203_3204delAG, E1068VfsX18) in DSP exon 23 (on the left) and of heterozygous C>T transition (c.2773C>T, P925S) in DSG2 exon 15 (on the right), in patient #88.

Identification of mutations in the patient #88 allowed further investigation of other family members. All available first-order relatives carried at least one mutation. The proband (II,1) and a sister (II,2), the only ones carrying both mutations, fulfilled clinical diagnostic criteria. The proband's mother (I,2) did not fulfil diagnostic criteria but raised a suspicion of incomplete disease expression; the proband's father (I,1) was clinically unaffected, and a sister was not available for clinical investigation.

Family #97

Patient #97 (II,3 in Family #97, Figure 4.43) was a female aged 47 with a classical form of ARVC/D.

A novel missense mutation (c.1224A>T) was identified by DHPLC analysis followed by sequencing of DSP exon 9 sequence (Figure 4.42). It resulted in the substitution (N375I) of an asparagine (carrying two functional chemical groups) whit a hydrophobic residue of lysine. This change was not found in 200 control subjects, and it involved a residue conserved in different species located in the N-terminus of desmoplakin.

A novel nucleotide change (c.1912G>A), showed by DHPLC analysis and confirmed by direct sequencing, was found in exon 13 of DSG2 gene (Figure 4.42). It causes the substitution G638R, in which a hydrophobic residue is replaced by an amino acid highly hydrophilic, in the desmoglein-2 transmembrane domain. Also in this case a control group of 200 healthy and unrelated subjects was used to exclude that detected mutation could be common DNA polymorphism.

The previously described insertion c.2687_2688insGA (Syrris et al., 2006) was detected in DSC2 exon 16 (Figure 4.42). This mutation causes a frame shift that leads to a premature termination codon (E896EfsX4) within the intracellular cadherin-typical segment (ICS) domain of desmocollin-2.

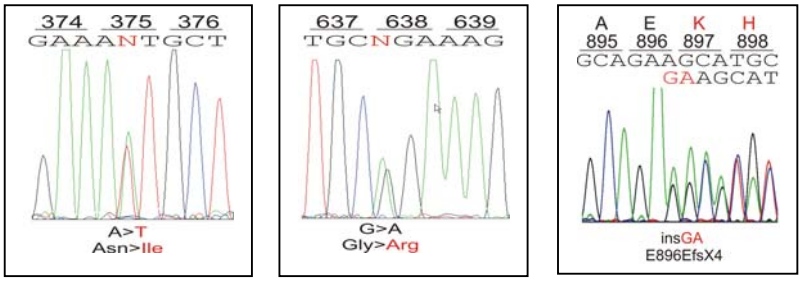

Figure 4.42. Sequencing analysis shows the presence of heterozygous A>T transversion (c.1224A>T, N375I) in DSP exon 9 (on the left), of heterozygous G>A transition (c.1912G>A, G638R) in DSG2 exon 13 (on the center), and of heterozygous 2bp insertion (c.2687_2688insGA, E896EfsX4) in DSC2 exon 16 (on the right) in patient #97.

The genetic study was extended to additional members of the family. Only patient #97 resulted to carry all three mutations. Two subjects were double heterozigotes for DSG2 and DSC2

mutations: the brother (II,7) showed left ventricle 2D-Echo abnormalities, and the sister (II,6) was fully asymptomatic.

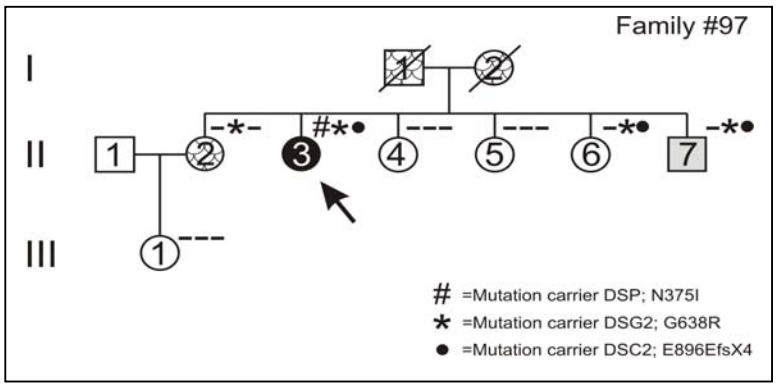

Figure 4.43. Pedigree of ARVC/D index patient #97 (indicated by arrow). Black, white, and grey symbols represent clinically affected, unaffected, and individuals showing minor signs of the disease, respectively; shaded symbols, individuals of unknown disease status. The line through symbol, deceased individuals. Presence (symbol) or absence (-) of the three mutations is indicated.

Family #105

Patient #105 (II,2 in Family#105, Figure 4.45) was a German woman from a family with recurrence of ARVC/D.

By DHPLC analysis, an abnormal elution profile for the amplicon of DSP exon 7 was identified, which showed two peaks. To confirm the presence of a heterozygous nucleotide change, sequencing analysis was performed. A novel nonsense substitution, c.817C>T, was identified (Figure 4.44), which produces a premature stop codon (Q273X) in N-terminal domain of desmoplakin molecule.

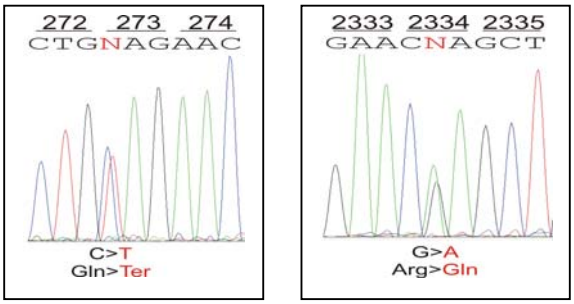

Figure 4.44. (Left) Sequencing analysis showing the presence of heterozygous C>T transition (c.817C>T, Q273X) in DSP exon 7 in patient #105. **(Right)** Sequencing analysis showing the presence of heterozygous G>A transition (c.7001G>A, R2334Q) in in DSP exon 23 in family subject II,4.

The genetic study was extended to additional members of the family.

Analysis of all the available family members showed that other two clinically affected subjects (II,4, and III,7) didn't carried this mutation.

Assuming that in family #105 distinct mutations could be carried, DNA of the two affected relatives was investigated for mutations in coding regions of desmosomal PKP2, DSP, DSG2 and DSC2 genes.

A novel DSP nucleotidic variation, c.7001G>A in exon 23, was detected by DHPLC analysis followed by direct sequencing of amplicons 23e in subject II,4. It results in the missense substitution R2334Q of a residue conserved among species (Figure 4.44), located within the subdomain B in the desmoplakin C-terminus. This amino acid change was not observed in 2--Italian control subjects screened by DHPLC analysis. To exclude that it can be a rare polymorphism in the German population, a further screening in German control subjects will be necessary.

However, DSP R2334Q variation was not detected in DNA of the affected family member III,7, thus suggesting that different mutation in unknown ARVC/D gene should be involved in the genetic determination of the disease in this family.

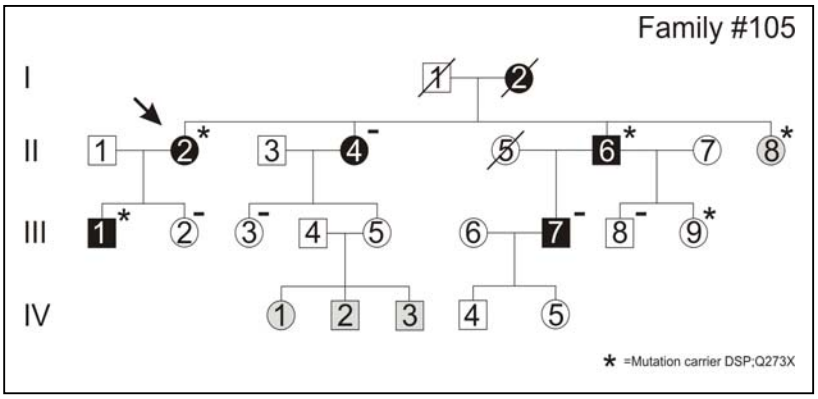

Figure 4.45. Pedigree of Family #97 (index patient is indicated by arrow). Black, white, and grey symbols represent clinically affected, unaffected, and individuals showing minor signs of the disease, respectively. The line through symbol, deceased individuals. Presence (symbol) or absence (-) of the DSP mutation is indicated.

4.1.7. Clinical expression and penetrance of mutations in ARVC/D genes

This study provides mutational analysis and clinical features in 110 unrelated consecutive patients fulfilling the ARVC/D criteria (McKenna et al, 1994). In 52 of them, one or more than one mutation was detected (Table 4.10).

Table 4.10. Mutations detected in 110 ARVC/D index cases.

Mutations carriers index cases	One PKP2 mutation carrier	One DSP mutation carrier	One DSG2 mutation carrier	One DSC2 mutation carrier	Multiple mutations carrier	Total
ARVC/D diagnosis	16	11	8	3	14	52

In 19 of these index patients, additional family members had been clinically and genetically investigated in order to study the segregation of mutations.

In 89 relatives one or more mutations were identified (Table 4.11). 16 subjects (18%) fulfilled the task force diagnostic criteria for ARVC/D; 19 (about 21%) were found to have isolated minor cardiac abnormalities, most often non-sustained ventricular arrhythmias.

Thirty family members (34%) resulted fully asymptomatic; the remaining 24 (27%) were not available to clinical investigation.

Table 4.11. Clinical diagnosis and mutations detected in family members of ARVC/D index cases.

Mutations carriers family members	One PKP2 mutation carrier	One DSP mutation carrier	One DSG2 mutation carrier	One DSC2 mutation carrier	Multiple mutations carrier	Total
ARVC/D diagnosis	-	7	5	-	4	16
Minor signs of ARVC/D	2	10	3	2	2	19
Clinically fully asymptomatic	2	13	9	1	5	30
Clinically not available	6	3	12	-	3	24
Total	10	33	29	3	14	89

Clinical characteristics of 87 probands and family members carrying one mutation in each of the three main desmosomal genes or multiple mutations were compared (Table 4.12). Only family members fulfilling ARVC/D diagnostic criteria or satisfying an incomplete set of criteria have been included.

Table 4.12. Clinical characteristics comparison in patients fulfilling ARVC/D diagnostic criteria or satisfying some criteria for ARVC/D.

87 mutation carriers	DSP (30 pts)	PKP2 (18 pts)	DSG2 (16 pts)	Multiple mutations (20 pts)	DSP vs PKP2	DSP vs DSG2	PKP2 vs DSG2	DSP vs Multiple	PKP2 vs Multiple	DSG2 vs Multiple
Males	20 (67%)	13 (72%)	9 (56%)	12 (60%)	0,71	0,46	0,33	0,61	0,44	0,81
Mean age (years)	42±17	46±18	53±20	49±15	0,44	0,05	0,36	0,14	0,08	0,49
Mean age at diagnosis (years)	32±15	34±17	41±19	40±16	0,67	0,08	0,26	0,07	0,26	0,86
Index cases	11 (37%)	16 (89%)	8 (50%)	14 (70%)	**0,001**	0,39	**0,01**	**0,02**	0,15	0,22
Ventricular arrhythmias	24 (80%)	14 (78%)	13 (81%)	19 (95%)	0,86	0,93	0,83	0,14	0,12	0,19
Non sustained VT	16 (53%)	6 (33%)	9 (56%)	9 (45%)	0,18	0,84	0,18	0,58	0,45	0,51
Sustained VT/VF	8 (27%)	8 (44%)	4 (25%)	10 (50%)	0,23	0,88	0,25	0,1	0,71	0,13
ICD implantation	3 (10%)	5 (28%)	3 (18%)	10 (50%)	0,11	0,44	0,49	0,02	0,17	0,05
Biventricular involvement	11 (37%)	8 (44%)	4 (25%)	7 (35%)	0,63	0,41	0,25	0,88	0,57	0,52
Pathological ECG	9 (30%)	16 (89%)	10 (62%)	15 (75%)	**0,0003**	0,04	0,07	**0,003**	0,27	0,4
Presence of late potentials	17 (57%)	12 (67%)	9 (56%)	17 (85%)	0,49	0,94	0,51	0,04	0,19	0,06
RV abnormalities	22 (73%)	15 (83%)	12 (75%)	19 (95%)	0,43	0,88	0,57	0,05	0,23	0,09
mild form	18 (60%)	6 (33%)	5 (31%)	5 (25%)	0,07	0,06	0,9	0,01	0,58	0,69
Moderate form	7 (23%)	9 (50%)	3 (19%)	9 (45%)	0,06	0,75	0,06	0,1	0,75	0,1
Severe forms	5 (17%)	5 (28%)	6 (37%)	6 (30%)	0,37	0,13	0,57	0,28	0,89	0,66
Major events	9 (30%)	10 (55%)	5 (31%)	11 (55%)	0,09	0,94	0,16	0,08	1	0,15
Age at major events	39±16	37±19	51±19	41±12	0,69	**0,02**	**0,03**	0,63	0,43	0,06

VT, ventricular tachycardia; VF, ventricular fibrillation; RV, right ventricular; pts, patients.

No significant differences in terms of electrocardiographic and structural abnormalities, major events and disease expression were noted.

Significant differences in clinical manifestations between DSP mutation carriers and PKP2 and multiple mutation carriers could be due to the lower number of probands in the DSP subgroup.

Interestingly, patients carrying DSG2 mutations were found be older at diagnosis and at the time of major arrhythmic symptoms than DSP and PKP2 carriers.

Kaplan-Mayer analysis was used to examine freedom from the major events (sustained VT, ventricular fibrillation, heart failure, death, unexplained syncope) since birth. Analysis was performed on individuals carrying one mutation in each of the three main desmosomal genes or multiple mutations (Figure 4.46).

No significant differences were identified between the different groups.

VT, ventricular tachycardia; VF, ventricular fibrillation; ICD, implantable cardioverter defibrillator, RV, right ventricular; Major events (VT, VF, HF heart failure , unexplained syncope).

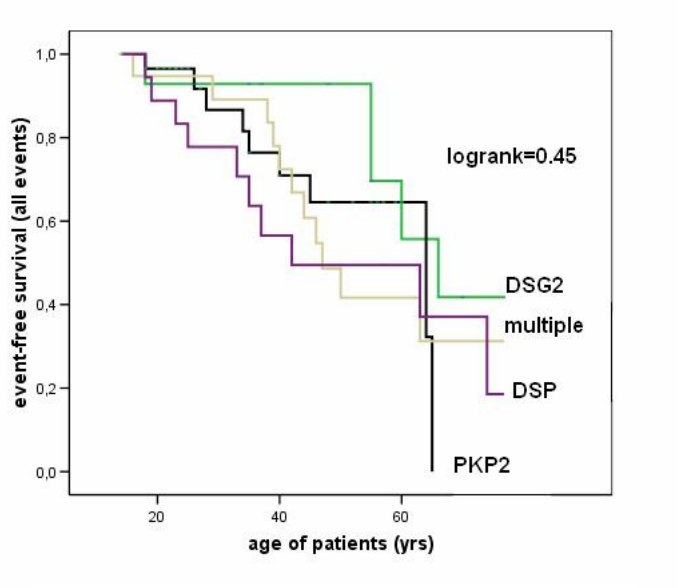

Figure 4.46. Event-free survival curve of patients carrying different gene-mutations considering major events (death, VF, sustained VT, unexplained syncope, heart failure) since birth

Presently, the penetrance of the ARVC/D phenotype is not known. An approximately penetrance estimation (defined as the probability that a person who has the genotype will manifest the character), for DSP and DSG2 mutations has been calculated among family members. Penetrance of PKP2 and DSC2 mutations cannot be estimated due to the small size of each group of mutation carriers.

Among the 35 DSP mutation carriers (5 index cases and 30 family members) clinically investigated, 12 (about 34%) were diagnosed with ARVC/D.

Family subjects carrying a DSG2 mutation and clinically investigated were 19 (of which 2 were index cases); 7 of them (about 37%) fulfilled the task force diagnostic criteria for ARVC/D.

4.2. MUTATION SCREENING IN CANDIDATES ARVC/D GENES

4.2.1. Mutations in DES gene

DES gene, coding for desmin, was considered a good candidate ARVC/D gene, because of its expression and function in heart tissue.

A systematic mutation screening in DES coding regions was performed in 80 (54 males and 26 females) among 110ARVC/D index cases.

The patients DNA was investigated by DHPLC and direct sequencing. PCR primers flanking each exon of the human DES were designed by PRIMER3 software.

Human DES gene (cDNA and translation sequences available in NCBI website, NM_001927 and NP_001918, respectively) has 9 coding exons. Exon 1 was split into three different and overlapping fragments for DHPLC analysis. Exons 2 and 3 were amplified into the same fragment. Exon 8 was analyzed only by direct sequencing, because the nucleotide sequence showed denaturation domains unsuitable for DHPLC analysis.

For amplicons size, primers sequences, amplification and analysis conditions see Appendix, Table 5.

A control group of 300 healthy and unrelated subjects (600alleles) from the Italian population was used to exclude (by DHPLC analysis or Arms test analysis) that detected mutations could be common DNA polymorphisms. DNA variations found in more than 1% of the healthy controls chromosomes have been considered polymorphisms.

Analysis of exon-by-exon sequences of the DES coding region resulted in identification of six nucleotide variations (five novel), not reported in dbSNP (Table 4.13).

Table 4.13. Variations detected in DES gene.

Mutation	Amino Acid Change	Type of mutation	Exon	Position (protein domain)	# Index case	Reference
721A>G	K241E	missense	3	1B	73	novel
736-11A>G	-	splice site	Intron 3	-	98	novel
Polymorphism	**Amino Acid Change**	**Type of variation**	**Exon**	**Position (protein domain)**	**# Index case**	**Reference**
4-8C>T	L136L	synonymous	1	1A	7,32,4-,101	novel
638C>T	A213V	missense	2	1B	65	Bär et al., 2005; Goudeau et al., 2006
735+2-C>T	-	intronic	Intron 3	-	21,95	novel
736-35C>A	-	intronic	Intron 3	-	several	novel

c.721A>G, K241E

A novel nucleotide change, c.721A>G, was identified in patient #73. An abnormal elution profile for the DES amplicon 2+3 was identified by DHPLC analysis, (Figure 4.47); then, sequencing analysis was performed to confirm the presence of a heterozygous nucleotide change (Figure

4.47). The missense mutation resulted in the substitution K241E of a residue highly conserved among species (Figure 4.48), located within the conserved subdomain 1B of desmin α-helical rod domain. Although both lysine and glutammic acid are hydrophilic amino acids, the positively charged amino group is replaced by a negative charged carbossilic group. This amino acid change was not detect in 300 Italian control subjects screened by ARMS test.

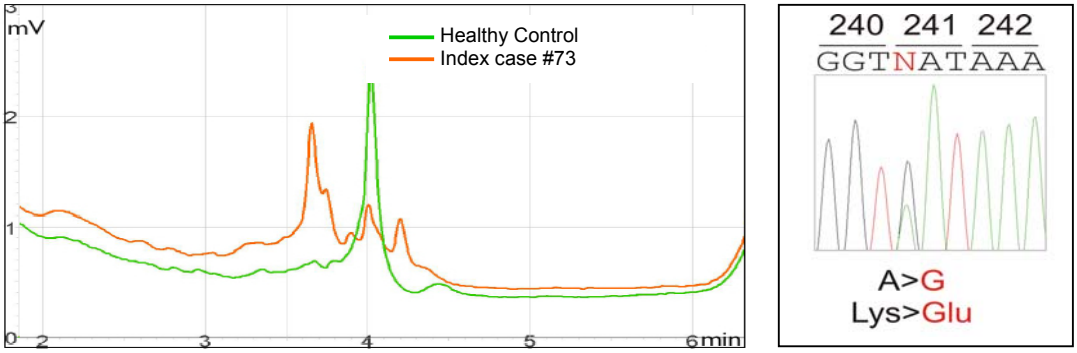

Figure 4.47. (Left) DHPLC elution profiles of PCR DES fragment 2+3 in the Healthy Control and in Index case #73 at analysis temperature of 61.5°C. **(Right)** DNA sequencing of PCR DES,2+3 fragment revealing c.721A>G transition (K241E substitution).

```
DES_Hs  202 EAENNLAAFRADVDAATLARIDLERRIESLNEEIAFLKKVHEEEIREL 250 NP_001918
DES_Cf  202 EAENNLAAFRADVDAATLARIDLERRIESLNEEIAFLKKVHEEEIREL 250 NP_001012394
DES_Dr  197 EAENNLSAFRADVDAATLARLDLERRIEGLHEEIAFLRKIHEEEIREL 244 NP_571038
DES_Gg  186 EAENNLAAFRADVDAATLARIDLERRIESLQEEIAFLKKVHEEEIREL 233 BAA_25132
DES_Mm  202 EAENNLAAFRADVDAATLARIDLERRIESLNEEIAFLKKVHEEEIREL 250 NP_034173
DES_Rn  202 EAENNLAAFRADVDAATLARIDLERRIESLNEEIAFLKKVHEEEIREL 250 NP_071976
DES_Ss  204 EAENNLAAFRADVDAATLARIDLERRIESLNEEIAFLKKVHEEEIREL 251 AAD46492
DES_Xl  191 DAENNLAAFRGDVDAATLARIDLERRIESLQEEIAFLKKIHEEEIREL 238 CAA34740
```

Figure 4.48. ClustalW alignment of highly conserved 1B desmin domain among species. Organism names, GenBank accession numbers, and amino acid termini are reported on sides. A213 (changing in valine in the index case #65) is reported on a yellow background; K241 (changing in valine in the index case #65) is reported on a green background. Not conserved residues are reported in pink colour (Hs= Homo sapiens, Cf= Canis familiaris, Dr= Danio rerio, Gg= Gallus gallus, Mm= Mus musculus, Rn= Rattus norvegicus, Ss= Sus scrofa, Xl= Xenopus laevis).

Patient #73 (II,1 in the Family #73, Figure 4.49) resulted to carry also a PKP2 frame shift mutation (T816RfsX9) predicted to encode truncated plakophilin-2 molecules. The genetic study was extended to an additional family member (II,2) who carried only the DES mutation and was fully clinically asymptomatic.

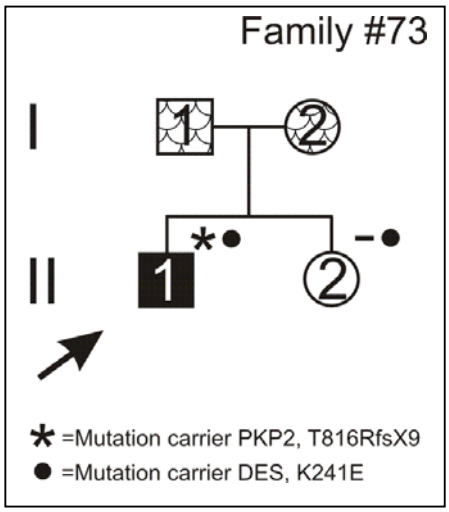

Figure 4.49. Pedigree of Family #73. Index patient #73 is indicated by arrow. Black, white, and shaded symbols represent clinically affected individuals, unaffected individuals, and individuals of unknown disease status, respectively. Presence (symbol) or absence (-) of the genes mutations is indicated.

c.736-11A>G

By means of DHPLC analysis of DES fragment 4, an abnormal elution profile was identified in the index case #98 (Figure 4.50). By direct sequencing of the amplicon a heterozygous nucleotide change close to the acceptor splice site of exon 4 of DES gene (c.736-11A>G) was identified (Figure 4.50). This variant was not detected in the SNP database and was never observed in 300 control chromosomes screened by ARMS test analysis.

The c.736-11A>G co-segregation with affected members in the family was investigated (Family #89, Figure 4.51), and DES intronic nucleotide variation was not detected in all clinically affected individuals.

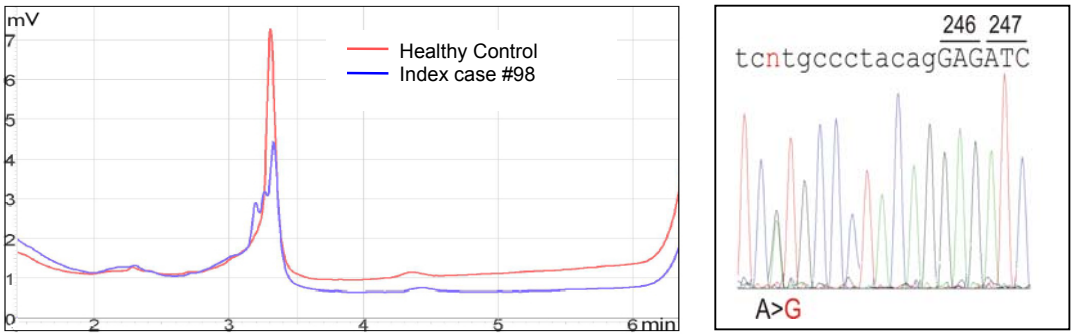

Figure 4.50. (Left) DHPLC elution profiles of PCR DES fragment 4 in the Healthy Control and in Index case #98 at analysis temperature of 62.8°C. **(Right)** DNA sequencing of PCR DES fragment 4 revealing c.736-11A>G intronic transition.

No mutation was detected in screened desmosomal ARVC/D genes in the index case #98. For these reason the hypothesis that other mutations, in addition to DES variation, could be carried in family #98 in not screened ARVC/D genes or in unknown ARVC/D genes, can be suggested.

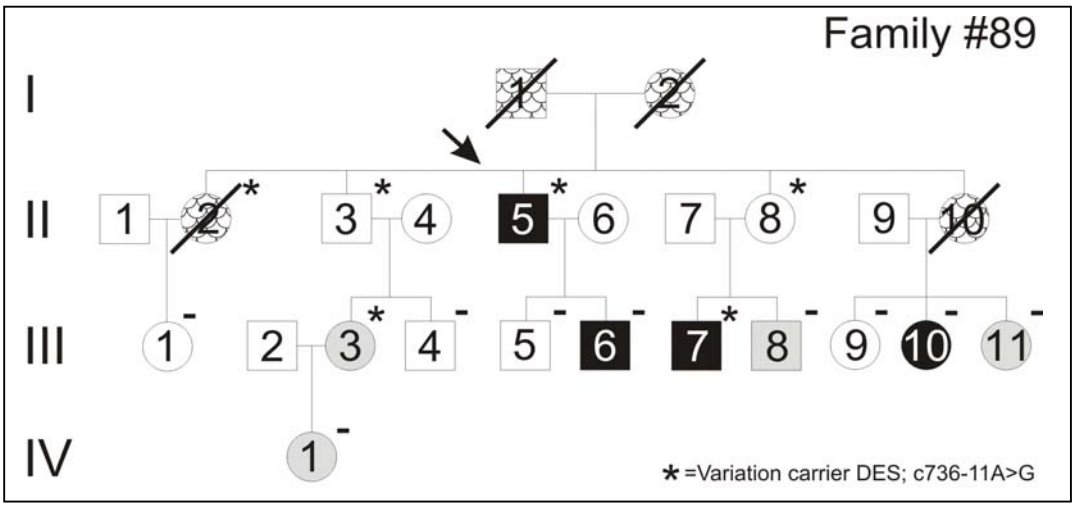

Figure 4.51. Pedigree of ARVC/D index patient #89 (indicated by arrow). Black, white, and grey symbols represent clinically affected individuals, unaffected individuals, and showing minor signs of the disease individuals, respectively; shaded square or circles, individuals of unknown disease status; the line through symbol, deceased individuals. Presence (symbol) or absence (-) of the DES variation is indicated.

In order to detect aberrant transcripts generated from this nucleotide change in the patient cDNA and since heart tissue sample was not available, desmin expression pattern across tissues was tested. RT-PCR experiments were carried out using specific primers to amplify the fragment corresponding to exons 2-5 of DES gene; cDNAs from heart, skin, skeletal muscle, kidney, and liver (MTC Multiple Tissue cDNA Panel I) and cDNA from lymphocytes (from a healthy donor) were available to verify and compare DES gene expression. DES gene resulted not expressed in lymphocytes (Figure 4.52). Therefore, to exclude that c.736-11A>G can be a rare polymorphism, a RT-PCR from RNA from patient skin cells (obtained by skin biopsy) could be carried out.

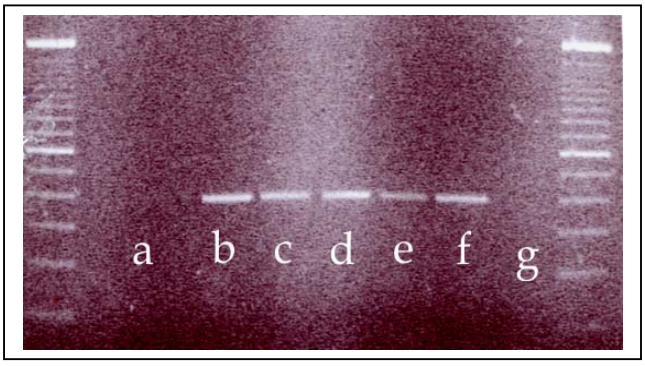

Figure 4.52. DES gene expression across tissues: lymphocytes from a healthy donor (a); heart (b), skin (c), skeletal muscle (d), kidney (e), and liver (f) from Human Multiple Tissue cDNA Panel I; negative control (g).

DES polymorphisms

In the course of the DES gene screening, some intronic and exonic SNPs (found in control population with an allelic frequency higher than 1%) were detected. In Table 4.13 only SNPs not reported in dbSNP are indicated.

The c.408C>T (L136L) synonymous variation detected in exon 1 in four index cases, was found in control subjects with a frequency of 3.6% by DHPLC analysis.

The c.638C>T nucleotidic change in exon 2 was identified in only one ARVC/D isolated case (index cases #65). It results in A213V amino acid change in a highly conserved residue among species, exception made for *Xenopus laevis* (Figure 4.48); both alanine and valine are apolar amino acids. The same change, previously described as a conditionally pathogenic recurring mutation involved in desminopathy (Bär et al., 2005; Goudeau et al., 2006), was detected in healthy controls with a frequency of 2.5% and therefore considered a polymorphism.

Two nucleotidic changes (c.735+20C>T and c.736-35C>A) were identified in intron 3. By DHPLC analysis the first variation was detected in control population at an allelic frequency of 5%; by restriction analysis using *ApaI* enzyme, the second variation showed an allelic frequency of 8%.

4.2.2. Mutations in PKP4 gene

PKP4 gene, coding for plakophilin-4, was considered a good candidate ARVC/D gene, because of its expression in heart tissue and its function in the desmosomal plaque.

A systematic mutation screening in PKP4 coding regions was performed in 8- (54 males and 26 females) among 11- ARVC/D index cases.

The patients DNA was investigated by DHPLC and direct sequencing. PCR primers flanking each exon of the human DES were designed by PRIMER3 software.

Human PKP4 gene (cDNA and translation sequences available in NCBI website, NM_003628 and NP_003619.2, respectively) has 22 exons. PKP4 gene encodes for two isoforms (PKP4a and PKP4b); PKP4b does not include exon 20 in the transcript. Exons 7 and 14 were split into two different and overlapping fragments for DHPLC analysis. Exons 15 and 21 were analyzed only by direct sequencing, because the nucleotidic sequence showed denaturation domains unsuitable for DHPLC analysis.

For amplicons size, primers sequences, amplification and analysis conditions see Appendix, Table 6.

A control group of 300 healthy and unrelated subjects (600 alleles) from the Italian population was used to exclude (by DHPLC analysis) that detected mutations could be common DNA polymorphisms. DNA variations found in more than 1% of the healthy controls chromosomes have been considered polymorphisms.

Three novel nucleotidic variations (neither found in 600 healthy control chromosomes) were identified in three different study subjects. Nine novel nucleotidic variations were classified as polymorphisms (Table 4.14).

Table 4.14. Variations detected in PKP4 gene.

Mutation	Amino Acid Change	Type of mutation	Exon	Position (protein domain)	# Index case	Reference
245+1-1A>G	-	intronic	intron 3	-	1-9	novel
1437G>A	A479A	synonymous	9	Head	95	novel
2391G>T	P797P	synonymous	14	between A6-A7	67	novel
Polymorphism	**Amino Acid Change**	**Type of variation**	**Exon**	**Position (protein domain)**	**# Index case**	**Reference**
66C>T	A22A	synonymous	2	Head	several	novel
413-34A>G	-	intronic	intron 5	-	several	novel
537A>C	S179S	synonymous	6	Head	2,16,29,55	novel
2-79G>A	T693T	synonymous	12	A5	7,3-,41,78	novel
21-6C>T	S7-2S	synonymous	13	A5	7,3-,41,78,86	novel
2175C>T	I725I	synonymous	13	A5	34	novel
2577+24C>T	-	intronic	Intron15	-	several	novel
3127+34C>A	-	intronic	intron19	-	several	novel
338-A>T	D1127V	missense	22	Tail	14	novel

c.245+1-1A>G

The novel intronic transition c.245+1-1A>G was identified in index patient #1-9. By means of DHPLC analysis of PKP4 exon 3, an abnormal elution profile was identified (Figure 4.53). By direct sequencing of the amplicon a nucleotide change was identified in intron 3 (Figure 4.53). This was not detected in the SNP database and was never observed in 600 control chromosomes screened by DHPLC analysis.

Although the c.245+101A>G change occurred 101bp downstream of splice site, intronic variants could activate cryptic splice sites; therefore, a functional effect of this alteration was not excluded.

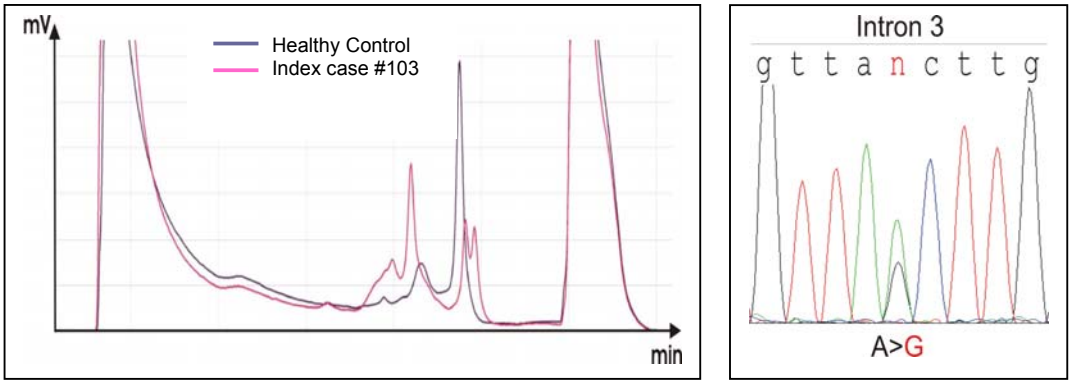

Figure 4.53. (Left) DHPLC elution profiles of PCR PKP4 fragment 3 in the Healthy Control and in Index case #103 at analysis temperature of 57.5°C. **(Right)** DNA sequencing of PCR PKP4,3 fragment revealing c.245+101A>G intronic transition.

In order to detect aberrant transcripts generated from this nucleotide change in the patient cDNA and since heart tissue sample was not available, PKP4 expression pattern across tissues

was tested. RT-PCR experiments were carried out using specific primers to amplify the fragment corresponding to exons 7-8 of PKP4 gene; cDNAs from lymphocytes (from a healthy donor) and cDNA from heart, skin, and kidney (MTC Multiple Tissue cDNA Panel I) were available to verify PKP4 gene expression. PKP4 gene resulted expressed in lymphocytes (Figure 4.54).

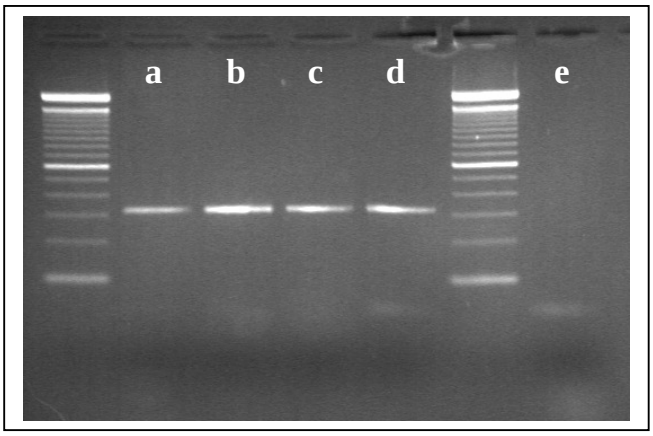

Figure 4.54. PKP4 gene expression across tissues: lymphocytes from a healthy donor (a); heart (b), skin (c), and kidney (d) from Human Multiple Tissue cDNA Panel I; negative control (e).

Patient's RNA was isolated from lymphocytes, reverse transcribed into cDNA, and investigated by amplification of the fragment corresponding to PKP4 exons 3-6. Only one amplification product was showed into agarose gel electrophoresis. It was gel isolated and sequenced. The chromatogram showed only the wild-type allele.

However, if aberrant transcripts will not be detected by nested PCR, real-time quantitative RT-PCR analysis will be performed in order to verify PKP4 expression in patient #103, since aberrant transcripts could be degraded, most likely through nonsense-mediated mRNA decay.

c.1437G>A, A479A

A novel synonymous transition, c.1437G>A (A479A), was identified in PKP4 exon 9 in patient #95, by DHPLC analysis followed by sequencing of PKP4 fragment 9 (Figure 4.55).

Since it was detected in neither of 300 healthy control subjects analyzed by DHPLC and synonymous variants could result in activation of a cryptic splice sequence or in mutating an exonic splice enhancer or silencer sequence, a transcriptional effect was supposed. RNA was isolated from patient lymphocytes, reverse transcribed into cDNA, and investigated. PKP4 cDNA corresponding to exons 8 to 1- was nested-PCR amplified. Sequencing of amplification product isolated by agarose gel failed to detect aberrant transcripts and showed only the wild-type allele.

If an aberrant transcript will not be showed by nested PCR, a real-time quantitative RT-PCR analysis will performed in order to verify PKP4 expression in patient #95.

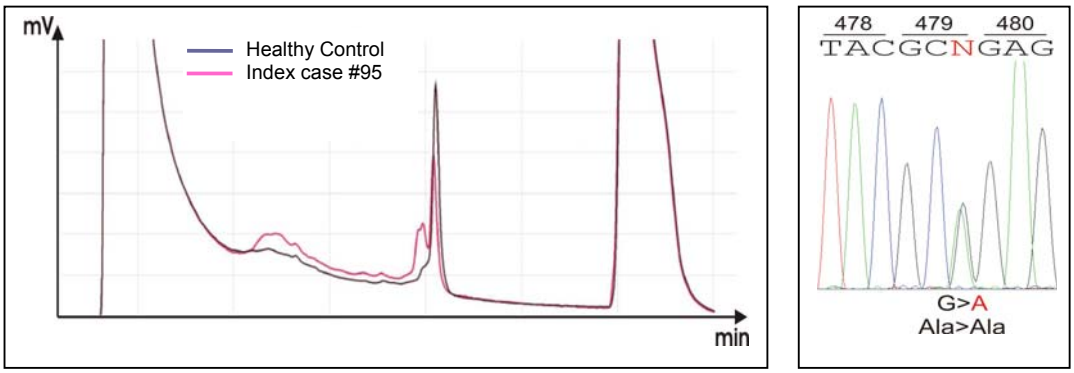

Figure 4.55. (Left) DHPLC elution profiles of PCR PKP4 fragment 9 in the Healthy Control and in Index case #95 at analysis temperature of 59.9°C. **(Right)** DNA sequencing of PCR PKP4 fragment 9 revealing c.1437G>A synonymous transition (A479A).

c.2391G>T, P797P

The third novel nucleotidic variation, c.2391G>T (P797P) detected in PKP4 gene, was identified in PKP4 exon 14 in DNA of index case #67. By DHPLC analysis, an abnormal chromatogram for amplicon 14b showing three abnormal elution peaks in comparison with the wild-type single peak, was identified (Figure 4.56). The presence of the nucleotide change was confirmed by direct sequencing (Figure 4.56). The same variation was not detected in 300 healthy controls screened by DHPLC analysis.

PKP4 patient cDNA corresponding to exons 10 to 13 was nested-PCR amplified and direct sequenced. The analysis failed to detect aberrant transcripts and showed only the wild-type allele.

As previously described, further cDNA investigations will be needed.

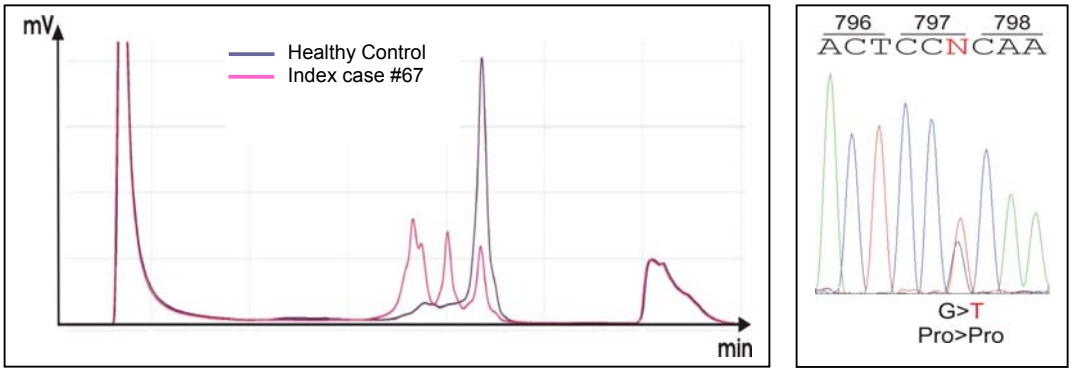

Figure 4.56. (Left) DHPLC chromatographic profiles of PCR PKP4 fragment 14b in the Healthy Control and in Index case #67 at analysis temperature of 57.4°C. **(Right)** DNA sequencing of PCR PKP4 fragment 14b revealing c.2391G>T synonymous transversion (P797P).

PKP4 polymorphisms

In the course of the PKP4 gene screening, three intronic and six exonic novel SNPs were detected. All the nucleotidic changes, exception made for c.3380A>T, were found in control population with an allelic frequency from 1.3% to 4.5% .

The missense nucleotidic variation c.3380A>T, resulting in D1127V amino acid change, and involving a residue conserved about species (Figure 4.57), presented an allelic frequency of 1.1%.

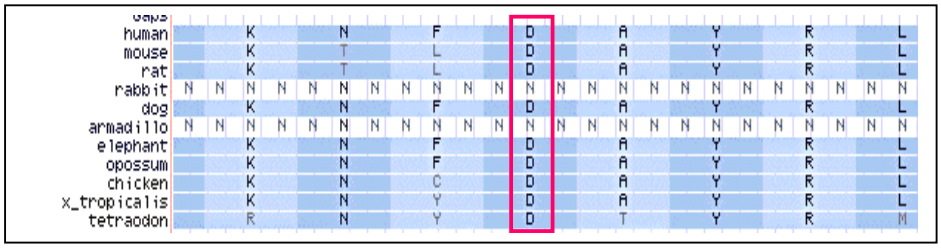

Figure 4.57. Genome Browser alignment of a small region of PKP4 tail domain showing conservation of human D1127 residue among species.

4.3. TARGETING VECTOR GENERATION FOR DEVELOPMENT OF A DSG2 KNOCK-IN MOUSE MODEL

In order to generate a knock−in mouse carrying a targeted mutation in DSG2 gene, three targeting vectors were created (Figure 4.58).

The A8B *dsg2* genomic clone (~16.1Kb in length) was isolated from the λ FIX II 129/SVJ mouse genomic library by screening with the radiolabelled probe 4-5. The clone was analyzed by restriction digestions and sequencing. Based on this information, the targeting vector was constructed cloning a 7041bp *dsg2* genomic fragment (corresponding to 7-9bp upstream exon 4 to 2249bp downstream exon 8) into *Sac*I restriction site of pBS-plyA vector (obtained by insertion of a new polylinker in the pBluescript II KS+ plasmid).

Three presumably pathogenic missense mutations, c.313G>C (G105R), c.812A>G (N271S), and c.895A>G (K299E), were introduced in exons 4, 7 and 8, respectively. Each of them was generated by site-directed mutagenesis PCR and the mutated PCR products were then inserted in targeting vector to replace wild-type fragments (1294bp amplicon carrying c.313G>C mutation was inserted into *Spe*I-*Spe*I restriction sites in the same transcriptional orientation; 823bp amplicons carrying c.313G>C or c.895A>G mutation were inserted into *EcoR*I-*Kpn*I restriction sites). Thus, three different targeting vectors were obtained.

In each of them, the neomycin resistance gene cassette (Neo, ~1900bp in length) was inserted into *Bln*I site of intron 8 and a herpes simplex virus thymidine kinase gene cassette (TK, ~1900bp in length) was cloned in *Xho*I – *Sal*I sites at the 5' end of each construct.

All correct insertions of the fragments in the targeting constructs were verified by restriction analysis and sequencing of the junctions.

In order to develop a knock-in mouse model, the resulting constructs (~11Kb in length) will be restricted from vectors by digestion with *Not*I enzyme and transfected into mouse embryonic stem cells. Neo and TK cassettes will allow positive-negative selection of the homologous recombination events.

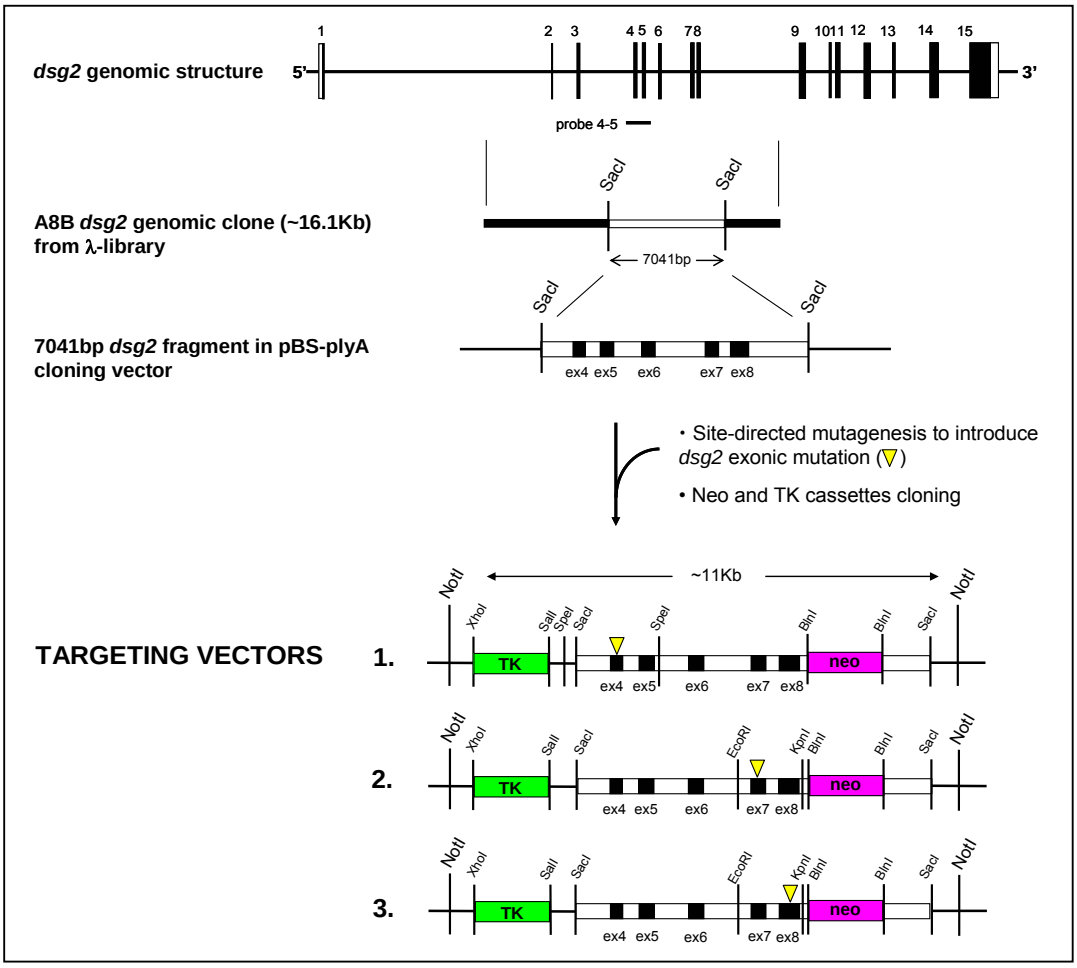

Figure 4.58. Targeting vector strategy for creating Knock-in mouse with a missense mutation (into exon 4, or 7 or 8). Targeting vectors (1, 2 and 3) carry a missense mutation (yellow triangle), a neomicina resistance cassette (neo) on intron 8 and herpes simplex virus thymidine kinase gene cassette (TK) at the 5' end of each construct.

5. DISCUSSION

Arrhythmogenic right ventricular cardiomyopathy/dysplasia (ARVC/D) is an inherited cardiac disorder characterized by right ventricular (fibro)-fatty replacement of myocardial tissue. Usually it presents with palpitations or syncope as a result of ventricular tachy-arrhythmias. It is an important cause of sudden cardiac death (SCD) at relatively young ages (Thiene et al., 1988; Fontaine et al., 1998).

Mutations in genes encoding proteins involved in myocardial cell–cell adhesion are increasingly recognized as a primary molecular defects in ARVC/D pathogenesis (McKoy et al., 2000; Rampazzo et al., 2002; Gerull et al., 2004; Pilichou et al., 2006; Syrris et al., 2006). To date, disease-causing mutations have been identified in five cell adhesion proteins genes: Junctional plakoglobin (JUP), Desmoplakin (DSP), Plakophilin-2 (PKP2), Desmoglein-2 (DSG2) and Desmocollin-2 (DSC2).

In the present clinical practice, genotyping is of most value in enabling cascade screening of relatives, particularly attractive in ARVC/D where, because of variable and age-related penetrance, lifelong clinical re-assessment of extended families would be otherwise needed. Identification of a pathogenic mutation in an index patient gives the opportunity to reassure family members not carrying the detected mutation; these persons can be dismissed from regular cardiological follow-up and the clinical resources can be targeted to proven mutation-carriers relatives.

Both the subtlety of clinical abnormalities in early ARVC/D and the diverse phenotypic manifestations of the disease, which include left ventricular arrhythmia and ECG changes, suggest a potential role for genotyping in confirmatory testing of index cases. In this regard, one of the foremost clinical challenges in ARVC/D is timely diagnosis of the so-called “concealed” phase, during which a dearth of symptoms may belie significant arrhythmic risk. Identification of a causative mutation facilitates timely diagnosis, with the subsequent possibility of preventing complications and reducing morbidity and mortality.

5.1. MUTATION SCREENING IN KNOW ARVC/D GENES

In this study, mutation screening of four desmosomal genes (PKP2, DSP, DSG2 and DSC2 genes) was performed in 110 ARVC/D index cases fulfilling the task force diagnostic criteria.

Mutations were detected in 47.3% (52 out of 110) of ARVC/D index cases: 14.7% of them resulted to carry one plakophilin-2 mutation, 10.0% one desmoplakin mutation, 7.3% a single desmoglein-2 mutation, 2.7% one desmocollin-2 mutation, and 12.7% carried multiple mutations. Present study provides for the first time an estimate of relative prevalence of mutations among ARVC/D genes encoding desmosomal proteins, in a series of unselected and unrelated cases, screened by using the same methodology. The relatively high incidence of

multiple mutations in ARVC/D suggests that potentially pathogenic variants might recur in the general population at higher rate than previously supposed. Taking into account the low penetrance of some mutations, prevalence of ARVC/D was probably underestimated.

A total of seventy-one mutations (55 different mutations, including 28 novel ones) were identified. Twenty-five of them (35.2%) (16 different changes) were identified in PKP2 gene, 20 (28.2%) (18 different ones) in DSP gene, 20 (28.2%) (17 different ones) in DSG2 gene, and 6 (8.4%) (4 different ones) in DSC2 gene.

These data are in agreement with those reported in the literature, suggesting a preponderance of private mutations in the "big3" ARVC/D genes, with defects occurring in every exon of plakophilin-2, in the N-terminus, rod, and C-terminus of desmoplakin, and along functional domains of desmoglein-2.

Llack of identification of disease-gene mutations in the remaining 52.7% of index cases is probably due to mutations in additional, as yet unidentified, genes. However, possibility of misdiagnosis in some cases, possible presence of mutations in sequences not covered by the study (promoter, 5'UTR and 3'UTR regions) and possible failure of mutation detection cannot be ruled out. Moreover, although literature established >95% sensitivity for DHPLC (Xiao and Oefner, 2001; Schollen et al., 2002; Bagattin et al., 2004), large rearrangements (duplications/deletions) would be missed by DHPLC analysis and direct sequencing of genomic DNA.

Not every single sequence variant detected in an affected person is necessarily pathogenic. Deciding whether a DNA sequence change is pathogenic can be really difficult. For example, among the detected changes, missense mutations DSP V30M and DSG2 L831F occurred in non-conserved amino acids and variation E58D was identified in the control population (at a frequency lower than 1%). Even more interesting is the case of DSC2 E896EfsX4, previously reported as pathogenic mutation (Syrris et al., 2007) and detected at 2% frequency in the Italian control population. In all these cases it is very difficult to decide whether the detected variation should be considered as a pathogenic mutation or a harmless variant.

According to Strachan (2003) present criteria to decide whether a sequence change is a pathogenic mutation or a benign variant, are (in decreasing order of reliability):

1) functional studies showing that the change is pathogenic;

2) change seen before in patients with the disease (and not seen in ethnically matched controls);

3) a *de novo* mutation (not present in the parents, but present in a person with *de novo* disease);

4) a novel sequence change that is absent in a panel of at least 100 normal controls;

5) the nature of the sequence change:

- deletions of the whole gene, nonsense mutations and frameshifts are almost certain to destroy the gene function;

- mutations that change the conserved GT-AG nucleotides flanking most introns affect splicing, and usually abolish the function of the gene product;

- a missense mutation is more likely to be pathogenic if it affects a part of the protein known to be functionally important (computer modeling of the protein structure may help suggest which residues are critical);
- changing an amino acid is more likely to affect function if that amino acid is conserved in related genes (orthologs or paralogs);
- amino acid substitutions are more likely to affect function if they are non-conservative (if an amino acid is replaced by another that is chemically dissimilar to it, for example a polar by a non-polar amino acid, or an acidic by a basic one).

On the base of these commonly accepted criteria, a detailed and exhaustive subdivision can be proposed to classify all the detected mutations lacking functional effect (confirmed by functional studies). Until now, names as "putative causing-mutations" (Ackerman et al., 2003), "unclassified variants" (Van Tintelen et al., 2006) or "rare variant" (Arnestad et al., 2007), have been used.
The mutation classification represents a possible approach to infer the significance of such variants (probability to be pathogenic). Variations identified in affected subjects and detected in control population at a frequency lower than 1%, can be classified as: definitely pathogenic, highly probably pathogenic, probably pathogenic or possibly pathogenic mutations (Table 5.1).

Table 5.1. Genetic variations: classification and criteria.

	Definition	Criteria
Polymorphism	Benign variation, most likely lacking any phenotypic effect	Common variant found in unaffected controls at a frequency of more than 1 %
Mutation	Variation, most likely producing a phenotypic effect	Variant found in unaffected controls at a frequency less than 1 %
• **Definitely Pathogenic**	Variation with definitive functional effect	• Truncating mutations • Splice-site mutations confirmed by *in vitro* functional studies • Missense mutations with demonstrated functional effects
• **Highly probably pathogenic**	Variation with very high confidence supposed to be pathogenic	• Probably pathogenic mutation segregating in a large family (lod score >3)
• **Probably pathogenic**	Variation with high confidence supposed to be pathogenic	• Missense mutations causing a non conservative amino acid substitution, and involving a conserved residue among species, not detected in unaffected controls • Mutations involving cysteine (by forming or breaking disulfide bonds) and proline (as for its unique ring structure) • Splice-site mutations changing the conserved GT-AG nucleotides, in the absence of *in vitro* functional studies

• **Possibly pathogenic**	Variation suspected to be pathogenic	• Missense mutations causing a conservative substitution, involving conserved residues, and not detected in unaffected controls • Missense mutations involving not conserved residues, and not detected in unaffected controls • Missense mutations involving conserved residues, but detected in unaffected controls • Variants near but not within the consensus splice regions without *in vitro* functional studies • Non coding, silent variants without demonstrated functional effect

According to the proposed mutation classification, all different mutations detected in this study in ARVC/D index cases can be considered as reported in Table 5.2.

Table 5.2. Classification of the detected mutations in desmosomal ARVC/D genes (PKP2, DSP, DSG2 and DSC2) in 110 ARVC/D index cases.

	Mutations detected in PKP2 gene	Mutations detected in DSP gene	Mutations detected in DSG2 gene	Mutations detected in DSC2 gene
Definitely pathogenic mutation	T50SfsX60	V30M	E418EfsX1	E102K
	Q62DfsX22	c.423-1G>A	Q558X	I345T
	Q133X	Q273X	c.1881-2A>G	
	Q211X	E1068VfsX18	G678AfsX2	
	G548VfsX14	R1113X	G997VfsX19	
	K672RfsX11	S2108X		
	Q707X			
	T816RfsX9			
Highly probably pathogenic mutation	-	S299R	-	-
Probably pathogenic mutation	N76S	N375I	Y87C	-
	K112N	N458Y	G100R	
	S140F	K470E	R146H	
	S209R	L1654P	E230G	
	I778T	R1775I	K294E	
			D297G	
			E331K	
			G638R	
			P925S	
Possibly pathogenic mutation	E58D	273+5G>A	N266S	631-10C>T
	Q62K	A566T	V392I	
	V587I	R1255K	L831F	
		D1258E		
		M1601I		
		R2541K		
Polymorphism	-	-	-	E896EfsX4

Among 59 different mutations, 21 can be considered pathogenic; 16 of them because are truncating mutations, 2 are splice-site mutations confirmed by *in vitro* functional studies (DSP, c.423-1G>A, Bauce et al., 2005; DSG2, c.1181-2A>G, Pilichou et al., 2006), and 3 are missense mutations with demonstrated functional effects (DSP V30M, Yang et al., 2006; DSC2, E102K and I345T, Beffagna et al., 2007).

For the remaining mutations, on the basis of available experimental data, it is impossible to infer a pathogenic role. Some of presumed causing mutations could be false-positive test results and

the inclusion of rare polymorphisms in the mutation class might result in overestimation of the success rate of ARVC/D population genotyping.

Only DSP S299R variant is a highly probably pathogenic mutation, showing a segregation in a large family (lod score >3) (Rampazzo et al., 2002). Due to the substantial small number and size of families of ARVC/D index cases, co-segregation of all mutations has not been determined. Such co-segregation data would provide further evidence that each mutation is correctly assigned.

Most detected amino acid changes result as probably pathogenic mutations, causing a non-conservative amino acid change, involving conserved residues among species (2 of which are proline residue), and not detected in unaffected controls.

Thirteen nucleotide variations can be classified as possible pathogenic mutations; 2 involve intronic nucleotides near consensus splice regions, without *in vitro* functional studies; 4 (PKP2 E58D, PKP2 Q62K, DSP R2541K and DSG2 L831F) are missense mutations involving not conserved residues among species and one of them (PKP2, E58D) was found in control population at a frequency of 0.7%. The remaining 7 variants cause a conservative amino acid change.

According to the proposed mutation classification, the variant DSC2 E896EfsX4, found in Italian control population at a frequency of 2%, should be considered a polymorphism.

However, in order to define the pathogenic role of a detected variant, functional studies are the gold standard. Pathogenic mechanisms of mutations in ARVC/D genes could be characterized both in vitro, by transient transfection of wild−type and mutated cDNA in cultured cardiomyocytes, and in vivo by generation of transgenic and knock−in mouse lines.

5.2. CLINICAL EXPRESSION AND PENETRANCE OF MUTATIONS IN ARVC/D GENES

This study provides mutational analysis and clinical features in 110 unrelated consecutive patients fulfilling the ARVC/D criteria (McKenna et al, 1994). In 52 of them, one or multiple mutations were detected.

In 19 index patients, additional family members have been clinically and genetically investigated. One or more mutations were identified in 89 relatives, 35 of which fulfilled ARVC/D diagnostic criteria or didn't entirely fulfil the conditions for being assigned to the category of "affected", though showing minor signs of the disease.

Clinical investigation of index cases and family members showed that clinical expression of ARVC/D mutations is heterogeneous even among relatives, ranging from a complete lack of symptoms and/or clinical manifestations to severe disease phenotype. Although environmental influences, variability in life style and level of physical activity may contribute to the differences, genetic factors are likely to play a significant role as well.

For this reason, describing ARVC/D as purely monogenic trait is probably an oversimplification.

It is widely accepted that phenotype of mendelian disorders, particularly those with autosomal dominant inheritance, may be affected by genetic factors (modifiers) other than the major pathogenic mutation. Modifier genes do not cause the disease *per se* but affect severity of phenotypic expression. This is particularly true for dominant disorders showing age−dependent onset and variable expressivity (Marian, 2002). In ARVC/D, mutations in demosomal genes are necessary to cause the disorder, but contribution of major pathogenic mutations to the severity of phenotype may appear relatively modest, while modifier genes (genetic background) and individual lifestyle appear to play a very relevant role. Unfortunately, chromosomal location of ARVC/D modifier genes is still unknown.

Clinical comparison of patients carrying single and multiple mutations showed no significant differences in terms of electrocardiographic and structural abnormalities, major events and disease expression. The only significant difference was that patients carrying DSG2 mutations were found older at diagnosis and at the time of major arrhythmic symptoms than DSP and PKP2 carriers. On the ground of these data, it is impossible to clinically differentiate different forms of ARVC/D due to mutations in different genes; thus, mutation screening in ARVC/D genes on DNA of probands should be planned only on the basis of relative prevalence of mutations in different genes.

It is interesting to notice that multiple mutations carriers did not show more severe phenotypes than single mutation carriers. On the contrary, in hypertrophic cardiomyopathy (HCM) families multiple gene mutations resulted in more severe clinical phenotypes (Richard et al., 2003; Van Driest et al., 2004): HCM patients with multiple mutations have been reported to develop more significant left ventricular hypertrophy, are diagnosed at an earlier age, and require more advanced and invasive treatments such as surgical myotomy and ICD implantation.

In two ARVC/D families (#40 and #83) the role of distinct mutations was confirmed, because each of them was known to be pathogenic by itself. On the contrary, the contribution of different mutations detected in all other families was impossible to be established because of the small size of families, or the low number of clinically evaluated family members.

In some cases (families #42 and #87), ARVC/D is apparently inherited as a recessive trait, since only the compound heterozygous patient show clinical manifestation of the disease manifestation. This raises the question of whether mutations detected in these families have a recessive or dominant mode of inheritance.

These contrasting data suggest that the genetics of ARVC/D may be more complex than hitherto appreciated. According to the evidence provided by present study, mutation screening should not be stopped after identification of a single mutation, but continued on the same gene and at least the three major genes (PKP2, DSP and DSG2). Moreover, before genetic counselling and before attempting to establish phenotype-genotype correlations, genetic status of each case should be fully investigated.

Penetrance of the ARVC/D phenotype is still poorly defined. Penetrance, estimated in the present study resulted 34% for DSP and 37% for DSG2. This estimate is imprecise, since complete cardiac evaluation was not performed in all first-degree relatives carrying ARVC/D

genes mutations, due to lack of collaboration of family members, unwilling or unable to undergo comprehensive testing. Till now, penetrance of mutations leading to ARVC/D was reported only for PKP2: Syrris and colleagues (Syrris et al., 2006) reported the penetrance among PKP2 mutation carriers to be nearly 50%; Dalal and colleagues (Dalal et al., 2006) studied 26 PKP2 mutation carriers, related to nine index cases and eight (31%) were diagnosed with ARVC/D.
Unfortunately, in the present study it was impossible to estimate the prevalence of such mutations, due to the low number of cases carrying variations in the PKP2 gene .

5.3. MUTATION SCREENING IN CANDIDATES ARVC/D GENES

The involvement of desmosomal protein genes in ARVC/D has led to the "desmosomal model" hypothesis. Desmosomes are most prevalent in tissues exposed to frictional and shear stress, such as the myocardium and epithelium, where they play a key role in imparting mechanical strength, both via cell–cell adhesion and through transmission of force between the junctional complex and the intermediate filaments in the cytoskeleton (Van Tintelen et al., 2007). Impaired desmosome function due to desmosomal gene mutations would led to detachment and death of cardiac myocytes followed by inflammation and fibrofatty replacement.
Mutation screening of four desmosomal ARVC/D genes (PKP2, DSP, DSG2, and DSC2) in 110 ARVC/D index cases led to identification of mutations in 47.3% of them. Since no causative mutations have been identified in more than 50% of ARVC/D index cases, DES gene (coding for desmin) and PKP4 gene (coding for plakophilin-4), considered as good candidate genes for ARVC/D because of their expression and function in heart tissue, were screened for mutations by DHPLC and direct sequencing.

5.3.1. Mutation screening in DES gene

Desmin is the main intermediate filaments protein in mature skeletal and heart muscles where it forms a three-dimensional scaffold around myofibrillar Z-discs connecting them to the plasma membrane and nuclear lamina, and aligning the myofibrils. Desmin interacts with other intermediate filaments proteins to form an intracytoplasmic network that maintains spatial relationship between the contractile apparatus and other structural elements of the cell (Lazarides, 1980). The linkage between the desmin intermediate filaments and the desmosomal adhesion structures in cardiomyocytes is mediated by desmoplakin I protein (Green and Gaudry, 2000).
Desmin is encoded by a single copy gene (DES) identified and sequenced in several mammalian species, and resulted highly conserved. The human DES gene is located in the chromosome 2q35 band (Viegas-Perqugnot et al., 1989); it encompasses nine exons and encodes for a single 53KDa protein monomer of 476 amino acids (Li et al., 1989).

Like all intermediate filaments proteins, desmin exhibits a tripartite structure consisting of an amphipathic central α-helical coiled-coil rod domain flanked by non-α-helical amino-terminal "head" and carboxy-terminal "tail" domains (Weber and Geisler, 1985). The head and tail domains are sites of post-translational modifications by phosphorylation and glycosylation, regulating dynamic aspects of desmin organization and structure during the cell cycle (Heins and Aebi, 1994). The α-helical organization of the central domain is interrupted at three sites (so-called "linkers" L1, L12 and L2) thereby leading to the formation of four separated α-helical segments, termed 1A, 1B, 2A, and 2B. The length of the individual α-helical segments is absolutely conserved in the cytoplasmic intermediate filaments proteins of vertebrates. The central domain maintains a 7-residue ("abcdefg") repeat pattern with a typical sequence of hydrophobic (in position "a" and "d") and hydrophilic amino acids (Brown at al., 1996). The heptad repeat structure guides two desmin polypeptides into formation of a parallel, in register, coiled-coil dimer, the elementary unit of the filament (Bär et al., 2004). Desmin dimers associate laterally to form distinct tetrameric complexes; tetramers associate laterally to yield so-called ULFs (unit-length filaments) which undergo a longitudinal and radial assembly leading to mature filaments (14nm diameter) (Herrmann et al., 1996; Herrmann and Aebi, 2000).

The beginning of segment 1A and the end of coil 2B include the "IF consensus motif" (TYRKLLEGEESRI). Fragments representing either of the conserved ends of the rod domain were shown involved in formation of tetrameric complexes (Herrmann et al., 2000).

There are increasing numbers of myopathies that are associated with abnormal accumulation and organization of desmin within muscle fibres, often reported as Desmin-related myopathies or Desminopathies (Goebel, 1995). Molecular studies of these disorders demonstrated that some are truly caused by mutations in desmin (Goldfarb et al., 1998). Identification of mutations in the desmin gene of humans suffering from cardiomyopathy, such as idiopathic dilated cardiomyopathy or restrictive cardiomyopathy, suggests that desmin abnormalities are most possibly the cause of the cardiac dysfunction, (Munoz-Marmol et al., 1998; Li et al., 1999).

Histological and electron microscopical analyses both in heart and skeletal muscle tissues of desmin knock-out mice reveals severe disruption of muscle architecture and degeneration. Structural abnormalities include loss of myofibril anchorage to the sarcolemma, perturbation of lateral alignment of myofibrils, and loss of nuclear shape and positioning. Loose cell adhesion and increased intercellular space are prominent defects in all muscles types; the heart exhibits extensive fibrosis, progressive degeneration and necrosis of the myocardium (Milner et al., 1996; Li et al., 1996). These data strongly supported the hypothesis that desmin mutations may have a causal effect.

So far several different mutations in desmin gene have been identified. Most of them are clustered in the α-helical rod domain and particularly in the 2B region. At present, there is no functional correlation between the position of the mutation and the phenotype. Generally, it seems that mutations at the rod domain will cause filament assembly perturbations, whereas it is impossible to predict the consequences for mutations found in other parts of the desmin molecule, since the function of the end domains is largely unknown.

On the base of high desmin expression in cardiomyocytes and of its involvement in heart muscle diseases, desmin has been considered a good ARVC/D candidate gene. Analysis of exon-by-exon sequences of the DES coding region, performed in 80 ARVC/D index cases, resulted in identification of several nucleotide variations, most of which reported in dbSNP or detected in control population at a frequency higher than 1% and thus considered polymorphisms.

The A213V desmin variant, detected in ARVC/D index cases #65, and located in the 1B α-helix, was previously described as a low penetrance mutation detected in two unrelated patients, one having restrictive cardiomyopathy (Bowles et al., 2002), the other (carrying also two additional causative mutations in α-glucosidase gene) with progressive skeletal myopathy with no cardiac involvement, and having an allele frequency on controls individuals of approximately 1% (Goudeau et al., 2006). *In vitro* functional characterization demonstrated that A213V amino acid change did not prevent the formation of a normal complete filamentous network, and this variant was considered a conditionally pathogenic mutation.

Since a functional effect was not shown and in this study it was detected in healthy controls with a frequency of 2.5%, it was considered a polymorphism.

The novel missense mutation K241E, not detected in control population, causes the non-conservative amino acid substitution (the positively charged amino group is replaced by a negative charged carbossilic group) of a residue highly conserved among species in the conserved 1B α-helix subdomain. This change should alter lateral interactions between desmin homopolymers into dimeric or tetrameric complexes as demonstrated for the desmin pathogenic amino acid change E401K located in 2B α-helix subdomain (Smith et al., 2002; Strelkov et al., 2002; Herrmann and Aebi, 2004).

The K241E DES variation was identified in the index case #73 affected by a severe form of ARVC/D but carrying a pathogenic frame shift mutation (T816RfsX9) in PKP2 gene. The patient's sister carried the same DES variant, and she was fully clinically asymptomatic. At the moment, no *in vitro* functional studies are available to demonstrate the effect of this amino acid change that should have a low penetrance, and the possibility of being a rare polymorphism cannot be excluded. On the basis of the proposed mutation classification, it should be considered a "possibly pathogenic" mutation.

The novel intronic nucleotide variation c.736-11A>G occurs 11bp upstream of acceptor splice site of exon 4. In order to determine if it could activate a cryptic splice site, a RT-PCR from RNA from patient skin cells (obtained by skin biopsy) should be carried out, since DES gene results not expressed in lymphocytes. Therefore, only speculative hypotheses about the effect of such mutation can be put forward. The intronic mutation could lead to skipping of the downstream exon 4 and the splicing apparatus uses an alternative legitimate splice site. However, it must be noticed that other outcomes are possible too, including usage of alternative exonic or intronic cryptic splice sites. The outcome is not always easily predictable. If the number of nucleotides in the exon is not divisible by three, a frame shift will introduce a premature termination codon, often resulting in an unstable RNA transcript and absence of the encoded polypeptide. If exon

skipping does not cause a frame shift, the absence of the normally encoded amino acids will often result in a non-functional or abnormal polypeptide, depending on the importance of these amino acids to protein function and/or structure. On the contrary, the intronic mutation could lead to intron retention due to complete failure in splicing, insertion of some nucleotides in the RNA and probable frame shift introducing a premature termination codon.

The genetic study of additional family members of ARVC/D index case #98 shoved co-segregation of DES variation in 4 out of 9 affected members. Thus, other mutations, in addition to DES variation, should be searched in not yet screened ARVC/D genes or in still unknown ARVC/D genes.

On the basis of present data, the involvement of desmin in genetic determination of ARVC cannot be excluded. However, even if it will be shown that the detected variants are pathogenic, DES mutations would account for only a small percentage of ARVC index patients.

5.3.2. Mutation screening in PKP4 gene

Plakophilin-4 is a *armadillo repeat* protein for which a dual localization pattern in desmosomes and adherens junctions, depending to the cell type, has been reported. Its expression is demonstrated in a wide variety of mammalian tissues (Hatzfeld and Nachtsheim, 1996).

Plakophilin-4 is the gene product of a single copy gene (PKP4) on chromosome 2q23-q31 (Bonne et al., 1998) and is coded in two splice variants, isoform “a” encompassing 1192 amino acids from transcription of exons 2 to 22, and isoform “b” lacking of transcription of exon 20 and encompassing 1149 amino acids.

The protein sequence covers three distinct domains. The amino-terminal head domain and the carboxy-terminal tail domain (amino acid residues 1 to 508 and 988 to 1192, respectively) lack significant homology to any protein in the data base. Isoforms a and b differ in the tail domain length. The central domain of 480 amino acids, forming ten imperfect ~45 amino acid repeats (arm repeats), shows strong homology to other members of the *armadillo* multigene family such plakoglobin and β-catenin (KÜssel and Frasch, 1995). Three short inserts are present between repeats 4 and 5, 5 and 6, and 6 and 7 (Hatzfeld and Nachtsheim, 1996). In particular, the stretch of 8 basic amino acids at the end or repeat 6 might function as a nuclear localization signal (Lu et al., 1999). Further experiments have to clarify whether or not armadillo related proteins are specifically translocated into the nucleus and how this transport is regulated.

Cultured epithelial murine cells studies show colocalization of plakophilin-4 with desmosomal markers (Hatzfeld and Nachtsheim, 1996). The N-terminal domain, carrying a highly conserved coiled-coil motif typically involved in protein-protein interaction (Anastasiadis and Reynolds, 2000), is demonstrated to be responsible for the interaction with cytoplasmic region of desmocollin-3, N-terminus of desmoplakin, and C-terminus of plakoglobin. Arms repeats can bind plakoglobin, plakophilin-2 in desmosoms, and non-desmosomal cadherins in adherens junctions (Hatzfeld et al., 2003).

Moreover, plakophilin-4 have a C-terminal conserved PDZ-binding motif (amino acids DSWV, 989 to 1192) (Hatzfeld, 1999) that allows the interaction with PDZ domains found in proteins involved in establishing cell polarity in epithelial cells. This suggests that plakophilin-4 should function not only as structural component of intercellular junctions, but also as scaffold for the junctional plaque organization and recruitment of signalling molecules to the region of cell-cell contact (Calkins et al., 2003).

The dual localization of placophilin-4 raises the possibility that it plays a role also in the molecular cross-talk that occurs between different junctions (as demonstrated for plakoglobin, Palka and Green, 1997), thus influencing a range of cellular events (Hatzfeld, 2006).

So far, plakophilin-4 has not been involved in genetic diseases.

A systematic mutation screening in PKP4 coding regions was performed in 80 ARVC/D index cases. In addition to several nucleotide variations, reported in dbSNP or detected in control population at a frequency higher than 1% and thus considered polymorphisms, three novel nucleotide variations c.245+101A>G, c.1437G>A (A479A) and c.2391G>T (P797P), were identified in three probands. None of the detected variations was found in a control group of 300 healthy and unrelated subjects (600 alleles) from the Italian population.

Although the first change occurred 101bp downstream of splice site, it could activate cryptic splice site; two exonic synonymous variations could result in activation of a cryptic splice sequence or in mutating an exonic splice enhancer (ESE) or silencer (ESS) sequence, important for regulating splice donor or splice acceptor recognition. In all cases, the effects could be the exon skipping or intron retention, both resulting in transcriptional effect.

RT-PCR investigations from patients RNA failed to detect aberrant transcripts and showed only the wild-type allele. However, real-time quantitative RT-PCR analysis will be performed in order to test PKP4 expression and verify aberrant transcripts degradation through nonsense-mediated mRNA decay.

Although, to date, functional effect of detected nucleotide variations has not been demonstrated, involvement of PKP4 in ARVC/D cannot be excluded.

Since no causative mutations in known ARVC/D genes have been detected in about 50% of index cases, additional disease-genes should be involved in genetic determination of the disease. Obviously, good candidate genes for ARVC are desmosomal proteins.

Recently, it has been reported that Perp, a tetraspan membrane protein, localizes specifically to desmosomes of heart tissue and is entirely absent from other regions of cell-cell contact (Marques et al., 2006). Numerous structural defects in desmosomes are observed in Perp-deficient skin, suggesting a role for Perp in promoting the stable assembly of desmosomal adhesive complexes (Ihrie et al., 2005). These characteristics make Perp a good candidate for ARVC/D.

Gap junctions, assembled from connexins, form the cell-to-cell pathways for propagation of the precisely orchestrated patterns of current flow that govern the synchronized rhythm of the healthy heart. The connexins Cx40, Cx43 and Cx45 are found in distinctive combinations and

relative quantities in different, functionally specialized subsets of cardiomyocytes. Alterations in connexin expression and gap junction organization, now a well-documented feature of human cardiomyopathies, potentially contribute to the pro-arrhythmic substrate (Severs et al., 2006). Thus connexins Cx43, Cx40 and Cx45 could be considered good candidate genes for ARVC.
Recently, it has been also reported that the binding of αT-catenin (encoded by CTNNA3 gene) to plakophilins can strengthen cell-cell adhesion in contractile cells by the formation of a unique type of junction that combines elements of classical desmosomes and adherens junctions (Goossens et al., 2007). For this reason, CTNNA3 mutations could be involved in the genetic determination of some forms of ARVC/D.
Identification of novel ARVC/D genes and of their primary products will represent a breakthrough for early diagnosis and treatment of ARVC/D patients.

5.4. DEVELOPMENT OF A KNOCK-IN MOUSE MODEL FOR ARVC/D

To fully understand the physiological consequences of detected mutations in disease-genes require understanding the physiological network that are perturbed as a result of the expression of the mutation or lack of the gene's product. There has been a drive to model the defined mutations in animal model so that the effect can be studied during cardiac development, maturation, and aging at the molecular, biochemical, cellular, organ, and whole animal levels.
The mouse has been the model of choice for creating genetic models of human ARVC/D, so as several other cardiac diseases (Yutzey and Robbins, 2007). Because the basic gene regulatory networks are often conserved between disparate organisms, insights into the underlying mechanisms driving heart development and function can be gained from studying such organisms as flies, worms, and fish (Olson, 2006). However, the advantages of dealing with a mammalian, 4-chambered heart in terms of the application of the data to human cardio-vascular disease remain compelling. With the development of abilities to manipulate proteins by genetic manipulation of the mouse genome, the mouse become the favoured model in which to make defined genetic changes to study the causes and mechanistic bases for human cardiac diseases.
Two techniques can be used for producing murine genetic heart disease models. Transgenesis involves the injection of naked DNA (containing the human gene sequence of choice and a cardiac-specific promoter to ensure expression only in the heart) into the nucleus of a fertilized 1-cell embryo. Thus, the endogenous gene is not affected, and no phenotype will be detectable unless the product of the transgene is dominant. In contrast, in knock-in mouse model, gene targeting depends on an exceedingly rare event in the mammalian genome, the homologous recombination, in which a suitably modified DNA is inserted into the endogenous genetic site and replaces the normal sequence. The DNA are electroporated into totipotent embryonic stem cells, and these targeted cells are microinjected into an early embryo, usually one at the 16-cell blastocyst stage. This technique is used to create a null allele (to "knock-out" a gene) or to

insert single base pair mutations (to “knock-in” a gene) in the gene of choice. By directing expression of an engineered protein to the heart, the consequences of a single genetic manipulation can be studied at the molecular, biochemical, cytological, and physiological levels, under both normal and stress stimuli.

As a model for ARVC, knock−in mice have the advantage of carrying the mutation responsible for the disease in the appropriate genomic and protein context; mutation is present in the full−length protein, correctly expressed under the control of the endogenous promoter. Because of the slow progression of the disease, knock−in mouse models offer a unique possibility of dissecting the pathogenic mechanism of ARVC/D in the precise genetic context of the human condition. Moreover, such animal models, through the means of precisely reproducing the key events in the pathology, would be essential for the development of effective pharmacological therapies.

Only few transgenic mouse models of mutant desmosomal proteins are presently available for ARVC/D.

Recently, *in vitro* and *in vivo* functional studies to test the pathogenic effects of DSP missense mutations have been reported (Yang et al., 2006). The N-terminal mutants (V30M and Q90R) failed to localize to the cell membrane in desomosome-forming cell line and failed to bind to and coimmunoprecipitate JUP; multiple attempts to generate V30M and Q90R cardiac-specific transgenes have failed and analysis of embryos revealed evidence of profound ventricular dilation resulting in embryonic lethality. Transgenic mice with cardiac-restricted overexpression of the C-terminal mutant (R2834H) showed increased cardiomyocyte apoptosis, cardiac fibrosis, and lipid accumulation, along with ventricular enlargement and cardiac dysfunction in both ventricles (Yang et al., 2006).

Although to date cardiac-specific transgenesis forms the bases for a majority of the murine models of ARVC/D, it remains a relatively blunt instrument because many of the models express the transgene at very high levels, raising the possibility of non-physiological consequences due to the aberrant levels of gene expression (even if transgenic animals are compared to animals in which a transgene encoding the normal protein is expressed at similar levels, so as to have a true control for the experiment).

For this reason, gene targeting, genetically more precise than transgenesis, has been choice as strategy to generate the first knock−in mouse carrying a targeted mutation in *Dsg2* gene as animal model for ARVC/D. DSG2 mutations have been recently associated with ARVC/D by our group and they appear to be frequently involved in the genetic determination of ARVC/D.

Since no common mutations have been detected or have been invariably associated to severe forms of the disease, the knock−in mouse model will be produced by introducing a DSG2 mutation, selected on the basis of in vitro and in vivo studies.

One out the three produced targeting vectors will be linearized and transfected into the murine embryonic stem cells to create a DSG2 knock−in mouse, in which a missense mutation in desmoglein-2, found in an ARVC/D index case, will be introduced into endogenous gene by

homologous recombination. The phenotypic characterization of the created mice will involve electrophysiological, histological and gene expression analyses.

The expected results will demonstrate the physiological effects of the inserted mutation, and will lead to identification of cellular mechanisms involved in the molecular pathogenesis of ARVC/D. Moreover, although the subtleties of the different cardiovascular physiology between mice and humans are crucial, particularly when therapeutic approaches are considered, basic organizational, developmental, and signalling pathways are conserved, and much can be learned from the mouse models. In perspective, such models should prove useful also for assessing the effects of selected pharmacological treatments and improving of targeted therapies for those patients who have already developed this life−threatening disease.

6. CONCLUSIONS

The mutation screening of four desmosomal ARVC/D genes was performed in 110 unrelated consecutive probands fulfilling the International ARVC/D Task Force criteria. Mutations were detected in 47.3% of cases.

In this series of patients screened for mutations, 14 (12.7%) compound genotypes were detected, suggesting that this condition may be more frequent than expected among ARVC/D patients. It is difficult to establish whether all of these cases are carriers for multiple pathogenic mutations, since it is almost impossible to discriminate between a rare variant with small pathogenic effect and a rare DNA polymorphism.

Present knowledge on the molecular genetics of the dominant forms of ARVC/D permitted detection of mutation carriers in 19 families. Genotyping of relatives is particularly attractive in ARVC/D where, because of variable and age-related penetrance, lifelong clinical re-assessment of extended families would be otherwise needed.

Clinical investigation of index cases and family members showed that clinical expression of ARVC/D mutations is heterogeneous even among relatives, ranging from a complete lack of symptoms and/or clinical manifestations to severe disease phenotype. It is interesting to notice that multiple mutations carriers did not show more severe phenotypes than single mutation carriers. Although environmental influences, variability in life style and level of physical activity may contribute to the differences, genetic factors are likely to play a significant role as well. For this reason, describing ARVC/D as purely monogenic trait is probably an oversimplification.

Since no causative mutations in known ARVC/D genes have been detected in about 50% of index cases, additional disease-genes should be involved in genetic determination of the disease. Even if the involvement of DES and PKP4 genes will be demonstrated, on the basis of present data, mutations in these genes will account for only a small percentage of ARVC/D patients.

Recent developments from in vitro and in vivo analyses of mutated proteins in mouse models are providing mechanistic explanations, with targeted therapies on the horizon for affected patients. The first knock−in mouse carrying a targeted mutation in *dsg2* gene will be generated as animal model for ARVC/D, by using created targeting vectors. The phenotypic characterization of the mice will involve electrophysiological, histological and gene expression analyses.

7. APPENDIX

TABLE 7.1. Primers sequences, amplification and analysis conditions for PKP2 gene.

Amplicon	bp	Forward 5'-3'	Reverse 5'-3'	PCR T_{ann}°C	T°C dHPLC
1	414	ACTCGAGCGGGGCGGGGCTCG	ACTCCCAGCACGCGGGGTGAG	68	Direct sequencing
2	329	ACTTGTTCTTGGCCTTCATT	TTGGGAAAAGTAAACACTCAAA	TD70>60	53.0 / 55.6 / 58.0
3	971	GGGGCAAACTTCTCGTCATC	GCAGCTGCCTGAAAAGTCATT	TD70>60	Direct sequencing
4	310	TGCTTCCCAGTATTCGCTGA	GGTTTCAGTGTGCAAAGTCACC	TD70>60	61.0
5 a	273	GCCTCAGTTGTGCTACACATAG	CAGCCACCTCCAATTTGTTG	TD70>60	56.0 / 60.0
5 b	304	CGTGGCATCCTCAAGCTTCT	TGAGCCCATCAATCATTTGC	TD70>60	58.1 / 59.1
6	308	TTCAGGGGAGGTGATGTTTG	GGATTACAGGCGCAGACC	TD70>60	Direct sequencing
7	333	GGAGTTGATGGCCTTGACTG	TCCTGACTTCCTTGGGGCTA	TD70>60	58.5
8	307	TGCCAGTTTCCAAACACCTG	AAACCTAAAACCAAGCGGCTA	TD70>60	55.2 / 56.5 / 58.7
9	291	TGATATCACACCTGCAAGGA	CACAAACACACACTCTCTCTCAT	TD70>60	56.9 / 58.7
10	330	CTGGTCTCCTGGTTTGAGTG	TTTCATCTCTGAATTGAATGTAG	TD70>60	57.8 / 60.8
11	330	AAACATCTTCATCAACCTCTGGT	CGGGAGGTGATACAGACAACA	TD70>60	55.3 / 57.1 / 61.2
12	406	GAAAAAGAATGTTCTTCACCCA	CATCCTGTTTGCTGCCATGT	TD70>60	Direct sequencing
13	307	ACCGAGTGGCCTGACTTCAT	CGATTTCTTCCCAGGGTCAA	TD70>60	58.5 / 59.9 / 61.0
14 a	284	TTGACCCTGGGAAGAAATCG	CAGGGGACCACGGAAATAGA	TD70>60	58.2
14 b	300	GGACTGCCAAAGCCTACCAC	TTCCCAGGAAGCCATGTACCA	TD70>60	57.4

TABLE 7.2. Primers sequences, amplification and analysis conditions for DSP gene.

Amplicon	bp	Forward 5'-3'	Reverse 5'-3'	PCR T_{ann}°C	T°C DHPLC
1	422	GGTAGCGAGCAGCGACCTC	AAAACCTTTCCACCTTCGGG	65	65.9 / 66.5
2	365	GATTCCGGGTAAAGGGTCTC	TCTGTTCTGAAAAAGCGTGTCT	62	60.5 / 62.6
3	433	TGGTTCATGAATCTCCGTCTGT	GGGAACATTTGTGCTGCCTT	62	57.2 / 59.2
4	471	TTAAGTCCTGGGGTAAAGAAAA	GGAGGAAAATCCTGCAAACAG	55	58.6 / 61.3
5	443	GCATTAGCCATTTGGGAACC	TTCCCCATTTAAGAAGTGGGATT	62	56.4 / 59.7 / 61.8
6	262	GGGATCTGAGGCCAGTATCTGA	ATCGATGAACAGGTGCCTCC	62	58.0
7	309	ACCTGCAGAGAACACCAGTCA	AGACCAATCATTCCCCGAGA	62	61.1 / 62.1
8	382	AACAGCGTGATTCTTTGGCA	CCAACCCCTGGTGTAGGGTA	55	Direct sequencing
9	312	AGCTTTCATGCAGGCTCACC	GCACTCAAAATCAATGAAGAGG	62	53.7 / 56.8 / 58.7
10	414	ATAGTTTCCCGCTGCCACAT	AAATGCTTGCTTGGCTCTGG	65	57.6 / 60.4
11	442	TGCCGACGAATTTGTGATTT	TTGTTCCATAGCTGCTGATTTC	60	55.7 / 56.4
12	394	TCAGCTTCATTTGAGGGGAAA	GGCAAGGCATCGTGTGTCTA	62	59.3 / 61.8
13	359	GGTTTTTGTGCAGTGGTGTGA	AGGAGGGCTGAGCTGACTTG	62	60.3
14	372	CCCATCTAGTGGGTGGCATT	CCAGTTTTATGCAAACTCCCTT	62	58.9 / 59.6
15	505	TTCTTCGTGCACTAAATTTTCA	AATCCTGCCAGAAGCCTGTT	62	56.6 / 58.0
16	480	CCATGGAAGTTGACTGATGTG	ATGCGAGGCTAGCGGAATTA	62	55.9
17	370	TCTGCTTTGACGTTGTTCCC	AACCTGTGTGGCCACTGAAA	62	57.6 / 58.2
18	437	TTTTATAAACTTTGCCGCCCA	GGCAGTCCATGAAAAGAGCAT	62	Direct sequencing
19	382	TCAAGTGAATTTCTGGGTGA	AAGCCTTCACAAAATGGGTT	58	57.0
20	323	TGCTCATCTCCTAAGCTGTAAC	CGCTTTACAACAAATCAGCA	62	53.6 / 55.3
21	312	TAGACGTGCAGCCCAATGAT	AAGACAGGCAGGAGACAGGG	65	57.0 / 58.8
22	489	TAGGGGAAACAGCCTGGAGA	CAGCGTATTGGAGCATGGAA	TD72>62	Direct sequencing
23 a	455	GAATGCACATTGGTCTGGGA	CACATTGCCTTGCTTTCTGC	62	56.9 / 58.5
23 b	477	TACCAGGCAGAGTGTTCCCA	CTCCTTGATGGTGGTCTTCG	62	58.0
23 c	471	AGGCACCCGGAAGAGAGAAT	GCCTCCTCCTGAAACTCAGC	62	56.0 / 57.0 / 60.7
23 d	461	ACTGAAGCAGGTCATGCAGC	CCAGCTGCTGTTTCCTCTGA	62	56.7 / 59.0
23 e Bg	326	TCACCCGAGAAAACAGGAGC	TCTCGCGTTTTCATCTTCCA	62	57.4 / 59.6
23 e End	271	TTGATGATGCTGCCAAAACC	AACCGCGTGATATCCTGGTC	62	57.0 / 59.4
23 f	503	GCAAACAGTAGTGCGACGGA	TGCTCATTCCTCAAGTGAGCTT	62	60.6 / 61.6
23 g	407	CGGAACCTGAGGCTGGAGTA	AAAGAACAGCAGGGCACACA	TD72>62	54.8 / 56.2 / 59.8
24 a	488	CAAGCTCACAGTGTATCCAGGG	TGCTTGGAGTCTTTCGATCTCA	62	Direct sequencing
24 b	471	GGAAGACTCAATATTCCCGCA	AAGCAGATGCTCCAGCGATA	62	57.8 / 59.3 / 59.8
24 c	476	GAAGGTGACAGCAATGCAGC	CTGAAGCAATCTGGGCTTCC	62	57.8 / 58.7
24 d	490	TTGATGATCCATTTTCAGGCA	CAGCTTGAACCCTGGAGGAA	62	58.0 / 59.1 / 59.7
24 e	472	CCTTCCAAGGAATCAGACAACC	CGAATACCGTGGCCCTTTT	65	58.3 / 59.3
24 f	502	CAGAACGAGCTGTCACTGGG	TGCTCACACAGTTCTTTGAAGG	62	Direct sequencing
24 g	493	CCTCAGGAAGCGTAGAGTGG	GTCAAAGATGGCTGCAATGG	TD72>62	57.2 / 58.5 / 59.3
24 h	500	TTAGCAGCTCCCGACATGAA	TTCGGTGCTTATCCTCCCAT	62	58.8 / 61.2 / 62.0
24 i	467	CATAGGCTTCGAGGGTGTGA	GTGGCGTCAAAGCTTCCTCT	65	Direct sequencing
24 l	479	GGATGCCATAAATCGCTCCA	GACGCACTGCATCCAAGTGTA	65	55.3 / 56.8

TABLE 7.3. Primers sequences, amplification and analysis conditions for DSG2 gene.

Amplicon	bp	Forward 5'-3'	Reverse 5'-3'	PCR T_{ann}°C	T°C DHPLC
1	314	CCAGGGAGGAGCCGAGTG	GATTTTCCGAAGCCCCAGGT	TD70>60	67.0 / 69,1
2	391	AGATTTCTCCTCGGGCACTT	TGCACTGAATACCCCTGGAT	TD70>60	54.8 / 55.1 / 57.5
3	463	GCCTCATAGGAAATACGAAGCA	CCGGAATGGGAAAGAGAATC	TD70>60	Direct sequencing
4	393	GGCTTTTGGCTAAGATCAAATC	GCATCCAAAGCGTAACCTGT	TD70>60	53.1 / 55.0
5	491	TCTTGATCGAGAAGAAACACCA	AAGCAATGGCATGTAAAGTCC	TD70>60	Direct sequencing
6	490	CCCATTCACGCTTATGTCCT	TGGACAGCACATCCCTAAAA	TD70>60	53.8 / 55.0 / 55.8
7+8	700	TCTGCAAAAGCTCTGACTGC	TTTTAAGTGTTCAGGGCTCAAA	TD70>60	Direct sequencing
9 a	343	TGCTGCTATATTTCCTGTGCAT	TCCAATTATTTGGCCTTTGC	TD70>60	54.7 / 55.7 / 56.5
9 b	355	CCTACACCCATTCCCATCAA	GGTGAAAATTCCCCCTCATC	TD70>60	54.8 / 56.9
10	373	AGAGGTTTCCAATTCATGCAG	CTTGACCTCGTGATCCACCT	TD70>60	52.3 / 53.7 / 54.3
11	421	TCTGTTGTCAGCAATAGGAACA	GGTTCAGGACCTCATTTCATAA	TD68>58	55.4 / 56.8 / 59.0
12	455	GCAATGAAAGAACATTTGTGGA	TTGTTTCCCTATTCACCCTCA	TD70>60	Direct sequencing
13	289	GACAAGTCCAGGAAGGGACA	CACTTCCCTAGGCCCCTTTA	TD70>60	55.0 / 57.5 / 59.5
14 a	292	CTGGCCTCAGTGGAAATAGC	GCAGGCTTCTGTGTTCTTCC	TD70>60	58.9 / 60.1
14 b	299	TCATTTCTGCCAGTGGATCA	TCTTCGTTCAGTGCAACAGC	TD70>60	60.6
14 c	225	GATGGAAGGTGGGAAGAACA	CCCCCACCACCAATACATAA	TD70>60	61.0 / 62.8
14 d	286	TGACCACTGAAACCACGAAG	GGGTCCCATTTCTCTTTCCT	TD70>60	Direct sequencing
15 a	273	TTTCCCTGATGGTTCCTTGT	GCGGTCATCTAGCTCTCCTT	TD70>60	53.8 / 54.5 / 57.5
15 b	331	CGGCCTCTTACACTGAGGAA	ACTGGGAAGCTACTGCCAGA	TD70>60	57.2
15 c	377	TCGCTGAATGCTTCTATTGG	CTAGAAGCCATTGGGTCAGG	TD70>60	56.5 / 57.9
15 d	263	TCTGGCAGTAGCTTCCCAGT	GCTGGAGCATACACCCTCTC	TD70>60	60.1
15 e	261	CACCTCTTCCTGACCCAATG	GAAGATGCTGAGTGCCTTCC	TD70>60	59.8
15 f	412	CCTTGGTAGATCAGCCTTATGC	TGCTTGGTAACTCTGGTGGA	TD70>60	58.0 / 59.0 / 60.0
15 g	305	ACGGTGTCTGGAGCTGGA	GGAAGCAGAGACAGTGTGGTC	TD70>60	57.2 / 58.5

TABLE 7.4. Primers sequences, amplification and analysis conditions for DSC2 gene.

Amplicon	bp	Forward 5'-3'	Reverse 5'-3'	PCR T_{ann}°C	T°C DHPLC
1	708	TCAGACCTCGCTCTGTAATTGA	TATCCCCGTTCCCCTAGTTT	58	Direct sequencing
2	199	ACACATTAAAGTTTTCTTTTTAT	GGCGTATATGTACCACAGCA	62	Direct sequencing
3	400	CCCCACGTGCATACATTACT	TGGTTTTCATTCGTCTTTAAGC	58	54.8 / 55.4
4	269	CCCCTACCCAGCTAATCCTC	GGAAACTATAGACTCCCACAGCA	58	55.6 / 58.5
5	332	TGAAAGCTCTGCTGAAATAAAGA	GGAGTAGCCAGAGCATTGGT	58	56.5 / 57.2
6	266	GCCAAAATGAATTTGAAGCATAC	TTGAAACACAGTTAATTTGCCATA	60	54.7
7	384	CATAGAACATGTGAATGTTTTGGA	CAAAACCAGCATACTCCAAGG	58	55.0 / 58.0 / 59.5
8	252	GTTGGTGCTTTCCCCCAATA	AGGCCAGAGATGTGCATATTA	58	54.3 / 55.6
9	324	CATCGTGTTCAATTTTTGTGA	CCTTTCTTTCCATTAAATTCTAGC	60	52.2 / 53.5 / 55.3
10	374	ACTCGTTAGCATTGCCAAAT	TAACGTAACAAAATAAGCTA	58	56.5 / 57.9
11	375	CAAGAAGTAGCAGTGGCATAAGG	AACAGAGTGCATGTATCCAGCTT	60	51.7 / 56.0
12	345	GTGTTCAGTGCATACTTTTGTGG	GCAGACATCCTGATGTTGAAAA	58	57.0 / 58.0 / 59.0
13	356	TGTTCAGAAGAAATCAGTGACA	GTGTCTTGAAAGTTACTTTAAAGG	58	57.2 / 58.0
14	263	GATTTATGTGTGTATTAACCATTG	CGCATTATAAGCGAATTCATCC	58	57.7
15 a	194	CATAATTTTGTGTTCCTCTCTGT	AGGATTCCGAGGTCTGGTGT	58	56.2 / 60.6 / 61.8
15 b	332	GGCTTCACAACCCAAACTGT	TGAAAATTATAGTCAGAATCCAGT	58	61.0 / 61.4 / 62.2
15'	226	GCCACATGCGTGACTTTTAG	ACTTTCTGCCAAGGGGAAAA	58	53.7 / 55.2
16 a	397	CAATGAAAGGTAAATCAAAGCAA	AAAAACCCCCACAAATAGCA	58	56.3 / 56.8

TABLE 7.5. Primers sequences, amplification and analysis conditions for DES gene.

Amplicon	bp	Forward 5'-3'	Reverse 5'-3'	PCR T_{ann}°C	T°C DHPLC
1 a	502	GGGGGCTGATGTCAGGAG	GTAGTTGGCGAAGCGGTCAT	TD72>65	65.7 / 67.5
1 b	514	TCTAAGGGCTCCTCCAGCTC	AGGCCTAGCCTCCTGTGC	TD72>65	65.0 / 66.5
2+3	413	CGTTTCCACTGCCAGCTTTA	CACCCTCACACCCCTATTCC	65	60.8 / 61.5 / 62.5
4	379	ATACCTTGGCCCCTCTTCCT	TACCACAGGCAGCACATCC	TD72>65	62.8
5	257	GTGCCCTGCATCCTTCTCAT	TCTATGATGGGCCCAAGGTC	65	61.6 / 63.4
6	386	GACCTGACCATCTGGAGTTGC	TCCTGGGGACAGAAATGGAC	65	61.9 / 63.2
7	220	GCCGATGGGAGGGTTCTTA	CCCCAGACTCCAGGTCTGTC	65	58.5 / 61.0 / 64.3
8	199	CTTGGTCAGGCTGAGTGTGC	CACAGCTGGGTGGAAGACAG	65	Direct sequencing
9 a	353	GCTGAGGCTCCATTCTCTGG	CAGGCTCACTCACTGCCAACA	65	62.5 / 63.4

TABLE 7.6. Primers sequences, amplification and analysis conditions for PKP4 gene.

Amplicon	bp	Forward 5'-3'	Reverse 5'-3'	PCR T_{ann}°C	T°C DHPLC
2	372	TGCTAGGAACCATCTGTAAAGC	CAGTCATCCCAATGTACTCAGG	TD68>58	60.5 / 62.4
3	432	GCATTTCACAAAGCCACACC	CAAGCACAGGACTGAGGGATT	TD68>58	57.5 / 59.7
4	330	TGCAAAACAGGTCCTAAGCTAAA	TGCTGCTGTTCAATGCTTTT	TD68>58	53.7
5	279	TGACAAACATCTGACCTTTTT	TCTGACACTCGCTTTCAAGA	55	54.0 / 58.3
6	296	TCTTGAAAGCGAGTGTCAGA	CCGGAAGGTATTTCTTTGC	TD68>58	56.0 / 59.1
7 a	361	TGTAATGGCAATGAACACAAAAC	GTTGGGATTGGAGGTCTGC	TD68>58	58.9 / 60.9 / 62.4
7 b	477	ACCTCTGAACCCCAGTGCAT	CCACCTTTTCATTCTTTGTTTCA	TD68>58	60.4 / 62.8
8	335	AGGGTTTATGTTTTTAACCTCAC	AGGGAACCCAATCTCAATAA	TD68>58	59.4 / 60.9
9	331	GATCTCATGGAGAACATACTAATCTT	ATGGAGGAACTGGCTGACT	TD72>62	54.8 / 56.8 / 59.9
10	220	TACAACATGGGCCTTCCTTT	GGCATTATTTTCCCCAGTCA	TD68>58	59.5 / 61.5
11	335	TCACTGATTAATTGCATGTTACTT	TATACAAGGGCACAGTCCAG	55	57.8 / 58.2
12	380	GATTAGGTTTGGAACAGACTGA	AATAAAGTAAGTCCTCCTAAAATCAA	62	53.6 / 55.6
13	311	CCTGTTGTTCGCTCTCTCAG	ATCCGCAGGTCAGAAAGAA	TD68>58	62.6
14 a	190	TCAGTACAGAAGTGTTTGCTCT	GCTGGGAGACTCTTTTCCTA	60	59.7 / 62.8
14 b	302	GCTCTAATGTGCCGAGTTGTT	GTGATTCCTCACTCCCAGAAA	58	57.4 / 59.7
15	535	CCGCAAAGGTGAATGTTTTC	ACCCCACAGCACATACATCC	58	Direct sequencing
16	251	ATGAGACTGGAACTCTGTTTT	TTTTGTAGCTGCTCTCACAT	58	58.1 / 59.7
17	309	AACAATAACAAAAACCTAGTACC	CAGGACAATCTCAGGAATAA	58	62.7
18	194	GAGGCTGTGTCACCCACATT	AAATGATTATGAGTGTGTGCTCTGA	55	57.4 / 58.0
19	375	TTAGCATTCATCAGAGCACAC	TGTGTGATTCCTACAGAAGGTT	TD65>55	57.5 / 59.4
20	525	AGCTTTGTGTTTCTGGAGAGGA	GACGGAGCAAAGGGACTGT	60	56.9 / 60.1
21	195	TAATGGACCAGAGTAATAAGCACTA	GACGTGGACCCCTTACTGT	60	Direct sequencing
22	449	GTGTGCACCAGAAACAGCTT	TCAATCTGAACAAGGTTAGAAAGAA	55	53.9 / 56.6

8. REFERENCES

Ackerman MJ, Tester DJ, Jones GS, Will ML, Burrow CR, Curran ME. Ethnic differences in cardiac potassium channel variants: implications for genetic susceptibility to sudden cardiac death and genetic testing for congenital long QT syndrome. Mayo Clin Proc 2003, 78:1479-1487.

Agah R, Frenkel PA, French BA, Michael LH, Overbeek PA, Schneider MD. Gene recombination in postmitotic cells. Targeted expression of Cre recombinase provokes cardiac-restricted, site-specific rearrangement in adultventricular muscle in vivo. J Clin Invest 1997, 100:169-179.

Ahmad F, Li D, Karibe A, Gonzalez O, Tapscott T, Hill R, Weilbaecher D, Blackie P, Furey M, Gardner M, Bachinski LL, Roberts R. Localization of a gene responsible for arrhythmogenic right ventricular dysplasia to chromosome 3p23. Circulation 1998, 98:2791-5.

Alcalai R, Metzger S, Rosenheck S, Meiner V, Chajek-Shaul T. A recessive mutation in desmoplakin causes arrhythmogenic right ventricular dysplasia, skin disorder, and woolly hair. J Am Coll Cardiol 2003, 42:319-27.

Anastasiadis PZ and Reynolds AB. The p120 catenin family: complex roles in adhesion, signaling and cancer. J Cell Sci 2000, 113:1319-34.

Angelini A, Thiene G, Boffa GM, Calliari I, Daliento L, Valente M, Chioin R, Nava A, Volta SD, Calliaris I [corrected to Calliari I. Endomyocardial biopsy in right ventricular cardiomyopathy. Int J Cardiol 1993, 40:273-82. Erratum in: Int J Cardiol 1993, 41:246.

Armstrong DK, McKenna KE, Purkis PE, Green KJ, Eady RA, Leigh IM, Hughes AE. Aploinsufficiency of desmoplakin causes a striate subtype of palmoplantar eratoderma. Hum Mol Genet 1999, 8:143-8.

Arnestad M, Crotti L, Rognum TO, Insolia R, Pedrazzini M, Ferrandi C, Vege A, Wang DW, Rhodes TE, George AL Jr, Schwartz PJ. Prevalence of long-QT syndrome gene variants in sudden infant death syndrome. Circulation 2007, 115:361-367.

Arnold N, Gross E, Schwarz-Boeger U, Pfisterer J, Jonat W, Kiechle M. A highly sensitive, fast, and economical technique for mutation analysis in hereditary breast and ovarian cancers. Hum Mutat 1999, 14:333-9.

Asimaki A, Syrris P, Wichter T, Matthias P, Saffitz JE, McKenna WJ. A novel dominant mutation in plakoglobin causes arrhythmogenic right ventricular cardiomyopathy. Am J Hum Genet 2007, 81:964-73.

Awad MM, Dalal D, Cho E, Amat-Alarcon N, James C, Tichnell C, Tucker A, Russell SD, Bluemke DA, Dietz HC, Calkins H, Judge DP. DSG2 Mutations Contribute to Arrhythmogenic Right Ventricular Dysplasia/Cardiomyopathy. Am J Hum Genet 2006, 79:136-142.

Awad MM, Dalal D, Tichnell C, James C, Tucker A, Abraham T, Spevak PJ, Calkins H, Judge DP. Recessive arrhythmogenic right ventricular dysplasia due to novel cryptic splice mutation in PKP2. Hum Mutat 2006, 27:1157.

Bagattin A, Veronese C, Bauce B, Wuyts W, Settimo L, Nava A, Rampazzo A, Danieli GA. Denaturing HPLC-based approach for detecting RYR2 mutations involved in malignant arrhythmias. Clin Chem 2004, 50:1148-1155.

Bär H, Strelkov SV, Sjöberg G, Aebi U, Herrmann H. The biology of desmin filaments: how do mutations affect their structure, assembly, and organisation? J Struct Biol 2004, 148:137-152. Review.

Bär H, Mücke N, Kostareva A, Sjöberg G, Aebi U, Herrmann H. Severe muscle disease-causing desmin mutations interfere with in vitro filament assembly at distinct stages. Proc Natl Acad Sci U S A. 2005, 102:15099-15104.

Basso C, Thiene G, Corrado D, Angelini A, Nava A, Valente M: Arrhythmogenic right ventricular cardiomyopathy: dysplasia, dystrophy or myocarditis ? Circulation 1996, 94:983-991.

Basso C and Thiene G: Adipositas cordis, fatty infiltration of the right ventricle, and arrhythmogenic right ventricular cardiomyopathy. Just a matter of fat? Cardiovasc Pathol 2005, 14:37-41.

Basso C, Czarnowska E, Della Barbera M, Bauce B, Beffagna G, Wlodarska EK, Pilichou K, Ramondo A, Lorenzon A, Wozniek O, Corrado D, Daliento L, Danieli GA, Valente M, Nava A, Thiene G, Rampazzo A: Ultrastructural evidence of intercalated disc remodelling in arrhythmogenic right ventricular cardiomyopathy: an electron microscopy investigation on endomyocardial biopsies. Eur Heart J 2006, 27:1847-1854.

Basso C, Nava A, Thiene G. Cardiomiopatia aritmogena. Monografie di cardiologia. SIC.

Bauce B, Nava A, Rampazzo A, Daliento L, Muriago M, Basso C, Thiene G, Danieli GA. Familial effort polymorphic ventricular arrhythmias in arrhythmogenic right ventricular cardiomyopathy map to chromosome 1q42-43. Am J Cardiol 2000, 85:573-579.

Bauce B, Basso C, Rampazzo A, Beffagna G, Daliento L, Frigo G, Malacrida S, Settimo L, Danieli G, Thiene G, Nava A. Clinical profile of four families with arrhythmogenic right ventricular cardiomyopathy caused by dominant desmoplakin mutations. Eur Heart J 2005, 26:1666-1675.

Beffagna G, Occhi G, Nava A, Vitiello L, Ditadi A, Basso C, Bauce B, Carraro G, Thiene G, Towbin JA, Danieli GA, Rampazzo A. Regulatory mutations in transforming growth factor-beta3 gene cause arrhythmogenic right ventricular cardiomyopathy type 1. Cardiovasc Res 2005, 65:366 –373.

Beffagna G, De Bortoli M, Nava A, Salamon M, Lorenzon A, Zaccolo M, Mancuso L, Sigalotti L, Bauce B, Occhi G, Basso C, Lanfranchi G, Towbin JA, Thiene G, Danieli GA, Rampazzo A. Missense mutations in desmocollin-2 N-terminus, associated with arrhythmogenic right ventricular cardiomyopathy, affect intracellular localization of desmocollin-2 in vitro. BMC Med Genet 2007, 8:65.

Blomstrom-Lundqvist C, Sabel KG, Olsson SB. A long term follow up of 15 patients with arrhythmogenic right ventricular dysplasia. Br Heart J 1987, 58:477-88.

Bonne S, van Hengel J, van Roy F. Chromosomal mapping of human armadillo genes belonging to the p120(ctn)/plakophilin subfamily. Genomics 1998, 51:452-454.

Bowles NE, Jimenez S, Vatta M, Chrisco M, Szmuszkovicz, Capetanaki. Familial restrictive cardiomyopathy caused by a missense mutation in the desmin gene. Pediatric Res 2002, 51 Suppl 2.

Brown Jh, Cohen C, Parry DA. Heptad breacks in α-elical coiled-coils: stutters and stammers. Proteins 1996, 26:134-145.

Buja GF, Nava A, Martini B, Canciani B, Thiene G. Right ventricular dysplasia: a familial cardiomyopathy? Eur Heart J 1989, 10 Suppl D:13-15.

Calabrese F, Angelini A, Thiene G, Basso C, Nava A, Valente M. No detection of enteroviral genome in the myocardium of patients with arrhythmogenic right ventricular cardiomyopathy. J Clin Pathol 2000, 53:382-7.

Calabrese F, Basso C, Carturan E, Valente M, Thiene G. Arrhythmogenic right ventricular cardiomyopathy/dysplasia: is there a role for viruses? Cardiovasc Pathol 2006, 15:11-17. Review.

Calabrese F, Carturan E, Thiene G, Towbin JA. Arrhythmogenic in right ventricular cardiomyopathy/ dysplasia. Possible causative or contributing role of viruses. In Arrhythmogenic Right Ventricular Cardiomyopathy/Dysplasia. Edited by Marucs FI, Nava A, Thiene G. Milano: Springer, 2007:79-85.

Calkins CC, Hoepner BL, Law CM, Novak MR, Setzer SV, Hatzfeld M, Kowalczyk AP. The Armadillo family protein p0071 is a VE-cadherin- and desmoplakin-binding protein. J Biol Chem 2003, 278:1774-1783.

Carvajal-Huerta L. Epidermolytic palmoplantar keratoderma with woolly hair and dilated cardiomyopathy. J Am Acad Dermatol 1998, 39:418-21.

Casolo GC, Poggesi L, Boddi M, Fazi A, Bartolozzi C, Lizzadro G, Dabizzi RP. ECG-gated magnetic resonance imaging in right ventricular dysplasia. Am Heart J 1987, 113:1245-8.

Chimenti C, Pieroni M, Maseri A, Frustaci A. Histologic findings in patients with clinical and instrumental diagnosis of sporadic arrhythmogenic right ventricular dysplasia. J Am Coll Cardiol 2004, 43:2305-2313.

Choi HJ, Park-Snyder S, Pascoe LT, Green KJ, Weis WI. Structures of two intermediate filament-binding fragments of desmoplakin reveal a unique repeat motif structure. Nat Struct Biol 2002, 9:612-20.

Corrado D, Basso C, Schiavon M, Thiene G. Screening for hypertrophic cardiomyopathy in young athletes. N Engl J Med 1988, 339:364–369

Corrado D, Thiene G, Nava A, Rossi L, Pennelli N. Sudden death in young competitive athletes: clinicopathologic correlations in 22 cases. Am J Med 1990, 89:588-96.

Corrado D, Basso C, Leoni L, Tokajuk B, Bauce B, Frigo G, Tarantini G, Napodano M, Turrini P, Ramondo A, Daliento L, Nava A, Buja G, Iliceto S, Thiene G: Threedimensional electroanatomic voltage mapping increases accuracy of diagnosing arrhythmogenic right ventricular cardiomyopathy/displasia. Circulation 2005, 111:3042-3050.

Dalal D, Molin LH, Piccini J, Tichnell C, James C, Bomma C, Prakasa K, Towbin JA, Marcus FI, Spevak PJ, Bluemke DA, Abraham T, Russell SD, Calkins H and and Judge DP.Clinical features of arrhythmogenic right ventricular dysplasia/cardiomyopathy associated with mutations in plakophilin-2. Circulation 2006, 113:1641-1649.

Daliento L, Rizzoli G, Thiene G, Nava A, Rinuncini M, Chioin R, Dalla Volta S. Diagnostic accuracy of right ventriculography in arrhythmogenic right ventricular cardiomyopathy. Am J Cardiol 1990, 66:741-5.

Daliento L, Caneve F, Turrini P, Buja G, Nava A, Milanesi O, Stellin G, Rizzoli G. Clinical significance of high-frequency, low-amplitude electrocardiographic signals and QT dispersion in patients operated on for tetralogy of Fallot. Am J Cardiol 1995, 76:408-11.

Dalla Volta S, Battaglia G, Zerbini E: "Auricularization" of right ventricular pressure curve. Am Heart J 1961, 61:25-33.

Dalloz F, Osinska H, Robbins J. Manipulating the contractile apparatus: Gentically defined animal models of cardiovascular disease. J Mol Cell Cardiol 2001, 33:9-25.

Don RH, Cox PT, Wainwright BJ, Baker K, Mattick JS. 'Touchdown' PCR to circumvent spurious priming during gene amplification. Nucleic Acids Res 1991, 19:4008.

Ellis LA, Taylor CF, Taylor GR. A comparison of fluorescent SSCP and denaturing HPLC for high throughput mutation scanning. Hum Mutat 2000, 15:556-64.

Feinberg AP and Vogelstein B. A technique for radiolabeling DNA restriction endonuclease fragments to high specific activity. Anal Biochem. 1983, 132:6-13.

Fixman M and Freire JJ. Theory of DNA melting curves. Biopolymers. 1977, 16:2693-2704.

Foale R, Nihoyannopoulos P, McKenna W, Kleinebenne A, Nadazdin A, Rowland E, Smith G, Klienebenne A. Echocardiographic measurement of the normal adult right ventricle. Br Heart J 1986, 56:33-44. Erratum in: Br Heart J 1986, 56:298298.

Fontaine G, Fontaliran F, Guiraudon G, Frank R, Laurenceau JL, Malergue C, Grosgogeat Y. The arrhythmogenic right ventricle. In : Iwa T, Fontaine G (eds) Cardiac Arrhythmias. Recent Progress in Investigation and Management. Amsterdam: Elsevier Science BV 1988,189-202.

Fontaine G, Fontaliran F, Frank R. Arrhythmogenic right ventricular cardiomyopathies: clinical forms and main differential diagnoses. Circulation. 1998, 97:1532-5. Review.

Furlanello F, Bertoldi A, Dallago M, Furlanello C, Fernando F, Inama G, Pappone C, Chierchia S. Cardiac arrest and sudden death in competitive athletes with arrhythmogenic right ventricular displasia. Pacing Clin Electrophysiol 1998, 21:331-5.

Gallicano GI, Kouklis P., Bauer C, Yin M, Vasioukhin V, Degenstein L, Fuchs E. Desmoplakin is required early in development for assembly of desmosomes and cytoskeletal linkage. J Cell Biol 1998, 143:2009-2022.

Gallicano GI, Bauer C, Fuchs E. Rescuing desmoplakin function in extra-embryonic ectoderm reveals the importance of this protein in embryonic heart, neuroepithelium, skin, and vasculature. Development 2001, 128:929-941.

Garcia-Gras E, Lombardi R, Giocondo MJ, Willerson JT, Schneider MD, Khoury DS, Marian AJ. Suppression of canonical Wnt/beta-catenin signaling by nuclear plakoglobin recapitulates phenotype of arrhythmogenic right ventricular cardiomyopathy. J Clin Invest 2006, 116: 2012–2021.

Garrod DR, Merritt AJ, Nie Z. Desmosomal cadherins. Curr Opin Cell Biol 2002, 14:537–545.

Gerull B, Heuser A, Wichter T, Paul M, Basson CT, McDermott DA, Lerman BB, Markowitz SM, Ellinor PT, MacRae CA, Peters S, Grossmann KS, Michely B, Sasse-Klaassen S, Birchmeier W, Dietz R, Breithardt G, Schulze-Bahr E, Thierfelder L. Mutations in the desmosomal protein plakophilin-2 are common in arrhythmogenic right ventricular cardiomyopathy. Nat Genet 2004, 36:1162-1164.

Getsios S, Amargo EV, Dusek RL, Ishii K, Sheu L, Godsel LM, Green KJ. Coordinated expression of desmoglein 1 and desmocollin 1 regulates intercellular adhesion. Differentiation 2004, 72:419–433.

Gibson UEM, Heid CA, Williams PM. A novel method for real time quantitative RT-PCR. Genome Res 1996, 6:995-1001.

Goebel HH. Congenital myopathies in the new millennium. J Child Neurol 2005, 20:94-101.

Goldfarb LG, Park KY, Cervenakova L, Gorokhova S, Lee Hs, Vasconcelos O, Nagle JW, Semino-Mora C, Sivakumar K, Dalakas MC. Missense mutations in desmin associated with familial cardiac and skeletal myopathy. Nat Genet 1998, 19:402-403.

Goossens S, Janssens B, Bonné S, De Rycke R, Braet F, van Hengel J, van Roy F. A unique and specific interaction between alphaT-catenin and plakophilin-2 in the area composita, the mixed-type junctional structure of cardiac intercalated discs. J Cell Sci 2007, 120:2126-2136.

Goudeau B, Rodrigues-Lima F, Fischer D, Casteras-Simon M, Sambuughin N, de Visser M, Laforet P, Ferrer X, Chapon F, Sjoeberg G, Kostareva A, Sejersen T, Dalakas Mc, Goldfarb LG, Vicart P. Variable Pathogenic Potentials of Mutations Located in the Deamin Alpha-Helical Domain. Hum Mut 2006, 27:906-913.

Green KJ and Gaudry CA. Are desmosome more than tethers for intermediate filaments? Nat Rew Mol Cell Biol 2000, 1:208-216.

Green KJ and Simpson CL. Desmosomes: new perspectives on a classic. J Invest Dermatol 2007, 127:2499-2515. Review.

Gross E, Arnold N, Goette J, Schwarz-Boeger U, Kiechle M. A comparison of BRCA1 mutation analysis by direct sequencing, SSCP and DHPLC. Hum Genet 1999, 105:72-8.

Grossmann KS, Grund C, Huelsken J, Behrend M, Erdmann B, Franke WW, Birchmeier W. Requirement of plakophilin 2 for heart morphogenesis and cardiac junction formation. J Cell Biol 2004, 167: 149-160

Grumbach IM, Heim A, Vonhof S, Stille-Siegener M, Mall G, Gonska BD, Kreuzer H, Andreas S, Figulla HR. Coxsackievirus genome in myocardium of patients with arrhythmogenic right ventricular dysplasia/cardiomyopathy. Cardiology 1998, 89:241-5.

Hamid MS, Norman M, Quraishi A, Firoozi S, Thaman R, Gimeno JR, Sachdev B, Rowland E, Elliott PM, McKenna WJ: Prospective evaluation of relatives for familial arrhythmogenic right ventricular cardiomyopathy/dysplasia reveals a need to broaden diagnostic criteria. J Am Coll Cardiol 2002, 40:1445-1450.

Hatzfeld M and Nachtsheim C. Cloning and characterization of a new armadillo family member, p0071, associated with the junctional plaque: evidence for a subfamily of closely related proteins. J Cell Sci 1996, 109:2767-2778.

Hatzfeld M. The armadillo family of structural proteins. Int Rev Cytol 1999, 186:179-224.

Hatzfeld M, Green KJ, Sauter H. Targeting of p0071 to desmosomes and adherens junctions is mediated by different protein domains. J Cell Sci 2003, 116:1219-1233.

Hatzfeld M. Plakophilins: Multifunctional proteins or just regulators of desmosomal adhesion? Biochim Biophys Acta 2006, 1773:69-77. Review.

Heid CA, Stevens J, Livak KJ, Williams PM. Real time quantitative PCR. Genome Res 1996, 6:986-94.

Heim A, Grumbach I, Stille-Siegener M, Figulla HR. Detection of enterovirus RNA in the myocardium of a patient with arrhythmogenic right ventricular cardiomyopathy by in situ hybridization. Clin Infect Dis 1997, 25:1471-1472.

Heins S and Aebi U. Making heads and tails of intermediate filament assembly, dynamics and networks. Curr Opin Cell Biol 1994, 6:25-33. Review.

Herrmann H, Haner M, Brettel M, Muller SA, Goldie KN, Fedtke B, Lustig A, Franke WW, Aebi U. Structure and assembly properties of the intermediate filament protein vimentin: the role of its head, rod and tail domains. J Mol Biol 1996, 264:933-953.

Herrmann H and Aebi U. Intermediate filaments and their associates: multi-talented structural elements specifying cytoarchitecture and cytodynamics. Curr Opin Cell Biol 2000, 12:79-90. Review.

Herrmann H, Strelkov SV, Feja B, Rogres KR, Brettl M, Lustig A, Harner M, Parry DA, Steinert PM, Burkhard P, Aebi U. The intermediate filament protein consensus motif of helix 2B: its atomic structure and contribution to assembly. J Mol Biol 2000, 298:817-832.

Herrmann H and Aebi U. Intermediate filaments: molecular structure, assembly mechanism, and integration into functionally distinct intracellular scaffolds. Annu Rev Biochem 2004, 73:749-789.

Heuser A, Plovie ER, Ellinor PT, Grossmann KS, Shin JT, Wichter T, Basson CT, Lerman BB, Sasse-Klaassen S, Thierfelder L, MacRae CA, Gerull B. Mutant desmocollin-2 causes arrhythmogenic right ventricular cardiomyopathy. Am J Hum Genet 2006, 79:1081–1088.

Ihrie RA, Marques MR, Nguyen BT, Horner JS, Papazoglu C, Bronson RT, Mills AA, Attardi LD. Perp is a p63-regulated gene essential for epithelial integrity. Cell 2005, 120:843-856.

James TN. Normal and abnormal consequences of apoptosis in the human heart. From postnatal morphogenesis to paroxysmal arrhythmias. Circulation. 1994, 90:556-573. Review.

Jones AC, Austin J, Hansen N, Hoogendoorn B, Oefner PJ, Cheadle JP, O'Donovan MC. Optimal temperature selection for mutation detection by denaturing HPLC and comparison to single-stranded conformation polymorphism and heteroduplex analysis. Clin Chem 1999, 45:1133-40.

Kannankeril PJ, Mitchell BM, Goonasekera SA, Chelu MG, Zhang W, Sood S, Kearney DL, Danila CI, De Biasi M, Wehrens XH, Pautler RG, Roden DM, Taffet GE, Dirksen RT, Anderson ME, Hamilton SL. Mice with the R176Q cardiac ryanodine receptor mutation catecholamine-induced ventricular tachycardia and cardiomyopathy. Proc Natl Acad Sci U S A 2006, 103:12179-12184.

Kaplan SR, Gard JJ, Protonotarios N, Tsatsopoulou A, Spiliopoulou C, Anastasakis A, Squarcioni CP, McKenna WJ, Thiene G, Basso C, Brousse N, Fontaine G, Saffitz JE. Remodeling of myocyte gap junctions in arrhythmogenic right ventricular cardiomyopathy due to a deletion in plakoglobin (Naxos disease). Heart Rhythm 2004, 1:3–11.

Kapoun AM, Liang F, O'Young G, Damm DL, Quon D, White RT, Munson K, Lam A, Schreiner GF, Protter AA. B-type natriuretic peptide exerts broad functional opposition to transforming growth factor-beta in primary human cardiac fibroblasts: fibrosis, myofibroblast conversion, proliferation, and inflammation. Circ Res 2004, 94:453-61.

Kearney DL, Towbin JA, Bricker JT, Radovancevic B, Frazier OH. Familial right ventricular dysplasia (cardiomyopathy). Pediatr Pathol Lab Med 1995, 15:181-189.

Klymkowsky MW, Williams BO, Barish GD, Varmus HE, Vourgourakis YE. Membrane–anchored plakoglobins have multiple mechanisms of action in Wnt signaling. Mol Biol Cell 1999, 10:3151-3169.

Ko KS, Arora PD, McCulloch CA. Cadherins mediate intercellular mechanical signaling in fibroblasts by activation of stretch-sensitive calcium-permeable channels. J Biol Chem 2001, 276:35967–35977.

Kopplin LJ, Tester DJ, Ackerman MJ. Prevalence and spectrum of mutations in the cardiac ryanodine receptor in patient referred for long QT syndrome genetic testing. J Am Coll Cardiol 2004, 43(Suppl A):136A.

Kostetskii I, Li J, Xiong Y, Zhou R, Ferrari VA, Patel VV, Molkentin JD, Radice GL. Induced deletion of the N-cadherin gene in the heart leads to dissolution of the intercalated disc structure. Circ Res 2005, 96:346–354.

Kuhn A, Kottkamp H, Thiele H, Schuler G, Hindricks G. [Idiopathic right ventricular tachycardia or arrhythmogenic right ventricular tachycardia?] Dtsch Med Wochenschr 2000, 125:692-7. German.

Küssel P and Frasch M. Pendulin, a Drosophila protein with cell cycle-dependent nuclear localization, is required for normal cell proliferation. J Cell Biol 1995, 129:1491-1507.
Laitinen PJ, Brown KM, Piippo K, Swan H, Devaney JM, Brahmbhatt B, Donarum EA, Marino M, Tiso N, Viitasalo M, Toivonen L, Stephan DA, Kontula K. Mutations of the cardiac ryanodine receptor (RyR2) gene in familial polymorphic ventricular tachycardia. Circulation 2001, 103:485-90.

Laitinen PJ, Swan H, Kontula K. Molecular genetics of exercise-induced polymorphic ventricular tachycardia: identification of three novel cardiac ryanodine receptor mutations and two common calsequestrin 2 amino-acid polymorphisms. Eur J Hum Genet. 2003, 11:888-891.

Lahtinen AM, Lehtonen A, Kaartinen M, Toivonen L, Swan H, Widén E, Lehtonen E, Lehto VP, Kontula K. Plakophilin-2 missense mutations in arrhythmogenic right ventricular cardiomyopathy. Int J Cardiol 2007. [Epub ahead of print]

Lancisi GM: De Motu Cordis et Aneurysmatibus. Naples: 1736.

Lazarides E. Intermediate filamnts as mechanical integrators of cellular space. Nature 1980, 238:249-256.

Leclercq JF, Potenza S, Maison-Blanche P, Chastang C, Coumel P. Determinants of spontaneous occurrence of sustained monomorphic ventricular tachycardia in right ventricular dysplasia. J Am Coll Cardiol 1996, 28:720-4.

Le Guludec D, Slama MS, Frank R, Faraggi M, Grimon G, Bourguignon MH, Motte G: Evaluation of radionuclide angiography in diagnosis of arrhythmogenic right ventricular cardiomyopathy. J Am Coll Cardiol 1995, 26:1476-1483.

Li ZL, Lilienbaum A, Butler-Browne G, Paulin D. Human desmin-coding gene: complete nucleotide sequence, characterization and regulation of expression during myogenesis and development. Gene 1989, 78:243-54.

Li Z, Colucci-Guyon E, Pinçon-Raymond M, Mericskay M, Pournin S, Paulin D, Babinet C. Cardiovascular lesions and skeletal myopathy in mice lacking desmin. Dev Biol 1996, 175:362-366.

Li D, Tapscoft T, Gonzalez O, Burch PE, Quiñones MA, Zoghbi WA, Hill R, Bachinski LL, Mann DL, Roberts R. Desmin mutation responsible for idiopathic dilated cardiomyopathy. Circulation 1999, 100:461-464.

Li D, Ahmad F, Gardner MJ, Weilbaecher D, Hill R, Karibe A, Gonzalez O, Tapscott T, Sharratt GP, Bachinski LL, Roberts R. The locus of a novel gene responsible for arrhythmogenic right-ventricular dysplasia characterized by early onset and high penetrance maps to chromosome 10p12-p14. Am J Hum Genet 2000, 66:148-56.

Lu Q, Paredes M, Medina M, Zhou J, Cavallo R, Peifer M, Orecchio L, Kosik KS. Delta-catenin, an adhesive junction-associated protein which promotes cell scattering. J Cell Biol 1999, 144:519-532.

MacRae CA, Birchmeier W, Thierfelder L. Arrhythmogenic right ventricular cardiomyopathy: moving toward mechanism. J Clin Invest 2006, 116:1825-1828.

Maniatis T, Sambrook J, Fritsch EF. Molecular cloning. A laboratory manual. 2nd ed ition. USA, Cold Spring Harbor Laboratory Press, 1989.

Mallat Z, Tedgui A, Fontaliran F, Frank R, Durigon M, Fontaine G. Evidence of apoptosis in arrhythmogenic right ventricular dysplasia. N Engl J Med 1996, 335:1190-6.

Manyari DE, Duff HJ, Kostuk WJ, Belenkie I, Klein GJ, Wyse DG, Mitchell LB, Boughner D, Guiraudon G, Smith ER. Usefulness of noninvasive studies for diagnosis of right ventricular dysplasia. Am J Cardiol, 57:1147-53.

Maquat LE. Nonsense-mediated mRNA decay: splicing, translation and mRNP dynamics. Nat Rev Mol Cell Biol 2004, 5:89-99. Review.

Marcus F, Fontaine G, Guirdaudon G, Frank R, Laurenceau JL, Malergue C, Grosgogeat Y: Right ventricular dysplasia: a report of 24 adult cases. Circulation 1982, 65:384-398.

Marcus FI, Fontaine GH, Frank R, Gallagher JJ, Reiter MJ. Long-term follow-up in patients with arrhythmogenic right ventricular disease. Eur Heart J 1989,10 (Suppl D):68-73.

Marcus FI, Fontaine G. Arrhythmogenic right ventricular dysplasia/cardiomyopathy: a review. Pacing Clin Electrophysiol 1995,18:1298-314. Review.

Marian AJ. Modifier genes for hypertrophic cardiomyopathy. Curr Opin Cardiol 2002, 17:242-52. Review.

Maron BJ. Right ventricular cardiomyopathy: another cause of sudden death in the young. N Engl J Med 1988, 318:178-180.

Marques MR, Ihrie RA, Horner JS, Attardi LD. The requirement for perp in postnatal viability and epithelial integrity reflects an intrinsic role in stratified epithelia. J Invest Dermatol 2006, 126:69-73.

Matsumori A, Kawai C. Coxsackie virus B3 perimyocarditis in BALB/c mice: experimental model of chronic perimyocarditis in the right ventricle. J Pathol. 1980, 131:97-106.

McKenna WJ, Thiene G, Nava A, Fontaliran F, Blomstrom-Lundqvist C, Fontaine G, Camerini F. Diagnosis of arrhythmogenic right ventricular dysplasia/cardiomyopathy: Task Force of the Working Group Myocardial and Pericardial Disease of the European Society of Cardiology and of the Scientific Council on Cardiomyopathies of the International Society and Federation of Cardiology. Br Heart J 1994, 71:215–218.

McKoy G, Protonotarios N, Crosby A, Tsatsopoulou A, Anastasakis A, Coonar A, Norman M, Baboonian C, Jeffery S, McKenna WJ. Identification of a deletion in plakoglobin in arrhythmogenic right ventricular cardiomyopathy with palmoplantar keratoderma and woolly hair (Naxos disease). Lancet 2000, 355:2119-24.

Melberg A, Oldfors A, Blomstrom-Lundqvist C, Stalberg E, Carlsson B, Larsson E, Lidell C, Eeg-Olofsson KE, Wikstrom G, Henriksson KG, Dahl N. Autosomal dominant myofibrillar myopathy with arrhythmogenic right ventricular cardiomyopathy linked to chromosome 10q. Ann Neurol 1999, 46:684-92.

Mertens C, Hofmann I, Wang Z, Teichmann M, Chong SS, Schnolzer M, Franke WW. Nuclear particles containing RNA polymerase III complexes associated with the junctional plaque protein plakophilin 2. Proc Natl Acad Sci USA 2001, 98:7795-7800.

Miller SA, Dykes DD, Polesky HF. A simple salting out procedure for extracting DNA from human nucleated cells. Nucleic Acids Res 1988, 16:1215.

Milner DJ, Weitzer G, Tran D, Bradley A, Capetanaki Y. Disruption of muscle architecture and myocardial degeneration in mice lacking desmin. J Cell Biol 1996, 134:1255-1270.

Missiaen L, Robberecht W, van den Bosch L, Callewaert G, Parys JB, Wuytack F, Raeymaekers L, Nilius B, Eggermont J, De Smedt H. Abnormal intracellular ca(2+)homeostasis and disease. Cell Calcium 2000, 28:1-21. Review.

Munoz-Marmol AM, Strasser G, Isamat M, Coulombe PA, Yang Y, Roca X, Vela E, Mate JL, Coll J, Fernandez-Figueras MT, Navas-Palacios JJ, Ariza A, Fuchs E. A dysfunctional desmin mutation in a patient with severe generalized myopathy. Natl Acad Sci USA 1998, 95:11312-11317.

Nagata M, Hiroe M, Ishiyama S, Nishikawa T, Sakomura Y, Kasanuki H, Toyosaki T, Marumo F. Apoptotic cell death in arrhythmogenic right ventricular cardiomyopathy: a comparative study with idiopathic sustained ventricular tachycardia. Jpn Heart J 2000, 41:733-41.

Nava A, Scognamiglio R, Thiene G, Canciani B, Daliento L, Buja G, Stritoni P, Fasoli G, Dalla Volta S. A polymorphic form of familial arrhythmogenic right ventricular dysplasia. Am J Cardiol 1987, 59:1405-1409.

Nava A, Thiene G, Canciani B, Scognamiglio R, Daliento L, Buja G, Martini B, Stritoni P, Fasoli G. Familial occurrence of right ventricular dysplasia: a study involving nine families. J Am Coll Cardiol 1988, 12:1222-8.

Nava A, Thiene G, Canciani B, Scognamiglio R, Daliento L, Buja GF, Martini B, Stritoni P, Fasoli G. Familial occurrence of right ventricular dysplasia: a study involving nine families. J Am Coll Cardiol 1989, 12:1222-1228.

Nava A, Canciani B, Thiene G, Scognamiglio R, Buja G, Martini B, Daliento L, Fasoli G, Stritoni P, Dalla Volta S. Analysis of the mode of transmission of right ventricular dysplasia Arch Mal Coeur Vaiss 1990, 83:923-928. Review. French.

Nava A, Thiene G, Canciani B, Martini B, Daliento L, Buja G, Fasoli G. Clinical profile of concealed form of arrhythmogenic right ventricular cardiomyopathy presenting with apparently idiopathic ventricular arrhythmias. Int J Cardiol 1992, 35:195-206.

Nava A, Bauce B, Basso C, Muriago M, Rampazzo A, Villanova C, Daliento L, Buja G, Corrado D, Danieli GA, Thiene G. Clinical profile and long term follow-up of 37 families with arrhythmogenic right ventricular cardiomyopathy. J Am Coll Cardiol 2000, 36:2226 –2233.

Nava A, Rossi L and Thiene G. editors. Arrhythmogenic right ventricular cardiomyopathy/displasia. Excerpta medica. International congress series.

Nerbonne JM. Studying cardiac arrhythmias in the mouse- a reasonable model for probing mechanisms? Trends Cardiovasc Med 2004, 14:83-93.

Nishikawa T, Ishiyama S, Nagata M, Sakomura Y, Nakazawa M, Momma K, Hiroe M Kasajima T. Programmed cell death in the myocardium of arrhythmogenic right ventricular cardiomyopathy in children and adults. Cardiovasc Pathol 1999, 8:185-9.

Norgett EE, Hatsell SJ, Carvajal-Huerta L, Cabezas JC, Common J, Purkis PE, Whittock N, Leigh IM, Stevens HP, Kelsell DP. Recessive mutation in desmoplakin disrupts desmoplakin-intermediate filament interactions and causes dilated cardiomyopathy, woolly hair and keratoderma. Hum Mol Genet 2000, 9:2761-6.

Norman MW, McKenna WJ: Arrhythmogenic right ventricular cardiomyopathy/dysplasia: perspectives on diseases. Z Kardiol 1999, 88:550-554.

Norman M, Simpson M, Mogensen J, Shaw A, Hughes S, Syrris P, Sen-Chowdhry S, Rowland E, Crosby A, McKenna WJ. Novel mutation in desmoplakin causes arrhythmogenic left ventricular cardiomyopathy. Circulation 2005, 112:636-642.

Olson EN. Gene regulatory networks in the evolution and development of the heart. Science 2006, 313:1922-1927. Review.

Palka HL and Green KJ. Roles of plakoglobin end domains in desmosome assembly. J Cell Sci 1997, 110:2359-2371.

Pilichou K, Nava A, Basso C, Beffagna G, Bauce B, Lorenzon A, Frigo G, Vettori A, Valente M, Towbin J, Thiene G, Danieli GA, Rampazzo A: Mutations in desmoglein-2 gene are associated with arrhythmogenic right ventricular cardiomyopathy. Circulation 2006, 113:1171-1179.

Pinamonti B, Sinagra G, Di Lenarda A, Morgera T, Bussani R, Silvestri F, Camerini F. Left ventricular involvement in right ventricular cardiomyopathy. Postgrad Med J 1992, 68 Suppl 1:S36-39.

Premstaller A and Oefner PJ. Denaturing high-performance liquid chromatography. Methods Mol Biol 2003, 212:15-35.

Priori SG, Napolitano C, Tiso N, Memmi M, Vignati G, Bloise R, Sorrentino V, Danieli GA. Mutations in the cardiac ryanodine receptor gene (hRyR2) underlie catecholaminergic polymorphic ventricular tachycardia. Circulation 2001, 103:196-200.

Priori SG, Napolitano C, Memmi M, Colombi B, Drago F, Gasparini M, DeSimone L, Coltorti F, Bloise R, Keegan R, Cruz Filho FE, Vignati G, Benatar A, DeLogu A. Clinical and molecular characterization of patients with catecholaminergic polymorphic ventricular tachycardia. Circulation 2002, 106:69-74.

Protonotarios N, Tsatsopoulou A, Patsourakos P, Alexopoulos D, Gezerlis P, Simitsis S, Scampardonis G. Cardiac abnormalities in familial palmoplantar keratosis. Br Heart J 1986, 56:321-6.

Rampazzo A, Nava A, Danieli GA, Buja G, Daliento L, Fasoli G, Scognamiglio R, Corrado D, Thiene G. The gene for arrhythmogenic right ventricular cardiomyopathy maps to chromosome 14q23-q24.Hum Mol Genet 1994, 3:959-62.

Rampazzo A, Nava A, Erne P, Eberhard M, Vian E, Slomp P, Tiso N, Thiene G, Danieli GA. A new locus for arrhythmogenic right ventricular cardiomyopathy (ARVD2) maps to chromosome 1q42-q43. Hum Mol Genet 1995, 4:2151-4.

Rampazzo A, Nava A, Miorin M, Fonderico P, Pope B, Tiso N, Livolsi B, Zimbello R, Thiene G, Danieli GA. ARVD4, a new locus for arrhythmogenic right ventricular cardiomyopathy, maps to chromosome 2 long arm. Genomics 1997, 45:259-63.

Rampazzo A, Nava A, Malacrida S, Beffagna G, Bauce B, Rossi V, Zimbello R, Simionati B, Basso C, Thiene G, Towbin JA, Danieli GA. Mutation in human desmoplakin domain binding to plakoglobin causes a dominant form of arrhythmogenic right ventricular cardiomyopathy. Am J Hum Genet 2002, 71:1200-6.

Rampazzo A, Beffagna G, Nava A, Occhi G, Bauce B, Noiato M, Basso C, Frigo G, Thiene G, Towbin J, Danieli GA. Arrhythmogenic right ventricular cardiomyophaty type 1 (ARVD1): confirmation of locus assignment and mutation screening of four candidate genes. Eur J Hum Gen 2003, 11: 69-76.

Rampazzo A and Danieli GA. Arrhythmogenic in right ventricular cardiomyopathy/dysplasia. Advances in genetics: Dominant forms. In Arrhythmogenic Right Ventricular Cardiomyopathy/Dysplasia. Edited by Marucs FI, Nava A, Thiene G. Milano: Springer, 2007:7-14.

Richard P, Charron P, Carrier L, Ledeuil C, Cheav T, Pichereau C, Benaiche A, Isnard R, Dubourg O, Burban M, Gueffet JP, Millaire A, Desnos M, Schwartz K, Hainque B, Komajda M; EUROGENE Heart Failure Project. Hypertrophic cardiomyopathy: distribution of disease genes, spectrum of mutations, and implications for a molecular diagnosis strategy. Circulation 2003, 107:2227-2232.

Rossi V, Beffagna G, Rampazzo A, Bauce B, Danieli GA. TAIL1: an isthmin-like gene, containing type 1 thrombospondin-repeat and AMOP domain, mapped to ARVD1 critical region. Gene 2004, 335:101-108.

Ruiz P, Brinkmann V, Ledermann B, Behrend M, Grund C, Thalhammer C, Vogel F, Birchmeier C, Günthert U, Franke WW, Birchmeier W. Targeted mutation of plakoglobin in mice reveals essential functions of desmosomes in the embryonic heart. J Cell Biol 2006, 135:215-225.

Schollen E, Martens K, Geuzens E, Matthijs G. DHPLC analysis as a platform for molecular diagnosis of congenital disorders of glycosylation (CDG). Eur J Hum Genet 2002, 10:643-8.

Scognamiglio R, Fasoli G, Nava A, Miraglia G, Thiene G, Dalla-Volta S. Contribution of cross-sectional echocardiography to the diagnosis of right ventricular dysplasia at the asymptomatic stage. Eur Heart J 1989, 10:538-542.

Severini GM, Krajinovic M, Pinamonti B, Sinagra G, Fioretti P, Brunazzi MC, Falaschi A, Camerini F, Giacca M, Mestroni L. A new locus for arrhythmogenic right ventricular dysplasia on the long arm of chromosome 14. Genomics 1996, 31:193-200.

Severs NJ, Dupont E, Thomas N, Kaba R, Rothery S, Jain R, Sharpey K, Fry CH. Alterations in cardiac connexin expression in cardiomyopathies. Adv Cardiol 2006, 42:228-242. Review.

Sharp PA, Sugden B, Sambrook J. Detection of two restriction endonuclease activities in Haemophilus parainfluenzae using analytical agarose-ethidium bromide electrophoresis. Biochemistry 1973, 12:3055-63.

Smith TA, Strelkov SV, Burkhard P, Aebi U, Parry DA. Sequence comparisons of intermediate filament chains: evidence of unique functional/structural role for coiled-coil segment 1A and linker L1. Struct Biol 2002, 137:128-145.

Strelkov SV, Herrmann H, Geisler N, Wedig T, Zimbelmann R, Aebi U, Burkhard P. Conserved segments 1 A and 2B of the intermediate filament dimer: their atomic structures and role in filament assembly. EMBO J 2002, 21:1255-1266.

Stokes DL and Wagenknecht T. Calcium transport across the sarcoplasmic reticulum: structure and function of Ca2+-ATPase and the ryanodine receptor. Eur J Biochem 2000, 267:5274-5279. Review.

Strachan T and ReadA.P. Human Molecular Genetics. 3th edition. Publisher: Garland Science, 2003.

Syrris P, Ward D, Evans A, Asimaki A, Gandjbakhch E, Sen-Chowdhry S, McKenna WJ. Arrhythmogenic right ventricular dysplasia/cardiomyopathy associated with mutations in the desmosomal gene desmocollin-2. Am J Hum Genet 2006, 79:978-984.

Syrris P, Ward D, Asimaki A, Sen-Chowdhry S, Ebrahim HY, Evans A, Hitomi N, Norman M, Pantazis A, Shaw AL, Elliott PM, McKenna WJ. Clinical expression of plakophilin-2 mutations in familial arrhythmogenic right ventricular cardiomyopathy. Circulation 2006, 113:356-364.

Syrris P, Ward D, Asimaki A, Evans A, Sen-Chowdhry S, Hughes SE, McKenna WJ. Desmoglein-2 mutations in arrhythmogenic right ventricular cardiomyopathy: a genotype-phenotype characterization of familial disease. Eur Heart J 2007, 28:581-588.

Tabib A, Miras A, Taniere P, Loire R. Undetected cardiac lesions cause unexpected sudden cardiac death during occasional sport activity. A report of 80 cases. Eur Heart J 1999, 20:900-903.

Tandri H, Saranathan M, Rodriguez ER, Martinez C, Bomma C, Nasir K, Rosen B, Lima JA, Calkins H, Bluemke DA: Noninvasive detection of myocardial fibrosis in arrhythmogenic right ventricular cardiomyopathy using delayed-enhancement magnetic resonance imaging. J Am Coll Cardiol 2005, 45:98-103.

Tavernier R, Gevaert S, De Sutter J, De Clercq A, Rottiers H, Jordaens L, Fonteyne W. Long term results of cardioverter-defibrillator implantation in patients with right ventricular dysplasia and malignant ventricular tachyarrhythmias. Heart 2001, 85:53-6.

Thiene G, Nava A, Corrado D, Rossi L, Pennelli N: Right ventricular cardiomyopathy and sudden death in young people. N Engl J Med 1988, 318:129-133.

Thiene G, Nava A, Angelini A, Daliento L, Scognamiglio R, Corrado D. Anatomoclinical aspects of arrhythmogenic right ventricular cardiomyopathy. In Advances in cardiomyopathies. Edited by Baroldi G, Camerini F, Goodwin JF. Milano: Springer Verlag, 1990:397-408.

Thiene G, Corrado D, Nava A, Rossi L, Poletti A, Boffa GM, Daliento L, Pennelli N. Right ventricular cardiomyopathy: is there evidence of an inflammatoryaetiology? Eur Heart J 1991, 12 Suppl D:22-5.

Thiene G, Basso C, Danieli GA, Rampazzo A, Corrado D, Nava A. Arrhythmogenic right ventricular cardiomyopathy: a still underrecognised clinical entità. Trends Cardiovascular Med 1997,7:84-90

Thiene G, Corrado D, Basso C. Arrhythmogenic right ventricular cardiomyopathy/dysplasia. Orphanet J Rare Dis 2007, 2:45.

Thomas NL, George CH, Lai FA. Functional heterogeneity of ryanodine receptor mutations associated with sudden cardiac death. Cardiovasc Res 2004, 64: 52-60.

Tiso N, Stephan DA, Nava A, Bagattin A, Devaney JM, Stanchi F, Larderet G, Brahmbhatt B, Brown K, Bauce B, Muriago M, Basso C, Thiene G, Danieli GA, Rampazzo A. Identification of mutations in the cardiac ryanodine receptor gene in families affected with arrhythmogenic right ventricular cardiomyopathy type 2 (ARVD2). Hum Mol Genet 2001, 10:189-94.

Valente M, Calabrese F, Angelini A, Basso C, Thiene G. Apoptosis in arrhythmogenic right ventricular cardiomyopathy. Circulation 1996, 26:339-257.

Van Driest SL, Maron BJ, Ackerman MJ. From malignant mutations to malignant domains: the continuing search for prognostic significance in the mutant genes causing hypertrophic cardiomyopathy. Heart 2004, 90:7-8.

Van Tintelen JP, Entius MM, Bhuiyan ZA, Jongbloed R, Wiesfeld AC, Wilde AA, van der Smagt J, Boven LG, Mannens MM, van Langen IM, Hofstra RM, Otterspoor LC, Doevendans PA, Rodriguez LM, van Gelder IC, Hauer RN: Plakophilin-2 mutations are the major determinant of familial arrhythmogenic right ventricular dysplasia/cardiomyopathy. Circulation 2006, 113:1650-1658.

Van Tintelen JP, Hofstra RM, Wiesfeld AC, van den Berg MP, Hauer RN, Jongbloed JD. Molecular genetics of arrhythmogenic right ventricular cardiomyopathy: emerging horizon? Curr Opin Cardiol 2007, 22:185-192. Review.

Vatta M, Yang Z, Towbin JA. Arrhythmogenic in right ventricular cardiomyopathy/dysplasia. Transgenic animal models. In Arrhythmogenic Right Ventricular Cardiomyopathy/Dysplasia. Edited by Marucs FI, Nava A, Thiene G. Milano: Springer, 2007:61-68.

Viegas-Perqugnot E, Li ZL, Dutrillaux B, Apiou F, Paulin D. Assignement of human desmin gene to band 2q35 by nonradioactive in situ hybridation. Hum Genet 1989, 83:33-36.

Virata ML, Wagner RM, Parry DA, Green KJ. Molecular structure of the human desmoplakin I and II amino terminus. Proc Natl Acad Sci U S A 1992, 89:544-8.

Weber K and Geisler N. Intermediate filaments: structural conservation and divergence. Ann N Y Acad Sci 1985, 455:126-143. Review.

Whittock NV, Wan H, Morley SM, Garzon MC, Kristal L, Hyde P, McLean WH, Pulkkinen L, Uitto J, Christiano AM, Eady RA, McGrath JA. Compound heterozygosity for non-sense and mis-sense mutations in desmoplakin underlies skin fragility/woolly hair syndrome. J Invest Dermatol 2002, 118:232-8.

Wichter T, Borggrefe M, Haverkamp W, Chen X, Breithardt G: Efficacy of antiarrhythmic drugs in patients with arrhythmogenic right ventricular disease. Results in patients with inducible and noninducible ventricular tachicardia. Circulation 1992, 86:29-37.

Xiao W and Oefner PJ. Denaturng high-performance liquid chromatography: A rewiew. Hum Mut 2001, 17: 439-74.

Yang Z, Bowles NE, Scherer SE, Taylor MD, Kearney DL, Ge S, Nadvoretskiy VV, DeFreitas G, Carabello B, Brandon LI, Godsel LM, Green KJ, Saffitz JE, Li H, Danieli GA, Calkins H, Marcus F, Towbin JA. Desmosomal dysfunction due to mutations in desmoplakin causes arrhythmogenic right ventricular dysplasia/cardiomyopathy. Circ Res 2006, 99:646-55.

Yoshida M, Romberger DJ, Illig MG, Takizawa H, Sacco O, Spurzem JR, Sisson JH, Rennard SI, Beckmann JD. Transforming growth factor-beta stimulates the expression of desmosomal proteins in bronchial epithelial cells. Am J Respir Cell Mol Biol 1992, 6:439-45.

Yutzey KE and Robbins J. Principles of genetic murine models for cardiac disease. Circulation 2007, 115:792-799. Review.